PREDICTING SHORELINE RESPONSE TO WAVE AND SEA LEVEL TRENDS

Stefano Corbella

University of KwaZulu-Natal

Submitted in fulfillment of the academic requirements for the degree of

Doctor of Philosophy, School of Engineering, University of KwaZulu-Natal, Durban.

November 2012

As the candidates supervisor I have approved this thesis for submission.

....
Professor Derek D. Stretch Date

Declaration 1 - Plagiarism

I, Stefano Corbella declare that:

1. The research reported in this thesis, except where otherwise indicated, is my original research.

2. This thesis has not been submitted for any degree or examination at any other university.

3. This thesis does not contain other persons' data, pictures, graphs or other information, unless specifically acknowledged as being sourced from other persons.

4. This thesis does not contain any other persons' writing, unless specifically acknowledged as being sourced from other researchers. Where other written sources have been quoted then:

    a. Their words have been re-written but the general information attributed to them has been referenced;

    b. Where their exact words have been used, then their writing has been placed in italics and inside quotation marks, and referenced.

5. This thesis does not contain text, graphics or tables copied from the Internet, unless specifically acknowledged, and the source being detailed in the thesis and in the Reference section.

Signed .....

Declaration 2 - Publications

All the publications represent research completed and compiled in their entirety by the author with Derek Stretch providing technical suggestions and amendments.

Published peer reviewed journal papers

Publication 1
Corbella, S. Stretch, D. 2012. The wave climate on the KwaZulu-Natal coast, *Journal of the South African Institution of Civil Engineering*, 54 (2), 45 – 54.

Publication 2
Corbella, S. Stretch, D. 2012. Shoreline recovery from storms on the east coast of Southern Africa, *Natural Hazards and Earth System Science*, 12, 11 – 12, www.nat-hazards-earth-syst-sci.net/12/11/2012/, doi:10.5194/nhess-12-11-2012.

Publication 3
Corbella, S. Stretch, D. 2012. Decadal trends in beach morphology on the east coast of South Africa and likely causative factors, *Natural Hazards and Earth System Science*, 12, 2515 – 2527, www.nat-hazards-earth-syst-sci.net/12/2515/2012/, doi:10.5194/nhess-12-2515-2012.

Publication 4
Corbella, S. Stretch, D. 2012. Predicting coastal erosion trends using non-stationary statistics and process-based models, *Coastal Engineering*, 70, 40 – 49, doi:10.1016/j.coastaleng.2012.06.004.

Publication 5
Corbella, S. Stretch, D. 2012. Multivariate return periods of sea storms for coastal erosion risk assessment, *Natural Hazards and Earth System Science*, 12, 2699 – 2708, www.nat-hazards-earth-syst-sci.net/12/2699/2012/, doi:10.5194/nhess-12-2699-2012.

Publication 6

Corbella, S. Stretch, D. 2012. Coastal Defences on the KwaZulu-Natal coast: a review with particular reference to geotextiles, *Journal of the South African Institution of Civil Engineering*, 54 (2), 55 – 64.

Publication 7

Corbella, S. Stretch, D. 2012. Geotextile sand filled containers as coastal defence: South African experience, *Geotextiles and Geomembranes*, 35, 120 – 130, doi:10.1016/j.geotexmem.2012.09.004.

Submitted peer reviewed journal paper

Publication 8

Corbella, S. Stretch, D. 2012. Simulating a multivariate sea storm using Archimedean Copulas, *Coastal Engineering*.

Signed .....

Acknowledgements

A special thanks must be extended to the eThekwini Municipality, especially to Godfrey Vella, the manager of the Coastal Department, for accommodating the study. Thanks to Andrew Mather for all the assistance and to my supervisor Professor Derek Stretch for his infinite revisions to my unfathomable English.

Thank you to Andre Theron and Gerhardus Diedericks for the valuable suggestions and discussions. Thanks to Zane Thackeray and Rio Leuci of EMS for the advice and all round enthusiasm for the coastal zone.

Thanks to Transnet Port Authority for the wave data and to Clive Greyling for mediating the data requests.

Thanks to Ricardo Vieira for putting his own work aside to debug my Matlab scripts.

Special thanks to my family for patiently accommodating the completion of the study.
To my wife Kaydee who's sacrifices exceeded mine during this study, the achievement is as much hers as it is mine.

Abstract

In March 2007 the KwaZulu-Natal coastline was devastated by an extreme storm event. There is international concern that such events are associated with climate change. There is evidence of global changes in climate but there is still uncertainty as to whether they are anthropogenic or part of natural decadal (or longer) cycles. The increase in frequency and intensity of extreme storm events will impact on the sediment dynamics of coastlines and the associated risks need to be modelled and quantified so that they can be included in coastal planning and management.

Durban is a coastal city on the east coast of South Africa and has been used as a case study to identify trends in wave parameters and beach profile volumes. The correlation between profile erosion, waves and tides was explored using singular spectral analysis. The dependence between wave parameters was modelled using copulas. The decadal trends were introduced into these models using a non-stationary generalised extreme value distribution. Numerical models (SWAN, SBEACH, XBEACH) were used to transform the statistical model to near shore waves and estimate the associated erosion. The copula model was used to investigate the relationship between multivariate return periods and erosion return periods. Coastal defence options were reviewed and those appropriate for Durban were identified.

This study provides a review of Durban and Richards Bay's 18 years of Waverider data. It presents wave parameter exceedance statistics and wave height return periods for Durban. Durban's wave data showed increasing trends in maximum significant wave heights, peak wave period, storm event frequencies and a trend towards a more southerly

mean wave direction. However, only the increase in peak period and wave direction was statistically significant. The trend in wave direction is considered a potential coastal hazard as it has the potential to increase the littoral drift by 1 % per annum. Durban's beach profiles have shown a long term erosion trend which is due to a combination of wave and sea level trends, and a reduction in sediment supply. The reduction in sediment supply from rivers was found to be both anthropogenic and natural. Storm, wave parameter and sea level trends were estimated to contribute more than 75 % to the total long term erosion. It was found that it takes an average of 2 years for a beach to recover to its pre-storm volume. Different types of coastlines recover at different rates and these recovery rates should be considered in risk assessments. A method for estimating future impacts due to storm and sea level trends has been proposed in the form of a non-stationary copula based statistical model. In general a bivariate return period of wave height and duration was found to approximate erosion return periods, while a method for estimating an analogous multivariate storm and erosion return period was developed. Geotextile sand filled containers were found to be a suitable coastal defence as they satisfy social, environmental and political pressure.

“ The key to a successful research project is to have a wife and a mistress,
and ensure that both are aware of the others existence.
Then when you are not with your wife she thinks you are with your mistress,
and when you are not with your mistress she thinks you are with your wife.

That way you have more time for research”.

(Adapted from a popular mathematics joke)

Contents

List of Figures

List of Tables

Nomenclature

Roman Symbols

L_q^F	iso-hyper-surface	29
A	wave direction	22
C	a copula	23
D	storm duration	22
d	water depth	54
F	a distribution function	24
fp	peak energy frequency	53
g	gravitational acceleration	54
H	wave height	22
H_{max}	maximum wave height	53
Hs	significant wave height	53
I	storm inter-arrival time	22
K_C	Kendall's distribution function	30
L	wave length	54
m_0	area under the wave spectrum	53

Greek Symbols

Acronyms

Chapter 1

General introduction

1.1 The risks associated with wave and sea level trends

Chronic coastal erosion is becoming an international concern. Beaches provide a natural buffer zone between the hazards posed by coastal erosion and land-based human developments and play a primary role in risk mitigation. While chronic erosion may be induced by anthropogenic factors or natural cycles, a potential contributor to these erosion trends is an increase in wave height, storm duration and frequency and an increase in sea levels.

The erosion potential of a storm event is dependent on the wave height, wave period, wave direction, storm frequency, storm duration and water level. Therefore the quantification and or estimation of this risk needs to consider all these factors. Furthermore the quantification of the risk associated with a given sea state needs to be understood in terms of it's relative erosion potential. i.e A sea storm with a recurrence interval of 100 years may not be representative of an erosion event of a 100 year recurrence interval. These statistical models also need to include the trends in wave height and sea level which requires a non-stationary model.

The statistical model can then be quantified in terms of coastal erosion using numerical wave and morphological models.

1.2 Problem Definition

The risks associated with trends in sea conditions are intuitive. The problem is identifying these trends and estimating them in a mathematically consistent way while maintaining a link to the physical characteristics of the sea states.

1.2.1 Research Questions

The main research question of this thesis is:

Can the risks from extreme waves be characterised by simple measures such as a recurrence interval that accurately reflects the associated hazards to developed coastal zones?

This research question will be investigated in the context of a case study in the Durban area where it can be posed specifically as:

What is the return period of the waves experienced during the March 2007 storm event, and what are the lasting effects of these storms on the coastline?

This question can be divided into the following questions:

1. Is there evidence of trends in Durban's wave climate and sediment movement?
2. What are the current and potential future impacts of these trends?
3. What is the global recovery time of storm damaged beaches?
4. Can a sea storm be described as a non-ambiguous multivariate return period, representative of its erosion potential?
5. What are the most sustainable coastal defences?

1.2.2 Motivation

The March 2007 storm event exhibited the largest wave height ever recorded off the KwaZulu-Natal coast and saw Durban's coastline seriously damaged, opening the debate regarding its return period. In the presence of global climate change and sea level rise it is felt that wave heights are increasing and/or storms are becoming more frequent resulting in serious storms having shorter return periods. If so, design wave characteristics need to be reviewed and adjusted for coastal engineering applications, and for developing sustainable coastal protection and recovery processes. Considering controversial developments such as the Durban small craft harbour and Promenade Upgrade, limited scientific analysis was available to argue that the developments' close proximity to the shoreline would be unsustainable. Return periods in combination with beach recovery processes and periods are vital for Durban's local authority, the eThekwini Municipality's Coastal Management Plan. This thesis will aid the Municipality in defending their sustainability policies, setback lines and implementing effective coastal protection solutions.

1.2.3 Aims and objectives

Aims:

- To analyse historic wave data and sand movements to determine if there has been a shift in the wave climate.
- To analyse post storm beach profiles to determine a sand replenish rate and so a storm recovery period. To study the effects of the March 2007 storm and determine the effectiveness of coastline protection options for increasing severity of storm events.
- To use the analysed data to create a copula based multivariate statistical model for estimating future storm events.
- To estimate future potential erosion by coupling a statistical model with numerical process-based morphological models.

Objectives:

- To determine a multivariate return period for the March 2007 storm event
- To determine a recovery period of storm damaged beaches
- To determine if there has been a shift in the Durban wave climate
- To understand the risk associated with the probability of wave parameter occurrences
- To critically evaluate and recommend appropriate options for sustainable coastal protection

1.3 Approach

Durban is a coastal city on the east coast of South Africa and was used as the thesis' case study.

1.3.1 Case Study: Durban

Durban is located on the east coast of South Africa and is a coastal city of the province of KwaZulu-Natal (Fig. 1.1). The eThekwini Municipality is Durban's local government authority and its jurisdiction stretches from the Tongati River Mouth to the Mahlongwa River Mouth, nearly 100 km of coastline (Figure 1.2). In this thesis Durban will refer to the stretch of coastline governed by the eThekwini Municipality. Figure 1.3 defines the percentage of the Durban coastline as either sand, rock or a mixture of sand and rock. The sand, rock and mixture categories are further divided into developed and natural coasts. Developed coasts refers to areas where the backshore has been stabilised by infrastructure and natural coasts refer to beaches whose sediment dynamics are not influenced by infrastructure. The eThekwini coastline is made up of approximately 44 % of sandy beaches and 49 % of a mixture of sand and rock coasts. The remaining 7 % is rocky coastline. 45 % of the coast has been impacted by development. Figures 1.2a to 1.2d illustrate typical examples of four different coastlines as well as their locations.

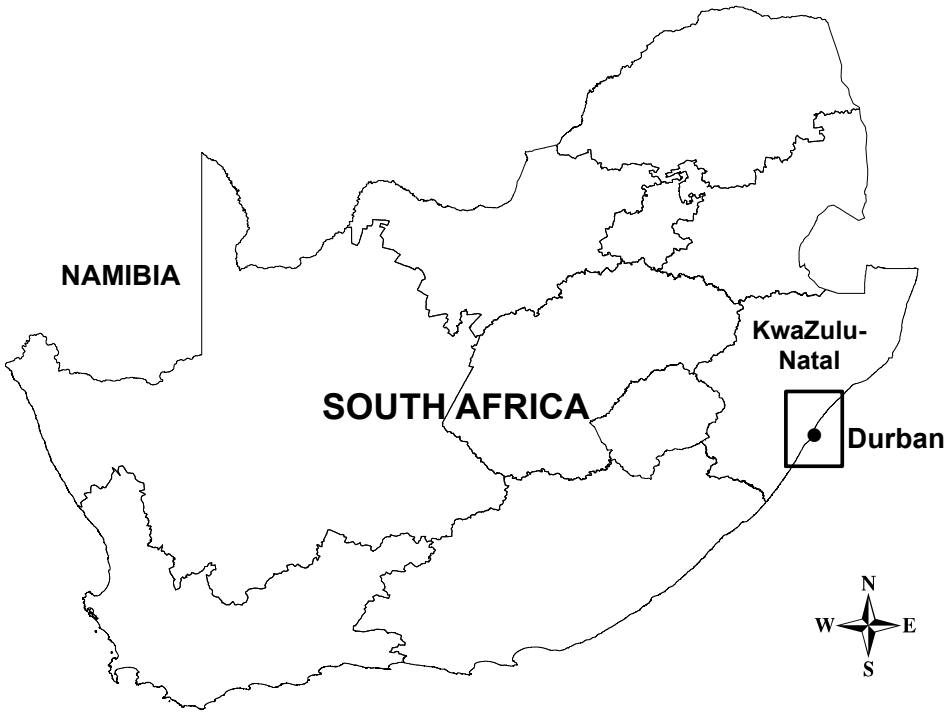

Figure 1.1: Map of South Africa showing KwaZulu-Natal and Durban

Durban has 18 years of wave data from 2 wave recording buoys and an acoustic doppler current profiler. This data was analysed for trends and used to create a statistical model. Richards Bay, a coastal city 170 km north of Durban, also has 18 years of wave data from a wave recording buoy and was used to verify and supplement the Durban data.

Durban has 37 years of beach profile data and this was used to identify erosion trends, recovery rates and recovery periods of storm damaged beaches.

Historical storm events and pre and post storm beach profile data was used to calibrate a SWAN and a 1D XBEACH model. The numerical models were used to quantify potential future erosion as well as to establish a method of determining physically appropriate sea storm return periods.

Durban's history of coastal defences was reviewed and compared to international practices. Experiences of successful shoreline protections were used to recommend a sustainable coastal defence.

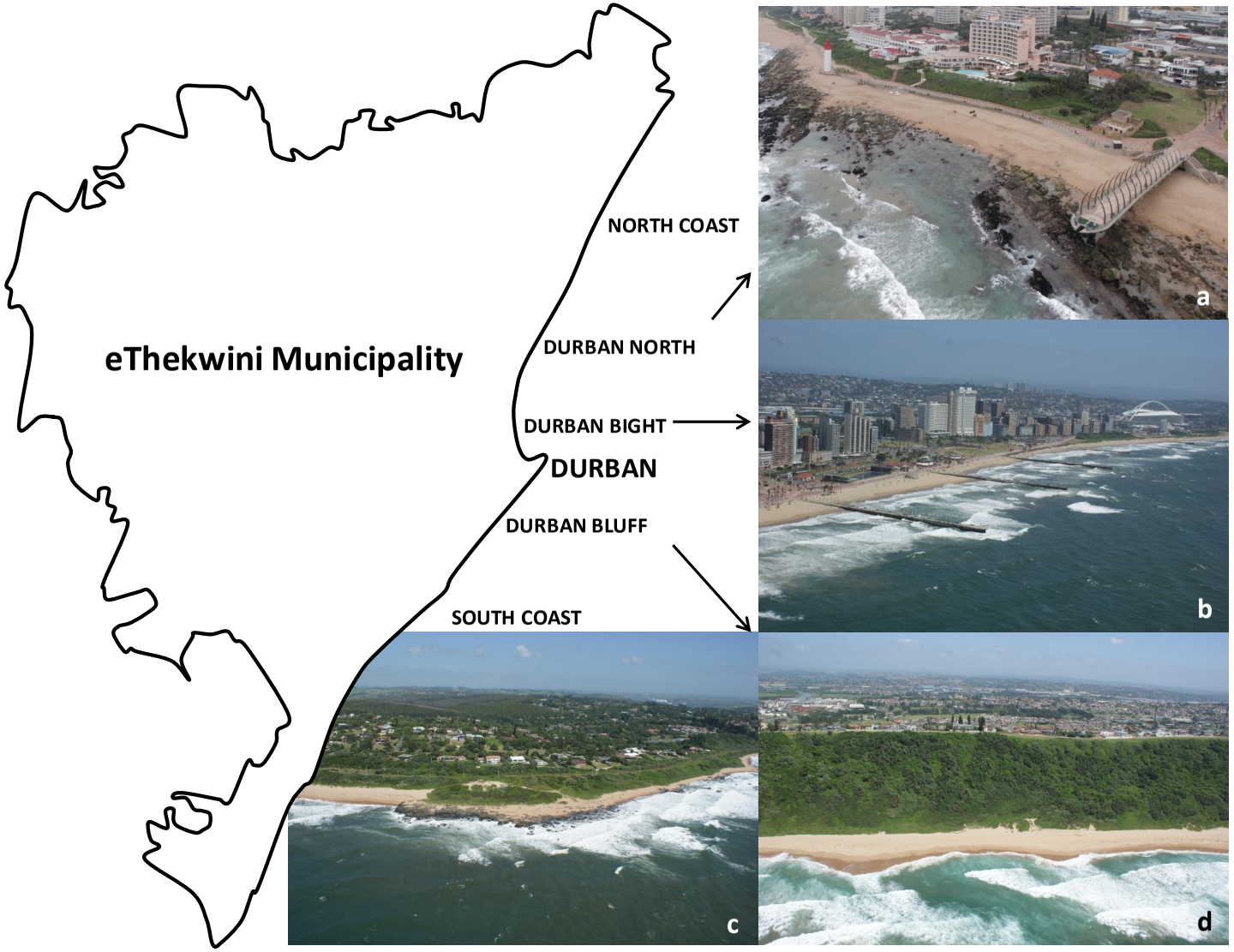

Figure 1.2: Map of the eThekwini Municipality showing typical locations of (a) mixed rock and sand developed coastlines, (b) sandy developed coastlines, (c) mixed rock and sand natural beaches and (d) natural sandy beaches

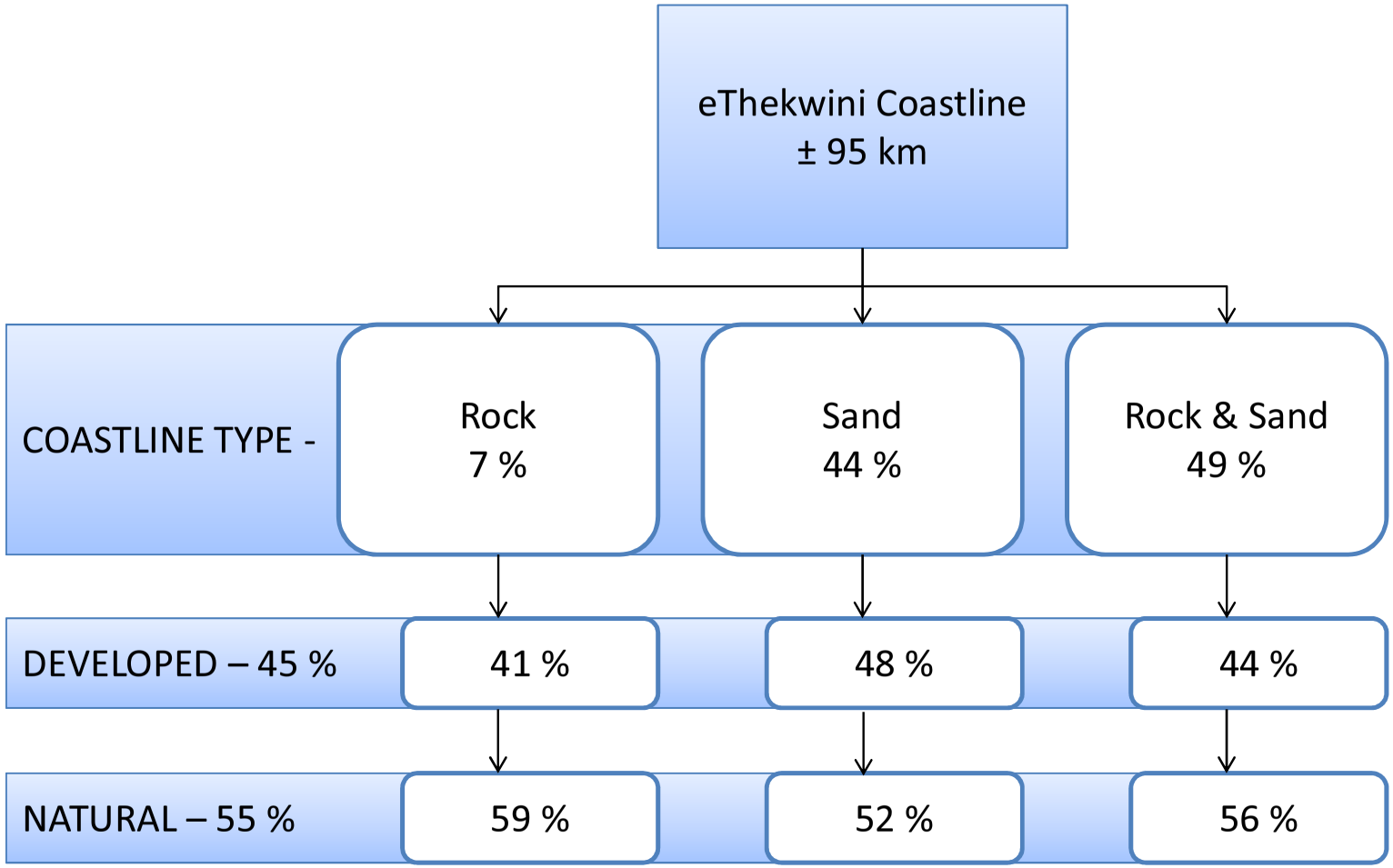

Figure 1.3: The estimated percentage of beach types along the eThekwini coastline

1.3.2 The 2007 storm event

The March 2007 storm event refers to the 19 – 20 March 2007 when the storm was most intense. The storm was a result of a "cut-off low" remaining trapped offshore for several days. The 40 knot winds blowing over a 450 km fetch produced a significant wave height of 8.5 m and a maximum wave height of 14 m. The highest astronomical tide of the year occurred on the 19 March 2007 almost at the peak of the 18.6 year Saros tidal cycle and only 2.4 cm below the highest astronomical tide. The 2.24 m above chart datum (CD) tide coincided with a peak storm setup of 40 cm to produce a total water level of 2.6 m CD. The combination of these two extreme events produced severe erosion on approximately 350 km of coastline. The wave heights were the largests ever recorded and only cyclone Imboa in February 1984 produced waves of a similar magnitude. A typical winter storm significant wave height ranges from 3.5 – 4.5 m.

1.3.3 Structure of the Thesis

This thesis begins with a literature review followed by eight chapters that are reproductions of papers. The papers follow a logical order and are explicitly linked. The key results of all the chapters are related in Chapter 11: Synthesis and conclusion. The Thesis is structured as follows:

Chapter 2 is a literature review of the main subject areas.

Chapter 3 is a review of Durban's existing wave data and a uni-variate analysis of the said data.

Chapter 4 determines the recovery rates and recovery periods of storm damaged beaches in Durban and relates the recoveries to physical processes.

Chapter 5 identifies erosion trends and their causative effects.

Chapter 6 discusses the use of copulas in constructing a statistical model of a sea state.

Chapter 7 uses the copula based statistical model with a non-stationary generalised extreme value model in conjunction with 3 morphological numerical models to quantify the impacts of future storm events on beach erosion.

Chapter 8 discusses the ambiguity of multivariate return periods and proposes a solution to the ambiguity problem.

Chapter 9 reviews Durban's shoreline defences and identifies their successes and failures.

Chapter 10 provides a detailed insight into the use of geotextiles as a coastal defence.

Chapter 11 relates the major results of the previous chapters, provides the conclusion and proposes future work in this field.

Chapter 2

Literature Review

2.1 Introduction

This section reviews literature that is relevant to the aims and objectives of this thesis. It initially looks at climate change (Sect. 2.2), wave climate trends (Sect. 2.3) and sea level trends and cycles (Sect. 2.4). These sections are to establish plausibility of a shift in wave climate along the east coast of South Africa.

Observations in morphological trends (Sect. 2.5) are investigated in an attempt to identify which factors and processes contribute to shoreline erosion and recovery after erosion events.

The literature review then focuses on methods that have been applied to achieve the thesis' objectives. The mathematical background of singular spectrum analysis (Sect. 2.6) is provided. This novel technique is used to identify trends in wave, wind, tide and beach profile data. Statistical modelling is used to produce univariate and multivariate recurrence intervals as well as simulate storm events based on parameter interdependence. Section 2.7 reviews statistical modelling methods in the context of copulas and Archimedean copulas.

Numerical modelling of coastal processes provide a means of quantifying the potential effects of trends in wave parameters and water levels. Section 2.9 provides motivation for the use of the numerical models in this thesis.

Finally a review of sustainable shoreline defences (Sect. 2.10) is provided.

2.2 Climate change

Climate changes have always occurred as a result of natural processes. There is also increasing evidence of human induced global warming due to increases in greenhouse gas emissions. This thesis focuses on the engineering and planning impacts of climate changes in the coastal zone. It is not concerned with the causes of climate change.

From the perspective of anthropogenic climate changes the following information is noteworthy. Annual carbon dioxide emissions grew by about 80 % between 1970 and 2004 and comprised 77 % of total anthropogenic greenhouse gas emissions in 2004 [IPCC, 2007]. Considering that coal fired power stations are economical and arguably a necessity for developing countries the use of coal is likely to remain an integral part of energy production. Institute of Mechanical Engineers [2009] suggest that the growth in greenhouse gas emissions is evidence that combating global warming will be politically delayed to such an extent that the impacts of climate change will already be affecting the global population.

From a perspective of natural cycles it is accepted that over the past two million years the earth has been subject to numerous glacial advances and retreats. These glaciations effect the sea level and are evidence of the existence of natural cycles in the absence of anthropogenic climate change.

In the context of coastal hazards, two important factors are a rise in sea level [Han *et al.*, 2010; Mather, 2008] and a change in wind regime [Rouault *et al.*, 2009, 2010]. The combination of increased sea levels and higher wind speeds has the potential to alter wave climates and produce significant storms more frequently.

Trends attributed to short data sets have the potential to be measures of natural variability rather than longterm systematic change. These issues of climate variabilty were highlighted in water level trends by Douglas [1992], in wave climate trends by WASA [1998] and in storm surge trends by Zhang *et al.* [2000]. These researchers have shown that over 50 years of data is required to define a coastal climate.

Even if coastal trends cannot be linked to anthropogenic climate change engineers still have to be prepared to design for natural climate cycles.

2.3 Trends in wave climates

The potential impacts of climate change need to be considered in formulating plans to mitigate future risks. Engineers worldwide are realising the potentially disastrous implications that climate change may have if design parameters are not adapted to a changing environment. Various global climate models have been used to predict these changes. In the northern hemisphere Wang & Swail [2001, 2002] and Wang *et al.* [2004a] found that between 1958 and 1997 changes did occur in winter and autumn significant wave heights. They also predicted future changes due to global warming. Wang *et al.* [2004b] found that in the past half century, the changes feature a significant increase in the number of strong winter and spring cyclones over the North Pacific sector, and of strong autumn and winter cyclones in the North Atlantic sector. Their findings also implied that the cyclone track may be shifting. The shift in cyclone track is significant as strong winds may become present in areas that do not have infrastructure to cater for such incidents. Perrie *et al.* [2004], focusing specifically on wave climate, found that wave heights in extreme events would slightly increase due to climate change while moderate events and low intensity storms seemed to experience little change. These results are consistent with those of Lambert [2004] and Knutson & Tuleya [2004] suggesting that intensities of the strongest storms should increase in a warmer climate. Analyses of a 45-year high resolution hindcast for the North Sea by Weisse & Stawarz [2004] showed that storm activity and extreme wave heights had increased from about 1960 onwards while the rate of increase reduced from about 1990 to 1995. Seymour [2002] analysed the recent history of El Nino events and found increases in the intensity, rate of occurrence and duration during the past two decades. Keim *et al.* [2004] concluded from their study of global climate models and empirical records that the past two decades have shown a decrease in the frequency of tropical storms but that there is a strong suggestion of an increase in the frequency of very strong (extreme) storms. Komar & Allan [2008], undertaking similar research to the present study, analysed 30 years of records from 3 wave data buoys in the Atlantic. They found from their analyses of the significant wave height histograms that there had been an increase in the number of occurrences of waves exceeding 3 m, those generated by

hurricanes, and in particular the most extreme significant wave heights recorded. It was concluded that these increases were a result of the increased intensity and occurrence of hurricanes produced from global climate changes. Although the literature shows no general agreement with regards to intensity they generally agree on two phenomena: the changing climate has the potential to produce storms in parts of the globe that do not traditionally experience that type of weather and that storms of high magnitude are occurring more often.

There is uncertainty to whether the documented trends are a result of anthropogenic climate change or are part of natural cycles [Ruggiero *et al.*, 2010].

2.4 Sea level trends

The prediction of sea levels is very important in coastal engineering for a multitude of reasons. The most important of these, in the context of this study, is the elevated damage a sea level can contribute to an impending storm. The basic variations in sea level are attributed to tidal cycles, storm surge and long term sea level rise. It is important to clarify the difference between global and relative sea level trends. Global sea level is the average height of all the world's oceans while relative sea level is a local sea level which varies temporally and spatially. The reader is refered to Pugh [1987] for a comprehensive overview on sea levels.

2.4.1 Astronomical tides

The astronomical tide is a long period wave that is generated by the gravitational pull of the moon and to a lesser extent by the sun. This makes the principal lunar tidal period 12.42 hours and the principal solar tidal period 12 hours [Sorensen, 2006]. Since lunar forces dominate, high and low tides progress by 0.84 hours (50.47 minutes).

The highest astronomical tide (HAT) is the maximum tidal height reached in an 18.6 year cycle of the precession of the moon's ascending node, also known as the Saros or nodal cycle. Extreme tides only occur at spring tides around full and new moons. Spring high tides will always peak in the period of spring and autumn.

Considering that tides are influenced by the gravitational pull of celestial bodies it is intuitive that extreme tides will occur when the sun and moon are inline as well as at the closest point to the earth. These closest points are known as the perigee for the moon and the perihelion for the sun. The moon and the sun should also have zero declination to create a maximum semidiurnal tide. The necessary condition to produce this maximum tide is simultaneous perihelion and zero declination which will only occur again in the year 6581 [Pugh, 1987].

In short there are 3 important high tide cycles: (1) the 18.6 year nodal cycle; (2) a 6 year cycle when the lunar perigee and zero lunar declination coincide and (3) the 4.5 year cycle when the lunar perigee coincides with either the March or September equinox.

2.4.2 Storm surge

If a storm has sufficient strength and the water body is shallow over a large enough area then the storm can generate large water level fluctuations [Sorensen, 2006]. Storm surge or meteorological tide is a result of: surface wind stress and the resulting bottom stress created by the generated currents; response to Coriolis acceleration; atmospheric horizontal pressure gradients; wind wave setup; long wave generation and precipitation and surface runoff.

Storm surge results in a water level increase above mean sea level that can become extremely significant if the surge coincides with high or spring tides [USACE, 2006; Sorensen, 2006; Woodroffe, 2003].

2.4.3 Sea level rise

Internationally much research has been done on the rate of sea level rise. Mather [2008] has initiated South African research into sea level rise and has found, from tide gauge recordings between 1970 and 2003, that sea level rise in Durban is 2.7 mm $\pm$ 0.05 mm per year at a 95 % level of confidence. This rise is comparable to that of the mid-Atlantic region from New York to North Carolina which ranged from a relative sea level rise of 2.4 mm to 4.4 mm per year, over the twentieth century [USEPA, 2009]. Recent studies have suggested that global sea-level may potentially rise a meter or more by the year 2100, and possibly several meters

within the next several centuries [USEPA, 2009]. The IPCC [2007] have predicted a somewhat less sensational worst case scenario of a 0.59 m rise by 2099. This estimate excludes accelerated ice discharges from Greenland and Antarctica and higher rates are possible.

2.5 Morphological trends

Morphological changes can be broadly thought of as anthropogenic and natural. In this thesis we are mostly concerned with erosion and recovery processes. Long term erosion of a coastline has three main contributors: sea level rise; wave climate and a reduction in sediment supply. Woodroffe [2003] identified waves as the principal energy source for erosion in the coastal zone, while Cowell *et al.* [2003a,b] estimated that sea level rise was the main cause of long-term erosion with waves causing variability. The recovery of storm damaged beaches is similarly dependent on waves, water levels and sediment supply.

2.5.1 Morphological effects of wave and sea level trends

Approximately 10 % of the world's population live near the coast and are highly vulnerable to storms and sea-level rise [Lichter *et al.*, 2011; McGranahan *et al.*, 2007]. Zhang *et al.* [2004] analysed the recovery of the U.S East Coast barrier beaches and found that the beaches recovered to their long term trend positions after storms regardless of storm severity. It was concluded that this finding strongly suggested that storm events are not responsible for long term coastal erosion. Zhang *et al.* [2004] stated that since no evidence has been given to show significant increases in storminess and since human interference is neither worldwide in extent nor uniform regionally, sea level rise is the most plausible contributor. It is worth noting that this statement may not consider sediment mining and river damming which is arguably a worldwide human interference and a contributor to long term coastal erosion.

Gratiot *et al.* [2008] showed that although tides have no long term effect on sea level trends they induce important fluctuations of the mean high water level. Gratiot *et al.* [2008] claimed that of the predicted 150 m of erosion along the

coast of the Guyanas between 2008 and 2015, 60 % would be attributed to the 18.6 year nodal cycle while the remaining 40 % would be a result of sea-level rise due to global change.

Dette & Raudkivi [2002] stated that the southern coastline of the practically tideless Baltic Sea has been retreating due to the locally rising sea level, at an estimated rate of 70 to 150 mm per century. Dette & Raudkivi [2002] claimed that this has led to erosion, narrow beaches and wave-cut dunes and cliffs.

2.5.2 The role of rivers in beach morphology

Rivers play an important role in sediment supply and have been estimated to supply 80 % of the global beach sediment [GESAMP, 1994]. Reduction in sediment yield from rivers may be natural and anthropogenic. River sediments are exported to the sea almost exclusively during large floods [Hsu *et al.*, 2004; Rovira *et al.*, 2005] and so steady erosion trends may exist between these episodic flood events. From a Durban perspective Cooper [2002] found that the Mgeni coastline had steadily eroded after 1931 but following a large flood in 1987 the shoreline accreted and continued to do so for at least another three years, re-establishing the shoreline further seaward than that of 1931.

Anthropogenic impact on fluvial yield has become a global concern and sediment mining and damming of rivers have been identified as significant impacts. Recent examples of related international research include Dai *et al.* [2008]; Dang *et al.* [2010]; Huang [2011]; Liquete *et al.* [2009]. In Durban the CSIR [2008] estimated that at least 400 000 m^3/annum are mined from the eThekwini rivers and that dams trap a third of the sediment that should reach the coastline. Anthropogenic reduction of sediment supply is therefore relevant to the case study site of this thesis.

2.5.3 Shoreline recovery from storm events

A storm event erodes a beach and reduces the natural buffer between the ocean and the hinterland. It is at this stage that an urbanized coastline is at risk of sustaining severe damage from a subsequent, possibly less extreme, storm event before it has fully recovered to its pre-storm level [Forbes *et al.*, 2004]. Recovery

times play an important role in the risk analysis of beaches as they describe a window of vulnerability. This considered there are not many publications on the recovery of beaches to their pre-storm positions [Morton *et al.*, 1994].

Choowong *et al.* [2009] found that the Bang Niang to Khuk Khak coastline of Phang-nga in Thailand after the 2004 Indian Ocean Tsunami took two years to recover, similarly Liew *et al.* [2010] found the Khao Lak coast in Sumatra took approximately two years to recover. Morton *et al.* [1995] found that the Texan coastline requires 4 to 5 years for volumetric and geomorphic beach recovery from moderate storm events. The consideration of geomorphic beach recoveries is thought to make the recovery periods identified by Morton *et al.* [1995] longer than those of Choowong *et al.* [2009] and Liew *et al.* [2010] who only considered volumetric recovery. A beach's recovery is dependent on its sediment supply and the severity of the erosion event in question [Houser *et al.*, 2008]. On steep coastlines the sediment that is transported offshore by undertow during an erosion event [Gracia *et al.*, 2002] is slowly worked back onshore under calm conditions [Shepard, 1950]. Depending on the severity of the event, the sediment may be carried sufficiently far offshore to prolong or even prevent its return [Forbes *et al.*, 2004]. Location is important for recovery, not only because of wave shoaling and refraction effects, but also because of the location of rivers (discussed in Sect. 2.5.2).

2.6 Singular spectrum analysis (SSA)

Numerous methods exist for analysis of time series (e.g ARAR algorithm, Box-Jenkins SARIMA models, Holt-Winter algorithm). Singular spectrum analysis (SSA) is a novel technique for analysing time series. SSA essentially decomposes a time series into the sum of its parts. From a coastal engineering perspective SSA can be used for (1) the identification of trends and (2) the extraction of seasonality components and cycles. The method has found application in numerous fields and recent examples include: short term load forecasting of electricity [Afshar & Bigdeli, 2011]; climatic variability [Ghil *et al.*, 2002]; exchange rates [Hassani, 2010] and rainfall and runoff forecasting [Sivapragasam *et al.*, 2001]. SSA has also found coastal applications and examples include the analysis of sea level [Mather,

2007; Jevrejeva, 2006], wave climate and shoreline trends [Rzynski, 2010].

Golyandina *et al.* [2001] and Hassani [2007] provide a good introduction to SSA. SSA can be broadly divided into two parts: (1) Decomposition and (2) Reconstruction.

The first step of decomposition is to embed the time series $Y_T = (y_1, ..., y_T)$ into a vector of dimension K. This is achieved by sliding a window length of L over the time series, making $K = T - L + 1$. The resulting trajectory matrix,

$$X = \begin{pmatrix} y_1 & y_2 & y_3 & \cdots & y_{K-1} \\ y_2 & y_3 & y_4 & \cdots & y_K \\ \vdots & \vdots & \vdots & \ddots & \vdots \\ y_{L-1} & y_L & y_{L+1} & \cdots & y_T \end{pmatrix},$$

is a Hankel matrix.

The next step is singular value decomposition (SVD) of the trajectory matrix. Let the eigenvalues of the $L \times L$ matrix XX' be λ_i. Where $i = 1, ..., L$ in decending order of magnitude. Denote the orthonormal system of eigenvectors corresponding to the eigenvalues as U_i. The eigenvector V_i can then be defined as $V_i = X'U_i/\sqrt{\lambda_i}$. Setting $d = rank(X)$ allows the trajectory matrix to be written as

$$X = X_1 + \ldots + X_d \tag{2.1}$$

$$X_i = s_i U_i V_i'. \tag{2.2}$$

Where s_i is the i^{th} singular value of X, and X_i $(i = 1, ..., d)$ are matrices of rank one.

The final step is reconstructing the time series. Firstly the matrices X_i are split into groups and summed within each group. Let I be a group of indices $i_1, ..., i_p$. The resultant matrix X_I is then defined as $X_I = X_{i1} + \ldots + X_{ip}$. The indices $J = 1, ..., d$ are grouped into m disjointed subsets $I_1, ..., I_m$. The trajectory matrix can then be represented as a sum of m resultant matrices

$$X = X_{I1} + \ldots + X_{Im} \tag{2.3}$$

The final step is diagonal averaging. This step transfers each matrix I into a component of the original time series Y_T. Diagonal averaging is perfomed by averaging the elements along diagonals $i + j = k + 2$. Diagonal averaging of the resultant matrix X_I produces a time series Y_n of length T. The orginal time series Y_T is therefore expressed as a decomposed time series

$$\tilde{Y} = Y_1 + \ldots + Y_m \tag{2.4}$$

2.7 Statistical modelling

In coastal engineering, compared to other areas of hydraulics, there are rarely long historical records of wave data. This shortage of data is a result of accurate and reliable wave recording data only being recently available and the expense and difficulty in operating and maintaining this equipment. Coastal management and development require return periods of storm events that can only be obtained through extrapolation of limited data sets. It should be noted that extrapolation of a data set based on a fitted probability distribution is limited. The rule of thumb is that a data set should not be extrapolated to more than 3 times the extent of the data set [Borgman *et al.*, 1977].

2.7.1 Univariate modelling

The average recurrence interval or return period of independent wave events can be estimated by fitting a theoretical probability distribution to the data and using it to extrapolate to the event of interest. There are many available probability distributions and the use of an appropriate one is important to accurately model the data and to realistically estimate the probability of rare events by extrapolation.

The literature identifies commonly used distributions but does not state which is preferred or superior. USACE [1985, 2006] recommends the guidelines of Isaacson & MacKenzie [1981] while providing guidelines for the Extremal Type I (Fisher Tippett I) distribution and also recommends Fisher Tippett II. Isaacson

& MacKenzie [1981] provide guidelines for the Lognormal, Extremal Type I and II and the Weibull distribution. Chadwick *et al.* [2004] noted that the Department of Energy recommends using the Gumbel, Fisher Tippett I or the Extremal value type I distribution. Goda [2008] provides guidelines for the use of the Fisher-Tippett I, Fisher-Tippett II, Weibull and Lognormal distributions. The Generalised Extreme Value distribution (GEV) encompasses the Fisher-Tippet distributions and the Extreme Value distribution is equivalent to the Gumbel distribution. The GEV distribution has been used extensively for extreme value analysis of hydrological events and specifically for wave heights by Guedes Soares & Scotto [2004] and Chini *et al.* [2010] while the Generalised Pareto (GP) distribution has been used by Callaghan *et al.* [2008] and Hawkes *et al.* [2002]. Ruggiero *et al.* [2010] considered both the GP and GEV distributions. Considering the above sources the: Weibull, Lognormal, Generalised Pareto, Extreme Value and the Generalised Extreme Value distributions are defined as follows,

$$\text{Weibull} \quad y = k^{-k} x^{k-1} e^{-(\frac{x}{\sigma})^k} \quad :0 \leq x < \infty \tag{2.5}$$

$$\text{Extreme value} \quad y = \sigma^{-1} e^{-\left(\frac{(x-\mu)}{\sigma}\right)^k} e^{-e\left(\frac{(x-\mu)}{\sigma}\right)} \quad :-\infty < x < \infty \tag{2.6}$$

$$\text{Lognormal} \quad y = \frac{1}{x\sigma\sqrt{2\pi}} e^{\frac{-(\ln x-\mu)^2}{2\sigma^2}} \quad :0 < x < \text{inf} \tag{2.7}$$

$$\text{GEV} \quad y = \sigma^{-1} e^{-\left(1+k\frac{x-\mu}{\sigma}\right)^{-\frac{1}{k}}} \left(1 + k\frac{x-\mu}{\sigma}\right)^{-1-\frac{1}{k}} \quad :-\infty < x < \infty \tag{2.8}$$

$$\text{GP} \quad y = \frac{1}{\sigma}\left(1 + k\frac{x-\theta}{\sigma}\right)^{-1-\frac{1}{k}} \quad :\theta < x, \quad \begin{array}{l} for\ k > 0 \\ \theta < x < -\sigma/k, \\ for\ k < 0 \end{array} \tag{2.9}$$

where μ is the location parameter, σ is the scale parameter, k is the shape parameter.

The fitting of these distributions requires the sampling of extreme events. The sampling of data needs to ensure the independence of consecutive storms and the simplest sampling method is the annual maximum method which fits a probability distribution to the annual maxima wave heights. This immediately solves some

problems by avoiding correlation among successive data, and by ensuring that the maximum values are not influenced by the mix of sea states of a different nature at lower probability levels [Guedes Soares & Scotto, 2004].

The use of this method requires at least 20 years of data [USACE, 2006]. The inherent problem with this method is that the quantity of data is limited often necessitating the use of the peak over threshold method. The peak over theshold method samples all events exceeding a specific threshold. Unlike the annual maximum method the peak over threshold method allows more than one event per year to be sampled and is therefore commonly used for analysing short data sets. The threshold is generally chosen so that the number of data values in the series is 1 – 3 times the number of recorded years [USACE, 2006].

The maximum likelihood method is probably the most popular parameter estimation method. The method maximises the probability of observing the data set that has been observed in the sample. This intuitive method has been referred to as the most popular and best technique for deriving estimators [Casella & Berger, 1990; Montgomery & Runger, 2003]. The maximum likelihood method is popular with statisticians as its characteristics can be examined mathematically [Goda, 2008].

2.7.2 Multivariate modelling

Univariate models are not approriate to describe a sea storm as it's rarity and destructivity is a function of it's wave height (H), wave period (T), storm duration (D), wave direction (A), water level (W) and storm inter-arrival time (I). With specific reference to coastal erosion the larger the wave height, storm duration and water level the greater the erosion. The contribution of wave period to erosion is less intuitive and van Gent *et al.* [2008] and van Thiel de Vries *et al.* [2008] found that an increase in wave period lead to an increase in erosion. The wave angle is not only important from a long shore and cross shore current perspective but also in terms of beach orientation. For example a beach sheltered in a given direction from a 100 year recurrence interval wave height may experience less erosion than a 50 year wave height from its exposed direction. The inter-arrival time is very similar to the storm duration. If the inter-arrival time between two consecutive

storms is short the beach will not have sufficent time to recover and so will be eroding from a lower level. In a sense a short inter-arrival time is similar to increasing the storm duration of a single event.
In order to provide an appropriate statistical model the inter-dependence between all these parameters needs to be considered. Numerous models exist for bivariate relationships but few of them are easily transformed into higher dimensions. Examples of bivariate models include the Gumbel logistic model [Yue, 2001]; the Gumbel mixed model [Yue *et al.*, 1999] and the log-normal model [Galiatsatou & Prinos, 2008]. A recent and novel approach to multivariate statistical modelling is the use of copulas. Copulas are not restricted to Gumbel marginals and so have greater flexibility. Copulas can also be used in higher dimensions and will make up the statistical model in this study.

2.8 Copulas

Copulas are, very basically, mathematical "functions that join or couple multivariate distribution functions to their one-dimensional marginal distribution functions" [Nelsen, 2006]. For a good introduction to copulas see Nelsen [2006] or De Michele *et al.* [2007] from which the following copula outline is drawn. Copulas may have n dimensions but we will first describe the concept of copulas in only 2 dimensions, in an attempt to simplify the explanation.

A 2 dimensional copula or 2-copula is a mathematical function that maps a bivariate probability distribution $H(x, y)$ onto the unit square I^2, using the marginal cumulative distribution functions $u = F(x)$ and $v = G(y)$ as coordinates (u, v). The unit square is the product $I \times I$ where $I = [0, 1]$. Figure 2.1 illustrates the concept of a 2-copula.

Before a n-copula can be formally defined the following notation is required. Let R denote the ordinary real line $(-\infty, \infty)$. We write $x < y$ when $x_i < y_i$ for all i. For $x < y$, the n-box $B = [x_1, y_1] \times \ldots \times [x_d, y_d]$ is denoted by $[x, y]$. The vertices of an n-box B are the points $c = (c_1, c_2, \ldots, c_n)$ where each c_i is equal to either x_i or y_i. A real function H is a function whose domain, $DomH$, is a subset of R^n, and whose range, $RanH$, is a subset of R. Let $B = [x, y]$ be an n-box all of whose vertices are in $DomH$. The H-volume of B can then be defined as

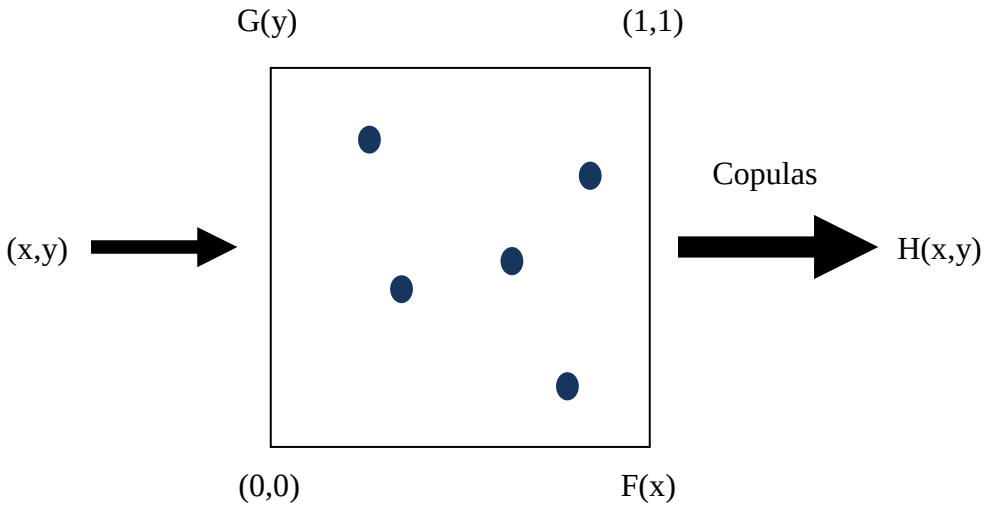

Figure 2.1: An illustration of how copulas are used to create multivariate distributions $H(x, y)$ from variables x and y and their marginal cumulative distributions $F(x)$ and $G(y)$.

$$V_H(B) = \sum sgn(c)H(c) \tag{2.10}$$

where the sum is taken over all vertices c of B, and $sgn(c)$ is given by

$$sgn(c) = \begin{cases} 1, & \text{if } c_i = x_i \text{ for an even number of } i's. \\ -1, & \text{if } c_i = x_i \text{ for an odd number of } i's. \end{cases} \tag{2.11}$$

A n-copula can now be formally defined as a function $C : I^n \to I$ such that:

1. For all $u \in I^n$, $C(u) = 0$ if at least one coordinate of u is 0, and $C(u) = u_i$, if all coordinates of u are 1 except u_i (uniform marginals);

2. For all $x, y \in I^n$ such that $x \leq y$,$V_C([x, y]) \geq 0$ (n-increasing)

Sklar's theorem [Sklar, 1959] provides a link between n-copulas and multivariate distributions.

Sklar's Theorem:
Let H be a multivariate distribution function with marginals $F_1, \ldots, F_n$. Then

there exists a n-copula C such that for all $x \in R^n$,

$$H(x_1, \ldots, x_n) = C(F_1(x_1), \ldots, F_n(x_n)) \tag{2.12}$$

If $F_1, \ldots, F_n$ are all continuous, then C is unique; otherwise C is uniquely defined on $Ran(F_1) \times \ldots \times Ran(F_n)$. Conversely if C is a n-copula and $F_1, \ldots, F_n$ are distribution functions, then the function H given by Eqn. 2.12 is a n-dimensional distribution function with marginals $F_1, \ldots, F_n$.

2.8.1 Archimedean Copulas

Archimedean copulas are a special class of copulas. They have been used in a wide range of applications because of their properties that make them easy to construct [Nelsen, 2006].

An Archimedean copula C is the solution of the functional equation

$$\varphi(C(u, v)) = \varphi(u) + \varphi(v) \tag{2.13}$$

where u and v are marginal distribution functions (u, v) and the generator function $\varphi : I \to [0, \infty]$ is a continuous, convex, strictly decreasing function such that $\varphi(1) = 0$. An example of an Archimedean copula is the Clayton copula (for an extensive list of Archimedean copulas see Nelsen [2006]). The Clayton generating function is

$$\varphi = \frac{1}{\theta}(t^\theta - 1) \tag{2.14}$$

where θ is the dependence parameter and $t \in I$. Kendall's tau τ_K is the sample version of the measure of association defined in terms of concordance, namely

$$\tau_K = \frac{(c - d)}{(c + d)} \tag{2.15}$$

where c is the number of concordant pairs and d is the number of discordant pairs. A valuable property of Archimedean copulas is that τ_K can be expressed as a function of the generator:

$$\tau_K = 1 + 4\int_0^1 \frac{\varphi(t)}{\varphi'(t)}dt \tag{2.16}$$

The dependence parameter θ can be found from the above expression using Kendall's tau.

2.8.2 Constructing multivariate Archimedean copulas

A 2-copula cannot simply be used to 'couple' another $(n-1)$-copula with a variate by setting them as its marginal distributions. For example

$$C^n(u_1, u_2, \ldots, u_n) = C(C^{n-1}(u_1, u_2, \ldots, u_{n-1}), u_n) \tag{2.17}$$

This technique often fails and is referred to as the compatibility problem [Nelsen, 2006]. The literature does however offer various techniques to create multivariate distributions from copulas. Some of these techniques are presented below.

Chakak & Koehler [1995] present one of the simplest ways of forming a 3-copula.

$$C_{XYZ}(u, v, w) = wC_{XY}\left(\frac{C_{XZ}(u, w)}{w}, \frac{C_{YZ}(v, w)}{w}\right) \tag{2.18}$$

where $u, v, w \in [0, 1]$. Application of Eqn. 2.18 is appealing because of its simple form and the fact that all the dependence parameters are available from the corresponding 2-copulas. However the resulting 3-copula is not uniquely determined and is dependent on the order the copulas are combined; there is no guarantee that

$$wC_{XY}\left(\frac{C_{XZ}(u, w)}{w}, \frac{C_{YZ}(v, w)}{w}\right) = vC_{XZ}\left(\frac{C_{XY}(u, v)}{v}, \frac{C_{YZ}(v, w)}{v}\right) \tag{2.19}$$

The conditional mixtures approach was used by Salvadori *et al.* [2007], Joe [1997] and De Michele *et al.* [2007] to combine two 2-copulas to form a 3-copula, combining F_{XY} and F_{YZ} to obtain F_{XYZ}. In this case the three dimensional distribution can be obtained from the conditional distributions by

$$F_{XYZ}(x,y,z) = \int_{-\infty}^{y} C_{XY}\left(F_{(X|Y)}(x|t), F_{(Z|Y)}(z|t)\right) F_Y(dt) \tag{2.20}$$

where $F_{(X|Y)}$,$F_{(Z|Y)}$ are the conditional distributions and can be found from the fitted two copulas

$$F_{(X|Y)}(x|y) = P(X \leq x|Y = y) = Q(F_X(x), F_Y(y)) \tag{2.21}$$

where $Q(a,b) = \partial_b C_{XY}(a,b) = \partial C_{XY}(a,b)/\partial b$.

A similar expression exists for $F_{(Z|Y)}$. Note that C_{XZ} is basically a measure of conditional dependence between X and Z, given the behaviour of Y. Generally an analytic solution of the integrals cannot be found and a numerical method has to be employed.

Other methods considered have mainly been used in financial modelling. They are the fully nested and partially nested methods suggested in Joe [1997] and presented by Savu & Trede [2006] as a joint distribution of asset returns. The method was also applied by Grimaldi & Serinaldi [2006], Nelsen [2006], Whelan [2004] and Embrechts *et al.* [2001]. The term used is 'hierarchical Archimedean copulas' which is a copula that joins two or more bivariate or higher order copulas by another Archimedean copula. The construction of a multi-level hierarchical Archimedean copula is conceptually simple but computationally and notationally challenging [Savu & Trede, 2006]. To make the notation slightly less confusing the operation " $\circ$ " is used to indicate the composition of functions such that $\varphi_{n-1} \circ \varphi_{n-2}^{-1}(y) = \varphi_{n-1}(\varphi_{n-2}^{-1}(y))$. The n-dimensional copula for the fully nested case requires $(n-1)$ generators, $\varphi_1, \ldots, \varphi_{1-n}$,

$$\begin{aligned} C(u_1,\ldots,u_n) =& \varphi_{n-1}^{-1}\left(\varphi_{n-1} \circ \varphi_{n-2}^{-1}\left[\ldots(\varphi_2 \circ \varphi_1^{-1}\left[\varphi_1(u_1) + \varphi_1(u_2)\right]\right.\right. \\ &\left.\left. + \varphi_2(u_3)) + \ldots + \varphi_{n-1}(u_{n-1})\right] + \varphi_{n-1}(u_n)\right) \end{aligned} \tag{2.22}$$

The partially nested method is more flexible than the fully nested [Savu & Trede, 2006]. It is however not possible to create a 3-copula as the lowest dimension is $n = 4$.

$$C(u_1,\ldots,u_4) = \varphi^{-1}\left(\varphi \circ \varphi_{12}^{-1}\left[\varphi_{12}(u_1)+\varphi_{12}(u_2)\right] + \varphi \circ \varphi_{34}^{-1}\left[\varphi_{34}(u_3)+\varphi_{34}(u_4)\right]\right) \tag{2.23}$$

with three generators φ, φ_{12} and φ_{34}. The conditions required for nesting are satisfied if $\theta < \theta_{12}$ and $\theta < \theta_{34}$ [Grimaldi & Serinaldi, 2006; Hofert, 2008, 2011; Savu & Trede, 2006]. Only the random variates U_1 and U_2 along with U_3 and U_4 are exchangeable. The major modelling limitation is that the joint distribution of (U_1, U_3) is equal to the joint distributions of (U_2, U_3), (U_1, U_4) and (U_2, U_4). This is not general enough for modelling a sea state and needs to be considered if the method is used for that application. The fully nested method provides a better model in this regard as in the $n = 4$ dimension, only (U_4, U_1), (U_4, U_2) and (U_4, U_3) will have the same joint distribution. Generally there are $n(n-1)/2$ (the number of bivariate marginals) ways to couple n variables and since there are only $n-1$ generators only part of all possible mutual dependences will be uniquely modeled.

The partially nested method has the benefit of producing a 4-copula from only two 2-copulas but is unable to produce a 3-copula. Three 2-copulas are required to create a 3-copula via the conditional mixtures approach (Eqn. 2.20) and by the Chakak & Koehler [1995] method (Eqn. 2.18). Equation 2.20 is likely to provide the most complete model as it allows all the dependencies to be modelled by different copulas.

2.8.3 Simulation

The aim of a simulation is to generate a vector $(U_1, \ldots, U_n)$ whose variables are interdependent and lie in the interval $[0, 1]$. Let their joint distribution be a copula $C = C(u_1, \ldots, u_n)$. A sample from C can be simulated by the conditional inversion method [De Michele *et al.*, 2007; Nelsen, 2006; Savu & Trede, 2006, 2010]. In general a sample u_n can be simulated from U_n based on the conditional law of U_n given the values $U_1, \ldots, U_{n-1}$.

$$C_n(u_n|u_1,\ldots,u_{n-1}) = P(U_n \leq u_n|U_1 = u_1\ldots,U_{n-1} = u_{n-1}) = \frac{\partial_{u_1,\ldots,u_{n-1}} C(u_1,\ldots,u_n,1,\ldots,1)}{\partial_{u_1,\ldots,u_{n-1}} C(u_1,\ldots,u_{n-1},1,\ldots,1)} \tag{2.24}$$

for $n = 2,\ldots,d$. The conditional law C_n can then be used in the following algorithm to generate u_n:

1. Simulate d independent random variables $t_1,\ldots,t_d$ on I.
2. Set $t_1 = u_1$
3. For $n = 2,\ldots,d$, evaluate the inverse of the conditional distribution function to generate $u_n = C_n^{-1}(t_n|u_1,\ldots,u_{n-1})$

Evaluation of the inverse conditional distribution becomes increasingly complicated as more variates are included in the model and can usually only be solved numerically. Other simulation algorithms have been proposed and examples of these can be found in Chebana & Ouarda [2011], Chakak & Koehler [1995], Whelan [2004] and Embrechts *et al.* [2001].

2.8.4 Multivariate return periods

A return period or average recurrence interval T_R is the average time (usually expressed in years) between the realisations of two successive events. It is common practice to use return periods to define a design event. Goda [2008] and Salvadori [2004] define a return period for a partial duration series as

$$\tau = \frac{\mu}{1-p}, \tag{2.25}$$

where μ is the average interval between events and p is the probability of non-exceedance. A multivariate return period can be described in numerous ways depending on the required combination of probabilities. Salvadori [2004] details

the probabilities of possible variate combinations in the bivariate case. The probability of u or v being exceeded can be expressed as

$$\rho_{u,\check{v}} = 1 - C(u, v) \tag{2.26}$$

and the probability of u and v being exceeded simultaneously can be expressed as

$$\rho_{u,\hat{v}} = \hat{C}(1 - u, 1 - v), \tag{2.27}$$

where $\hat{C}(u, v)$ is the survival copula defined by Salvadori [2004] and Nelsen [2006] as

$$\hat{C}(u, v) = u + v - 1 + C(1 - u, 1 - v). \tag{2.28}$$

Substituting these probabilities into the denominator of Eqn. 2.25 will produce the associated return period.

A multivariate return period is inherently ambiguous because different combinations of probabilities may produce the same return period. These events that have an equal probability of occurence are called iso-hyper-surfaces or critical layers L_q^F for a critical level q. Salvadori *et al.* [2011] expressed a critical layer as

$$L_q^F = \left\{ x^d : F(x) = q \right\}, \tag{2.29}$$

where F is a d-dimensional distribution $F = C(F_1, ..., F_d)$ and $q \in$ (0,1). This definition provides 3 probability regions:

1. the sub-critical region $R_q^<$ which encompasses all the points that are less than the critical layer L_q^F;

2. the critical layer L_q^F where the points equal the constant value q;

3. and the super-critical $R_q^>$ region which encompasses all the points that exceed L_q^F.

Salvadori *et al.* [2011] propose using the Kendall's distribution function K_C [Genest *et al.*, 2001] to define multivariate return periods. $K_C(q)$ is a measure of the

probability of a multivariate copula C being less than or equal to a critical level q. An estimate of Kendall's distribution function may be expressed as

$$\hat{K}_C(q) = \frac{1}{m} \sum_{i=1}^{m} 1(C(u_i) \leq q). \tag{2.30}$$

The corresponding multivariate return period can then be expressed as

$$T_x = \frac{\mu}{1 - K_C(q)}, \tag{2.31}$$

where μ is defined in Eqn. 2.25. Although work has been performed on multivariate return periods and multivariate quantiles, it has been limited to bivariate return periods [Chebana & Ouarda, 2011; Belzunce *et al.*, 2007]. Only Salvadori *et al.* [2011] provide a detailed methodology for describing higher order return periods. Expressing multivariate return periods in terms of K_C is currently the best technique.

2.9 Numerical modelling

Numerical modelling is an integral part of all engineering. Modelling of coastal processes can be divided into 4 parts: waves, flow, morphology and water quality. In this thesis we are essentially interested in morphology driven by flow which is governed by waves (including tide). Morphology is linked to long-shore or cross-shore sediment movements. Since erosion due to storms is dominated by cross-shore processes we limit the review to cross-shore models.

2.9.1 Spectral wave models

There are numerous spectral wave models. Arguably the most popular are SWAN (Simulating WAves Nearshore) [Booij *et al.*, 1999] and Mike 21 [DHI, 2005]. Strauss *et al.* [2007] showed that both models produced similar results. Generally the SWAN model is preferred as the model and source code are freely available. SWAN solves the spectral action balance equation. The spectral action balance equation encompasses the effects of spatial propagation, refraction, shoaling,

generation, dissipation and nonlinear wave-wave interactions [The SWAN Team, 2008]. Offshore boundary conditions for the SWAN model are usually produced by the Wavewatch III model [Tolman, 2009].

2.9.2 Cross-shore beach response models

There are numerous numerical models available for estimating cross-shore erosion [Schoonees & Theron, 1995]. Schoonees & Theron [1995] concluded from their evaluation of 10 cross-shore models that it was not possible to determine which models are superior. The Bailard model [Bailard, 1981] was determined to be amongst the models having the best theoretical basis as well as being substantially validated. The other two models that have received extensive validation are the Kriebel and Dean Time Convolution model [Kriebel & Dean, 1993] and SBEACH [Larson *et al.*, 1990].

Although SBEACH has been found to under estimate erosion [Seymour *et al.*, 2005; Zheng & Dean, 1997], it generally provides reasonable predictions [Schoonees & Theron, 1995; Zheng & Dean, 1997].

The Convolution model was not intended to accurately reproduce erosion processes but provide a fast and easy estimate of profile retreat [Kriebel & Dean, 1993]. It has recently been applied by Callaghan *et al.* [2008].

Schoonees & Theron [1995] evaluation did not include the relatively new XBEACH model. XBEACH is a public-domain model which is still under development. Although XBEACH has not been verified to the extent of the SBEACH and the Convolution model it has been used in numerous recent studies that have shown it's results to be satisfactory (examples include Hartanto *et al.* [2011]; Roelvink *et al.* [2009]). The Bruun Rule [Bruun, 1962] is also a cross-shore model and provides a simple relationship between sea level rise and profile retreat. The Bruun Rule has no consideration of wave heights and is widely applied because of its simplicity.

2.10 Shoreline defence

There are numerous shoreline defences that have been implemented throughout the world. There has been a global trend away from "hard" defences or those defences that interrupt the dynamics of a coastline and are unsustainable. Examples of "hard" defences are: groynes; rock revetments and sea walls. This review is limited to defences that the author deems the most sustainable. Namely: Beach nourishment and geotextile sand filled containers (GSCs). Natural defences such as vegetated dune systems are also precluded from the review.

2.10.1 Beach nourishment

Beach nourishment is the supply of sand to beaches usually from offshore dredging and is an environmentally preferred method of shore protection [Belkessa *et al.*, 2008]. This technique is used worldwide usually in combination with a shoreline stabilisation technique. Europe and the United States of America have adopted beach nourishment as central to their soft engineering strategy [Hamm *et al.*, 2002; Hanson *et al.*, 2002; Dean, 2003]. The additional sediment on the beach essentially shifts the wave run-up further away from inland infrastructure creating a buffer.

To protect dunes from erosion the dry beach has to be flat and wide enough to approximate to the Bruun-type equilibrium profile at the raised water level [Dette & Raudkivi, 2002]. This is usually ensured by numerical modelling or historical beach profiles.

2.10.2 Geotextile sand filled containers

The use of GSCs was initiated in the USA, the Netherlands and in Germany more than 50 years ago [Saathoff *et al.*, 2007]. The application of GSCs can be divided into the following 3 broad categories: (1) Geotextile sand bags; (2) geotextile tubes and (3) geotextile wraps.

GSCs are often spoken of as a soft engineering solution. This is not entirely correct because a soft solution is one that does not impede the natural morphology of the coast. The GSCs prevent erosion and so can develop a static shoreline.

They are considered a soft solution because if an unforeseen environmental impact ensues they can easily be sliced open and removed spilling sand back onto the beach.

Allan & Komar [2002] observed the effectiveness of an artificial dune for shore protection by surveying a dune constructed with sand-filled geotextile bags covered by loose sand and dune vegetation from 1999 to 2002. They reported that the dune survived fairly extreme conditions which included overtopping, but noted that it remained to be seen if it would cope with the expected more severe storms. GSC revetments at Jumaira Beach, Dubai, UAE had similar success [Saathoff *et al.*, 2007]. Heerten *et al.* [2008] found that securing the bags to each other with a Velcro strip significantly increased their stability and verified this stating that Oumeraci *et al.* [2003] claimed similar results.

Heerten *et al.* [2008] reported extensive research into the effectiveness of GSCs for mitigating coastal erosion. They described the successful use of GSCs on the island Sylt in Germany where geotextile cushions were covered with sand and sand trap fences. Although the GSCs was exposed after a large storm they prevented the high tide levels (2.5 m above normal) and large waves (exceeding 5 m) from eroding the dune.

Hornsey *et al.* [2011] and Restall *et al.* [2002] described the successes of GSC revetments at Stockton and Maroochydore beaches in Australia where they have been in place since 1996 and 2001 respectively.

Recio & Oumeraci [2008] also did extensive research on geotextile bags. Through rigorous model testing they were able to consider all the forces acting on the containers as well as the effects of container deformation. The impact of wave action and submergence causes sand to be moved inside the bag from the back to the exposed face. This movement has two negative effects. It decreases the contact area between bags thus reducing the friction forces and it increase the surface area in the front of the bag making it more susceptible to drag forces. Heerten *et al.* [2008] noted in their model testing that bags constituting the crest failed before those making up the slope. They found that the crest had an obvious dependence on the freeboard and so developed two separate stability formulae.

The advantages of geotextile sand bags include being cost effective and easily transported, which makes them ideal for emergency work. Their major disadvan-

tage is also one of its desirable attributes. The material can be easily cut and removed if it is required but at the same time permanent containers are susceptible to vandalism. This issue has been combatted by a composite vandal-deterrent geotextile which traps 3 kg of sand per square meter within the geotextile. This significantly increases the resilience and durability of the container [Saathoff *et al.*, 2007].

Geotextile tubes are several meters in length with a diameter exceeding 1 m. They have been particularly successful in the construction of artificial reefs as well as in other applications [Alvarez *et al.*, 2007; Cantr *et al.*, 2002; Shin & Oh, 2007].

A geotextile wrap is essentially a geotextile blanket that is covered with sand and wrapped back onto itself creating insitu sand tubes. The geotextile wrap is usually only considered as an alternative to sand bags and tubes when there are cost and access restriction for construction machinery. Wraps have been shown to be a realiable alternative to geotextile sand bag defences [Yasuhara & Recio-Molina , 2007].

2.11 Literature review conclusion

Climate change and variability, be it anthropogenic or natural, is becoming an increasing concern as people and nations begin to realise that these trends have far reaching effects on our everyday lives. Sea level rise and shifts in global wave climates are trends that have been associated with climate change.

There is general consensus within the greater scientific community that sea levels are currently rising and weather conditions are changing. Both of which, have a significant influence on wave behaviour. A higher sea level means waves can penetrate further inland with higher energy capable of increased erosion. The change in weather conditions is characterised by an increased frequency of high magnitude events with associated high waves and storm surge. Although no firm conclusions can be drawn from the literature about the changes in the intensity of storms there is enough evidence to conclude that the increase in sea level and an altered wave climate will impact internationally on coastlines and mitigating measures are required.

There is a need to estimate and minimise the risks associated with coastlines. Singular spectrum analysis provides a means of identifying trends and periodicity within wave and water level time series. The use of copula based statistical models is an appropriate risk management and design tool for coastal engineering. They allow more flexibility in statistical modelling than the common bivariate distributions like the Gumbel logistic model. Archimedean copulas are a class of copulas that can be expressed in terms of a generating function and Kendall's tau. Kendall's tau is a non-parametric correlation easily determined from empirical data. Multivariate copulas can be created to model various wave parameters and to define multivariate return periods. However, the construction of multivariate copulas is complicated and the legitimacy of these functions is still debated. Regardless, the literature presents various methods for constructing multivariate copulas, the easiest of which, in the author's opinion, is the partially nested method.

Once trends in waves and water levels have been identified using singular spectrum analysis and statistically modelled the implications of these trends need to be quantified. Numerical modelling is widely used to investigate coastal processes. The open source SWAN model is probably the most commonly used and extensively verified spectral wave model. There are also numerous cross-shore models available, some of which are too theoretically simple to provide confident estimates, while others require commercial licences. XBEACH is a promising model as it is technically appropriate and freely available.

Shoreline protection is inevitable as the value of certain land exceeds the cost of defence. In the face of climate change there has been an increased realisation that the dynamic natural environment needs to be preserved and so there has been a definite shift away from hard engineering options to soft options. Undeveloped land should be protected from future development through good management techniques that consider the effects of global sea level rise. Developed land is preferably protected by the often cost effective beach nourishment with GSCs providing a favourable transition between hard and soft engineering options.

References

Afshar, K. Bigdeli, N.: Data analysis and short term load forecasting in Iran electricity market using singular spectral analysis (SSA), Energy, 36, 2620 – 2627, 2011. 17

Allan, J. C. Komar, P. D.: A dynamic revetment and artificial dune for shore protection. In: Proceedings, The 28th International Coastal Engineering Conference, Cardiff, 2, 2044 – 2056, 2002. 33, 259, 276

Alvarez, I. E., Rubio, R., Ricalde, H.: Beach restoration with geotextile tubes as submerged breakwaters in Yucatan, Mexico. Geotextiles and Geomembranes, 25, 233 – 241, 2007. 34, 266, 296

Bailard, J. A.: Energitics model for cross-shore sediment transport. J. Geophys. Res. 84(C12), 7827 – 7833, 1981. 31

Belkessa, R., Houma, F., Ciortan, R., Mezouar K.: Protection works of the sea coast in Algeria. Seventh International Conference of Coastal and Port Engineering in Developing Countries, COPEDEC VII, 196, 11. Dubai, 2008. 32, 253

Belzunce, F., Castano, A., Olvera-Cervantes, A., Suarez-Llorens, A.: Quantile curves and dependence structure for bivariate distributions, Comp. Stat. Data Anal., 51, 5112 – 5129, 2007. 30

Booij, N. Ris, R.C. Holthuijsen, L.H.: A third-generation wave model for coastal regions, part I: model description and validation. Journal of Geophysical Research, 104 (C4), 7649 – 7666, 1999. 30

Borgman, L. E. Resio, D. T.: Extremal Prediction in Wave Climatology. Proceedings, Ports 77, 1, New York, 394 – 412, 1977. 19, 74

Bruun, P.: Sea Level Rise as a Cause of Shore Erosion, Journal of Waterway, Port, Coastal and Ocean Engineering, American Society of Civil Engineering, 88, 117 – 130, 1962. 31, 114, 133

Cantr, S.: Geotextile tubes - analytical design aspects. Geotextiles and Geomembranes 20, 305 – 319, 2002. 34, 266

Callaghan, D. P. Nielsen, P. Short, A. Ranasinghe, R.: Statistical simulation of wave climate and extreme beach erosion. Coastal Engineering, 55, 375 – 390, 2008. 20, 31, 58, 85, 121, 155, 182, 191, 192, 207, 236

Casella, G. & Berger, R. L.: Statistical Inference. Pacific Grove, CA: Wadsworth and Brooks/Cole. 1990. 21, 59, 188

Chadwick, C. Morfett, J. Borthwick, M.: Hydraulics in Civil Engineering and Environmental Engineering, (4th Edition). Abingdon: Spon Press. 2004. 20, 58

Chakak, A. Koehler, K. J.: A strategy for constructing multivariate distributions, Communications Statistics-Simulation and Computation, 24, 537 – 50, 1995. 25, 27, 28, 152, 154, 155, 162, 165, 170, 174, 313, 316

Chebana F. Ouarda T.B.M.J.: Multivariate quantiles in hydrological frequency analysis, Environmetrics, 22 (1), 63 – 78, 2011. 28, 30, 316

Chini, N. Stansby, P. Leake, J. Wolf, J. Roberts-Jones, J. Lowe, J.: The impact of sea level rise and climate change on inshore wave climate: A case study for East Anglia (UK), Coastal Engineering, 57, 973 – 984, 2010. 20, 58, 140, 156, 185, 223

Choowong, M., Phantuwongraj, S., Charoentitirat, T., Chutakositkanon, V., Yumuang, S., and Charusiri, P.: Beach recovery after 2004 Indian Ocean tsunami from Phang-nga, Thailand, Geomorphology, 104, 134 – 142, 2009. 17, 86, 105

Cooper, J.A.G.: The role of extreme floods in estuary-coastal behaviour: contrasts between river- & tide-dominated microtidal estuaries, Sedimentary Geology, 150, 123 – 137, 2002. 16, 140

Cowell, P.J. Stive, M.J.F. Niederoda, A.W. de Vriend, H.J. Swift, D.J.P. Kaminsky, G.M. Capobianco, M. The coastal-tract (part 1): a conceptual approach to aggregated modelling of low-order coastal change. Journal of Coastal Research, 19(4), 812 – 827, 2003a. 15

Cowell, P.J. Stive, M.J.F. Niederoda, A.W. Swift, D.J.P. de Vriend, H.J. Buijsman, M.C. Nicholls, R.J. Roy, P.S. Kaminsky, G.M. Cleveringa, J. Reed, C.W. de Boer, P.L. The coastal-tract (part 2): Applications of aggregated modelling of lower-order coastal change. Journal of Coastal Research, 19(4), 828 – 848, 2003b. 15

CSIR: Sand Supply from Rivers within the eThekwini Jurisdiction, implications for coastal sand budgets and resource economics, Report No. CSIR/NRE/ECO/ER/2008/0096/C, Stellenbosch, 2008. 16, 51, 87, 101, 106, 139, 140

Dai, S.B. Yang, S.L. Cai, A.M.: Impacts of dams on the sediment flux of the Pearl River, southern China, Catena, 76, 36 – 43, 2008. 16, 115

Dang , T. H. Coynel, A. Orange, D. Blanc, G. Etcheber, H. Le, L. A.: Long-term monitoring (19602008) of the river-sediment transport in the Red River Watershed (Vietnam): Temporal variability and dam-reservoir impact, Science of the Total Environment, 408, 4654 – 4664, 2010. 16, 115

Dean, R. G.: Beach Nourishment: Theory and Practice. World Scientific Publishing Company,New Jersey. 399, 2003. 32

De Michele, C. Salvadori, G. Passoni, G. Vezzoli, R.: A multivariate model of sea storms using copulas, Coastal Engineering, 54, 734 – 751, 2007. 22, 25, 27, 78, 152, 154, 155, 156, 162, 171, 174, 189, 190, 223, 224, 313, 315

Dette, H. H. Raudkivi, A. J.: Beach and storm-tide protection on the coast of the Baltic Sea. Proceedings of the 28th International Coastal Engineering Conference, 3, 3298 – 3307, Cardiff. 2002. 16, 32, 253

DHI: Mike21 spectral wave module. Scientific documentation, Danish Hydraulic Institute (DHI), 2005. 30

Douglas, B. C.: Global sea level acceleration, J. Geophys. Res., 97, 12, 699 – 12,706. 1992. 11

Embrechts, P. Lindskog, F. McNeil, A.J.: Modelling dependence with copulas and applications to risk management, http://www.risklab.ch/ftp/papers/DependenceWithCopulas.pdf 2001. 26, 28, 154, 316

Forbes, D. L., Parkes, G. S., Manson, G. K., & Ketch, L. A.: Storms and shoreline retreat in the southern Gulf of St. Lawrence, Mar. Geol., 210, 169 – 204, 2004. 16, 17, 85, 86

Galiatsatou, P. Prinos, P.: Bivariate models for extremes of significant wave height and period. An application to the Dutch Coast. International Conference in Coastal Engineering. 322, 2008. 22

Gracia, V., Morón, D., Jiménez, J. A., Guillén, J., Palanques, A., & Sanchez-Arcilla, A.: Near-bottom transport seaward of the surf zone under storms: On the role of currents, wind and infragravity waves in microtidal environments, Proceedings of the 28th International Coastal Engineering Conference, Cardiff, 7 – 12 July 2002, 2, 2517 – 2527, 2002. 17, 86

Genest, C. & Rivest, L. P.: On the multivariate probability integral transformation, Stat. Probab. Lett., 53, 391 – 399, 2001. 29, 226

GESAMP: Anthropogenic Influences on Sediment Discharge to the Coastal Zone and EnvironmentalConsequences, Joint Group of Experts on the Scientific Aspects of Marine Environmental Protection (GESAMP), GESAMP Reports and Studies No 52, UNESCO, 1994. 16, 86, 114

Ghil, M.R. Allen, M. Dettinger, M.D. Ide, K. Kondrashov, D. Mann, M.E. Robertson, A.W. Saunders, A. Tian, Y. Varadi, F. Yiou,P.: Advanced spectral methods for climatic time series. Rev. Geophys., 40, 3-1 – 3-41, 2002. 17

Goda, Y.: Random Seas and Design of Maritime Structures (2nd Edition). Singapore: World Scientific Publishing Co. Pte. Ltd. 2008. 20, 21, 28, 58, 59, 151, 187, 188, 225, 233

Golyandina, N. Nekrutkin, V. Zhigljavsky, A.: Analysis of Time Series Structure: SSA and related techniques, Chapman and Hall/CRC, London 305 pp., 2001 18, 118

Gratiot, N. Anthony, E. J. Gardel, A. Gaucherel, C. Proisy, C. Wells J.T.: Significant contribution of the 18.6 year tidal cycle to regional coastal changes. Nature geosciences, 1 (3), 169 – 172, 2008. 15

Grimaldi, S. Serinaldi, F.: Asymmetric copula in multivariate flood frequency analysis, Advances in Water Resources, 29, 1155 – 1167, 2006. 26, 27, 154, 315

Guedes Soares, C. Scotto, M. G.: Application of the r largest-order statistics for long-term predictions of significant wave height. Coastal Engineering, 51, 387 – 394, 2004. 20, 21, 58, 156, 185, 223

Hamm, L. Capobianco, M. Dette, H. H. Lechuga, A. Spanhoff, R. Stive, M. J. F.: A summary of European experience with shore nourishment. Coastal Engineering, 47, 237 – 264, 2002. 32, 253

Han, W. Meehl, G. A. Rajagopalan, B. Fasullo, J.T. Hu, A. Lin, J. Large, W.G. Wang, J. Quan, X. Trenary, L. L. Wallcraft, A. Shinoda, T. Yeager, S.: Patterns of Indian Ocean sea-level change in a warming climate, Nature Science, 3, 546 – 550, 2010. 11, 114, 139

Hanson, H. Brampton, A. Capobianco, M. Dette, H. H. Hamm, L. Laustrup, C. Lechuga, A. Spanhoff, R.: Beach nourishment projects, practices, and objectives - a European overview. Coastal Engineering. 47, 81 – 111, 2002. 32, 253

Hartanto, I.M., Beevers, L., Popescu, I., Wright, N.G.: Application of a coastal modelling code in fluvial environments. Environmental Modelling & Software, 26 (12), 1685 – 1695, 2011. 31, 192, 228

Hassani, H.: Singular Spectrum Analysis: Methodology and Comparison, Journal of Data Science, 5, 239 – 257, 2007. 18, 118

Hassani, H. Soofi, A. S. Zhigljavsky, A. A.: Predicting daily exchange rate with singular spectrum analysis, Nonlinear Analysis: Real World Applications, 11, 2023 – 2034, 2010. 17

Hawkes, P. J. Gouldby, B. P. Tawn, J. A. Owen, M. W.: The joint probability of waves and water levels in coastal engineering design. Journal of Hydraulic Research, 40 (3), 241 – 251, 2002. 20, 58

Heerten, G. Klompmaker, J. Partridge, A.: Design and construction of waterfront structures with special designed non-woven geotextiles, In: Proceedings, Seventh International Conference of Coastal and Port Engineering in Developing Countries, COPEDEC VII, Dubai. 2008. 33, 259, 276

Hofert, M.: Sampling Archimedean copulas, Computational Statistics and Data Analysis, 52, 5163 – 5174, 2008. 27, 315

Hofert, M.: Efficiently sampling nested Archimedean copulas, Computational Statistics and Data Analysis, 55, 57 – 70, 2011. 27, 315

Hornsey, W. P., Carley, J. T., Coghlan, I.R., Cox, R. J.: Geotextile sand container shoreline protection systems: Design and application. Geotextiles and Geomembranes, 29 (4), 425 – 439, 2011. 33, 260, 262, 263, 274, 276, 282, 283, 286, 287, 290, 291, 292, 294, 296, 299, 300

Houser, C., Hapke, C., & Hamilton, S.: Controls on coastal dune morphology, shoreline erosion and barrier island response to extreme storms, Geomorphology, 100, 223 – 240, 2008. 17, 86

Hsu, S. Lin, F. Jeng, W. Chung, Y. Shawb, L. Hung, K.: Observed sediment fluxes in the southwesternmost Okinawa Trough enhanced by episodic events:

flood runoff from Taiwan rivers and large earthquakes Deep-Sea Research I 51, 979 – 997, 2004. 16, 115

Huang, G.: Time lag between reduction of sediment supply and coastal erosion, International Journal of Sediment Research, 26, 27 – 35, 2011. 16, 115

Institute of Mechanical Engineers: Climate Change: Adaption to the inevitable, London, 30 pp. Available from http://www.imeche.org/ [Accessed 19 May 2009], 2009. 11

IPCC. Pachauri, R.K. Reisinger, A. (Eds.): Climate Change 2007: Synthesis Report, Geneva, Switzerland, 104 pp., Available from http://www.ipcc.ch/ [Accessed 31 March 2009], 2007. 11, 15

Isaacson, M. Q. & MacKenzie, N. G.: Long-term distributions of ocean waves: a review. Journal of Waterway, Port, Coastal and Ocean Division, ASCE, 107(WW2): 93-109, 1981. 19, 58, 59, 150

Jevrejeva, S. Grinsted, A. Moore, J. C. Holgate, S.: Nonlinear trends and multi-year cycles in sea level records, J. Geophys. Res., 111, C09012, doi:10.1029/2005JC003229, 2006. 18

Joe, H.: Multivariate Models and Dependence Concepts, Chapman & Hall, London, 1997. 25, 26, 152, 154, 313

Keim,B.D. Muller, R.A. Stone, G.W.: Spatial and temporal variability of coastal storms in the North Atlantic Basin, Marine Geology, 210, 7 – 15, 2004. 12, 115, 140

Knutson, T.R. Tuleya, R.E.: Impact of $C0^2$- Induced warming on simulated hurricane intensity and precipitation: Sensitivity to the choice of climate model and convective parameterization, J. Climate, 17, 3477 – 3495, 2004. 12, 138

Komar, P. D. Allan, C. J.: Increasing Hurricane-Generated Wave Heights along the U.S. East Coast and Their Climate Controls, Journal of Coastal Research, 24 (2), 479 – 488, 2008. 12, 115, 140, 275

Kriebel, D.L., Dean, R.G.: Convolution method for time-dependent beach-profile response. Journal of Waterway, Port, Coastal and Ocean Engineering, 119 (2), 204 – 226, 1993. 31, 85, 182, 191, 204, 207, 228

Lambert, S.: Changes in winter cyclone frequencies and strengths in transient enhanced greenhouse warming simulations using two coupled climate models, Atmosphere-Ocean, 42(3), 173 – 181, 2004. 12, 138

Larson, M. Kraus, N. C. Byrnes, M. R.: SBEACH: Numerical model for simulating storm-induced beach change, Report 2, Numerical formulation and model tests, Technical report CERC-89-9, US Army Engineer Waterways Experiment Station, Vicksburg, MS, 1990. 31, 191, 228

Lichter, M. Vafeidis, A. T. Nicholls, R. J. Kaiser, G.: Exploring Data-Related Uncertainties in Analyses of Land Area and Population in the "Low-Elevation Coastal Zone" (LECZ). Journal of Coastal Research, 757 – 768, 2011. 15

Liew, S. C., Gupta, A., Wong, P. P., & Kwoh, L. K.: Recovery from a large tsunami mapped over time: The Aceh coast, Sumatra, Geomorphology, 114, 520 – 529, 2010. 17, 86, 105, 106

Liquete, C. Canals, M. Ludwig, W. Arnau, P.: Sediment discharge of the rivers of Catalonia, NE Spain, and the influence of human impacts, Journal of Hydrology, 366, 76 – 88, 2009. 16, 115

Mather, A. A.: Linear and nonlinear sea level changes at Durban, South Africa, South African Journal of Science, 103, 509 – 512, 2007. 17, 116, 133, 141, 186

Mather, A. A.: Sea Level Rise for the East Coast of Southern Africa, Seventh International Conference of Coastal and Port Engineering in Developing Countries, COPEDEC VII, 2008, 173, 11, Dubai, UAE, 2008. 11, 14, 114, 186, 275

McGranahan, G. Balk, D. Anderson, B.: The rising tide: assessing the risks of climate change and human settlements in low elevation coastal zones. Environment & Urbanization, 19(1), 17 – 37,

International Institute for Environment and Development (IIED). http://eau.sagepub.com/cgi/content/abstract/19/1/17, 2007. 15

Montgomery, D. C. & Runger, G. C.: Applied Statistics and Probability for Engineers (3rd Edition). New York: John Wiley & Sons, 2003. 21, 59, 188

Morton, R. A., Paine, J. G., & Gibeaut, J. C.: Stages and Durations of Post-Storm Beach Recovery, Southeastern Texas Coast, U.S.A., J. Coast. Res., 10, 4, 884 – 908, 1994. 17, 86, 105

Morton, R. A., Gibeaut, J. C., & Paine, J. G.: Meso-scale transfer of sand during and after storms: implications for prediction of shoreline movement, Mar. Geol., 126, 161 – 179, 1995. 17, 86, 105

Nelsen, R.B.: An introduction to copulas, (second edition), Springer Series in Statistics, Springer, New York, 2006. xxi, xxviii, 22, 24, 25, 26, 27, 29, 152, 153, 154, 158, 159, 162, 171, 172, 173, 175, 189, 190, 223, 224, 315

Oumeraci, H., Hinze, M., Bleck, M., dan Kortenhaus, A.: Sand-Filled geotextile containers for Shore protection. In: Proceedings, Sixth International Conference of Coastal and Port Engineering in Developing Countries, COPEDEC VI, Colombo, Sri Lanka, 2003. 33, 262, 291

Perrie, W. Jiang, J. Long, Z. Toulany, B. Zhang, W.: NW Atlantic wave estimates and climate change, Proceedings of the Eighth International Workshop on Wave Hindcasting and Forecasting, Oahu, Hawaii, 2004. 12, 138

Pugh, D.T.: Tides, Surges and Mean Sea Level, John Wiley and Sons, Avon, United Kingdom, 472, 1987. 13, 14, 131, 187

Recio, J., Oumeraci, H.: Hydraulic Stability of Geotextile Sand Containers for Coastal Structures: Process Oriented Studies Towards New Stability Formulae. In: Proceedings, Seventh International Conference of Coastal and Port Engineering in Developing Countries, COPEDEC VII, Dubai, 2008. 33, 259, 263, 279, 294, 297

Restall, S. J. Jackson, L. A. Heerten, G. Hornsey, W. P.: Case studies showing the growth and development of geotextile sand containers: an Australian perspective. Geotextiles and Geomembranes, 20(5), 321 – 342, 2002. 33, 260, 276, 277, 296

Roelvink, D., Reniers, A., van Dongeren, A., van Thiel de Vries, J., McCall, R., Lescinski, J.: Modelling storm impacts on beaches, dunes and barrier islands. Coastal Engineering, 56, 1133 – 1152, 2009. 31, 191, 192, 220, 228

Rouault, M. Penven, P. Pohl, B.: Warming in the Agulhas Current system since the 1980's, Geophysical Research Letters, 36, L12602, 2009. 11, 114

Rouault, M. Pohl, B. Penven, P.: Coastal oceanic climate change and variability from 1982 to 2009 around South Africa, African Journal of Marine Science, 32(2), 237 – 246, 2010. 11, 114, 138

Rovira,A. Batalla,R.J. Sala, M.: Fluvial sediment budget of a Mediterranean river: the lower Tordera (Catalan Coastal Ranges, NE Spain), Catena, 60, 19 – 42, 2005. 16, 115

Rzynski, G.: Long-term evolution of Baltic Sea wave climate near a coastal segment in Poland; its drivers and impacts Ocean Engineering, 37 (2-3), 186 – 199, 2010. 18

Ruggiero, P. Komar, P. D. Allan, J. C.: Increasing wave heights and extreme value projections: The wave climate of theU.S. Pacific Northwest, Coastal Engineering, 57, 539 – 552, 2010. 13, 20, 58, 115, 139, 156, 185, 186, 196, 223

Salvadori, G.: Bivariate return periods via 2-Copulas, Statistical Methodology, 1, 129 – 144, 2004. 28, 29, 188, 225

Salvadori, G. De Michele, C. Kottegoda, N.T. Rosso, R.: Extremes in Nature. An Approach Using Copulas, Water Science and Technology Library, Springer, 56, 292, 2007. 25, 154, 155, 225, 313

Salvadori, G. De Michele, C. Durante, F.: On the return period and design in a multivariate framework, Hydrol. Earth Syst. Sci., 15, 3293 – 3305, 2011. 29, 30, 152, 219, 220, 225, 226, 227, 240

Saathoff, F. Oumeraci, H. Restall, S.: Australian and German experiences on the use of geotextile containers. Geotextiles and Geomembranes, 25 (4-5), 251 – 263, 2007. 32, 33, 34, 258, 260, 275, 277, 285, 286, 287, 288, 289

Savu, C. Trede, M.: Hierarchical Archimedean copulas, http://www.uni-konstanz.de/micfinma/conference/Files/papers/Savu_Trede.pdf (2008-11-01), 2006. 26, 27, 154, 190, 224, 314, 315

Savu, C. Trede, M.: Hierarchies of Archimedean copulas, Quantitative Finance, 10 (3), 295 – 304, 2010. 27, 190, 224, 315

Schoonees, J.S. Theron, A.K.: Evaluation of 10 cross-shore sediment transport/morphological models, Coastal Engineering, 25, 1 – 41, 1995. 31, 191, 228

Seymour, R, J.: The Influence of Global Climate Change on Extreme Wave Occurrence on the West Coast of the United States, Proceedings of the 28th International Coastal Engineering Conference, Cardiff, 1, 52 – 60, 2002. 12, 140

Seymour, R. Guza, R.T. OReilly, W. Elgar, S.: Rapid erosion of a small southern California beach fill, Coastal Engineering, 52, 151 – 158, 2005. 31, 191

Shepard, F. P.: Longshore Bars and Longshore Troughs, Technical Memorandum 41, Beach Erosion Board, U.S. Army Corps of Engineers, Washington, DC., 1950. 17, 86

Shin, E. C., Oh, Y. I.: Coastal erosion prevention by geotextile tube technology. Geotextiles and Geomembranes, 25, 264 – 277, 2007. 34, 266, 296

Sivapragasam, C. Shie-Yui Liong, Pasha, M. F. K.: Rainfall and runoff forecasting with SSASVM approach, Journal of Hydroinformatics, 3 (3), 141 – 152, 2001. 17

Sklar, A.: Fonctions de repartition a n dimensions et leurs marges, Publications de l'Institut de Statistique de l'Universit de Paris, 8, 229 – 231, 1959. 23

Sorensen, R. M.: Basic Coastal Engineering, Third Edition. Springer Science + Business Media, Inc. New York, 2006. 13, 14, 150

Strauss, D. Mirferendesk, H. Tomlinson, R.: Comparison of two wave models for Gold Coast, Australia, Journal of Coastal Research 50, 312 – 316, 2007. 30

The SWAN Team: SWAN scientific and technical documentation, Faculty of Civil Engineering and Geosciences, Environmental Fluid Mechanics Section, Delft University of Technology, The Netherlands, 2008. 31

Tolman, H. L.: User manual and system documentation of WAVEWATCH III version 3.14. NOAA / NWS / NCEP / MMAB Technical Note 276, 194 & Appendices, 2009. 31

U.S. Army Corps of Engineers: Reliability of long-term wave conditions predicted with data sets of short duration. Coastal Engineering Technical Note, Report No. CENT-I-5. [Internet]. Available from http://chl.erdc.usace.army.mil/library/publications/chetn/pdf/cetn-i-5.pdf [Accessed 05 June 2009], 1985. 19, 58

USACE: Coastal Engineering Manual, EM 1110-2-1100, Part II: (Chapter 1), pp 8 and Part II: (Chapter 5), pp 38 – 43. Part II: (Chapter 8), pp 6 – 11. 2006. xxvi, 14, 19, 21, 56, 58

USEPA: Coastal sensitivity to sea level rise: A focus on the Mid-Atlantic Region. U.S Climate Change Science Program. Synthesis and assessment product 4.1. 2009. 14, 15

van Gent, M.R.A van Thiel de Vries, J.S.M. Coeveld, E.M. de Vroeg, J.H. van de Graaff, J.: Large-scale dune erosion tests to study the influence of wave periods, Coastal Engineering, 55, 1041 – 1051, 2008. 21, 54, 138, 151, 219

van Thiel de Vries, J.S.M. van Gent, M.R.A. Walstra, D.J.R. Reniers, A.J.H.M.: Analysis of dune erosion processes in large-scale flume experiments, Coastal Engineering, 55, 1028 – 1040, 2008. 21, 54, 138, 151, 219

Wang, X. L. Swail, V. R.: Changes of Extreme Wave Heights in Northern Hemisphere Oceans and Related Atmospheric Circulation Regimes, J. Climate, 14, 2204 – 2221, 2001. 12, 115, 138

Wang, X. L. and Swail V. R.: Trends of Atlantic wave extremes as simulated in a 40-year wave hindcast using kinematically reanalyzed wind fields, J. Climate, 15(9), 1020 – 1035, 2002. 12, 115, 138

Wang, X. L. Zwiers, F. W. Swail, V. R.: North Atlantic Ocean Wave Climate Change Scenarios for the 21st Century. J. Climate, 17, 2368 – 2383, 2004a. 12, 115, 138

Wang X. L. Swail V.R Zwiers F.W.: Changes in extra-tropical storm tracks and cyclone activity as derived from two global reanalyses and the Canadian CGCM2 projections of future, Proceedings of the Eighth International Workshop on Wave Hindcasting and Forecasting, Oahu, Hawaii, 2004b. 12, 115

WASA Group: Changing waves and storms in the Northeast Atlantic? Bull. Am. Met. Soc., 79, 741 – 760, 1998. 11

Weisse, R. Stawarz M.: Long-term changes and potential future developments of the North sea wave climate. Proceedings of the Eighth International Workshop on Wave Hindcasting and Forecasting, Oahu, Hawaii., 2004. 12, 115, 138, 140

Whelan, N.: Sampling from Archimedean copulas Quantitative Finance, 4 (3), 339 – 352, 2004. 26, 28, 154, 316

Woodroffe C. D.: Coasts: form, process and evolution, Cambridge University Press, Cambridge, United Kingdom, 2003. 14, 15, 114, 131, 150

Yasuhara, K., Recio-Molina, J.: Geosynthetic-wrap around revetments for shore protection, Geotextiles and Geomembranes, 25, 221 – 232. 2007. 34, 267, 268

Yue, S. Ouarda, T. B. M. J. Bobee, B. Legendre, P. Bruneau, P.: The Gumbel mixed model for flood frequency analysis. Journal of Hydrology, 226, 88 – 100, 1999. 22, 78

Yue, S.: The Gumbel logistic model for representing a multivariate storm event. Advances in Water Resources. 24, 179 – 185, 2001. 22, 78

Zhang, K. Douglas, B.C. Leatherman, S. P.: Twentieth-Century storm activity along the U.S. East Coast. Journal of Climate 13, 1748 – 1761, 2000. 11

Zhang, K. Douglas, B. C. Leatherman, S. P.: Global warming and coastal erosion, Climatic Change 64(1-2), 41 – 58, 2004. 15, 114, 186

Zheng, J. Dean, R. G.: Numerical models and intercomparisons of beach profile evolution, Coastal Engineering, 30, 169 – 201, 1997. 31, 191

Chapter 3

The wave climate on the KwaZulu-Natal coast

This chapter is based on a paper published in the Journal of the South African Institution of Civil Engineering, 54 (2), 45 – 54, 2012.

Abstract

The east coast of South Africa has been the subject of numerous coastal developments over recent years. The design of such developments requires a thorough analysis of the local wave climate. Richards Bay and Durban's Waverider data are two relatively long east coast data sets (18 years). These data sets have not been formally reviewed since Rossouw [1984] analysed existing wave data for South African and Namibian coastal waters. This paper aims to provide a formal analysis of the east coast wave data.

Seasonal exceedance probability plots, wave roses and typical wave parameter statistics are presented. Return periods for extreme waves are estimated from the generalised extreme value distribution and the associated limitations are discussed.

The average peak period on the east coast of South Africa is 10.0 seconds,

the average significant wave height is 1.65 m and the mean wave direction is 130 degrees. Autumn has the most frequent and the largest wave events while summer is the only season unlikely to produce either large or frequent events. The recurrence interval of the largest recorded significant wave height (8.5 m) was determined to be between 32 and 61 years.

3.1 Introduction

The estimation of statistical return periods (average recurrence interval) of storm events is imperative for coastal managers and design engineers. An average recurrence interval T_R is the average time (usually expressed in years) between the realisations of two successive events. If the risk of engineering failure due to an event of a specified recurrence interval is not acceptable then it should be redesigned or relocated accordingly. In light of recent developments, from promenade and harbour upgrades to a prospective port and small craft harbour being undertaken in vulnerable coastal zones, the accurate estimation of design waves of specified return periods has become increasingly important.

The KwaZulu-Natal coastline on the east coast of South Africa (Fig. 3.1) experienced its largest recorded wave event in March 2007. The storm coincided with the March equinox (highest astronomical tide of the year) and had devastating effects on the shoreline. Considering coincidence of tide and significant wave height, Theron & Rossouw [2008] (cited by Wright [2009] and Smith *et al.* [2010]) referred to the event as having a 500 year recurrence interval. Phelp *et al.* [2009] found the recurrence interval of the significant wave height to be between 34 and 85 years, but noting that a 35 year occurrence was more likely. CSIR [2008] estimated the significant wave height return period of the storm to be 10 to 35 years, but noted that it was probably closer to a 10 year return period. Apart from the 500 year recurrence interval that considers the coincidence of the tide and storm, the analysis of the significant wave height return period therefore ranges from 10 to 85 years. This wide range further highlights the need for additional research on the characteristics of design waves for the east coast of South Africa.

Once a coastal project has been designed in consideration of a specific return period, the construction or operation of the project becomes the point of focus.

Construction and operation of a development often depends on the exceedance statistics of a given wave parameter (see Sect. 3.2). Exceedance graphs are a tool used to identify the percentage of time parameters will be exceeded. Exceedance statistics are not very useful to the design engineer as the probability of exceedance does not preclude dependent or related recordings of the same event. Therefore this does not yield a recurrence interval estimate of independent storm events. Exceedance graphs are however of value during coastal construction work as a management tool. It allows the contractor, resident engineer or project manager to estimate how often work will be disrupted. For example if a specific height of a cofferdam is installed, exceedance statistics may be used to determine the probable number of days that the temporary works will be overtopped.

The wave climate on the east coast of South Africa has not been formally reviewed since Rossouw [1984] analysed existing wave data for South African and Namibian coastal waters. Rossouw [1984] concluded that only the Waverider data (refer Sect. 3.2) is reliable enough to consider for design purposes. The relatively long records of data (18 years) making up the current east coast record are from Durban and Richards Bay. Rossouw's analysis was of a time when no wave recording buoys were operational in Durban. Durban's reliable data has been analysed by various South African consultants and researchers (examples include van der Borch van Verwolde [2004] and Rossouw [2001]).

From a coastal design point of view it was felt that there was a need to identify what data was available for design applications and how representative it was since Durban's record was made up of three different instruments at three different locations. Fortunately Richards Bay has a continuous wave data set from its Waverider buoy that could be used to verify the results.

Storm waves are generated off the KwaZulu-Natal coast by tropical cyclones, cold fronts or cut-off lows. Cold fronts move from west to east and generally exist closer to the coast than cut-off lows and cyclones. Cold fronts occur more regularly than the other forcings and produce relatively smaller wave heights and wave periods with southerly direction. Tropical cyclones are rarely responsible for extreme waves in Durban and between 1962 and 2005 only seven cyclones affected the eastern parts of South Africa [Kruger *et al.*, 2010]. Generally tropical cyclones produce north easterly swell. Cut-off lows have been associated with the

largest wave events on the KwaZulu-Natal coast (March 2007). They form further offshore than cold fronts and are generally associated with large south easterly waves with long wave periods. For a detailed description of South African weather conditions the reader is referred to Hunter [1987], Preston-Whyte & Tyson [1993] and Taljaard [1995].

This paper aims (1) to determine the reliability of the Durban and Richards Bay Waverider data and to use it to establish return periods of wave heights for the east coast of South Africa; (2) to present exceedance statistics of wave heights and peak period and to provide other typical wave statistics; (3) to analyse wave height return periods by different methods to illustrate the uncertainties and risks of basing designs on a short wave record.

The methods of analysis as well as definitions of the wave parameters considered are described under Sect. 3.2 We then present the exceedance statistics and other typical wave parameter statistics with seasonal variations. A discussion of multivariate return periods is given prior to summarising the conclusions.

3.2 Methods

The first phase of the analysis was verifying the validity of the available data. Analysis of the wave climate could then be performed with respect to seasonal distributions; exceedance graphs; typical statistics; and a univariate statistical analysis of extreme wave heights.

The wave parameters analysed included the significant wave height, Hs, which, in deep water, is equal to $4\sqrt{m_0}$ where m_0 is the area under the wave spectrum; the maximum wave height, H_{max}, is the largest wave recorded in a recording period; the peak period, Tp, is the period at which the maximum energy density occurs and is the inverse of the peak energy frequency fp, $Tp = 1/fp$; and the wave direction is the mean wave direction from its genesis measured from true north. Hs should be used to model coastal processes and shoreline response while H_{max} is more appropriate to calculate wave loading on structures. Tp is used to define the surf similarity parameter and is consequentially used to quantify wave runup, scour and forces on structures (the larger the period the larger the wave runup and forces on structures), an increase in period has also been

shown to increase erosion [van Gent *et al.*, 2008; van Thiel de Vries *et al.*, 2008].

3.2.1 Validity of the wave data

Durban's 18 years of wave records are a combination of three different wave recording instruments at three different locations (Table 3.1), two Waverider buoys and an acoustic doppler current profiler (ADCP). Waverider is the trade name of Datawell's wave recording buoy, it is a spherical accelerometer buoy that calculates wave heights from accelerations. The ADCP is located on the ocean floor and uses sonar to measure wave heights. The different locations were a concern because of the shoaling and refraction effects due to the different water depths. Diedericks [2009] found that the Richards Bay data has a good correlation with Durban's data. Diedericks [2009] findings were verified by finding a Pearson correlation coefficient and a ratio between the Durban Waverider buoy and the Richards Bay Waverider buoy and between the Durban ADCP and the Richards Bay Waverider buoy (Table 3.5).

There was still a concern that the ADCP data was not representative enough of deepwater wave conditions and so the recorded waves were classified as either deep water, transitional or shallow water by considering the range of their depth over wave length ratio (Table 3.2). Newton's method was used to iteratively solve for the wave length L using the peak wave period Tp, depth d and gravitational acceleration g (Eqn. 3.1).

$$x_2 = x_1 - \frac{y(x_1)}{y'(x_1)} = x_1 - \frac{x_1 - Dcoth(x_1)}{1 + D(coth^2 x_1 - 1)}, \tag{3.1}$$

where $D = 4\pi^2 d/gTp^2$ and $x = 2\pi d/L$, is the wave number.

It was decided that since the ADCP did not record the 2007 event, in addition to being in much shallower water than the other instruments, that this entire data set would be replaced by the Richards Bay data which had a strong correlation to the Durban waverider buoys. The Richards Bay data is a continuous set from a constant location and so it was also analysed to confirm and compare the Durban results. Unfortunately Richards Bay was not without its limitations and although it recorded the 2007 event it did not record the second and third largest events.

Figure 3.1: Map of South Africa showing KwaZulu-Natal with locations of Waverider buoys and ADCP.

Table 3.1: Historical wave recording instruments, their operating periods, water depth and coordinates

Instrument	Date	Depth (m)	Coordinates (WGS 84)	Missing data (%)
Durban Waverider	1992-2001	42	-29.99 S; 31.00 E	18
Durban ADCP	2002-2006	15	-29.86 S; 31.07 E	13
Durban Waverider	2007-2009	30	-29.88 S; 31.07 E	26
Richards Bay Waverider	1992-2009	22	-29.00 S; 32.50 E	14

Table 3.2: Classification of water waves by the ratio of water depth d to the wave length L (Adapted from USACE [2006])

Classification	d/L (m/m)
Deep water	1/2 to ∞
Transitional	1/20 to 1/2
Shallow water	0 to 1/20

These events had to be incorporated into the Richards Bay data from the Durban records. Richards Bay is approximately 155 km away from Durban. If we apply linear wave theory and assume deep water waves with a wave period of 10 seconds the wave celerity would be 15.5 m/s. This means that if waves are formed south of Durban they can take as long as 3 hours to reach Richards Bay and vice versa. Similarly for large wave periods this time can be as short as an hour. Since the data sets are in three hour intervals there is no reason to apply a shift to the sets.

3.2.2 Seasonal distribution of wave parameters

Each data set was analysed independently to establish if there were any inconsistencies or biases. The sets were analysed annually and seasonally. The months were divided into seasons using the meteorological convention as defined in Table 3.3.

All the recordings were counted and used to determine what percentage of a specific season and year made up a data set. The data sets were made up of 3 hourly readings, meaning that a season may contribute a larger percentage to the data set in terms of data points but be missing a significant amount of days

Table 3.3: Seasonal definition of months

Seasonal	Months
Summer	12 – 2
Autumn	3 – 5
Winter	6 – 8
Spring	9 – 11

of data. This problem was resolved by calculating a percentage of days missing. The percentage of data and the percentage of days missing showed which seasons or years had the potential to skew results or create bias and identified which periods needed to be supplemented by the other data set. A few days of missing data was deemed to be insignificant, if not during a storm event, but months to years of missing data was supplemented.

Average direction was only available from the Durban ADCP (2002 - 2006) and the Durban Waverider (2007 - 2009), making H_{max}, Hs and Tp the only parameters analysed for the full 18 years of data. The Richards Bay data had wave directions from 1997 to 2009 and only differed from the Durban data as a result of different local wind conditions.

3.2.3 Exceedance graphs

Supplementing Durban's data with Richards Bay's data created an 18 year data set for Durban. Exceedance graphs were created for Hs, H_{max} and Tp for each of the four seasons. The exceedance graphs provided an initial idea of event occurrences and allowed an Hs value to be selected for the peak over threshold method.

The exceedance graphs were created by binning the parameter in question and then calculating the frequency of occurrence per bin. The frequencies were then used to find the frequency of events that exceeded each bin. The exceedance frequencies were then divided by the total number of data points and expressed as a percentage exceedance. The parameters were plotted against the percentage on a log scale to produce the exceedance graphs. A best fit line was then used to interpret the percentage of time a given wave height is equalled or exceeded.

3.2.4 Wave climate variation and typical statistics

The following parameters were extracted from the data set annually and seasonally: The maximum H_{max}, Hs, Tp, and the average Tp, Hs and wave direction. Comparing the parameters seasonally illustrated the degree of seasonal variation.

The mean wave direction was calculated as well as the significant wave height weighted average direction. The results differed negligibly and so only the weighted average directions are presented.

Since minor events had the potential of dampening major events in specific seasons, the analysis of the Hs data was also done by only considering events exceeding 3.5 m wave heights.

3.2.5 Univariate statistical analysis of extreme waves

The average recurrence interval or return period of independent wave events can be estimated by fitting a theoretical probability distribution to the data and using it to extrapolate to the event of interest. There are many available probability distributions and the use of an appropriate one is important to accurately model the data and to realistically estimate the probability of rare events by extrapolation.

The literature identifies commonly used distributions but does not state which is preferred or superior. USACE [1985, 2006] recommends the guidelines of Isaacson & MacKenzie [1981] while providing guidelines for the Extremal Type I (Fisher Tippett I) distribution and also recommends Fisher Tippett II. Isaacson & MacKenzie [1981] provide guidelines for the Lognormal, Extremal Type I and II and the Weibull distribution. Chadwick *et al.* [2004] noted that the Department of Energy recommends using the Gumbel, Fisher Tippett I or the Extremal value type I distribution. Goda [2008] provides guidelines for the use of the Fisher-Tippett I, Fisher-Tippett II, Weibull and Lognormal distributions. The Generalised Extreme Value distribution (GEV) encompasses the Fisher-Tippet distributions and the Extreme Value distribution is equivalent to the Gumbel distribution. The GEV distribution has been used extensively for extreme value analysis of hydrological events and specifically for wave heights by Guedes Soares & Scotto [2004] and Chini *et al.* [2010] while the Generalised Pareto (GP) distribution has been used by Callaghan *et al.* [2008] and Hawkes *et al.* [2002]. Rug-

giero *et al.* [2010] considered both the GP and GEV distributions. Considering the above sources the: Weibull, Lognormal, Generalised Pareto, Extreme Value and the Generalised Extreme Value distributions were used in the analysis.

Weibull	$y = k^{-k}x^{k-1}e^{-(\frac{x}{\sigma})^k}$	$:0 \leq x < \infty$
Extreme value	$y = \sigma^{-1}e^{-\left(\frac{(x-\mu)}{\sigma}\right)^k}e^{-e\left(\frac{(x-\mu)}{\sigma}\right)}$	$: -\infty < x < \infty$
Lognormal	$y = \frac{1}{x\sigma\sqrt{2\pi}}e^{\frac{-(\ln x-\mu)^2}{2\sigma^2}}$	$:0 < x <$ inf
GEV	$y = \sigma^{-1}e^{-\left(1+k\frac{x-\mu}{\sigma}\right)^{-\frac{1}{k}}}\left(1+k\frac{x-\mu}{\sigma}\right)^{-1-\frac{1}{k}}$	$: -\infty < x < \infty$
GP	$y = \frac{1}{\sigma}\left(1+k\frac{x-\theta}{\sigma}\right)^{-1-\frac{1}{k}}$	$:\theta < x,$ $for\ k > 0$ $\theta < x < -\sigma/k,$ $for\ k < 0$

where μ is the location parameter, σ is the scale parameter, k is the shape parameter.

There are numerous fitting methods available but probably the most popular is the maximum likelihood. The method maximises the probability of observing the data set that has been observed in the sample. This intuitive statement has led to the method being referred to as the most popular and best technique for deriving estimators [Casella & Berger, 1990; Montgomery & Runger, 2003]. The maximum likelihood method is popular with statisticians as its characteristics can be examined mathematically [Goda, 2008]. It shows a small amount of negative bias but seems to have the smallest degree of deviation [Goda, 2008]. The method requires lengthy iterative manipulation [Isaacson & MacKenzie, 1981], an issue that has largely been removed with modern computing capabilities. The maximum likelihood method is therefore used in this study. The Akaike information criterion (Eqn. 3.2) was used to determine the best fitting probability

distribution.

$$AIC = 2k - 2\ln(L) \tag{3.2}$$

where k is the number of parameters in the probability distribution and L is the maximised value of the likelihood function for the estimated parameters.

The length of the wave data record was only 18 years and so it was decided to statistically analyse the H_{max} and Hs wave heights with both the annual maxima method and peak over threshold method (POT). The peak over threshold method was only applied to the Hs data for a threshold of 3.5 m. A 3.5 m wave height was used because experience has shown that a wave height exceeding 3.5 m is associated with erosion. When performing the POT method it is imperative that only independent events are considered. To ensure this, data was divided into events using the following definition: a storm event commences when Hs exceeds 3.5 m and ends when Hs falls below 3.5 m and remains below for approximately one month, based on the decay time of the autocorrelation. The Richards Bay data was similarly analysed.

The 95 % confidence intervals were found for the return periods using bootstrapping. Bootstrapping is a resampling technique with replacement. The bootstrapped samples were used to calculate the critical t statistic which was in turn used to bound the estimated return intervals. For a given value μ of a sample there is a probability $(1-\alpha)$ of selecting a sample for which the confidence interval will contain the true value of μ. The $100(1-\alpha)$ percent confidence interval for the t distribution is given by Eqn. 3.3.

$$\overline{x} - t_{\alpha/2,n-1}\frac{s}{\sqrt{n}} \leq \mu \leq \overline{x} + t_{\alpha/2,n-1}\frac{s}{\sqrt{n}} \tag{3.3}$$

where $\overline{x}$ is the mean of the bootstrapped sample, s is the standard deviation, n is the number of samples and $t_{\alpha/2,n-1}$ is the upper $100\alpha/2$ percentage point of the t distribution with $n-1$ degrees of freedom.

3.3 Results

The Richards Bay data is shown to be a representative measure of the Durban wave conditions. The two data sets are used in conjunction to establish exceedance probabilities, typical wave parameter statistics, seasonal trends and average recurrence intervals of wave heights along the east coast of South Africa.

3.3.1 Wave data validity

The wave data showed that the Richards Bay data was an acceptable supplement to the Durban Waverider data. The waves recorded from all the recording instruments were largely transition water waves (Table 3.4). The Durban Waveriders, being in deeper water, recorded the most deep water waves and although the Richards Bay Waverider data consisted of only 2 % deep water waves, it was still ten times larger than the ADCP, making Richards Bay's recorded waves more similar to that of the Durban Waveriders than the ADCP.

Richards Bay's Waverider showed a stronger correlation between the Durban Waverider than the ADCP (Table 3.5). When comparing the average ratios of significant wave height the Richards Bay data showed a 1.08 ratio with Durban's Waverider data while only a 0.85 with the ADCP data.

The final justification in replacing the ADCP data is shown in Fig. 3.2 and 3.3. These time series plots of the largest wave events (overlapping the data sets) illustrate that the Richards Bay data is more representative of the Durban Waverider than the Durban ADCP. Figure 3.4 shows a comparison of the wave roses for the entire data sets of the Durban Waverider (2007 - 2009), the Durban ADCP (2002 - 2006) and the Richards Bay Waverider (1997 - 2009). The Durban and Richards Bay Waveriders show a similar southerly distribution reaffirming the strong representation of one another. The Durban ADCP has a dominant easterly component and is essentially the result of refraction occurring at the ADCP's shallow depth.

Consequently the Richards Bay data was substituted in for the ADCP data and used to supplement other missing data points and a complete 18 year data set was attained.

The Richards Bay data on the other hand was a continuous set from the same

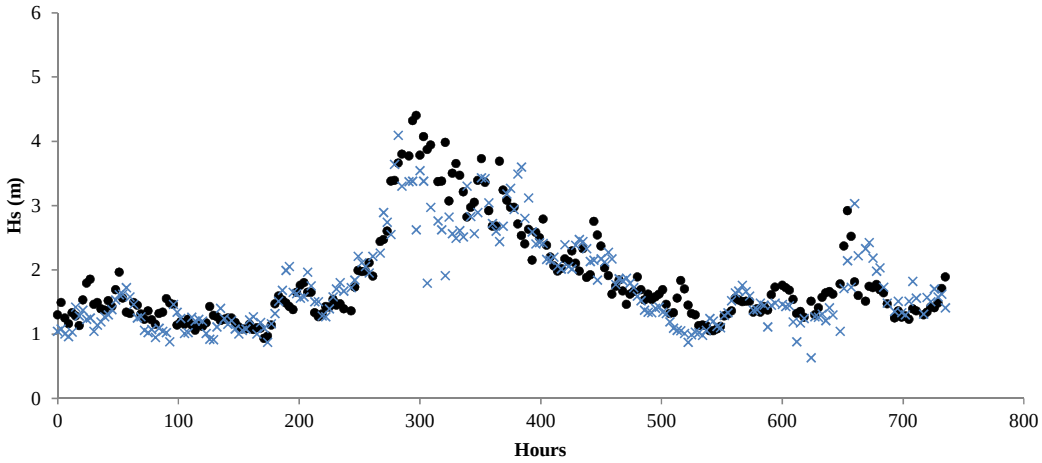

Figure 3.2: Comparison of Richards Bay's Waverider (×) and Durban's Waverider (•) during May 1998

location, having wave direction recordings from 1997. The Richards Bay data did contain minor gaps and Durban's data was used to supplement two missing wave events. The Richards Bay data was analysed to compare and verify the results of the Durban data.

3.3.2 Exceedance probabilities and wave roses

As previously mentioned exceedance graphs are not useful in a design application but are valuable in project planning.

The exceedance graphs are shown seasonally. Fig. 3.5 shows an exceedance graph of significant wave height (Hs) and Fig. 3.6 shows an exceedance graph of maximum wave height (H_{max}). Wave direction barely shows a seasonal variation and it is presented as wave roses in Fig. 3.8.

Fig. 3.5 and 3.6 show that autumn experiences the largest waves followed by winter and spring and then summer. Autumn with regards to wave height exceedance (Hs and H_{max}) is the only season that shows a significant statistical difference from the other seasons at a 95 % confidence limit. Based on the available data, wave heights will exceed the 2007 event ($Hs = 8.5\ m$, $H_{max} = 12.4\ m$) 0.01 % of the time. However from the regression line the Hs exceedance of 8.5 m

Table 3.4: The percentage of different water waves recorded by the various recording instruments

Data Set	**Water Depth (m)**	**Deep Water Waves (%)**	**Transition Water Waves (%)**	**Shallow Water Waves (%)**
Durban Waverider (1992-2001)	42	22.7	77.3	0.0
Durban ADCP (2002-2006)	15	0.2	99.7	0.1
Durban Waverider (2007-2009)	30	10.1	89.9	0.0
Richards Bay Waverider (1992-2009)	22	2.2	97.8	0.0

Table 3.5: Pearson correlation, standard deviation and ratio between different instrument recorded Hs

Data Sets	**Correlation (Pearson)**	**Average Ratio of Hs**	**Standard Deviation**
Durban Waverider (1992-2001) Vs Richards Bay Waverider (1992-2009)	0.84	1.08	0.25
Durban ADCP (2002-2006) Vs Richards Bay Waverider (1992-2009)	0.77	0.85	0.28

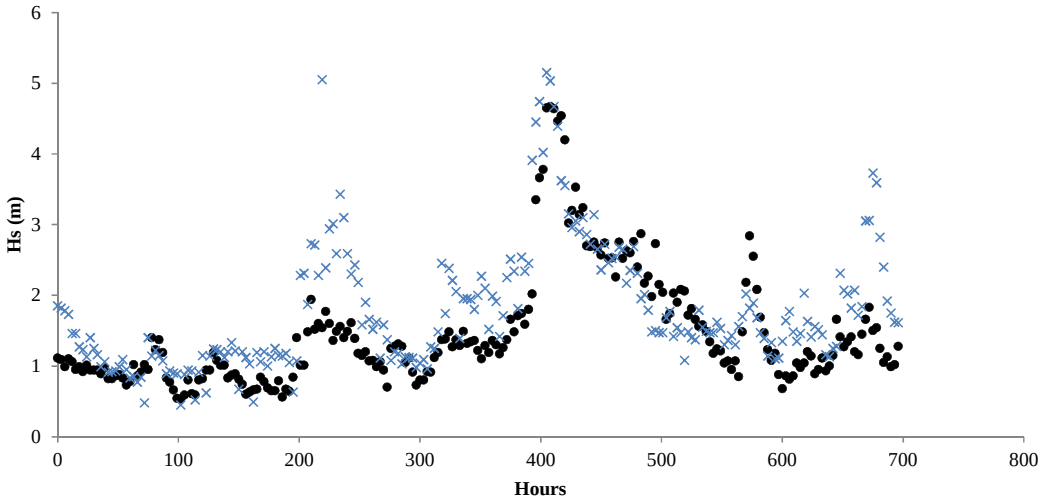

Figure 3.3: Comparison of Richards Bay's Waverider (×) and Durban's ADCP (•) during July 2002

Table 3.6: Intercepts and slopes of significant wave height exceedance regression lines for summer, autumn, winter and spring and their associated R^2 values. The bracketed values show the 95 % confidence intervals

Season	**Intercept**	**Slope**	R^2
Summer	1.21 (1.01; 1.42)	-0.37 (-0.41; -0.33)	0.99
Autumn	0.82 (0.54; 1.09)	-0.68 (-0.73; -0.64)	0.99
Winter	1.25 (1.04; 1.46)	-0.45 (-0.49; -0.41)	0.99
Spring	1.24 (1.01; 1,46)	-0.45 (-0.50; -0.41)	0.99

is 0.0015 % of the time and the H_{max} exceedance is 0.005 %. The event was evidently rare relative to the data set. Table 3.6 and 3.7 define the regression lines for Hs and H_{max} respectively.

Fig. 3.7 and Table 3.8 show that the peak period does not exhibit a statistically significant seasonal variation. The important result is that 90 % of the peak periods fall between 10 and 20 seconds.

Fig. 3.8 shows the seasonal wave direction roses for summer, autumn, winter and spring. The dominant wave angle is approximately south east and is consistent with the south - north littoral drift as expected.

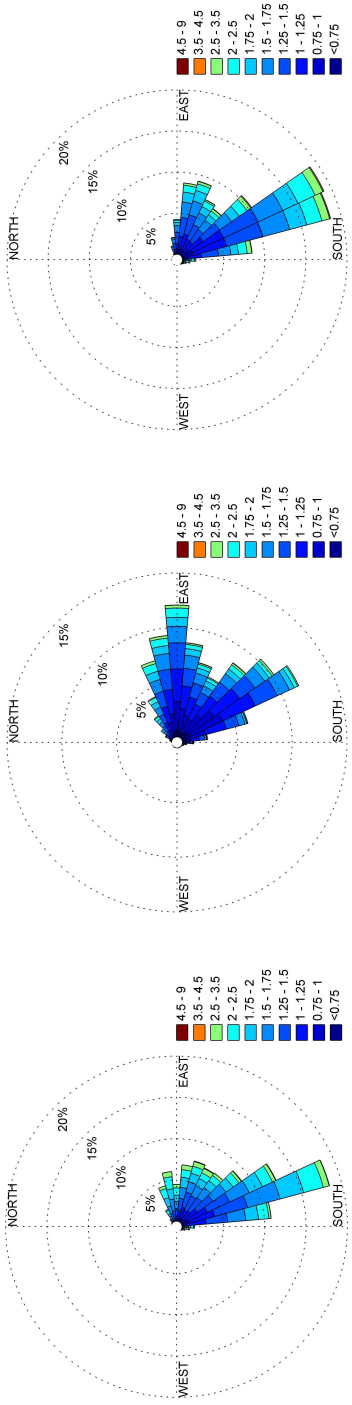

(a) (b) (c)

Figure 3.4: Comparison of the entire data set wave roses for (a) Durban Waverider (2007 – 2009), (b) Durban ADCP (2002 – 2006) and (c) Richards Bay Waverider (1997 – 2009)

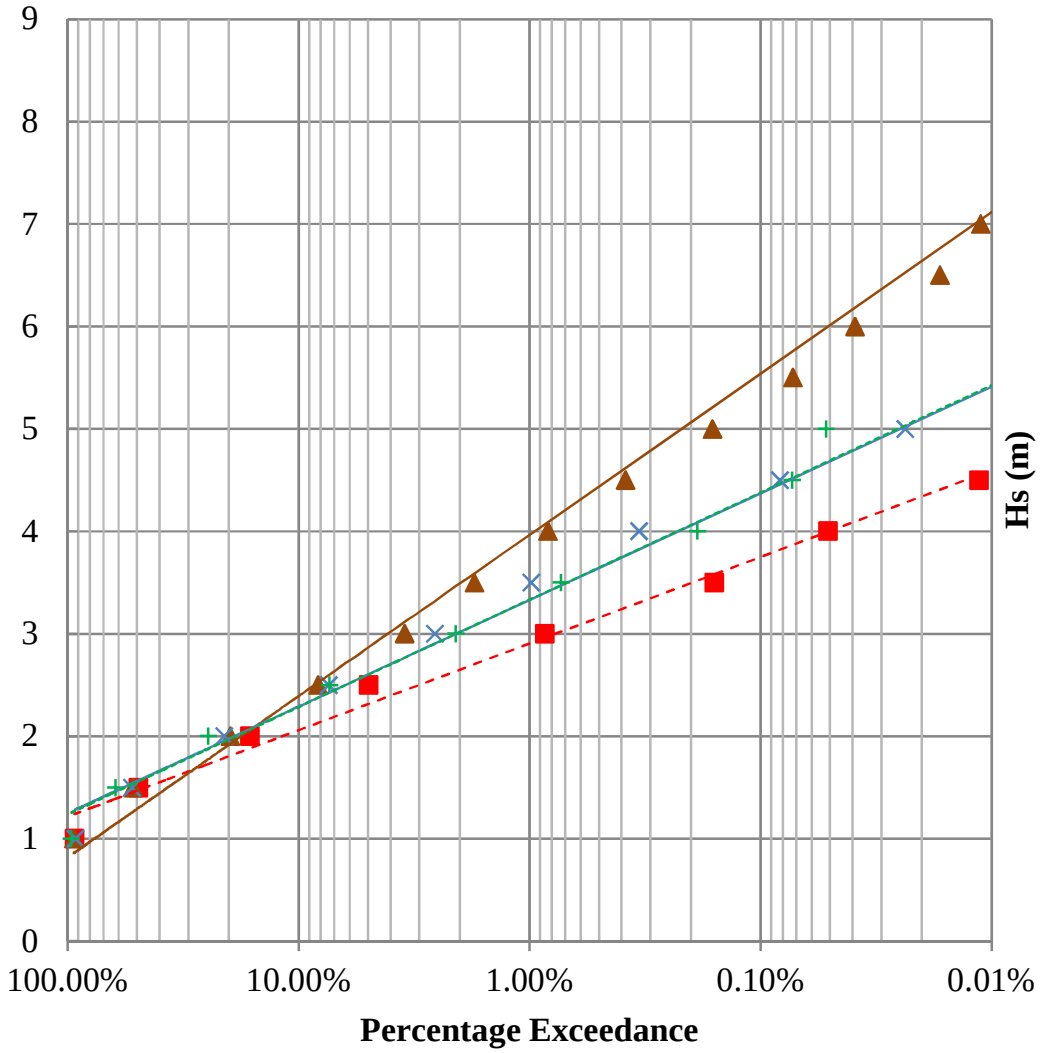

Figure 3.5: Significant wave height (Hs) percentage exceedance for summer (■), autumn (▲), winter (×) and spring (+)

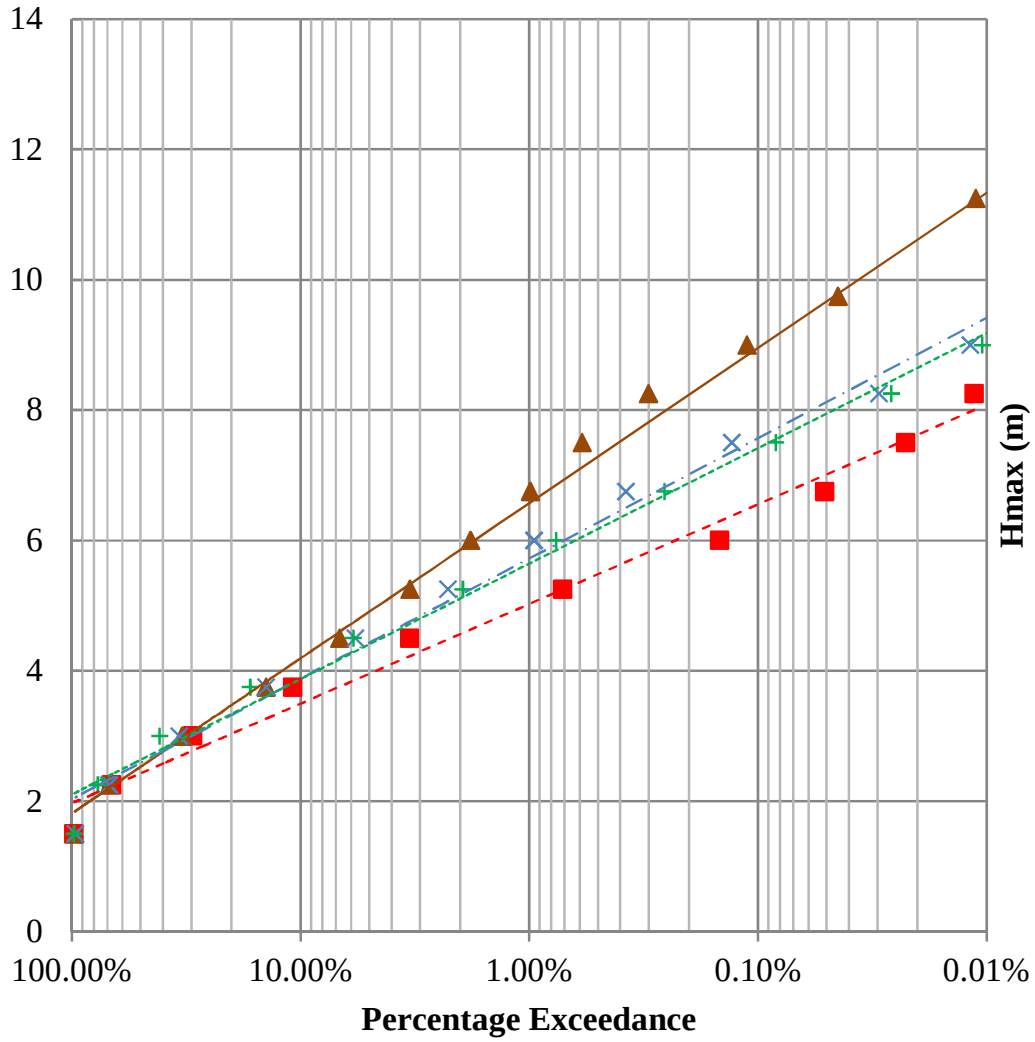

Figure 3.6: Maximum wave height (H_{max}) percentage exceedance for summer (■), autumn (▲), winter (×) and spring (+)

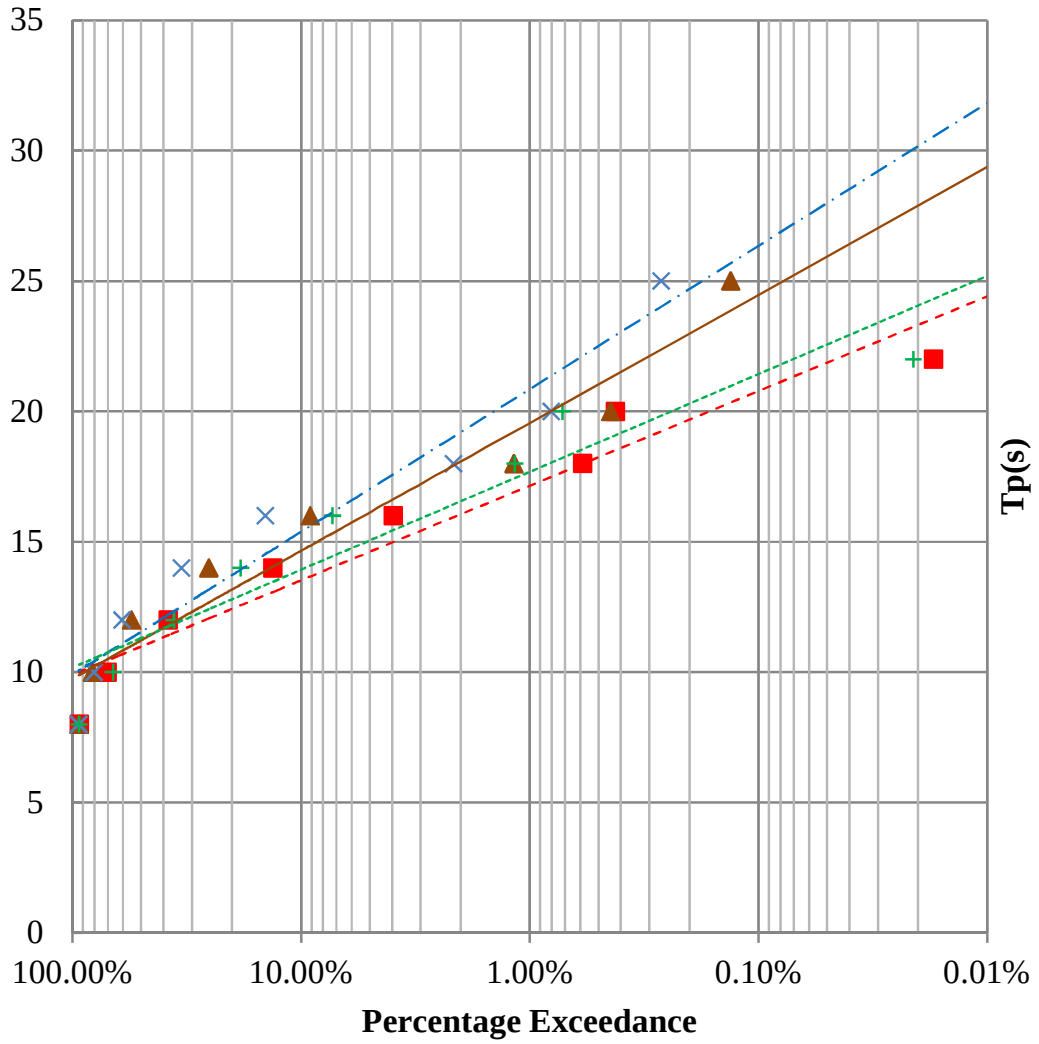

Figure 3.7: Peak period (Tp) percentage exceedance for summer (■), autumn (▲), winter (×) and spring (+)

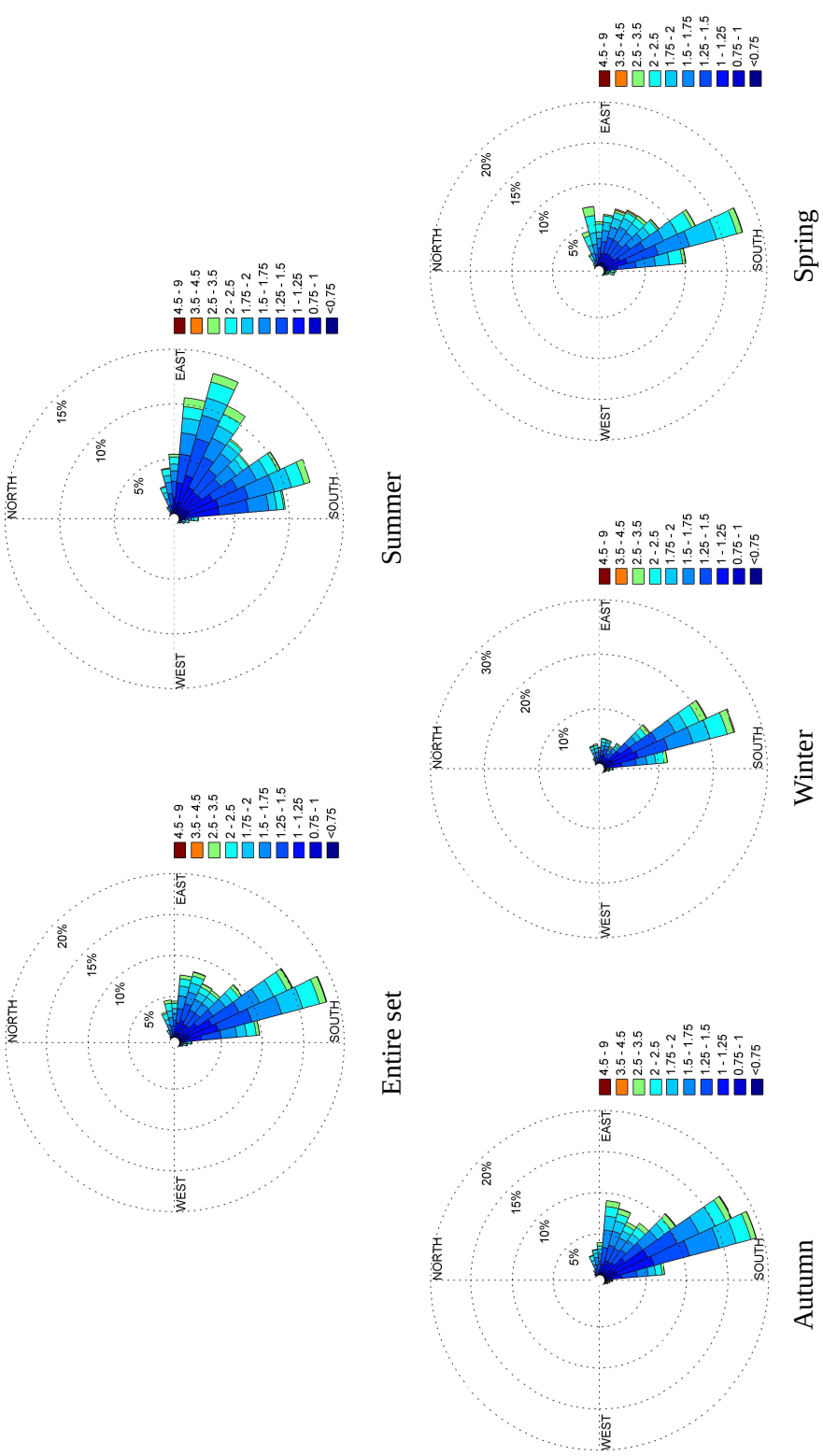

Figure 3.8: Wave roses of the entire set, summer, autumn, winter and spring. The significant wave heights associated with the various directions are illustrated by different colours shown in the legends

Table 3.7: Intercepts and slopes of maximum wave height exceedance regression lines for summer, autumn, winter and spring and their associated R^2 values. The bracketed values show the 95 % confidence intervals

Season	**Intercept**	**Slope**	R^2
Summer	2.0 (1.6; 2.3)	-0.66 (-0.73; -0.60)	0.99
Autumn	1.8 (1.5; 2.1)	-1.0 (-1.1; -0.98)	1.0
Winter	2.0 (1.7; 2.4)	-0.80 (-0.87; -0.74)	0.99
Spring	2.1 (1.8; 2.4)	-0.77 (-0.82; -0.72)	1.0

Table 3.8: Intercepts and slopes of peak period exceedance regression lines for summer, autumn, winter and spring and their associated R^2 values. The bracketed values show the 95 % confidence intervals

Season	**Intercept**	**Slope**	R^2
Summer	9.0 (7.0; 11)	-1.7 (-2.2; -1.2)	0.95
Autumn	8.9 (6.9; 11)	-2.3 (-2.9; -1.7)	0.96
Winter	9.1 (7.0; 11)	-2.6 (-3.3; -1.9)	0.96
Spring	9.3 (7.0; 11)	-1.8 (-2.4; -1.2)	0.93

3.3.3 Typical wave parameter statistics

The wave parameters were compared over the entire data set annually and seasonally.

Referring to Fig. 3.9 the highest wave height occurred in 2007. The next highest waves were in 2001. The year 2001 also had the highest average wave height, indicating a particularly rough year in terms of sea conditions. The average Hs for the entire data set was 1.65 m with an average direction of 130 degrees. The maximum Tp occurred in 2008.

Figures 3.10 to 3.13 are identical to Fig. 3.9 except they show the seasonal results as opposed to the entire data set.

Summer's maximum H_{max} occurred in 1999 and summer's largest Hs_{max} occurred in 2001. Its largest average Hs occurred in 1997. The average Hs for summer is 1.58 m, the average peak period is 9.52 s and the average direction is 135 degrees.

Figure 3.11 highlights that the largest H_{max} and Hs_{max} of autumn correspond to the 2007 event, while the largest average Hs was significantly higher in 2001

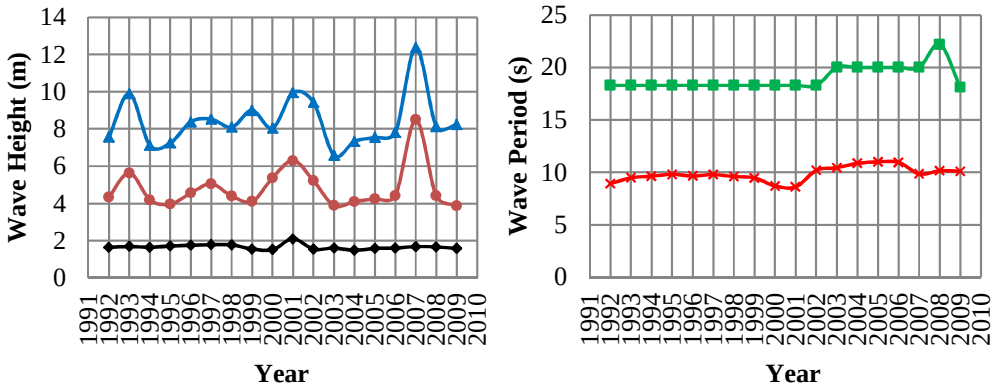

Figure 3.9: H_{max} (▲), Hs_{max} (●), average Hs (◆), maximum peak wave period (■) and average peak wave period (×) for the entire data set

than in the other years. Autumn of 2001 had the second highest Hs_{max} and the third highest H_{max}. The average Hs was 1.65 m, the average peak period is 10.4 s and the mean wave direction was 132 degrees.

Figure 3.12 shows that H_{max}, Hs_{max} and the maximum average Hs of winter all occurred in 2001. This further enforces the expectation of 2001 being a particularly rough year. The average Hs of winter is 1.64 m, the average peak period is 10.8 s and the average direction is 124 degrees.

The largest H_{max} and Hs_{max} of spring occurred in 1993, while the largest average Hs occurred in 1996. The average Hs for spring is 1.72 m, the average peak period is 9.56 s and the average direction is 129 degrees.

The data illustrates that 2001 had particularly rough sea conditions. It also demonstrates that in terms of average Hs, Tp and direction there is not much seasonal variation. The above statistics are those of the combined Durban and Richards Bay data set.

3.3.4 Seasonal Trends

Seasonal trends, with regards to large wave heights, were identified by considering only the events that exceeded a significant wave height threshold of 3.5 m. Table 3.9 shows the seasonal percentage of events, the maximum and minimum Hs and the average Hs for the events exceeding a wave height of 3.5 m.

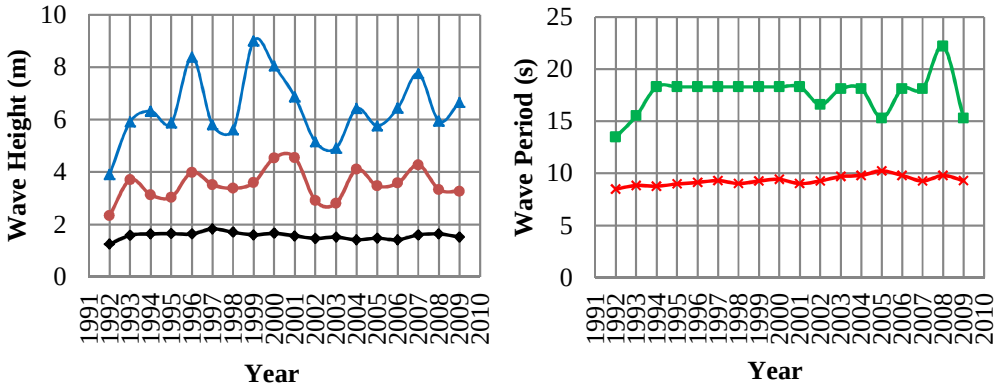

Figure 3.10: H_{max} (▲), Hs_{max} (●), average Hs (◆), maximum peak wave period (■) and average peak wave period (×) for summer

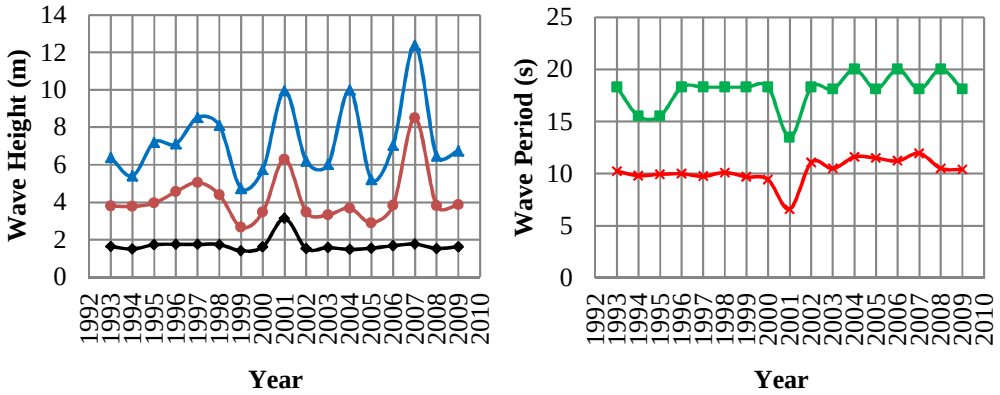

Figure 3.11: H_{max} (▲), Hs_{max} (●), average Hs (◆), maximum peak wave period (■) and average peak wave period (×) for autumn

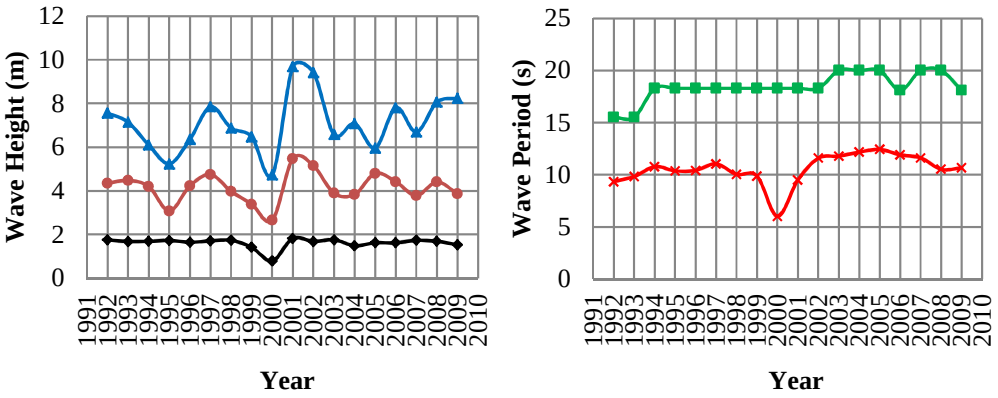

Figure 3.12: H_{max} (▲), Hs_{max} (●), average Hs (◆), maximum peak wave period (■) and average peak wave period (×) for winter

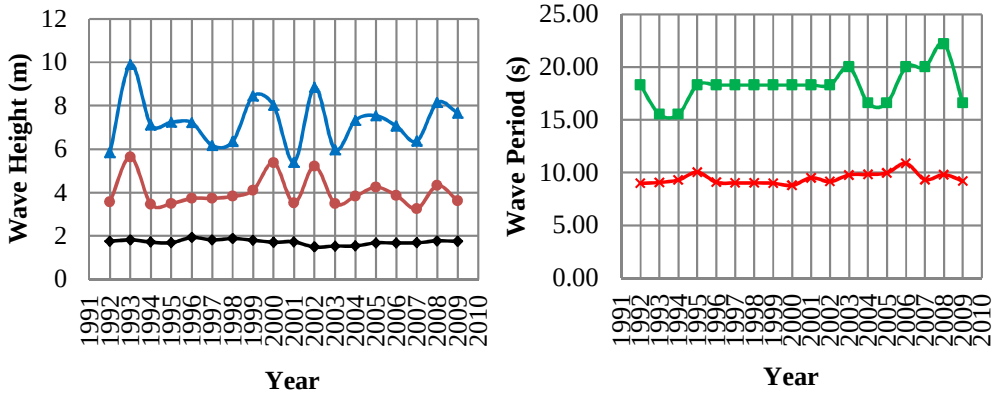

Figure 3.13: H_{max} (▲), Hs_{max} (●), average Hs (◆), maximum peak wave period (■) and average peak wave period (×) for spring

Table 3.9 shows that autumn has the highest frequency of events followed by spring and winter and then summer. Summer is definitely the calmest season having the lowest frequency and smallest Hs_{max} and average Hs. Autumn is the roughest period of the year having the largest Hs_{max}, Hs_{min} and average Hs. It is important to note that autumn still experienced the highest Hs of 6.3 m when not considering the 2007 event.

The results show that large events most frequently occur in autumn as well as the largest events. Winter and spring have very similar events and event occurrences, while summer appears to be the only season unlikely to produce either large or frequent events.

3.3.5 Wave height return periods

For the estimation of average recurrence intervals of independent extreme wave events, Borgman *et al.* [1977] suggest that a data set should not be extrapolated to more than 3 times the extent of the data set. The results can also vary extensively based on the distribution used as well as the data selected from the data set. These two limitations were considered by using numerous probability distributions and by applying the annual maxima method as well as the POT method of sampling. The GEV was determined to be the best fitting probability density function for all the data sets based on the Akaike information criterion.

Table 3.10 demonstrates the variations in the different methods. The annual maxima method of both Hs and H_{max} have the largest return periods, estimated for the 2007 event, of 48 and 61 years respectively. The 95 % confidence intervals are a function of the number of data points. Since the annual maxima method only uses 18 data points the confidence intervals are relatively large, ranging between 37 and 60 years for Hs and 49 and 76 for H_{max}. It should be noted that the H_{max} values and the Hs values do not always coincide with the same event evident by the different results.

The POT method uses 53 data points and yields significantly lower return period estimates and confidence intervals. The Hs POT estimated the event to have a recurrence interval of 32 years, with a 95 % confidence interval of 28 to 35 years. The estimates using the Richards Bay data were comparable (Table 3.10).

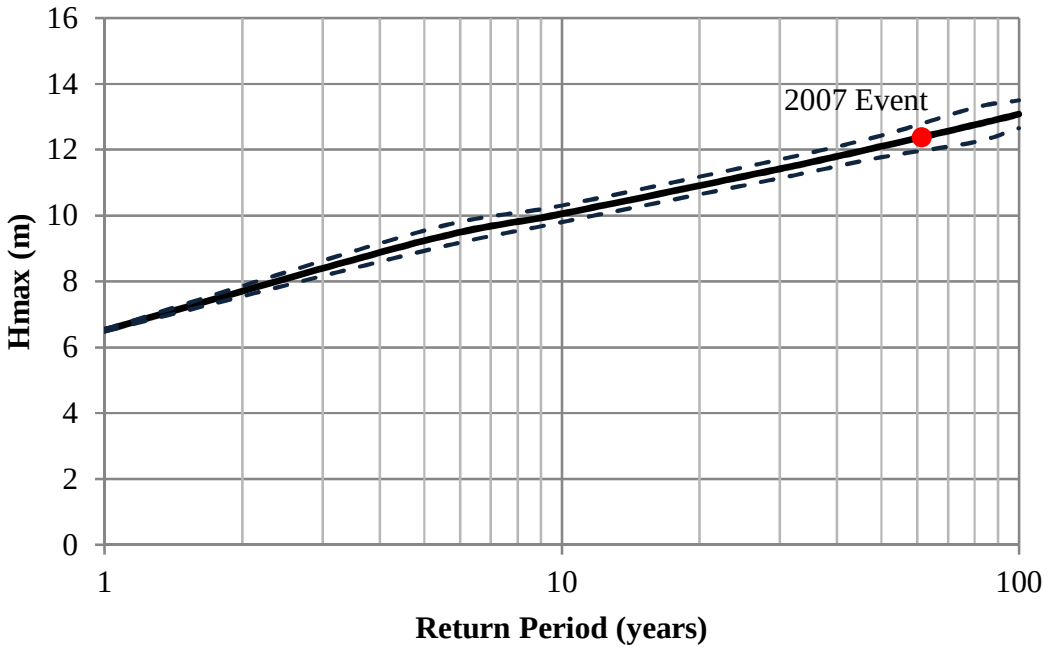

Figure 3.14: Extreme wave height, H_{max}, return periods with a 95 % confidence interval (- - -) and the 2007 event (•) for the annual maxima method

The variations in the estimates are indicative of the short data set. The estimates are limited to conclude that the event was between a 32 and 61 year event. This is similar to the 35 to 85 year return period that was determined by Phelps et al (2009). It should be noted that similar wave heights were experienced during Cyclone Imboa in 1984 (prior to the wave record analyzed herein). The 23 year period between these major events suggests that the actual return period of the 2007 event is at the lower end of the estimated range. Figures 3.14 to 3.16 have been created to allow easy estimation of return periods using any of the two methods, considering the associated uncertainty demonstrated in Table 3.10.

3.4 Discussion of multivariate return periods

We have demonstrated that the estimation of average recurrence intervals is dependent on the probability distribution used for estimation and the threshold used to sample wave heights. Apart from the analysis limitations the estima-

Table 3.9: Seasonal exceedance and maximum, minimum and average Hs of conditionally sampled significant wave heights using a 3.5 m Hs threshold as the condition

Season	**Percentage events exceeding an Hs of 3.5 m (%)**	**Max Hs (m)**	**Min Hs (m)**	**Average Hs (m)**
Summer	13.2	4.55	3.52	4.01
Autumn	30.2	8.50	3.59	4.64
Winter	28.3	5.47	3.53	4.12
Spring	28.3	5.64	3.50	4.02

Table 3.10: Comparison of the wave height recurrence intervals for the 2007 event. The results of Durbans data is un-bracketed and Richards Bays data is bracketed

Method	**Distribution**	**Wave Height (m)**	**Return Period (years)**	**95 % Confidence Interval**	
				Lower RI	**Upper RI**
Hs Annual Maxima	GEV	8.5	48 (58)	37 (47)	60 (70)
H_{max} Annual Maxima	GEV	12	61 (53)	49 (43)	76 (63)
Hs POT ($Hs > 3.5$ m, one month)	GEV	8.5	32 (46)	28 (40)	35 (53)

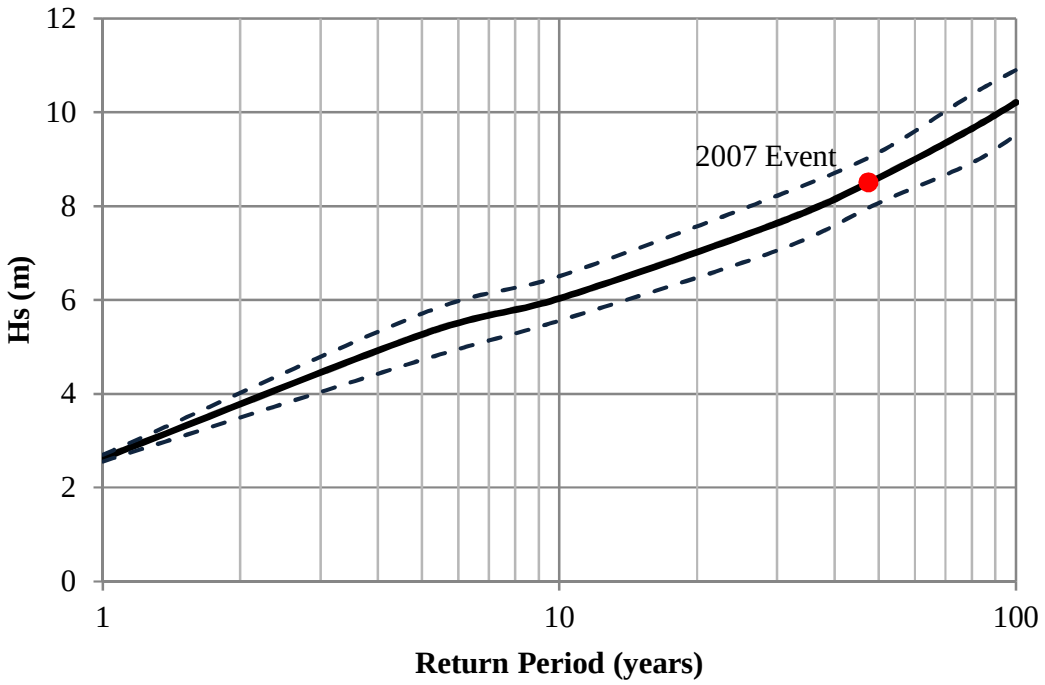

Figure 3.15: Significant wave height, Hs, return periods with a 95 % confidence interval (- - -) and the 2007 event (●) for the annual maxima method

tion of a univariate return period is not a true estimate of the storm risk. The 2007 event's wave height occurrence was estimated as a 32 year return period but its coincidence with the highest astronomical tide (HAT) would make the combined event far rarer. Considering two independent events the probability of both events being exceeded is the product of the exceedance probability of each event. In the case of the 2007 event, coincidence of the HAT (an 18.6 year return period) and wave height (a 32 year return period) yields an average recurrence interval of 595 years.

This extreme return period is actually incorrectly defined as it assumes the HAT is a random process that has equal probability of occurence each year. The HAT is deterministic and the coincidence of a wave height needs be described by the probability of a wave height exceedance for that period of heightened water level. Furthermore the 595 year return period is not a useful measure of risk since the HAT only exceeds mean high water springs by approximately 30 cm. This

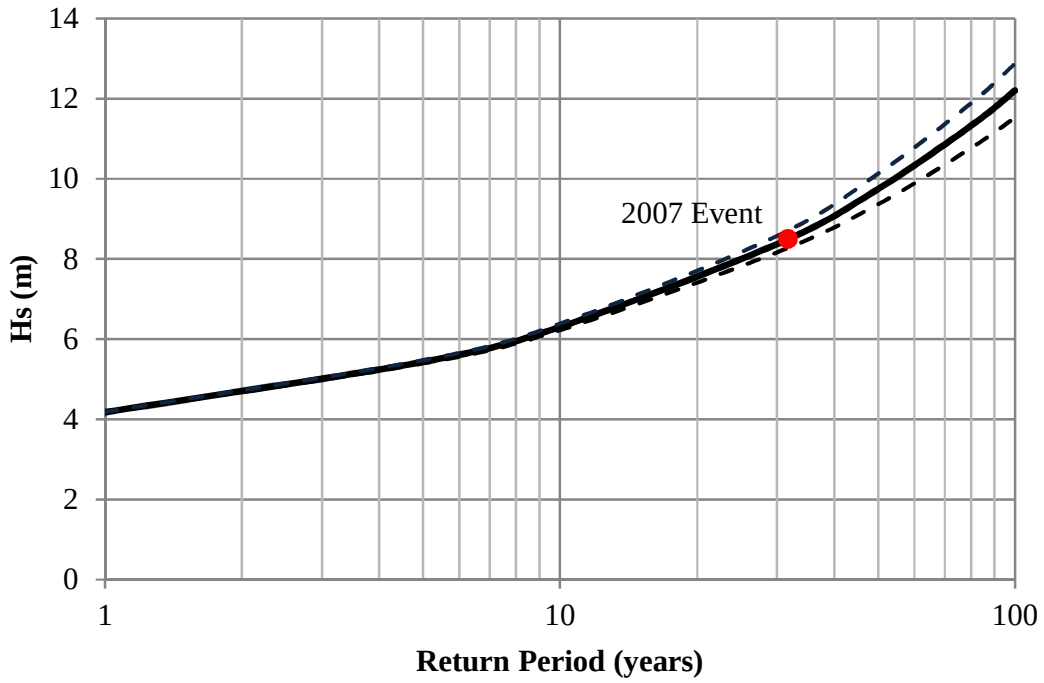

Figure 3.16: Significant wave height, Hs, return periods with a 95 % confidence interval (- - -) and the 2007 event (•) for the peak over threshold method. Events defined by one month below the wave height threshold

demonstrates that the event characteristics should be related to their contribution to the risk of failure. For example, the same amount of damage may have occurred at any highest astronomical tide of the year for the given wave heights but would have resulted in a significantly shorter return period estimate.

The estimation of risk becomes more complicated when events are interdependent and requires more advanced statistics. The Gumbel mixed model [Yue *et al.*, 1999]; the Gumbel logistic model [Yue, 2001] and copulas [De Michele *et al.*, 2007] are examples of multivariate models that may be appropriate for considering event dependencies in the estimation of return periods. Depending on the requirements of the risk estimation the multivariate analysis can be extended to include storm duration, wave direction, peak wave period and any other parameters that may contribute to a storms damage potential.

3.5 Conclusions

We have re-analysed 18 years of reliable wave data for the KwaZulu-Natal coast and provided a timely update to the existing statistics. Typical statistics of wave parameters are now available without having to re-analyse the integrity of the data sets. The average peak period of the data set is 10.0 seconds, the average significant wave height is 1.65 m and the mean wave direction is 130 degrees. Exceedance curves are now available to aid the programming and risk identification for coastal and marine projects. Autumn has been shown to be responsible for the most frequent and the largest amplitude wave events while winter and spring are similar with fewer events than autumn. Summer is the only season where large events are infrequent.

Five probability distributions have been fitted to the extreme wave events of which the generalised extreme value distribution best modelled the available data. Design waves are now available for coastal projects and the return periods of future events can be quickly estimated. The largest wave event on record occurred in autumn and had an 8.5m significant wave height, with an estimated return period between 32 and 61 years. Given past records, which have not been considered in the analysis, it is most probable that the average recurrence interval is at the lower end of the range. The Richards Bay return periods were found to be longer and so it is recommended that the more conservative return periods calculated for Durban's data be used in design.

The 32 year estimated return period of the 2007 event would suggest that it was not as rare as first assumed. This return period highlights the limitations of risk analysis when only considering a single variable. Coastal storm damage is caused by a combination of high waves, long duration storms, sea levels, and possibly other factors. In order to fully assess the risks from the 2007 event, the probability of the event's wave heights coinciding with the highest astronomical tide as well as other characteristics such as the storm duration, should be accounted for.

References

Borgman, L E & Resio, D T 1977. Extremal Prediction in Wave Climatology. Proceedings, Ports 77, vol. 1, New York, pp 394 – 412. 19, 74

Callaghan, D P, Nielsen, P, Short, A & Ranasinghe, R 2008. Statistical simulation of wave climate and extreme beach erosion. Coastal Engineering, 55: 37 – 390. 20, 31, 58, 85, 121, 155, 182, 191, 192, 207, 236

Casella, G & Berger, R L 1990. Statistical Inference. Pacific Grove, CA: Wadsworth and Brooks/Cole. 21, 59, 188

Chadwick, C, Morfett, J & Borthwick, M 2004. Hydraulics in Civil Engineering and Environmental Engineering, (4th Edition). Abingdon: Spon Press. 20, 58

Chini, N, Stansby, P, Leake, J, Wolf, J, Roberts-Jones, J & Lowe, J 2010. The impact of sea level rise and climate change on inshore wave climate: A case study for East Anglia (UK). Coastal Engineering, 57: 973 – 984. 20, 58, 140, 156, 185, 223

CSIR 2008. Durban Beach Monitoring Progress Report: July 2006 to June 2007. Report No. CSIR/NRE/ECO/ER/2008/0424/BVol1. Stellenbosch. 16, 51, 87, 101, 106, 139, 140

De Michele, C, Salvadori, G, Passoni, G & Vezzoli, R 2007. A multivariate model of sea storms using copulas. Coastal Engineeing, 54: 734 – 751. 22, 25, 27, 78, 152, 154, 155, 156, 162, 171, 174, 189, 190, 223, 224, 313, 315

Diedericks, H 2009. Personal Communication, eThekwini Municipality Coastal and Stormwater Department 166 KE Masinga Road, Durban, RSA, 29 June 2009. 54, 120

Goda, Y 2008. Random Seas and Design of Maritime Structures (2nd Edition). Singapore: World Scientific Publishing Co. Pte. Ltd. 20, 21, 28, 58, 59, 151, 187, 188, 225, 233

Guedes Soares, C & Scotto, M G 2004. Application of the r largest-order statistics for long-term predictions of significant wave height. Coastal Engineering, 51: 387 – 394. 20, 21, 58, 156, 185, 223

Hawkes, P J, Gouldby, B P, Tawn, J A & Owen, M W, 2002. The joint probability of waves and water levels in coastal engineering design. Journal of Hydraulic Research, 40 (3): 241 – 251. 20, 58

Hunter, I 1987. The Weather of the Agulhas Bank and the Cape Town South Coast. Thesis for the Department of Oceanography, University of Cape Town. 53

Isaacson, M Q & MacKenzie, N G 1981. Long-term distributions of ocean waves: a review. Journal of Waterway, Port, Coastal and Ocean Division, ASCE, 107(WW2): 93 – 109. 19, 58, 59, 150

Kruger, A C, Goliger, A M, Retief, J V, Sekele, S 2010. Strong wind climatic zones in South Africa, Wind and Structures, 13, 1, 2010. 52, 172

Montgomery DC & Runger G C 2003. Applied Statistics and Probability for Engineers (3rd Edition). New York: John Wiley & Sons. 21, 59, 188

Phelps, D, Rossouw, M, Mather, A A, & Vella, G F 2009. Storm damage and rehabilitation of coastal structures on the East coast of South Africa, Proceedings, Institute of Civil Engineers Conference, Edinburgh, Scotland. 51, 250, 277

Preston-Whyte R A & Tyson P D, 1993. The Atmosphere and Weather of Southern Africa. Oxford University Press, Southern Africa. 53

Rossouw, J 1984. Review of Existing Wave Data, Wave Climate and Design Waves for South African and South West African (Namibian) Coastal Waters.

Coastal Engineering and Hydraulics National Research Institute for Oceanology Council for Scientific and Industrial Research. CSIR report No. T/SEA 8401. Stellenbosh. 50, 52, 120

Rossouw, M 2001. Re-evaluation of the Extreme Wave Climate of Southern Africa. Ph.D thesis (in preparation). University of Stellenbosch, South Africa. 52

Ruggiero, P, Komar, P D, Allan, J C 2010. Increasing wave heights and extreme value projections: The wave climate of theU.S. Pacific Northwest. Coastal Engineering, 57: 539-552. 13, 20, 58, 115, 139, 156, 185, 186, 196, 223

Smith, A M, Mather, A A, Bundy, S C, Cooper, J A G, Guastella, L A, Ramsay, P J & Theron, A 2010. Contrasting styles of swell-driven coastal erosion: examples from KwaZulu-Natal, South Africa. Geological Magazine, 147: 940 – 953. 51, 103

Taljaard, J J 1995. Atmospheric Circulation Systems, Synoptic Climatology and Weather Phenomena of South Africa, Part 2: Atmospheric Circulation Systems in the South African region. South African Weather Bureau, Pretoria, SA. 53

Theron, A & Rossouw, M 2008. Analysis of Potential Coastal Zone Climate Change Impacts and Possible Response Options in the Southern African Region. CSIR Report. 51

U.S. Army Corps of Engineers 1985. Reliability of long-term wave conditions predicted with data sets of short duration. Coastal Engineering Technical Note, Report No. CENT-I-5. [Internet]. Available from http://chl.erdc.usace.army.mil/library/publications/chetn/pdf/cetn-i-5.pdf [Accessed 05 June 2009]. 19, 58

U.S. Army Corps of Engineers 2006. Coastal Engineering Manual, EM 1110-2-1100, Part II: (Chapter 1), pp 8 and Part II: (Chapter 8), 6 – 11. xxvi, 14, 19, 21, 56, 58

van der Borch van Verwolde, E 2004. Characteristics of extreme wave evcnts and the correlation between atmospheric conditions along the South African coast. MSc dissertation. University of Cape Town, South Africa. 52

van Gent, M R A, van Thiel de Vries, J S M, Coeveld, E M, de Vroeg, J H & van de Graaff, J 2008. Large-scale dune erosion tests to study the influence of wave periods. Coastal Engineering, 55: 1041 – 1051. 21, 54, 138, 151, 219

van Thiel de Vries, J S M, van Gent, M R A, Walstra, D J R, Reniers, A J H M 2008. Analysis of dune erosion processes in large-scale flume experiments. Coastal Engineering, 55: 1028 – 1040. 21, 54, 138, 151, 219

Wright, K 2009. Storm Warning. Wavescape. [Internet]. Available from http://www.wavescape.co.za/severe-weather-watch/storm-warning.html. [Accessed 27 March 2009]. 51

Yue, S, Ouarda, T B M J, Bobee, B, Legendre, P & Bruneau, P 1999. The Gumbel mixed model for flood frequency analysis. Journal of Hydrology, 226: 88 – 100. 22, 78

Yue, S 2001. The Gumbel logistic model for representing a multivariate storm event. Advances in Water Resources. 24: 179 – 185. 22, 78

Chapter 4

Shoreline recovery from storms on the east coast of Southern Africa

This chapter is based on a paper published in Natural Hazards and Earth System Sciences, 12, 11 – 22, 2012.

Abstract

Episodic extreme waves due to sea storms can cause severe coastal erosion. The recovery times of such events are important for the analysis of risk and coastal vulnerability. The recovery period of a storm damaged coastline represents a time when the coastline is most vulnerable and nearby infrastructure is at the greatest risk. We propose that identification of the beach recovery period can be used as a coastal management tool when determining beach usage.

As a case study, we analyse 37 yr of beach profile data on the east coast of South Africa. Considering beach length and cross-sectional area, we establish a global recovery period and rate and identify the physical characteristics of the coastlines that either accelerate or retard recovery.

The beaches in the case study were found to take an average of two years to recover at a rate of approximately $90\,\mathrm{m}^3\,\mathrm{m}^{-1}\,\mathrm{yr}^{-1}$. Beach profiles with vegetated dunes recovered faster than urbanized beaches. Perpendicular beach structures have both positive and negative effects on beach recovery. Coastlines with rock outcrops in the surf zone tend to recover slowly and long-term sediment loss was identified in cases where storm damaged beaches have not recovered to pre-erosion levels.

4.1 Introduction

Erosion of coastlines is an age old problem faced by coastal communities. Durgappa [2008] claimed that sandy shores make up approximately 20 % of the world's coastline and of this more than 60 % has experienced severe erosion over the past few decades. Apart from anthropogenic effects and sea level rise contributing to erosion, various elements of wave climate cause erosion. It is easy to perceive that a large wave height sustained for a long duration can produce erosion (e.g,. Callaghan *et al.*, 2009; Kriebel & Dean, 1993). An increase in wave period has also been shown to increase erosion [van Gent *et al.*, 2008; van Thiel, 2008]. The inter-arrival time of storm events does not necessarily influence the quantity of sediment removed during a given event. This is because a new equilibrium profile is established during the initial storm and a subsequent storm of less or equal wave power will not erode the profile any more. However, the new equilibrium profile does effect the vulnerability of coastal developments. A storm event erodes a beach and reduces the natural buffer between the ocean and the hinterland. It is at this stage that an urbanized coastline is at risk of sustaining severe damage from a subsequent, possibly less extreme, storm event before it has fully recovered to its pre-storm level [Forbes *et al.*, 2004].

During these periods of heightened vulnerability, a global estimate of the recovery time of storm damaged beaches is valuable to coastal managers for estimating the probability of storm events falling within the recovery period. The analysis of inter-arrival times in sea storm applications has been used in risk modelling by De Michele *et al.* [2007]. Research regarding shoreline erosion is plentiful [recent examples include Callaghan *et al.*, 2008; Miller & Dean, 2004; van Rijn,

2009], but there is much less on the recovery of beaches to their pre-storm positions [Morton *et al.*, 1994]. Coastal management is fraught with uncertainty [Otter & Capobianco, 2000] and social conflicts abound over the use of coastal resources [Cooper *et al.*, 2008]. Information on beach recovery periods enables coastal managers to make more informed decisions in planning for coastal hazards and appropriate use of coastal resources. Choowong *et al.* [2009] found that the Bang Niang to Khuk Khak coastline of Phang-nga after the 2004 Indian Ocean Tsunami took two years to recover, similarly Liew *et al.* [2010] found the Khao Lak coast took approximately two years to recover. Morton *et al.* [1995] found that the Texan coastline requires 4 to 5 yr for volumetric and geomorphic beach recovery from moderate storm events. The consideration of geomorphic beach recoveries is thought to make the results of Morton *et al.* [1995] longer than Choowong *et al.* [2009] and Liew *et al.* [2010] who only considered volumetric recovery. A beach's recovery is dependent on its sediment supply and the severity of the erosion event in question [Houser *et al.*, 2008]. The sediment that is transported offshore by undertow during an erosion event [Gracia *et al.*, 2002] is slowly worked back onshore under calm conditions [Shepard, 1950]. Depending on the severity of the event, the sediment may be carried sufficiently far offshore to prolong or even prevent its return [Forbes *et al.*, 2004]. Location is important for recovery, not only because of wave shoaling and refraction effects, but also because of the location of rivers which have been estimated to supply about 80 % of global beach sediments [GESAMP, 1994].

The KwaZulu-Natal coastline on the east coast of South Africa experienced its largest recorded wave event in March 2007. The event caused severe coastal damage. Peoples' perceptions about the recovery of the beaches vary with many of them saying the coastline has fully recovered while others say it has not. This chapter will show how both perceptions may be correct as well as providing an average recovery period.

This paper reports observations of recovery times and recovery rates for beach erosion from storm events on the east coast of South Africa. It also explores the implications of cases where shorelines do not recover to their pre-storm level prior to subsequent storm events.

The methods used for the case study are described in Sect. 4.2. We then

present the recovery results of all the identified major erosion events in Sect. 4.3 before focusing on the largest erosion event on record (March 2007). Finally we summarise the conclusions of the study.

4.2 Methods

4.2.1 Case study site

Durban is a coastal city on the east coast of South Africa (Fig. 4.1). Durban's local authority, the eThekwini Municipality, is responsible for almost 100 km of predominantly sandy coastline. Durban's struggle to balance the establishment of a port against beach erosion has resulted in a substantial beach monitoring and sand bypass scheme [Barnett *et al.*, 1999]. Beach profiles have been recorded since 1973, but were restricted to the central beaches (Fig. 4.2c). Numerous profiles have since been included in the monitoring programme, some as recent as 2007. All the profiles are measured at least every 3 months. Since not all the profiles had the same record length, it was decided to analyse a period that contained most of the profiles which conveniently coincided with the first records from wave recording buoys, 1992 to 2010. The profile lengths and volumes were also analysed from 1973 to 2010 for those that were available. All profile locations are shown in Figs. 4.1 and 4.2.

The profiles are recorded relative to chart datum (CD) which is the height of the lowest astronomical tide. The length and elevation of each profile is measured from a constant and unique bench mark. Beach profiles are rarely measured below 1 m CD and, therefore, all volumes were calculated above the 1 m CD contour which is approximately equal to mean sea level (Fig. 4.4). Based on the concept of an equilibrium profile, an area well below CD would be inappropriate as the sediment eroded from above CD would be deposited below CD, but above the closure depth and no net profile erosion would be measured.

The average wave conditions on the east coast of South Africa are a significant wave height of 1.65 m with an average direction of 121 degrees. These conditions produce a net littoral drift towards the north of between 300 000 m^3 and 500 000 m^3 per annum [CSIR, 2008; Schoonees, 2000].

Figure 4.1: A map of South Africa showing KwaZulu-Natal and Durban and a map of the eThekwini Municipality showing the locations of the beach profiles

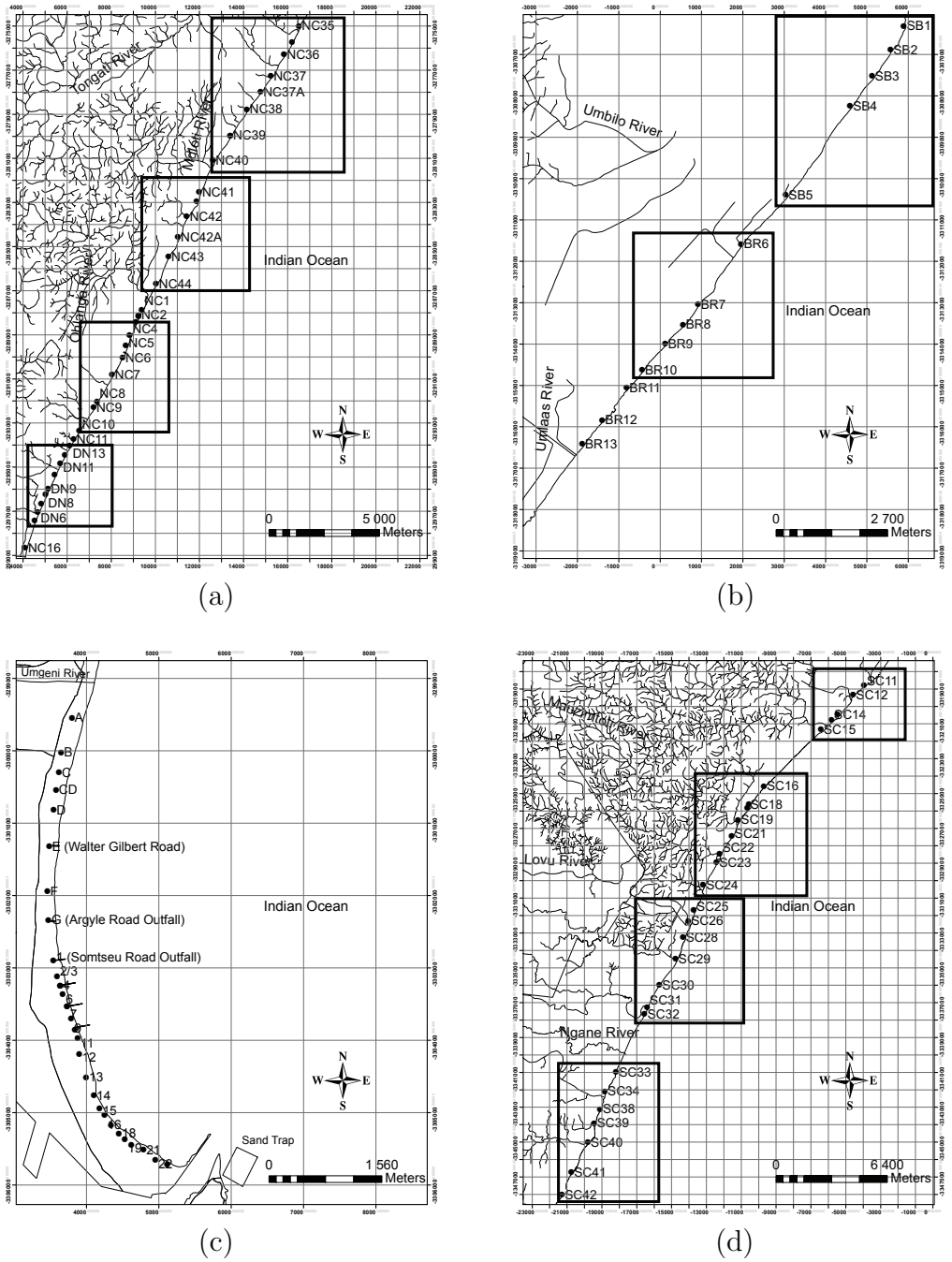

Figure 4.2: Locations of beach profiles and rivers. Coordinate system: Lo 31 – WGS84. **(a)** From DN6 to DN13 of Durban North and from NC16 to NC35 of the North Coast **(b)** From SB1 to BR13 of the Durban Bluff **(c)** From A to 23 of the Durban Bight and the sand trap **(d)** From SC11 to SC42 of the South Coast

.

4.2.2 Recovery

The recovery of both profile volumes and profile lengths were considered. The pre-erosion values before the event were used to establish an average level. The profile was only considered to have recovered once it had passed the average level on at least three consecutive recordings. The difference between the recovery date and the event date defines the recovery period while the recovery rate is defined as the volume recovered per unit time during the recovery period. Whence

$$\text{recovery period} = D_{\text{recovery}} - D_{\text{event}} \tag{4.1}$$

$$\text{recovery rate} = \frac{V_{\text{recovered}}}{\text{recovery period}} \tag{4.2}$$

where D_{event} denotes the date of the erosion event, D_{recovery} the recovery date and $V_{\text{recovered}}$ the volume recovered. The definitions of recovery period and recovery rate are illustrated in Fig. 4.3. On occasion, the profiles did not recover to the average – these were noted along with the value that they were able to recover, then used to estimate a recovery rate. This recovery rate was then used to establish what the recovery period would have been at that estimated rate. Volumes were determined from the profile cross-sectional areas and the distances between the profiles by the end areas method. The profiles are measured at different intervals ranging from 112 m to 1809 m. The profiles with large gaps between them may not be representative of the actual beach volume changes and so the areas (or volume per metre) are the preferred analysis quantity. The volume recovery periods and rates are ultimately the same measure as those of the volume per metre. The volume results are, therefore, not presented as they can be estimated by multiplying the length of coastline by the average profile volume per metre.

4.2.2.1 Volume recovery

The profile volume per unit length (Fig. 4.4) was defined as the profile area above 1 m CD. Beach profile volumes were analysed chronologically to determine erosion events.

Since the recovery period depends on the location of the profile and the severity of the event, these dependencies had to be considered when estimating a global

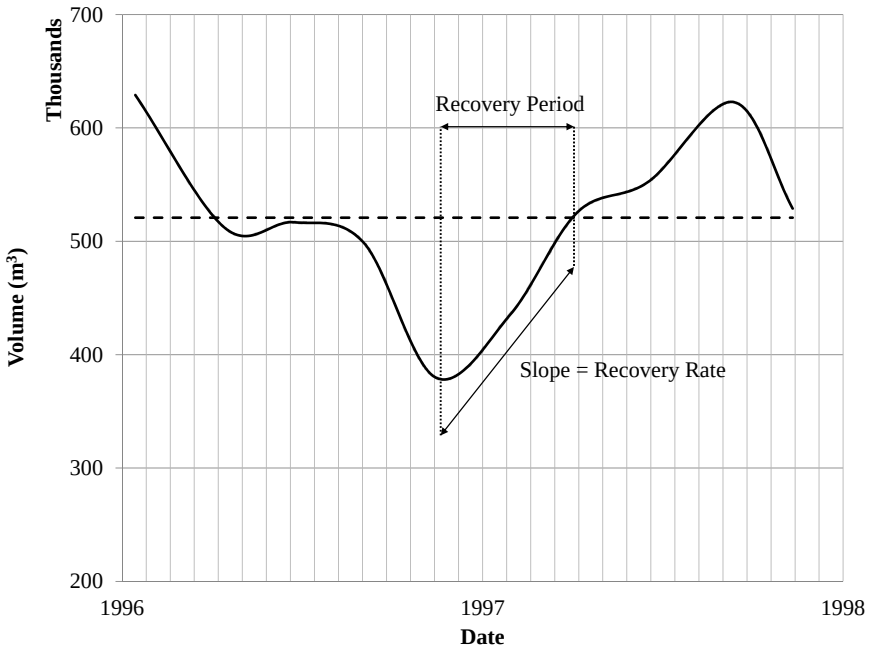

Figure 4.3: Illustration of the recovery period and recovery rate of beach volume.

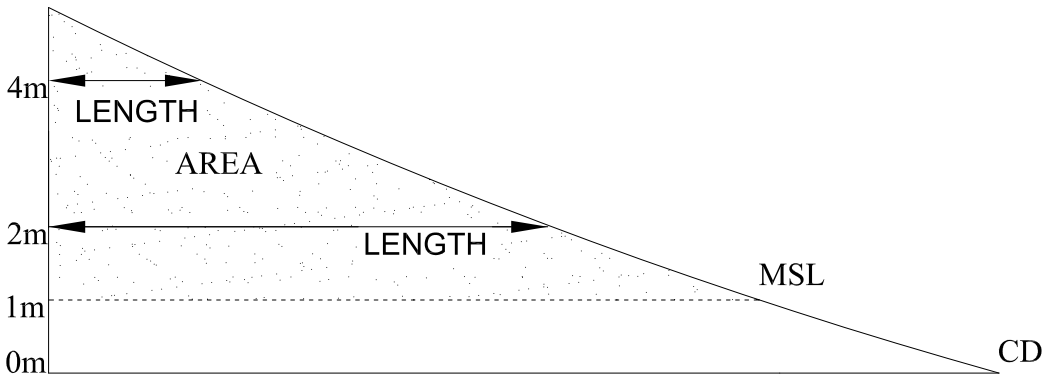

Figure 4.4: Beach profile area (volume per metre) above 1 m chart datum (CD) and profile length at the 2 m and 4 m CD contour.

beach recovery period. Ensemble averaged recovery periods and rates were estimated using three different groupings of data, namely:

- *Location grouped volume recovery:* The profiles were grouped together into blocks based on location, especially with regards to rivers. The groups created were: A – 23 shown in Fig. 4.2c, BR6 – BR10 and SB1 – SB5 indicated in Fig. 4.2b, DN6 – DN13, NC3 – NC10, NC34 – NC40 and NC41 – NC44 shown in Fig. 4.2a, SC11 – SC15, SC16 – SC24, SC25 – SC32 and SC33 – SC44 indicated in Fig. 4.2d. Ensemble averaged recovery periods and rates were then calculated for each location group.

- *Event grouped volume recovery:* The profiles were grouped into erosion events and then an average recovery period and rate were determined per event.

- *Individual profile volume recovery:* An average recovery period and rate was established for each profile by considering all the erosion events that the profile experienced.

A global recovery period and rate was calculated from the average of all three groupings.

Note that in some cases specific profiles could not be included in the above analysis because they were inconsistent in their responses and no recovery period or rate could be established. This is probably due to local sheltering effects.

4.2.2.2 Length recovery

Location group A – 23 was unique as it had the longest data record as well as being directly affected by the sand bypass scheme. Certain profiles within A – 23 have been recorded since 1973. The Durban Bight has historically been a major concern to the eThekwini Municipality as a result of the port's dredging activities. Profiles (1 – 23) were not useful in terms of recovery periods as they are dependent on the sand bypass volumes. Only profiles A – G were considered as they are furthest away from the sand pumping influence.

The lengths were not considered with the volumes as they are not truly representative of recoveries. This is because a change in length does not necessarily

mean a net change in the profile sediment amount and may simply describe an evolution in profile shape.

The extensive record of lengths were analysed differently to that of the volumes. The profile lengths at the 2 m CD and the 4 m CD contour (see Fig. 4.4) were analysed as they represent approximately the lower and upper bounds of the swash zone, respectively. A recovery period was defined as recovery to the average length instead of the pre-event average as in the case of the volume calculation.

The results in location group A – G were ensemble averaged by grouping according to events.

4.3 Results

Major events were defined as the profiles' lowest levels and did not necessarily coincide with the responsible storm event. The periods around 1998, 2004 and 2007 were identified as major erosion events between 1992 and 2009.

Before the results are presented, it must be noted that the majority of Durban's beach profiles have been showing a long-term decreasing trend [Corbella, 2010]. New erosion events are, therefore, recovering to lower average levels. One of the more extreme examples of this is shown in Fig. 4.5.

4.3.1 Sediment balance

The Durban Bight is affected by a sand bypass scheme (Fig. 4.2c). This provided the opportunity to identify erosion events by considering profile changes in conjunction with sand bypass volumes. The sediment balance is presented in Fig. 4.6 and shows the events of 1997, 2007 and 2003 (in descending order of erosion magnitude) to be the main erosion events. The 1997 event is also referred to as the 1998 event as this presented the lowest beach level following the 1997 event. Reference to the 2004 event similarly applies to the 2003 event. These events will be referred to as the major erosion events.

Figure 4.6 shows that 2005 was the only year that recorded a gain in volume. This is likely a result of the calm sea conditions and the fact that the beach volume was already at a low level. The percentage annual change in volume

relative to the previous year was used to identify major erosion events. The year 2007 had the largest percentage loss corresponding to a volume loss of 35 % of the previous year's volume. The year 1997 and 2003 accounted for a 33 % loss. Note that pumped volumes from the sand bypass scheme are included in the sediment balance so the loss of sand shown could have occurred even if the profile volumes increased.

The major erosion events are typically attributable to individual severe storms, while smaller storms may also play a secondary role. Storms in this context are defined as episodic events with significant wave heights exceeding 3.5 m [Corbella & Stretch, 2012a]. For example, the low level of sediment in 1998 was a result of a large storm in 1997 followed by several smaller storms in 1998. The low of 2004 similarly resulted from the second largest storm on record in 2001 followed by a series of smaller storms. The low in 2007 was the result of the largest storm on record. The severity of erosion events may also be due to the coincidence of high waves with a 4.4 yr extreme tidal cycle [Corbella & Stretch, 2012b]. The extreme and infrequent events tend to have a general impact on all the profiles while smaller storms may have more localized impacts. The smaller storms also occur more frequently as part of the normal wave climate and are, therefore, not expected to individually affect the recovery rates in a significant way. The recovery rates that are being recorded in this paper may, therefore, be linked directly to the largest storms and extreme tidal cycles that were the main factors underpinning the major erosion events.

4.3.2 Location grouped profile volumes

Table 4.1 shows the location and event grouped profile volumes. The Durban Bight (A – G) has a large variation in recovery period as its recovery is dependent on sand being delivered via the sand bypass scheme which is limited to operate when sand is available from the sand trap and when conditions are appropriate for dredging. This recovery period is also dependent on the significance of the erosion event. The recovery rate of the Durban Bight is also expected to have a large standard deviation for similar reasoning. The Durban Bight is obviously a unique portion of the coastline and may not be appropriate for comparing to the

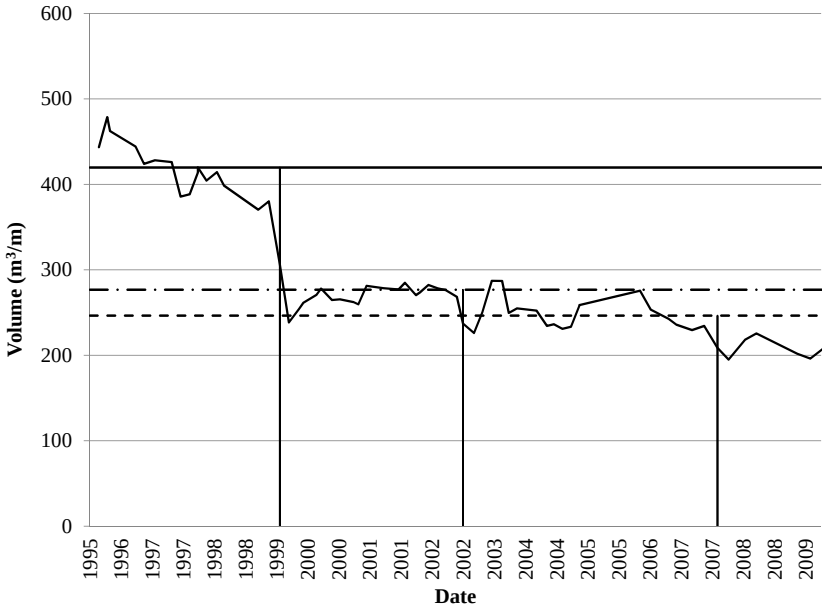

Figure 4.5: The moving average volume of profile DN6 in Durban North (–). The average profile levels prior to the following erosion events are shown: 29 June 1999 by the solid line; 4 December 2002 by the dashed and dotted line; 12 September 2007 by the dashed line.

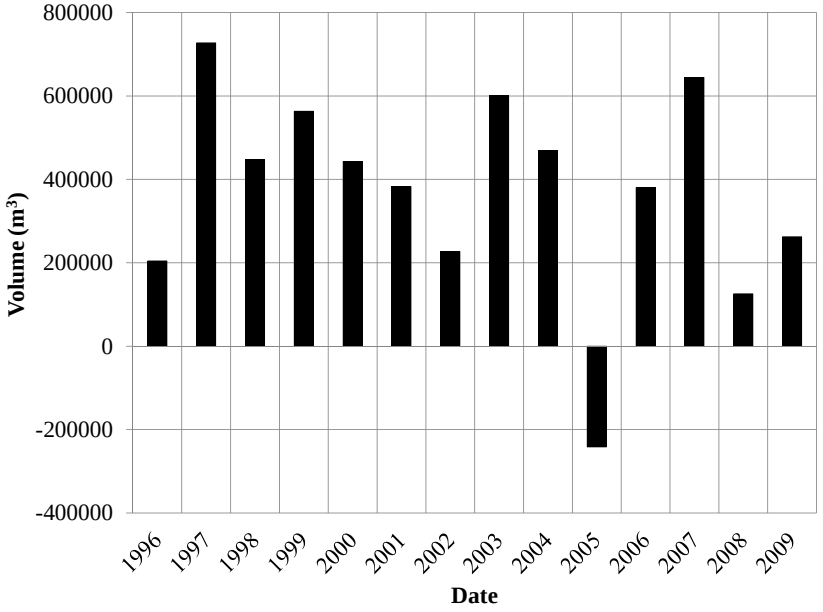

Figure 4.6: Annual sediment losses for the Durban Bight (A – 23) accounting the sediment volumes contributed by the sand bypass scheme.

remainder of the coast.

Excluding the Durban Bight, the average beach recovery period is 1.82 yr at a rate of 61.3 $m^3 m^{-1} yr^{-1}$ and the inclusive recovery period is 2.15 yr at a rate of 80.3 $m^3 m^{-1} yr^{-1}$. The results show that the different blocks recover differently from the same events. This difference in recoveries is the result of the different locations as well as that some blocks are more eroded than others from the same event. This suggests that erosion of a beach is dependent on the wave direction and orientation of a beach to the impending storm. It must be remembered that since the profiles show a decreasing trend, the 2007 event is generally recovering to a lower average profile level and, thus, may have a shorter recovery period relative to the other event.

It is interesting that the Bluff shows the shortest recovery time, but it has the slowest recovery rate. This would seem to imply that the Bluff beaches erode less from the events. This is only partly true, the reason they recover so quickly is a consequence of the majority of the beaches consisting of vegetated dunes (further discussed in Sect. 4.3.8) as well as the long-term erosion causing consequent recoveries at lower levels. This is visually depicted in Fig. 4.8 showing the pre-erosion event averages.

4.3.3 Event grouped profile volumes

It was evident from the location grouped recovery that recovery periods and rates are dependent on the profile location and the erosion event. Therefore, the profiles were divided into erosion events to establish how much the recovery periods and rates varied from the location groups.

The events with the largest recovery periods in descending order are 2007, 2004 and 1998 (see Table 4.2). The average recover period is 2 yr and the rate is 97.3 $m^3 m^{-1} yr^{-1}$. This is comparable with the averaged location grouped events.

Table 4.1: Location averaged profile recovery periods and rates for the Durban North, Bight and Bluff blocks and for the major erosion events

	Durban North (DN6 – DN13)		**Durban Bight (A – G)**		**Durban Bluff (BR6 – BR10)**	
Event	**Period (yr)**	**Rate ($m^3\,m^{-1}\,yr^{-1}$)**	**Period (yr)**	**Rate ($m^3\,m^{-1}\,yr^{-1}$)**	**Period (yr)**	**Rate ($m^3\,m^{-1}\,yr^{-1}$)**
1998	2.28	101	2.91	79.0	1.50	50.9
2004	1.82	64.3	2.52	92.6	2.19	45.4
2007	1.52	74.9	2.97	204	1.63	50.7
Std. Dev.	0.38	27.8	0.25	74.8	0.36	3.12
Mean	1.87	73.7	2.80	118	1.77	49.0

Table 4.2: Event grouped ensemble average recovery period and rate for the major erosion events

Event	**Period (yr)**	**Rate ($\mathbf{m^3\,m^{-1}\,yr^{-1}}$)**
1998	1.89	90.0
2004	2.13	57.9
2007	2.11	118
Std. Dev.	0.13	34.2
Mean	2.04	97.3

4.3.4 Individual profile volumes

Finally, to explore the recovery dependence on location, individual profile recovery was averaged across all erosion events. Figure 4.7 clearly demonstrates that the profiles are affected differently by storm events and also recover differently. Profiles E and F are adjacent to one another and are affected by the same events. Profile F recovers more than 4 times faster than profile E. This is a result of F having an exceptionally fast recovery following the 2007 event. This is a consequence of the location of low lying stormwater outfalls. Profile F is situated between two outfalls while E is immediately up-drift of an outfall (Fig. 4.2c). This causes E to erode less than F during storm events, but also results in it recovering slower. F, on the other hand, erodes more, but consequently recovers faster as sediment is trapped between the outfalls. Other location factors influencing recovery are identified in Sect. 4.3.8 concerning recovery from the 2007 event.

The average recovery period is 2.27 yr and the average rate is $104.2\,\mathrm{m^3\,m^{-1}\,yr^{-1}}$. Considering the averages in their location groups provides a very similar result. Analysis of the volumes once again showed that each profile reacts differently to erosion events as well as recovers differently.

4.3.5 Profile length recovery

The Durban Bight beach length data from 1973 to 2009 was put through a similar recovery analysis to that of the volumes. Once again the profiles 1 to 23 were not considered as they are thought to be too dependent on the sand bypass system.

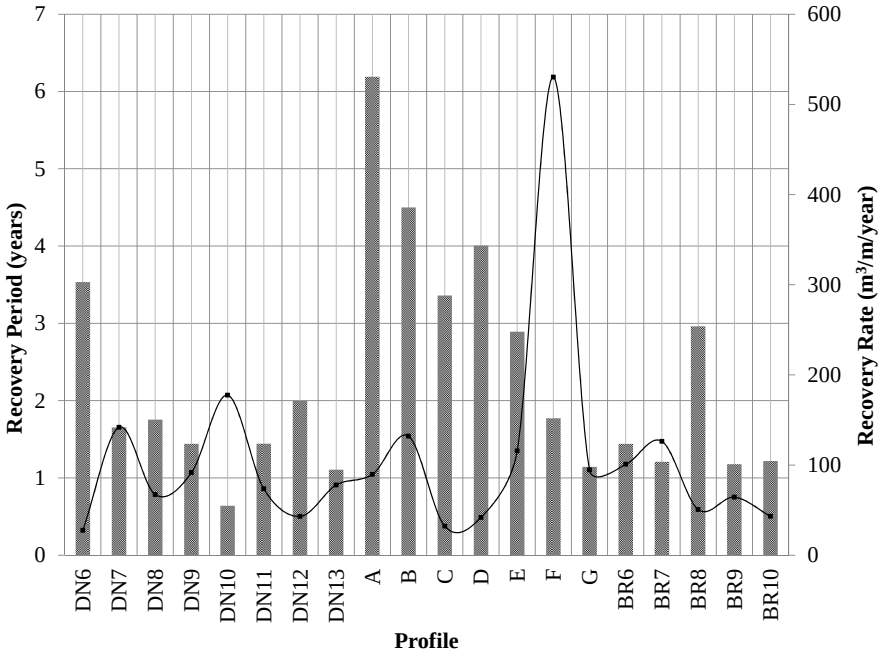

Figure 4.7: Profile area recovery period shown by the bar graph and recovery rate shown by the line graph.

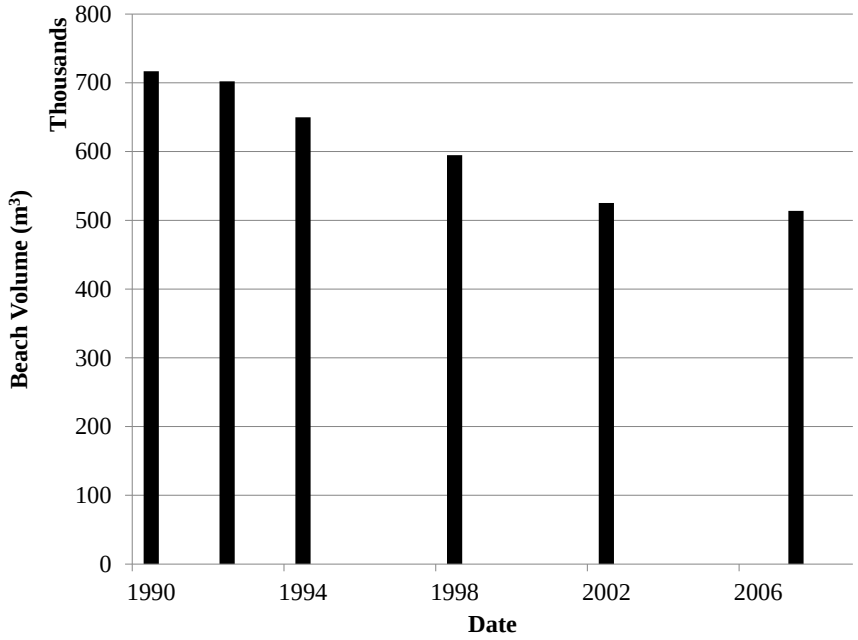

Figure 4.8: The Bluff Block (BR6 – BR10) average pre-erosion event volumes.

The 37-yr data set was significantly longer than the others and so the analysis was performed slightly differently to that of the volumes. Instead of creating a dynamic average that depends on the profiles pre-storm average, an average for all the profile lengths were created and this was used to establish a recovery period and rate.

The years 1980, 1986/1987, 1998 and 2007 were identified as significant erosion events. The recovery rates and periods were calculated and since they all made up the same location group they were averaged into events. The 2 m contour has an average recovery period of 1.3 yr and a standard deviation of 0.24 yr. It also recovers an average of $39.4\,\mathrm{m\,yr^{-1}}$. The standard deviations are relatively small for the 2 m contour with the 1979/1980 event being the only event responsible for a significantly longer recovery period. The 4 m contour length has a recovery period of 1.8 yr and a large standard deviation of 0.95 yr. The recovery rate is $26.6\,\mathrm{m\,yr^{-1}}$.

The difference in the recovery period between the 2 m CD contours and the 4 m CD contours is half a year. This demonstrates the effect of the beach morphology – although it may take only a year for the length to recover it may take much longer for the profile to recover to its pre-storm shape. This recovery process is what causes the perception of beach recovery. The beach is perceived to have recovered once it returns to its pre-storm length, but it is yet to recover to its full pre-storm cross-sectional volume.

4.3.6 Recovery comparison

Analysing the average recoveries of the profiles in different groups highlighted the different dependencies in erosion and recovery. The various recovery periods and rates were then compared and averaged to establish an appropriate global recovery period and rate for the coastline. Table 4.3 gives a summary of the results.

The volumes take between 1.82 and 2.27 yr to recover while the recovery rate is between 61.3 and 104 $\mathrm{m^3\,m^{-1}\,yr^{-1}}$. The blocks and profiles erode and recover differently as a result of location. This results in the beaches recovering from storm events in 1.5 to 2.5 yr, depending on their location. These are consistent

Table 4.3: Area recovery periods and recovery rates

Grouping Method	Average Recovery Period (yr)	Average Recover Rate ($m^3\,m^{-1}\,yr^{-1}$)
Location & event	1.82	61.3
Event	2.04	97.3
Profile	2.27	104
Mean	2.04	87.5

results since, by the end of 2009, the beaches had made a full visual recovery from the 2007 event although they had not entirely recovered (recall that the decreasing trend means it has recovered to a lower average level). Since the waves are very similar along the 100 km of coastline [Corbella & Stretch, 2012a], it is safe to assume that erosion and the subsequent recovery is highly dependent on the location of the profile. In this regard the bathymetry, proximity of rivers (Fig. 4.2) and orientation of the coast affects the sediment supply and the shoaling and refracting of waves.

4.3.7 Unrecovered profiles

Two factors responsible for long-term sediment loss, apart from sea level rise, are an overall decrease in sediment supply and the occurrence of multiple erosion events within the recovery period.

Reduced fluvial sediment supply to the coast in this region has been attributed to a combination of sediment mining and trapping of sediments in dams along rivers [CSIR, 2008]. Large episodic flood events also contribute major sediment inputs when lower river reaches are eroded [CSIR, 2008]. The last major regional flood event was in 1987 and the KwaZulu-Natal coastline may require another such event to counteract the chronic erosion.

If significant erosion events occur before a beach has recovered from previous events, the outcome will be a long-term decrease in sediment. Since there has not been any significant erosion events subsequent to the 2007 event, this factor cannot be considered in the analysis of that event.

Table 4.4 shows the profiles that do not recover before the next erosion event

Table 4.4: Unrecovered profiles from the corresponding erosion event

Event Year	Profile	Response
1996	A	Does not recover before next event
1998	DN6	Does not recover before next event
	DN7	Does not recover before next event
	DN9	Never recovers
	DN12	Does not recover before next event
	DN13	Does not recover before next event
	E	Does not recover before next event
	BR6	Does not recover before next event
	BR7	Does not recover before next event
	BR8	Does not recover before next event
2004	B	Does not recover before next event
2006	DN9	Does not recover before next event

or do not recover at all. The 1996, 2004 and 2006 erosion events virtually made a full recovery prior to the subsequent events, with only 5 % of the analysed profiles not recovering. The 1998 event was far more significant and over 6 yr 45 % of the analysed profiles were unable to recover. Only the Durban Bight, which is heavily stabilized and protected, recovers from the 1998 event before the 2004 event. The Durban North and Bluff beaches do not recover from the 1998 event before the 2007 event.

4.3.8 Recovery from the 2007 event

The recovery analysis demonstrated that the profiles recover differently depending on their location and the severity of the storm event. The recovery of all the profiles were analysed for the 2007 event to identify which physical features affect the recovery of beaches. Recovery periods were not calculated for profiles SC11 – SC44 and NC10 – NC35 because there was insufficient data to calculate a pre-erosion level. Figure 4.9 presents the recovery rates and the recovery periods.

It can be seen from Fig. 4.9 that of the northern beach profiles DN6 and DN8 are amongst the profiles that take the longest time to recover. This is thought to be a result of this stretch of coast being exposed to direct wave attack. Profiles A to D take the longest to recover. This is a result of them being dependent

on the sand bypass system and being the last beaches to receive the bypassed sediment subsequent to it being trapped by numerous outfalls and groynes along the way. In the Bluff area BR8 takes the longest time to recover. This appears to be a result of the rock outcrop in front of the profile that limits the deposition of sediment onto the beach profile. A stormwater outfall up-drift of the profile may also contribute to its slow recovery as a result of sediment being trapped.

Numerous profiles had extremely slow recovery rates. Slow recovery rates seem to be associated with open, unsheltered coastlines with rocky nearshore profiles. The main Umhlanga beach, NC3 – NC5, and NC36, the Bluff, BR6 – BR8, and the majority of the south coast, SC14 – SC33 are examples of this type of coastline. The recovery rates of BR6 and BR8 were further hindered by a large stormwater outfall intercepting sediment up-drift of their location. Profile SC21 is located between two rocky headlands. It has a slow recovery rate as a result of the up-drift headland starving the profile of sand as well as possible wave focusing as they are refracted around the headland creating a rip current which further erodes the profile. Two profiles, SC33 and SC25, have continued to lose sediment after the event and, therefore, have negative recovery rates. In the case of SC33 this is thought to be due to the large rock outcrop just up-drift of that location. The continued losses at profile SC25 are due to northward migration of the estuary mouth at that location which has significantly eroded the profile (see Fig. 4.2d and photographs provided in supplementary material). The high water table due to the perched back-barrier lagoon may also be contributing to on-going erosion.

Amongst the profiles with the shortest recovery periods were DN10, DN13, F and BR9. Profile DN13 has well established vegetated dunes while DN10 and BR9 have the same type of dune system as well as small outfalls that aid the trapping of sediment. A similar observation was made by Smith *et al.* [2010] who noted natural beaches recovered faster than urbanized coastlines. Profile F has an extremely fast recovery rate and, thus, a very short recovery period (only presented in Fig. 4.7 to allow for an appropriate scale in Fig. 4.9). Apart from the explanation given in Sect. 4.3.4, profile F was one of the few stretches of beach that had vegetated dune protection.

The profiles with the fastest recovery rates seem to be associated with beaches

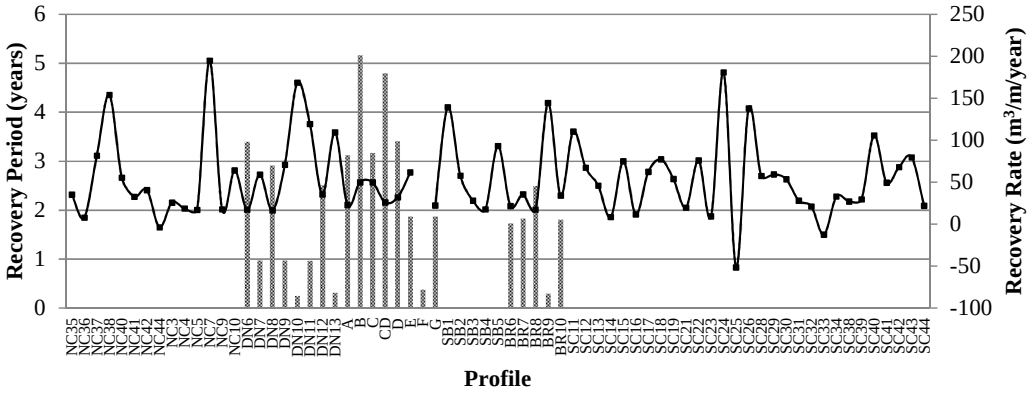

Figure 4.9: Profile volume recovery period and recovery rate of the 2007 event shown by the bar graph and line graph, respectively.

having densely vegetated dunes. Profiles NC38, NC7, DN10, F and BR9 are examples of this type of coast. Profile SB1 on the Bluff has a fast recovery as the storm is thought to have caused minimal erosion since the area consists of a rock revetment along the road and is enclosed by a large rock outcrop. As noted previously, profile BR9, DN10 and F are also affected by their proximity to stormwater outfalls. Profiles SC24 and SC26 are both down drift of river mouths and this sediment supply is thought to contribute to their rapid recovery.

The volumes took an average of 2.08 yr to recover at a rate of 62.2 $m^3\,m^{-1}\,yr^{-1}$. This is comparable with the recoveries from other events. Tables 4.5 shows a comparison of the volume recovery periods as well as the corresponding means. The average recovery time of the 2007 event was 2.08 yr.

It should be noted that 33 % of the analysed profiles had still not recovered from the 2007 event by the end of 2010 and their recovery periods are projected from their recovery rates. Although they have virtually recovered, they are still slightly below their pre-storm levels and in light of the long-term erosion trend many are not expected to ever recover.

Considering the location averaged areas, only the northern beaches do not fully recover which contribute to about a third of the recorded beach data. At the end of 2009, this was a noticeable feature of the KwaZulu-Natal coastline where there was visible evidence that the beaches had recovered, but still exhibited

Table 4.5: Average volume recovery periods

Areas	Average Recovery Period (yr)
Profile Areas	2.11
Location Areas	2.05
Mean	2.08

traces of the past event.

4.4 Discussion

The 2007 event was the largest event in 18 yr and although it showed profile recovery times ranging from 0.5 yr to potentially 6 yr it still suggests an average recovery time of 2 yr. This is similar to a global average calculated for all the major erosion events and is consistent with the findings of Choowong *et al.* [2009] and Liew *et al.* [2010] who found that the Thai coastline took two years to recover from the 2004 tsunami.

After erosion events, many of the profiles initially accrete very quickly creating the perception of recovery while as much as half may not yet have recovered. This is evident from the shorter recovery period associated with beach length. Morton *et al.* [1994] reported similar perceptions. The 2 m CD contour profile length recovery period is shorter than the 4 m CD contour length which in turn is shorter than the volume recovery. These recoveries imply that a full volumetric and geomorphic recovery of storm damaged beaches may require 4–5 yr as suggested by Morton *et al.* [1995].

It was found that open, rock sheltered coastlines (NC3 – NC5 and BR8) take longer to recover than the sandy vegetated dune coastlines (NC38, NC7, DN10, F and BR9). Although a rock outcrop in the nearshore zone protects beaches from eroding under normal conditions, it also restricts accretion after an extreme event such as the 2007 event. Profiles up-drift of perpendicular beach structures (F) recovered the fastest while down-drift profiles (BR6) eroded further in the aftermath of the erosion events. Perpendicular beach structures include headlands (SC21) which can also accentuate erosion before and after a storm event by

focusing waves. Liew *et al.* [2010] also observed variations in recoveries as a result of anthropogenic activities. Harris [2008] made similar observations with regards to intensely developed coastlines. The dunes of natural beaches aid recovery by providing a source of sand to replenish the eroded beach. During the storm event, the lower portion of the dune is stripped of vegetation. The destabilized dune then slowly collapses, contributing to the recovery. The remaining dune vegetation traps wind blown sediment and the dune recovers. These observations suggest that coastal managers should attempt to maintain natural coastlines with vegetated dunes.

River mouths and estuaries seem to influence the recovery of beaches (SC24 and SC26) by providing a replenishing supply of sediment. The influence of alluvial sediment is only evident in the later stage of recovery as the rapid initial recovery is from offshore sediments being returned to the shoreline. Even with the benefit of rivers, adjacent profiles are still considered as a management risk because the mouth can potentially migrate, especially after large storm events.

The profile recoveries demonstrate how both longshore and cross-shore transport processes contribute. The profiles that recover by both processes recover faster than those that only recover by one. This is evident from the profiles down-drift of stormwater outfalls and those sheltered by nearshore rock outcrops. The profiles down-drift of stormwater outfalls (BR6) can only recovery by cross-shore transport. The rock sheltered profiles (NC3 – NC5 and BR8) are not replenished by cross-shore transport and can only recover from longshore transport. CSIR [2008] estimated the longshore transport along the Bluff (SB1 – BR13) as $460\,000\,\mathrm{m^3\,yr^{-1}}$, along the Bight (A – 23) as $260\,000\,\mathrm{m^3\,yr^{-1}}$ and north of the Umgeni River (Fig. 4.2a) as $315\,000\,\mathrm{m^3\,yr^{-1}}$. The Bluff may recover faster than the northern beaches because it has a larger longshore sediment transport rate. However, this cannot explain why profiles A – G recover fastest while having the smallest longshore transport, which suggests that cross-shore processes contribute more to recovery in this instance.

Short [1999] presented various indices for the classification of beach types as reflective, intermediate or dissipative. Harris [2008] used these indices to characterise the KwaZulu-Natal beaches. Considering our division of the study area, the Durban Bight (A – G) beaches are mainly intermediate with dissipative beaches

being restricted to the southern end of the Durban Bight (1 – 23) while the southern (BR6 – BR10) and northern (DN6 – DN13) beaches are largely reflective. Reflective, intermediate and dissipative beaches are characterised by potentially low, medium and high cross-shore sediment transport, respectively [Short, 1999]. These characterisations explain why the southern and northern beaches have a slow recovery rate and the intermediate central beaches have a relatively faster recovery rate. Unfortunately the dissipative beaches are the ones influenced by the sand bypass scheme and so do not represent a natural recovery. Based on the analysed data, it can be generalized that the profile areas above 1 m CD of reflective beaches recover approximately $60\,\mathrm{m^3\,m^{-1}\,yr^{-1}}$ and intermediate beaches recover approximately $120\,\mathrm{m^3\,m^{-1}\,yr^{-1}}$ along the KwaZulu-Natal coast.

The dependance of recovery rates on the beach type can also be linked to sediment grain size. Based on two sediment samples taken in 2007 for all the profiles the average D_{50} grain sizes were 0.88 mm on the northern beaches (N6 – NC44), 0.38 mm on the Durban Bight (A – G) and 0.43 mm on the southern beaches (SB1 – SC44). This implies that finer sediments are associated with faster recovery which can be attributed to the fact that they are more readily suspended and transported. Sediment grain sizes also affect the beach slope and, thus, determine whether the beach is reflective, intermediate or dissipative.

4.5 Conclusion

We have analysed 37 yr of beach profile data. Profile lengths and volumes were calculated along with their pre-erosion average levels. These were then used to determine recovery rates and recovery periods. The recovery of storm damaged beaches has been shown to be dependent on the location of the beach and the severity of the storm event.

The beaches in the case study were found to take an average of two years to recover at a rate of about $90\,\mathrm{m^3\,m^{-1}\,yr^{-1}}$. Long-term (chronic) sediment loss was identified in cases where storm damaged beaches have not recovered to pre-erosion levels. Beach profiles with vegetated dunes (NC38, NC7, DN10, F and BR9) recovered faster than urbanized beaches (G). Perpendicular beach structures have both positive (F) and negative (SC21) effects on beach recovery. Coastlines with

rock outcrops in the surf zone (BR8) tend to recover slowly. These observations are consistent with simple physical arguments concerning the roles of longshore and cross-shore sediment transport processes, the effect of different sediment characteristics, and with changes in the overall supply of fluvial sediments to the coastal zone. We, therefore, expect that the results from our case study may be widely applicable.

Considering the observed differences in recovery rates, even for profiles that erode similarly, it is recommended that the recovery period of post storm profiles be included in risk analyses for coastal development. A fast recovering profile possesses less of a development risk than a slow recovering profile since it has a smaller probability of experiencing a subsequent erosion event before it has recovered from the initial event.

The results reported here may have important applications for the management of vulnerable coastlines.

References

Barnett, K. A.: The Management of Durban's Beaches: An Historical Perspective, Fifth International Conference of Coastal and Port Engineering in Developing Countries, COPEDEC V, Cape Town, 19 – 25 April 1999, 1999. 87, 249, 277

Callaghan, D. P., Nielsen, P., Short, A., and Ranasinghe, R.: Statistical simulation of wave climate and extreme beach erosion, Coast. Eng., 55, 375 – 390, 2009. 20, 31, 58, 85, 121, 155, 182, 191, 192, 207, 236

Callaghan, D. P., Ranasinghe, R., and Short, A.: Quantifying the storm erosion hazard for coastal planning, Coast. Eng., 56, 90 – 93, 2009. 85

Choowong, M., Phantuwongraj, S., Charoentitirat, T., Chutakositkanon, V., Yumuang, S., and Charusiri, P.: Beach recovery after 2004 Indian Ocean tsunami from Phang-nga, Thailand, Geomorphology, 104, 134 – 142, 2009. 17, 86, 105

Cooper, J. A. G. and McKenna, J.: Social justice in coastal erosion management: The temporal and spatial dimensions, Geoforum, 39, 294 – 306, 2008. 86

Corbella, S.: A review of Durban's wave climate and storm induced changes, M.Sc, University of KwaZulu-Natal, Durban, 308 pp., 2010. 93

Corbella, S. & Stretch, D. D.: The wave climate on the KwaZulu-Natal coast of South Africa, J. S. Afr. Inst. Civ. Eng., 54 (2), 45 – 54, 2012a. 94, 101, 155, 183, 220

Corbella, S. & Stretch, D. D.: Decadal trends in beach morphology on the east coast of southern Africa and likely causative factors, Nat. Haz. Earth Sys. Sci., 12, 2515 – 2527, 2012b. 94, 183, 186, 196, 199, 204, 205

CSIR : Sand Supply from Rivers within the eThekwini Jurisdiction, implications for coastal sand budgets and resource economics, Report No. CSIR/NRE/ECO/ER/2008/0096/C, Stellenbosch, 2008. 16, 51, 87, 101, 106, 139, 140

De Michele, C., Salvadori, G., Passoni, G., & Vezzoli, R.: A multivariate model of sea storms using copulas, Coast. Eng., 54, 734 – 751, 2007. 85

Durgappa, R.: Coastal protection works, Seventh International Conference of Coastal and Port Engineering in Developing Countries, COPEDEC VII, Dubai, 1 – 15 March 2008, 97, 2008. 85, 246, 275

Forbes, D. L., Parkes, G. S., Manson, G. K., & Ketch, L. A.: Storms and shoreline retreat in the southern Gulf of St. Lawrence, Mar. Geol., 210, 169 – 204, 2004. 16, 17, 85, 86

GESAMP: Anthropogenic Influences on Sediment Discharge to the Coastal Zone and Environmental Consequences, Joint Group of Experts on the Scientific Aspects of Marine Environmental Protection (GESAMP), GESAMP Reports and Studies No 52, UNESCO, 1994. 16, 86, 114

Gracia, V., Morón, D., Jiménez, J. A., Guillén, J., Palanques, A., & Sanchez-Arcilla, A.: Near-bottom transport seaward of the surf zone under storms: On the role of currents, wind and infragravity waves in microtidal environments, Proceedings of the 28th International Coastal Engineering Conference, Cardiff, 7 – 12 July 2002, 2, 2517 – 2527, 2002. 17, 86

Harris, L. R.: The ecological implications of sea-level rise and storms for sandy beaches in KwaZulu-Natal, M.Sc, University of KwaZulu-Natal, Westville, 184 pp., 2008. 106

Houser, C., Hapke, C., & Hamilton, S.: Controls on coastal dune morphology, shoreline erosion and barrier island response to extreme storms, Geomorphology, 100, 223 – 240, 2008. 17, 86

Kriebel, D. L. & Dean, R. G.: Convolution method for time-dependent beach-profile response J. Waterway Port. C. Ocean Eng., 119 (2), 204 – 226, 1993. 31, 85, 182, 191, 204, 207, 228

Liew, S. C., Gupta, A., Wong, P. P., & Kwoh, L. K.: Recovery from a large tsunami mapped over time: The Aceh coast, Sumatra, Geomorphology, 114, 520 – 529, 2010. 17, 86, 105, 106

Miller, J. K. & Dean, R. G.: A simple new shoreline change model, Coast. Eng., 51, 531 – 556, 2004. 85

Morton, R. A., Gibeaut, J. C., & Paine, J. G.: Meso-scale transfer of sand during and after storms: implications for prediction of shoreline movement, Mar. Geol., 126, 161 – 179, 1995. 17, 86, 105

Morton, R. A., Paine, J. G., & Gibeaut, J. C.: Stages and Durations of Post-Storm Beach Recovery, Southeastern Texas Coast, U.S.A., J. Coast. Res., 10, 4, 884 – 908, 1994. 17, 86, 105

Otter, H. S. & Capobianco, M.: Uncertainty in integrated coastal zone management, J. Coastal Conservation, 6, 23–32, 2000. 86

Shepard, F. P.: Longshore Bars and Longshore Troughs, Technical Memorandum 41, Beach Erosion Board, U.S. Army Corps of Engineers, Washington, DC., 1950. 17, 86

Schoonees, J. S.: Annual variation in the net longshore sediment transport rate, Coast. Eng., 40, 141 – 160, 2000. 87

Smith, A. M., Mather, A. A., Bundy, S. C., Cooper, J. A. G., Guastella, L. A., Ramsay, P. J., & Theron, A.: Contrasting styles of swell-driven coastal erosion: examples from KwaZulu-Natal, South Africa, Geol. Mag., 1 – 14, Cambridge University Press, 2010. 51, 103

Short, A. D.: Handbook of Beach and Shoreface Morphodynamics, John Wiley & Sons, Chichester, 379 pp., 1999. 106, 107

van Gent, M. R. A., van Thiel de Vries, J. S. M., Coeveld, E. M., de Vroeg, J. H., & van de Graaff, J.: Large-scale dune erosion tests to study the influence of wave periods, Coast. Eng., 55, 1041 – 1051, 2008. 85

van Rijn, L. C.: Prediction of dune erosion due to storms, Coast. Eng., 56, 441 – 457, 2009. 85

van Thiel de Vries, J. S. M., van Gent, M. R. A., Walstra, D. J. R., Reniers, A. J. H. M.: Analysis of dune erosion processes in large-scale flume experiments, Coastal Engineering, 55, 1028 – 1040, 2008. 85

Chapter 5

Decadal trends in beach morphology on the east coast of southern Africa and likely causative factors

This chapter is based on a paper published in Natural Hazards and Earth System Sciences, 12, 2515 – 2527, 2012.

Abstract

Sandy shorelines are dynamic with constant changes that can cause hazards in developed areas. The causes of change may be both natural or anthropogenic. This paper evaluates evidence for shoreline changes and their causative factors using a case study on the east coast of South Africa. Beach morphology trends were found to be location specific but overall the beaches show a receding trend. It was hypothesized that wave, tide, sea level and wind trends as well as anthropogenic influences are causative factors and their contributions to shoreline changes were evaluated. Maximum significant wave heights, average wave direction, peak pe-

riod and storm event frequencies all show weak increasing trends but only the increases in peak period and change in wave direction are statistically significant. The chronic beach erosion cannot be attributed to wave climate changes since they are still too small to explain the observations. Instead the impacts of sea level rise and reductions in the supply of beach sediments are suggested as the main causative factors. The analysis also identifies a trend in the frequency of severe erosion events due to storms that coincide with a 4.5-yr extreme tide cycle, which demonstrates the potential impact of future sea level rise.

5.1 Introduction

Shoreline erosion has long been a concern to engineers [Kinmont *et al.*, 1954]. Long term erosion of a coastline has three main causes – sea level rise [e.g. Han *et al.*, 2010; Mather, 2008], meterological changes [Rouault *et al.*, 2009, 2010] that may result in wave climate changes, and a reduction in sediment supply. Woodroffe [2003] identified waves as the principal energy source for erosion in the coastal zone, while erosion due to an increase in water level is a well-developed concept [Bruun, 1962]. Zhang *et al.* [2004] analyzed the recovery of the U.S East Coast barrier beaches and found that the beaches recovered to their long term trend positions after storms regardless of storm severity. It was concluded that storm events are not responsible for long term coastal erosion. Zhang *et al.* [2004] stated that since no evidence has been given to show significant increases in storminess and since human interference is neither worldwide in extent nor uniform regionally, sea level rise is the most plausible contributor. It is worth noting that this statement may not consider dams and sediment mining on rivers that are arguably a worldwide human interference and contribute to long term coastal erosion. Singh [1997] has previously analysed beach profile data from Trinidad and Tobago in an attempt to identify climate related changes. Wave data was not considered and Singh [1997] identified significant erosion. Since anthropogenic impacts such as sediment mining are not an issue in Trinidad it was speculated that the erosion was from sea level rise.

Rivers play an important role in sediment supply and have been estimated to supply 80 % of the global beach sediment [GESAMP, 1994]. Reduction in

sediment yield from rivers may be natural and anthropogenic. River sediments are exported to the sea almost exclusively during large floods [Hsu *et al.*, 2004; Rovira *et al.*, 2005] and so steady erosion trends may exist between these episodic flood events. Anthropogenic impacts on fluvial yield has become a global concern and sediment mining and damming of rivers have been identified as significant impacts. Recent examples of related international research include Dai *et al.* [2008]; Dang *et al.* [2010]; Huang [2011]; Liquete *et al.* [2009].

In March 2007 the KwaZulu-Natal coastline on the east coast of South Africa suffered severe erosion due to an extreme storm event. This event stimulated local debate on whether the wave climate on the east coast of South Africa had changed causing more serious wave impacts more often. Changing wave climates have been investigated by numerous authors. In the northern hemisphere Wang & Swail [2001, 2002] and Wang *et al.* [2004a] found that between 1958 and 1997 changes did occur in winter and autumn significant wave heights. Wang *et al.* [2004b] found that in the past half century, the changes feature a significant increase in the number of strong winter and spring cyclones over the North Pacific, and of strong autumn and winter cyclones in the North Atlantic. Analysis of a 45-yr high resolution hindcast for the North Sea by Weisse & Stawarz [2004] showed that storm activity and extreme wave heights had increased from about 1960 onwards. Keim *et al.* [2004] concluded from their study of global climate models and empirical records that the past two decades have shown a decrease in the frequency of tropical storms but that there is a strong suggestion of an increase in the frequency of very strong (extreme) storms. Komar & Allan [2008] analysed 30 years of records from 3 wave buoys in the Atlantic. They found that there has been an increase in the number of occurrences of waves exceeding 3 m, those generated by hurricanes, and in particular the most extreme significant wave heights recorded. Theron *et al.* [2010] analysed wave data from Slangkop in South Africa and found that significant wave heights of storm events were increasing. There is uncertainty as to whether the above-mentioned documented trends are a result of anthropogenic climate change or are part of natural cycles [Ruggiero *et al.*, 2010].

Decadal trends in beach morphology need to be considered in formulating coastal management plans to mitigate future risks. Through a case study of the

east coast of South Africa, this paper aims to evaluate evidence for (1) trends in shoreline/beach evolution; (2) changes in wave climate such as trends in wave parameters and/or the frequency of extreme events; (3) links between shoreline/beach changes and wave climate trends or other causative factors.

5.2 Methods

5.2.1 Case study site

The city of Durban is a popular tourist destination on the east coast of South Africa (Fig. 5.1). Like many coastal cities Durban is concerned about the risks posed by wave and sediment trends. The eThekwini Municipality (Durban's local authority) has adopted a pro-active approach to addressing climate change issues and has recently begun to quantify the potential impacts. Mather [2007] initiated this process when he analysed South African tide gauge recordings from between 1970 and 2003. He found that sea level rise in Durban is 2.7 mm $\pm$ 0.05 mm per year at a 95% confidence level. A rise in sea level combined with possible changes in wave characteristics can cause significant impacts. This has motivated further research into the trends of the east coast wave climate and erosion of its beach profiles.

5.2.2 Beach profile data and analysis

The Durban Bight (Profiles A – 23 in Fig. 5.3a) has historically suffered from erosion as a result of the adjacent harbour activities (Sect. 9.2). Consequentially the Bight has a comprehensive data set from 1973. As the Municipality grew so did the monitoring of profiles and some profiles have been introduced to the monitoring programme as recently as 2007. The analysis of the profiles was restricted to those with data including or preceding the year 1992. The profiles are measured at least every 3 months using a theodolite referenced to fixed benchmarks. Profile lengths were analysed at the 1 m, 2 m and 4 m relative to chart datum (CD) contours as they approximate the swash zone. Profile areas (volume per meter) and beach volumes were also analysed and were calculated above 1 m CD

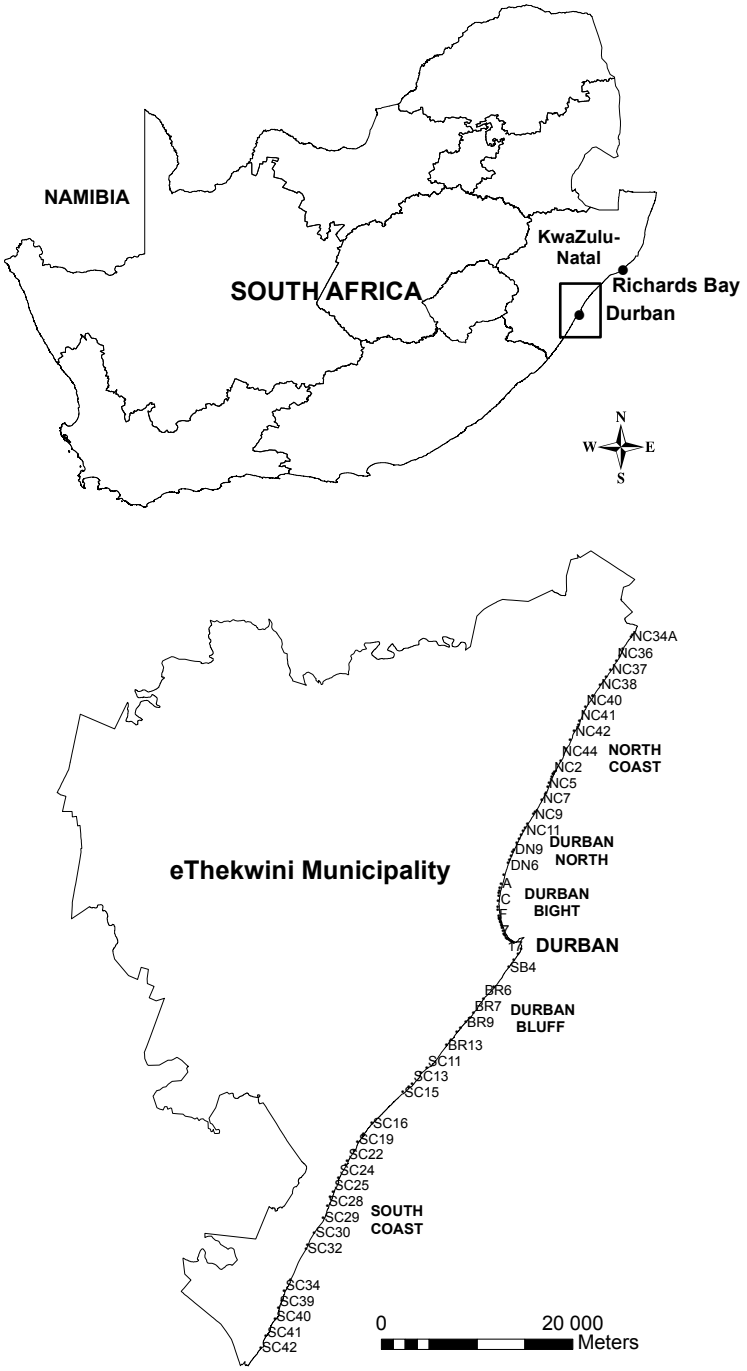

Figure 5.1: A map of the South African coastline showing the location of the case study site at Durban and Richards Bay and a map of the eThekwini Municipality showing the beach profiles

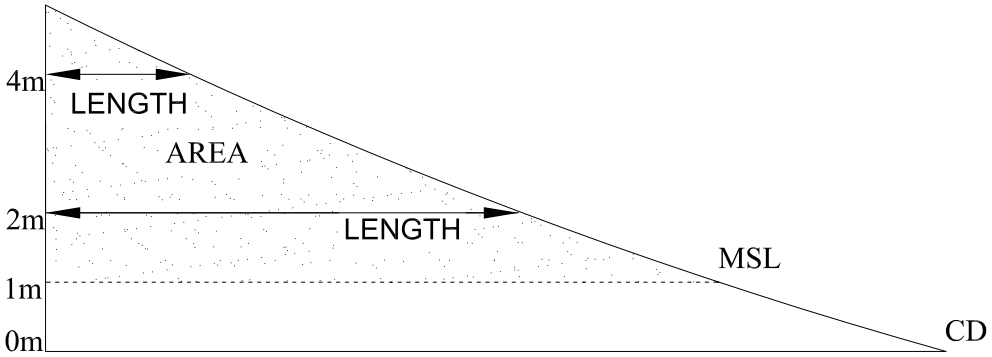

Figure 5.2: Beach profile area (volume per meter) above 1 m chart datum (CD) (approximately mean sea level, MSL) and beach profile length at the 2 m and 4 m CD contour

(about mean sea level at this location). The definition of profile area or volume per meter and profile length are shown in Fig. 5.2. The beach volume was calculated from the profile areas and the distances between the profiles using the end areas method.

The available data can be summarized as comprising three time histories: (1) a time series of profile lengths at the 1 m, 2 m and 4 m CD contour; (2) a time series of profile areas or volumes per meter; and (3) a time series of beach volumes.

5.2.3 Singular spectrum analysis

Singular spectrum analyses (SSA) was performed on the profiles' time series to filter the data and identify any trends. SSA decomposes a time series into a sum of constituent parts that characterize variations over different time scales. The reader is referred to Golyandina *et al.* [2001] or Hassani [2007] for detailed descriptions of SSA.

SSA was done on all the profile data from 1973 to 2009 and from 1995 to 2009. The beach profiles were grouped into blocks based on their position and data record. Four blocks were created: B – F; 1 – 18; 19 – 23; BR6 – BR9 (see Fig. 5.3). The end areas method was then used to create block volumes. A single slowly varying eigenvector was used to approximate the volume time series trends.

Figure 5.3: Locations of beach profiles and wave recording instruments. Coordinate system: Lo 31 WGS84. (a) Profiles A to 23 of the Durban Bight and the Durban Waverider Buoy (b) Profiles BR6 to BR10 of the Durban Bluff Beaches and the Durban ADCP.

SSA was also used to gauge the appropriateness of inferring a cause and effect relationship between sea storm trends and erosion trends. Wave height and tidal trends were compared to the four block volumes and Kendall's τ_B correlation coefficients were used to identify their association. Finally, SSA was used to analyze the trends in local wind speed data for the period 1995 to 2009 and to assess any influence on erosion trends.

5.2.4 Wave and wind data

Rossouw [1984] reviewed all of South Africa's then available wave data and concluded that only the wave recording buoy (Datawell's Waverider Buoy) data was reliable enough to use for design work. This limited Durban's wave data set to 18 years between 1992 and 2009 from two Waverider buoys and an acoustic doppler current profiler (ADCP). The two Durban Waveriders have a comprehensive set of data while the Durban ADCP data has large gaps and is measured at a shallower water depth than the other instruments (Table 5.1). Diedericks [2009] found that the Richards Bay Waverider (the buoy is sited 170 km north-east of Durban, Fig. 3.1) data has a good correlation with Durban's data. His conclusions were verified by finding a Pearson correlation between the Richards Bay's data, Durban's Waveriders and the ADCP. There is a strong correlation between the Waveriders but not the ADCP. The Richards Bay data was therefore used in place of the ADCP as well as to supplement any missing data. Since any trends in the Durban data may represent the shoaling and refraction effects of waves being recorded in different water depths, the Richards Bay data were also analysed to confirm the results of the Durban data. The Durban data will be the focus of this paper and the Richards Bay data will only be refered to as required.

The Waveriders sample at a rate of 10 Hz and wave statistics are calculated at 102 second intervals. The maximum wave parameters were then extracted at three hour intervals and the following parameters were analysed annually and seasonally: The maximum wave height H_{max} is the largest wave recorded in a recording period; the significant wave height H_s which in deep water is equal to $4\sqrt{mo}$ where mo is the area under the wave spectrum; the peak period T_p is the period at which the maximum energy density occurs and is the inverse of the

Table 5.1: Historical wave recording instruments, their operating periods and water depth.

Instrument	Period of operation	Depth (m)
Durban Waverider	1992 – 2001	42
Durban ADCP	2002 – 2006	15
Durban Waverider	2007 – 2009	30
Richards Bay Waverider	1992 – 2009	22

peak energy frequency f_p, $T_p = 1/f_p$ and the average peak period and average significant wave height. The average wave direction is the azimuth from true north and was analyzed as a vector of significant wave height.

Storm events were also analyzed in terms of occurrence, duration and calm period. A storm event was defined as a wave event that exceeded a 3.5 m significant wave height. The duration was defined as the time from when the significant wave heights exceeded the 3.5 m threshold until the significant wave heights fell below this threshold for at least two weeks. The two week interval is intended to ensure independent consecutive storm events and is similar to that used in previous work (e.g. Callaghan *et al.* [2008]. The Spearman autocorrelation coefficient of H_s shows a decay to low values (< 0.1) within two weeks which supports the assumption that the selected storm events are statistically independent. The calm period was defined as the time between consecutive storm events.

A linear regression analysis was performed on the wave data to evaluate trends.

Wind measurements at 20 minute intervals from the Durban port were obtained for the years 1995 and 2009. The measurements were at elevations between 80 m and 90 m above sea level. The data was corrected for altitude using a $1/7^{th}$ power law approximation for the velocity profile. Wind data were analysed similarly to the wave data using a threshold value of 14 m/s.

5.3 Results

5.3.1 Beach Profile trends

The profile trends were extracted from the beach volume time series using SSA. The trends were limited to a single slowly varying eigenvector. Figure 5.4 shows the time series for the block volumes of B – F, 1 – 18, 19 – 23 and BR6 – BR9. Figure 5.4 illustrates that beaches have been eroding over the 37 year period in an approximately linear manner. Blocks B – F, 1 – 18 and 19 – 23 have more erratic beach volumes relative to BR6 – BR9. This is because they are more strongly influenced by the harbour sand bypass scheme and the beach profile evolution is unnatural.

5.3.2 Quantifying long term trends

Following the results of the singular spectrum analysis it was evident that the long term trends could be approximated by a linear trend. Long term beach profile trends were therefore analyzed using linear regression. Figure 5.5 shows the results of the long term analysis of profile volumes per meter from 1973/1988 to 2009. Figure 5.6 similarly shows the results from 1995 to 2009. The majority of the central beach profiles (4 to 18) have been increasing over the past 37 years (Fig. 5.5). This is expected as it is an area intensely managed by the eThekwini Municipality in an attempt to mitigate the erosion potential developed by the harbour breakwaters and maintenance dredging. The Vetch's Bight (19 to 23) and the majority of the Bluff beaches (BR6 to BR10) have been receding over the years (Fig. 5.5 & Fig. 5.6).

Table 5.2 shows the percentage of profiles with regards to volume and length that have increasing or decreasing trends. The percentage of statistically significant trends is also shown. Statistically significant trends are defined as trends whose 95 % confidence intervals have the same signs. Over 37 and years (1973 to 2009) the length of the 2 m and 4 m CD contours has been increasing for almost 60 % of the profiles (Table 5.2). However over the same time period almost 60 % of the profile areas and 100 % of the beach volumes have been decreasing. This implies that the 2 m and 4 m CD contours describe profile shape changes but not

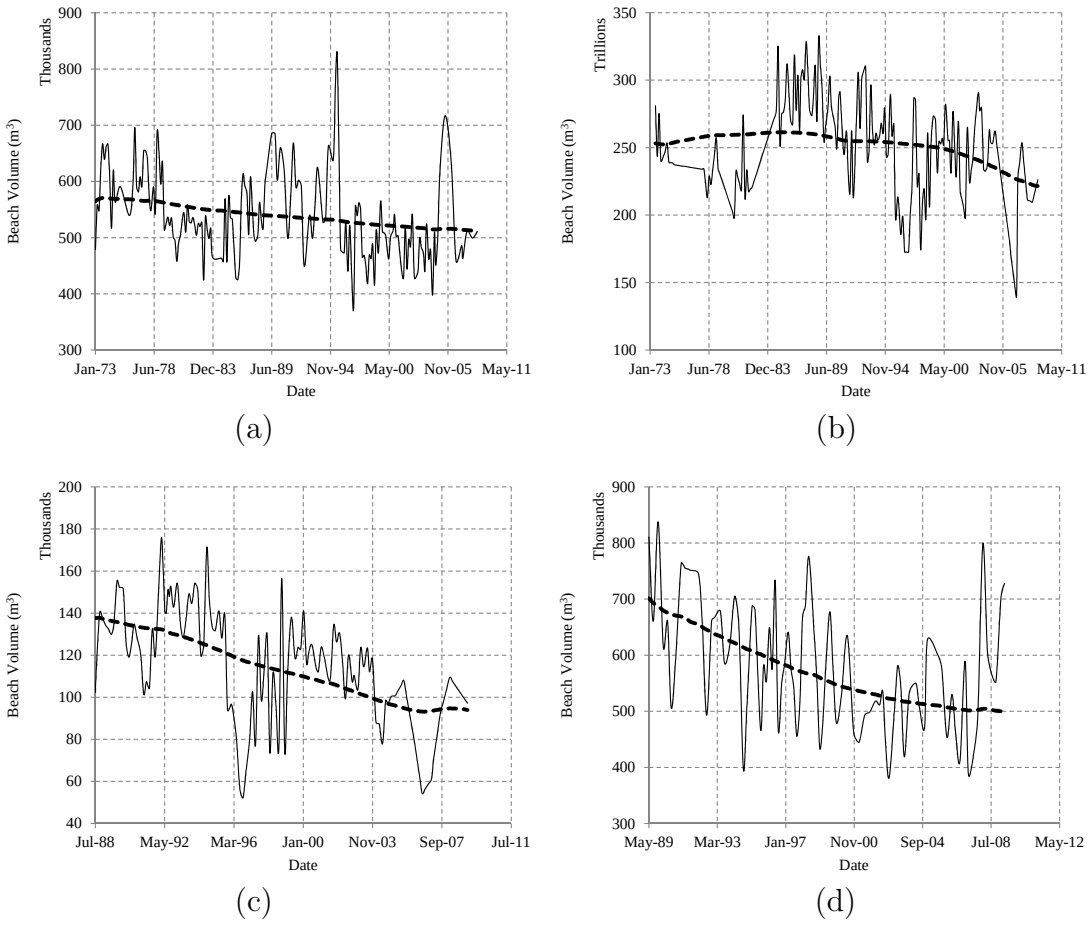

Figure 5.4: Singular Spectrum Analysis of beach volume blocks showing the original time series by the solid line and the reconstructed time series shown by the dashed line. Each data point represents a 3 month interval. (a) Block Volume B – F, (b) Block Volume 1 – 18, (c) Block Volume 19 – 23, (d) Block Volume BR6 – BR9 (refer to Fig. 5.3)

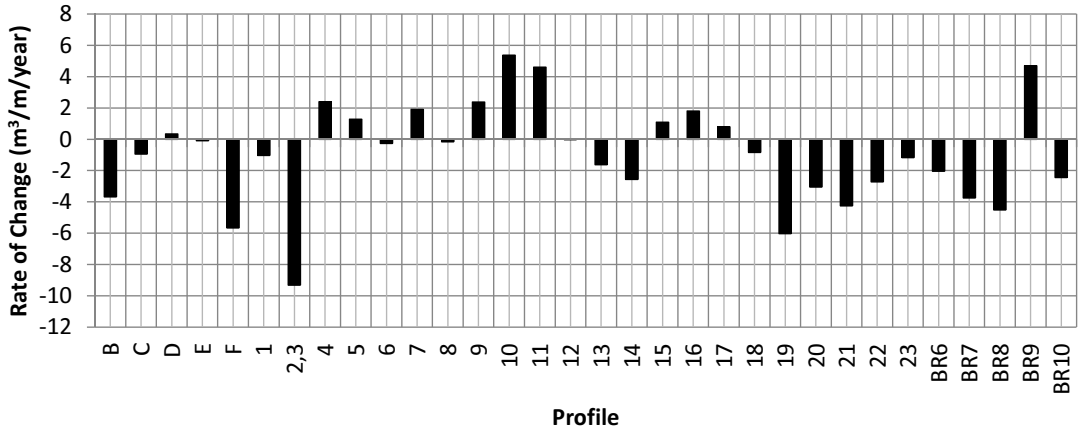

Figure 5.5: Profile volume per meter annual rate of change (1973/1988-2009)

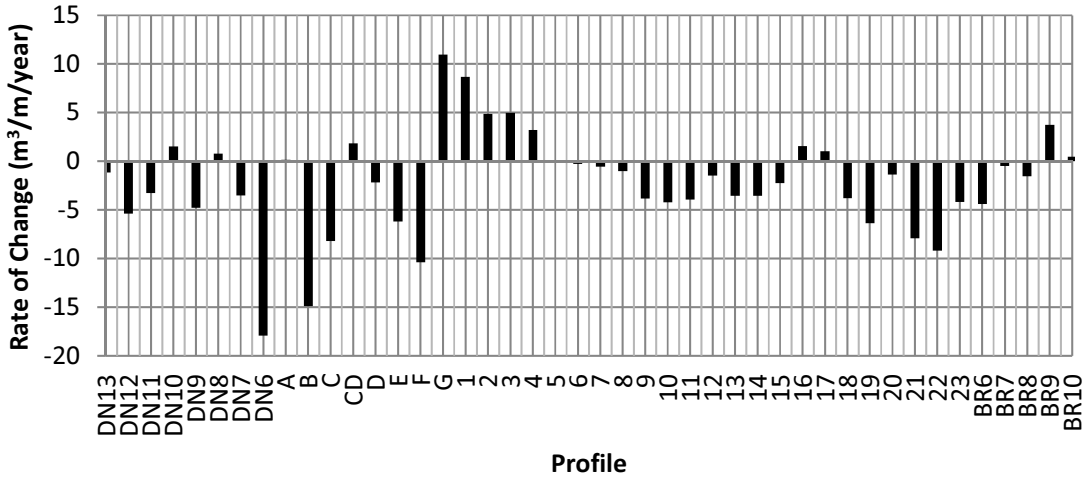

Figure 5.6: Profile volume per meter annual rate of change (1995-2009)

losses or gains. The volume per meter and volume measurements are therefore more appropriate for quantifying long term erosion trends.

The 15 years (1995 to 2009) of data show approximately 70 % of the profiles to be decreasing in terms of length and area.

5.3.2.1 Beach gains

From Fig. 5.6 it can be seen that the beaches have had significant gains from profiles G to 4 in descending order. This is a result of stormwater outfalls stretching across the shoreline. Profile 4 marks the location of the Bay of Plenty groyne. Profile 1 corresponds to Somtseu Road stormwater outfall and profile G is Argyle Road stormwater outfall. Profile BR9 and BR10 are the only profiles in the Bluff region that have accreted, which is also a result of stormwater outfalls. Unlike the semi-permeable Bay of Plenty groyne which is designed to retard the littoral transport, the stormwater outfalls are intended only for discharging stormwater into the ocean. However the large concrete stormwater outfalls intercept the littoral transport and trap sand on their up-drift sides. This causes accretion on the up-drift beaches but consequentially starves down-drift beaches and induces erosion.

5.3.2.2 Beach losses

Other than isolated gains Fig. 5.5 and Fig. 5.6 show that most of the profiles have lost sediment. It is no surprise that north of the groyne field (G and 4) there is a high loss rate which decreases gradually until it becomes a gain at profile CD. As previously explained this happens because the groynes trap sediment on their up-drift side and starve the down-drift beaches of sediment. The remaining profile losses cannot be attributed to beach structures. They could be the result of a reduction in sediment supply to the beaches or a result of increased frequency and or intensity of storms. The potential contribution of these three factors is discussed in Sect. 5.3.5 to Sect. 5.3.8.

Table 5.2: Type of trend experienced by the beach length at the 2 m and 4 m CD contour, volume per meter and volume during the period of 1973/1988 to 2009 and the beach length at the 1 m CD contour and volume per meter during the period of 1995 to 2009. The percentage of data contributing to the type of trend is shown as well as the percentage of statistically significant data

Trend		**Increase**		**Decrease**	
Time Period	**Measurement**	**Data (%)**	**Statistically Significant (%)**	**Data (%)**	**Statistically Significant (%)**
1973/1988 – 2009	Length (2 m CD)	59	90	41	79
	Length (4 m CD)	56	84	44	80
	Volume per meter	33	91	67	77
	Volume	0	NA	100	100
1995 – 2009	Length (1 m CD)	27	25	73	53
	Volume per meter	30	46	70	58

5.3.3 Wave parameter trends

Tables 5.3 and 5.4 show the annual rate of change of wave parameters over the past 18 years for Durban and Richards Bay respectively. Wave directions were only measured at Durban after 2002 while Richards Bay has wave direction data from 1997 onwards.

Table 5.3 shows that the maximum H_{max} has been slowly increasing in each season except for spring which has not experienced a change. The maximum H_s also shows an increasing trend in all seasons except spring where it has been decreasing. Average H_s shows virtually no annual change.

The maximum T_p behaves similarly to the maximum H_s. There is a trend towards a more southerly mean wave direction in all the seasons except winter where there is slow northerly trend.

The 95 % confidence intervals in Table 5.3 show that the majority of the calculated trends are not statistically significant. The only exceptions are the increasing trends in average and maximum T_p, and in the average wave direction.

Richards Bay's data (Table 5.4) shows somewhat different results to Durban's data. In this case the only statistically significant trends are in autumn and show a decrease in the maximum T_p and an increase in the average T_p. Furthermore the average autumn wave direction is decreasing which contrasts with increases in the other seasons, but the latter are not statistically significant at the 95 % confidence level.

The limitations of short duration data are illustrated by considering the effects of the 2007 storm event. The storm occurred in March and therefore affects the results for the autumn season in particular, but also affects those for the data set as a whole. For Durban, without the 2007 event, the autumn season showed a decreasing trend in maximum H_s. This single storm event was large enough to change the trend, and similarly for the combined all season results. In the case of Richards Bay, the 2007 event did not affect the trends of the combined seasons but did affect the autumn trend. These results, taken together with the inconsistencies between the two locations, indicate that trends in the wave parameters cannot yet be deduced with confidence from the available data. A much longer data record is required to balance out the effects of extreme events

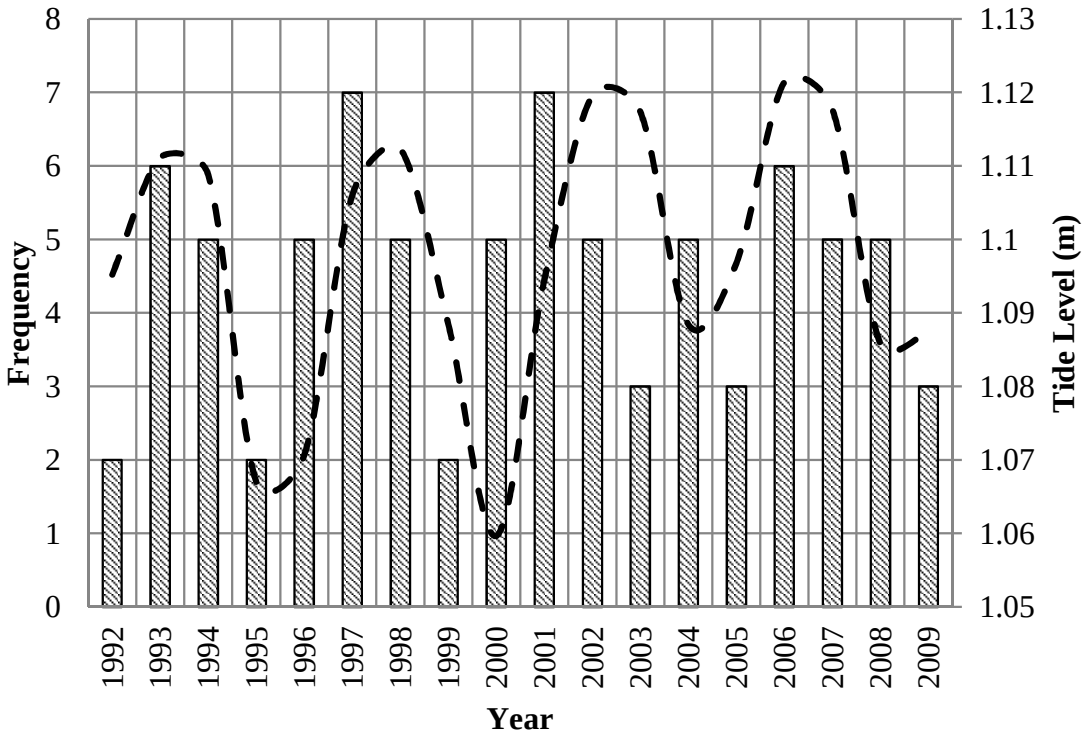

Figure 5.7: Frequency of events exceeding 3.5 m shown by the column chart and simulated highest astronomical tides of each year relative to mean sea level shown by the dashed line.

such as the 2007 storm event.

5.3.4 Storm trends

All the storm events, as per the definition in Sect. 5.2.4, were extracted from the data to determine if there had been an increasing trend in the frequency and duration and a decreasing trend in the calm period of these storm events. Figure 5.7 shows the frequency of events exceeding an H_s of 3.5 m.

The data show an increasing trend in the frequency of events exceeding 3.5 m at a rate of 0.015 ± 0.16 events per year which is not statistically significant at the 95 % confidence level. There does however seem to be a four year cycle in which a multitude of events occur within a year, namely 1993, 1997, 2001 and 2006. This cycle is similar to the time of the lunar perigee coinciding with either the

Table 5.3: Annual rate of change of Durban's wave parameters. The bracketed values are the 95 % confidence intervals

Parameter	Entire Data Set	Summer	Autumn	Winter	Spring
Maximum H_{max} (m)	0.04 (-0.09; 0.17)	0.04 (-0.09; 0.16)	0.09 (-0.12; 0.30)	0.07 (-0.06; 0.19)	0.0 (-0.11; 0.11)
Maximum H_s (m)	0.03 (-0.08; 0.14)	0.03 (-0.03; 0.08)	0.04 (-0.11; 0.19)	0.01 (-0.06; 0.07)	-0.01 (-0.08; 0.06)
Average H_s (m)	-0.01 (-0.02; 0.01)	0.00 (-0.02; 0.01)	0.00 (-0.05; 0.04)	0.00 (-0.03; 0.02)	-0.01 (-0.02; 0.00)
Maximum T_p (s)	0.14 (0.05; 0.22)	0.10 (-0.08; 0.27)	0.14 (-0.02; 0.31)	0.17 (0.08; 0.26)	0.13 (-0.02; 0.28)
Average T_p (s)	0.07 (0.02; 0.13)	0.06 (0.03; 0.09)	0.26 (0.03; 0.49)	0.11 (-0.03; 0.24)	0.04 (-0.002; 0.09)
Average Direction (Deg.)	0.91 (0.12; 1.7)	3.5 (-3.8; 11)	0.71 (-2.5; 3.9)	-0.06 (-0.53; 0.41)	0.25 (-0.67; 1.2)

Table 5.4: Annual rate of change of Richards Bay's wave parameters. The bracketed values are the 95 % confidence intervals

Parameter	**Entire Data Set**	**Summer**	**Autumn**	**Winter**	**Spring**
Maximum H_{max} (m)	0.08	-0.01	0.06	0.01	0.08
	(-0.05; 0.21)	(-0.12; 0.09)	(-0.14; 0.26)	(-0.09; 0.10)	(-0.11; 0.11)
Maximum H_s (m)	0.07	0.01	0.04	-0.00	0.06
	(-0.04; 0.17)	(-0.04; 0.06)	(-0.09; 0.18)	(-0.05; 0.05)	(0.01; 0.12)
Average H_s (m)	-0.00	-0.00	-0.00	-0.00	0.00
	(-0.01; 0.01)	(-0.01; 0.01)	(-0.02; 0.01)	(-0.02; 0.01)	(-0.01; 0.01)
Maximum T_p (s)	-0.05	-0.22	-0.22	0.01	0.02
	(-0.25; 0.15)	(-0.46; 0.03)	(-0.39; -0.05)	(-0.18; 0.21)	(-0.22; 0.26)
Average T_p (s)	0.02	0.01	0.05	0.04	-0.01
	(-0.00; 0.05)	(-0.05; 0.06)	(0.01; 0.08)	(-0.01; 0.08)	(-0.09; 0.07)
Average Direction (Deg.)	0.07	0.18	-0.75	0.16	-0.02
	(-0.15; 0.28)	(-0.49; 0.84)	(-1.12; -0.37)	(-0.49; 0.80)	(-0.58; 0.54)

Table 5.5: Annual rate of change of storm attributes with 95 % confidence bounds

Storm attribute	Annual rate of change
Frequency (no.)	0.015 (-0.14 ; 0.18)
Duration (h)	−0.44 (-2.15 ; 1.27)
Calm period (h)	−28.4 (-150 ; 93)

March or September equinox, a 4.5 yr extreme tide cycle [Pugh, 1987]. The tide levels shown in Fig. 5.7 were simulated from the general astronomical tide formula using the 8 most relevant astronomical constituents. Since both tidal levels and storm frequency are associated with erosion the occurrence of the two mechanisms simultaneously is a significant erosion concern. The cycle is not as clear in the Richards Bay data and is not evident in the wind data. Table 5.5 shows the trend in storm frequency, duration and calm period. The storm events and wind data show a decreasing trend in duration and calm period. The smaller the calm period the less time the beaches have to recover from storm events. However, once again the trends are not statistically significant at the 95 % confidence level. The Richards Bay results are similar.

5.3.5 Link between sea storms and erosion trends

Figures 5.8a – d compare the SSA filtered significant wave height trends to the volume trends in blocks B – F; 1 – 18; 19 – 23 and BR6 – BR9. Table 5.6 gives the Kendall's τ_B correlation coefficients (with corresponding p-values) between wave heights and beach volumes. The correlation coefficients for the first three blocks are small and negative, but not statistically significant at a 95 % confidence level. However the correlations for block BR6 – BR9 are larger and statistically significant. A negative correlation is expected because wave height is a driver for erosion that reduces beach volumes [e.g. Woodroffe, 2003]. However the profiles north of the harbour entrance are strongly influenced by the sand bypass system. The trends in erosion for blocks B – F; 1 – 18; 19 – 23 are better explained by variations in the sediment supply from the sand-pumping scheme, as discussed further in Sect. 5.3.8.

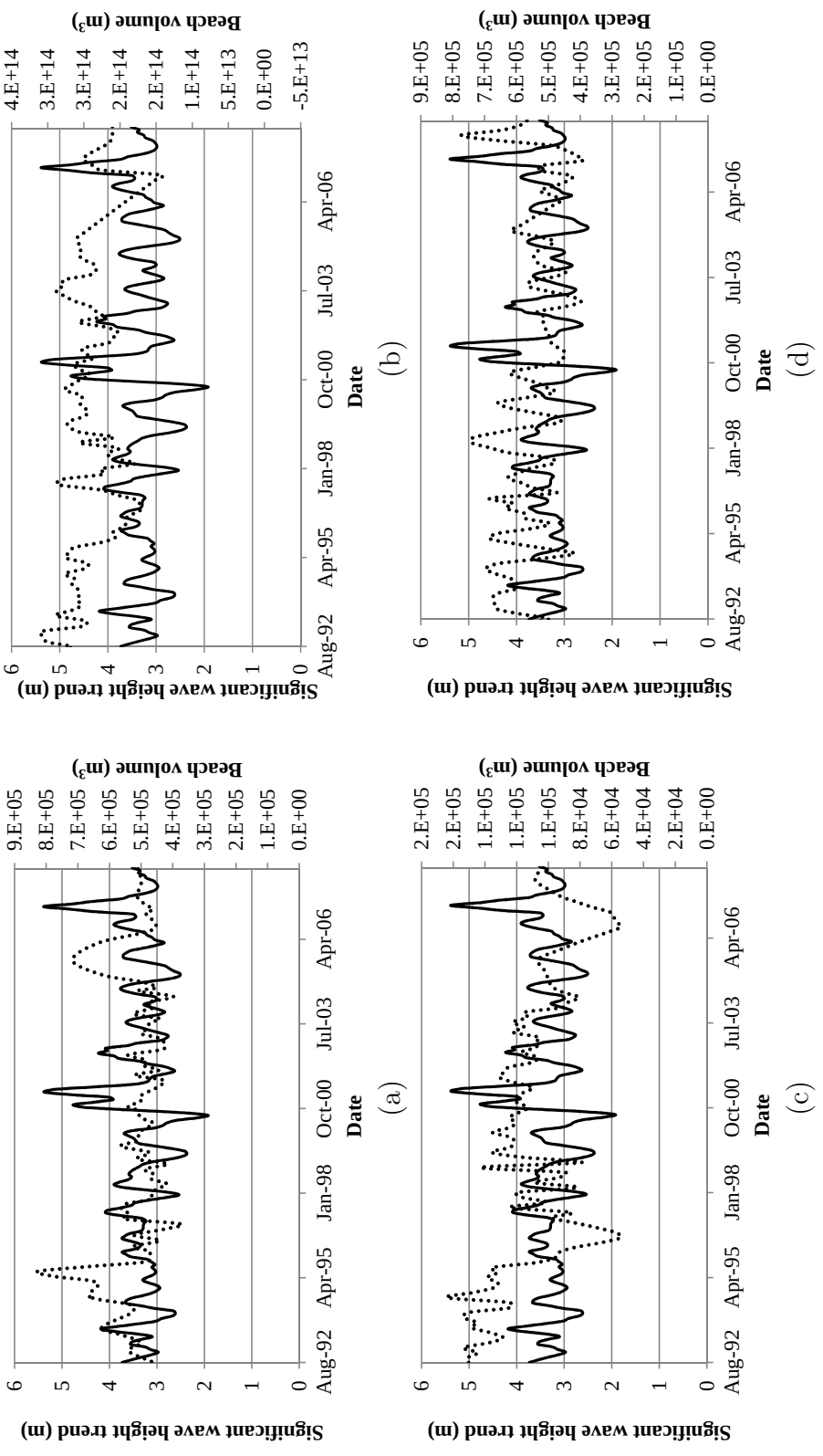

Figure 5.8: The relationship between the significant wave height trends (shown by the solid line) and the beach volume trends (shown by the dotted line) for the blocks (a) B – F, (b) 1 – 18, (c) 19 – 23, (d) BR6 – BR9 (refer to Fig. 5.3).

Table 5.6: Kendall's τ_B correlation coefficients and corresponding p-values between significant wave heights and beach volumes.

Correlation variables	**Kendall's τ_B**	**p-value**
(Volumes B – F) : H_s	-0.13	0.063
(Volumes 1 – 18) : H_s	-0.059	0.38
(Volumes 19 – 23) : H_s	-0.13	0.052
(Volumes BR6 – BR9) : H_s	-0.32	1.3×10^{-6}

5.3.6 Link between water levels and erosion trends

Figure 5.9 shows the tide trends and the four block volume trends deduced from SSA while correlation coefficients are compiled in Table 5.7. The plots show a distinctive dip in beach volumes during the peak in tidal trend. Blocks B – F and 1 – 18 have been recorded over 2 tidal peaks and have the largest correlation coefficients with a mean of -0.25 and with p-values less than 0.002 (Table 5.7). A significant negative correlation is again expected because higher water levels extend the onshore penetration of wave energy. Blocks 19 – 23 and BR6 – BR9 are only recorded over one peak of the tidal trend and both of these blocks have weaker correlations with the tidal trend that are not statistically significant at the 95 % confidence level. The weaker correlation at block 19 – 23 may be related to effects of the sand bypass system, while block BR6 – BR9 has a weak correlation because it is dominated by chronic erosion.

The Bruun rule [Bruun, 1962] provides a simple relationship between sea level rise and profile retreat although is not always appropriately applied [see e.g. Cooper & Pilkey, 2004]. In the present study it was used to identify and evaluate the contribution of sea level rise to the observed chronic erosion. Closure depths were calculated for profiles C, D, F and 13 (Fig. 5.3) and the Bruun rule was applied to them. A linear sea level rise of 0.0027 m yr^{-1} was assumed based on the estimate by Mather [2007]. Table 5.8 shows a comparison between measured volume changes and those estimated by the Bruun Rule. The average measured loss in profile volume is 1.97 $m^3m^{-1}yr^{-1}$ with an estimated average loss due to sea level rise of 2.06 $m^3m^{-1}yr^{-1}$. Profile D has a measured annual gain and if we remove it from the average the measured volume increases to 2.74 $m^3m^{-1}yr^{-1}$.

Table 5.7: Kendall's τ_B correlation coefficients and corresponding p-values between tide levels and beach volumes.

Correlation variables	**Kendall's τ_B**	**p-value**
Volume B – F : tide level	-0.15	4×10^{-3}
Volume 1 – 18 : tide level	-0.34	7.7×10^{-12}
Volume 19 – 23 : tide level	-0.11	0.056
Volume BR6 – BR9 : tide level	-0.099	0.10

Table 5.8: Comparison of measured annual erosion volumes (m^3m^{-1}) and estimated annual erosion volumes (m^3m^{-1}) calculated from the Bruun Rule using a sea level rise of 0.0027 m yr^{-1}.

.

Profile	**Measured erosion** ($m^3m^{-1}yr^{-1}$)	**Estimated erosion** ($m^3m^{-1}yr^{-1}$)
C	0.95	1.51
D	-0.34	1.99
F	5.66	2.62
13	1.62	2.12
Average	1.97	2.06

Taken together with the correlation between tide levels and erosion these results suggest that sea level rise is contributing significantly to chronic erosion.

5.3.7 Link between wind and erosion

The wind data shows a strong seasonal trend in which high wind speeds are experienced from August to December. The majority of the wind in all seasons is from the northeast and southwest and there is no evidence of directional trends or associated erosion consequences. Figure 5.10 shows the seasonal trends in the wind speed and its relationship with erosion. There is no correlation between wind and erosion evident in Fig. 5.10a. Figures 5.10b and 5.10c have a weak negative correlation as a result of a long term trough in wind speed coinciding with relatively high beach volumes. Overall there is no clear evidence of significant correlation between wind speed and erosion in Figs. 5.10a – c. On the other hand

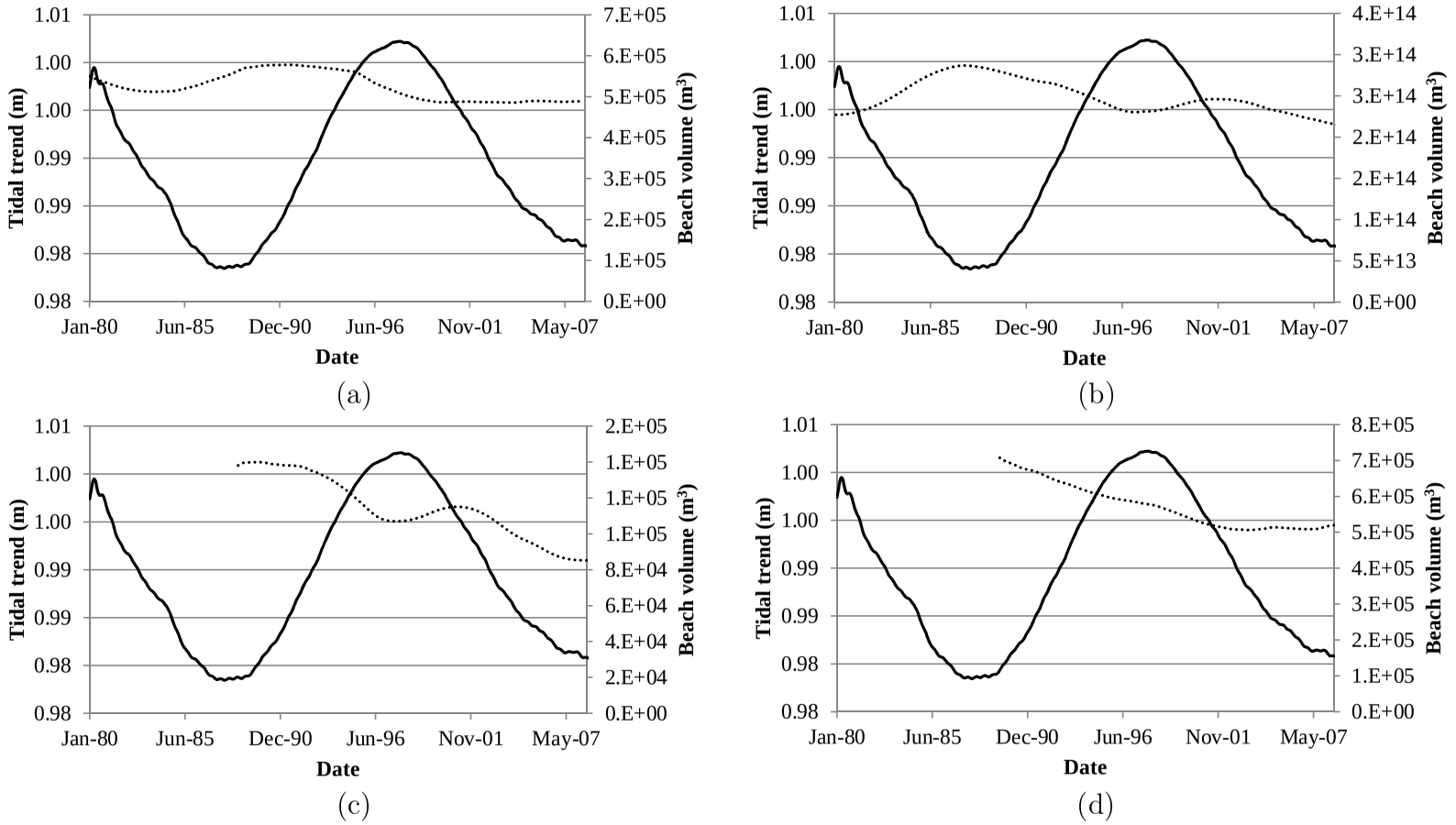

Figure 5.9: The relationship between the tidal trends (shown by the solid lines) and the beach volume trends (shown by the dotted lines) for the blocks (a) B – F, (b) 1 – 18, (c) 19 – 23, (d) BR6 – BR9 (refer to Fig. 5.3).

Fig. 5.10d shows the more exposed Bluff block which is expected to be more dependent on the wind. The seasonal peaks in wind speed coincide with the troughs in beach volume and explain the seasonal variations in beach morphology. This is a significant result since if seasonal winds can explain beach morphology then long term wind trends are a plausible contributor to long term erosion. However the available data set is too short to provide meaningful information on long term trends.

5.3.8 Link between sediment supply and erosion

The relationship between sediment supply and erosion was investigated by considering dredger operations for Durban's sand bypass scheme. Durban's sand bypass system consists of a dredged sand trap (Fig. 5.3a) south of the harbour entrance that intercepts sand movements up the coast to prevent shoaling of the entrance channel. The sand trap is emptied by dredging and the sediment is then pumped to the northern beaches. The Port of Durban regularly empties the sand trap because excess sand blocks the harbour entrance channel and disrupts port activities. The sand trap is not expected to have a 100 % trapping efficiency but it is assumed that the pumped volume closely represents the sediment volume entering the sand trap and thus approximates the average littoral drift.

Figure 5.11 shows a time series of the volume of bypassed sand and the associated decreasing trend. This means that less sediment is being deposited on the beaches and suggests that the littoral transport is decreasing. Although the stormwater outfalls are responsible for erosion on up-drift profiles they cannot be accountable for the net volume loss as the gains should balance the losses. A comparison of Fig. 5.11 and Fig. 5.8c illustrates the extent that the immediate beach profiles are dependent on the sediment supply. The least sediment was bypassed in the years 1996 and 2006 (Fig. 5.11) and the corresponding decrease in beach volume is clearly visible in Fig. 5.8c.

Only limited studies are available on the effects of dams and episodic storm events on sediment supply for the study area. These are discussed in Sect. 5.4.

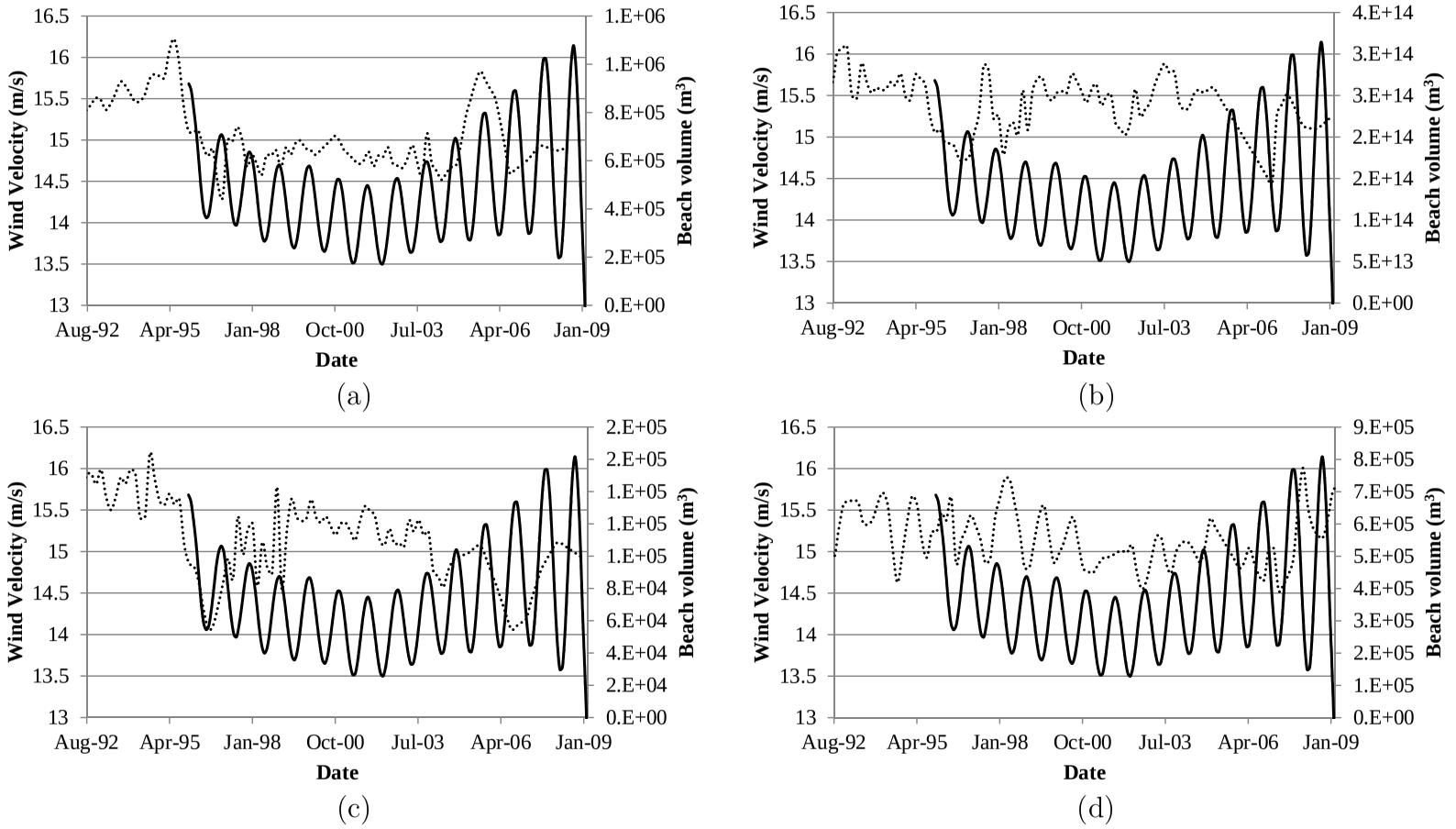

Figure 5.10: The relationship between the wind trends (shown by the solid lines) and the beach volume trends (shown by the dotted lines) for the blocks (a) B – F, (b) 1 – 18, (c) 19 – 23, (d) BR6 – BR9 (refer to Fig. 5.3).

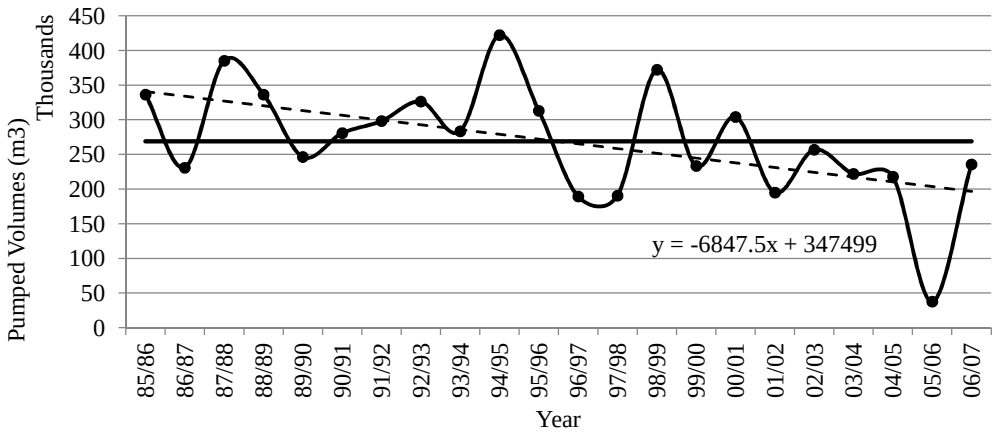

Figure 5.11: Annual volumes pumped by the sand bypass scheme. The solid horizontal line shows the average annual volume while the dashed line shows a fitted linear trend.

5.4 Discussion

Durban's beach profile records are long enough to confidently say that the beaches have been eroding but there is uncertainty concerning the factors that are contributing to this erosion.

Average H_s shows virtually no change, a result consistant with the findings of Perrie *et al.* [2004], while all the other parameters showed increases when considering the entire data set. The maximum H_s, maximum H_{max} and maximum T_p are increasing in all seasons except spring. An increase in wave period is a concern as it has been shown to increase erosion [van Gent *et al.*, 2008; van Thiel de Vries *et al.*, 2008]. The fact that large events are getting larger is consistent with recent findings elsewhere [Knutson & Tuleya, 2004; Lambert, 2004; Perrie *et al.*, 2004; Weisse & Stawarz, 2004]. Considering that spring is responsible for some of the largest historical storm events it is surprising that it is moving against the general trend. This difference may imply a shift in the wave climate, which is consistent with the findings of Dodet *et al.* [2010]; Wang & Swail [2001, 2002]; Wang *et al.* [2004a]. Rouault *et al.* [2010] hypothesised that a poleward shift of westerly winds as well as an increase in the magnitude of the trade winds is causing a warming of the Agulhas Current system on the east coast of South

Africa. Han *et al.* [2010] noted an increase in anomalous south-easterly winds from the Southern hemisphere. These changes in seasonal wind conditions could explain the wave height and direction trends. It is also reiterated that prior to the March 2007 event, autumn (responsible for the largest events) was experiencing a negative trend in H_{max} and H_s. Ultimately the wave data set at our case study site is still too short to confidently establish any trends. However, Ruggiero *et al.* [2010], Theron *et al.* [2010] and Dodet *et al.* [2010] found similar increases in wave parameters which were determined to be statistically significant.

Only Durban's peak period and mean wave direction showed statistically significant trends for the case study. Thetrend towards a more southerly wave direction is potentially important. At this location the net littoral transport is from south to north and the mean wave direction is from the south east. The increasing trend towards a more southerly wave direction implies that the littoral drift should be increasing. A simple application of the CERC formula [Shore protection manual, 1984] shows that an annual increase in wave direction of 0.91° translates to a 1 % annual increase in littoral drift. However there is no increase evident in the measured sand bypass volumes. In conjunction with the fact that there has been a net sediment loss over the past 37 yr, this implies that there is sediment being removed from the system.

One possible sediment "sink" has been identified as the low-lying concrete stormwater outfalls that trap sediment movement. Other anthropogenic impacts are dams that trap sediments in rivers and sand-mining for construction. CSIR [2008] estimated that at least 400 000 m^3/annum are mined from the eThekwini rivers. They further estimated that dams trap a third of the sediment that should reach the coastline. Although there are no significant dams on the rivers that flow into the harbour, all of the sediment deposited in the harbour is removed by maintenance dredging and dumped offshore. The cumulative effects of harbour dredging, dams, and sand-mining results in a 63 % reduction in the total fluvial yield into the area north of the harbor [CSIR, 2008].

The Richards Bay data on the other hand showed a statistically significant decrease in autumn wave direction, which may eventually have an important impact on Richards Bay's sand bypass scheme. In this case the CERC formula translates the trend into a 0.3 % annual decrease in littoral drift.

Large episodic flood events also contribute major sediment inputs to the sediment budget because they erode accumulated sediments from rivers [CSIR, 2008]. The Mgeni river is located immediately north of profile A (Fig. 5.3). Cooper [2002] found that the Mgeni coastline had steadily eroding after 1931 but that following a large flood in 1987 the shoreline accreted and continued to do so for at least another three years, re-establishing the shoreline further seaward than that of 1931. The steady erosion between major flood events in 1917 and 1987 is consistent with the slow overall retreat of the coastline since the 1987 flood. Tinmouth *et al.* [2010], based on 2005/2006 measurements, reported that there was more sediment present within the Mgeni Estuary than prior to the 1987 flood. The KwaZulu-Natal coastline may require another major flood event to flush these sediments and balance the current sediment deficit.

Increases in storm frequency and intensity are potential contributors to beach erosion – the more storms or the longer their duration, the more erosion is likely to occur. Since sediment moves offshore during storm events and is then slowly worked back during calm conditions the shorter the calm period between storms means consecutive storms could be experienced before the beaches have fully recovered. Durban's data show a decrease in storm duration and so is unlikely to be contributing to erosion. However there was an increase in storm frequency and a corresponding decrease in average calm period. Storm events, as per the definition, were found to be increasing at 1.5 events per 100 years. This slight increase in wave events may be related to the minor increase in cyclone days that has been reported by [Mavume *et al.*, 2009] in the south-west Indian Ocean. The increase in frequency is consistent with observations elsewhere by Komar & Allan [2008]; Keim *et al.* [2004]; Seymour [2002]; Weisse & Stawarz [2004] and is possibly contributing to beach erosion. The limited 13 yr of wind data was unable to provide statistically significant long term trends but did provide an explanation for seasonal trends in beach morphology. The fact that wind has a seasonal effect on the beaches implies that any long term trend in wind conditions will have a consequence on beach morphology. It was found that a number of storm events coincided with a 4.5 yr extreme tidal cycle. The coincidence of these two erosion mechanisms compounds the erosions effects and is a demonstration of potential future sea level rise impacts [Chini *et al.*, 2010]. However, as with most

of the wave parameters at this location, none of the changes in storm attributes are statistically significant and apart from the results being consistent with other literature their interpretation remains speculative.

Sea level rise is a plausible contributor to chronic erosion. Bruun's Rule with a sea level change of 0.0027 m/yr [Mather, 2007] suggests that sea level rise can explain a significant portion of the observed erosion. The difference is expected to be made up by reduced fluvial sediment supply and the trends in wave and storm parameters.

5.5 Conclusions

Shoreline changes can have significant implications for coastal planning and management in developed coastal zones. It is therefore important to monitor and understand trends over decadal and longer time scales. In this study 37 yr of beach profile data on the east coast of South Africa have been analyzed for evidence of trends. This has been combined with an analysis of 18 yr of local wave data to investigate corresponding trends in wave parameters and storm attributes and causative links to shoreline changes. To the authors knowledge this is the first such analysis done for the east coast of southern Africa.

The beach profile data shows that the beaches in the region have been eroding over decadal time scales.

Most wave parameters showed an increasing trend except for the average significant wave height, which remained nearly constant over the 18 yr. However, only the trends in peak period and average direction are statistically significant at the 95 % confidence level. There is evidence of an increase in storm frequency and decrease in the duration of calm periods, but neither are statistically significant. Local wind velocity was shown to have a significant effect on beach morphology but the data set was unable to provide any significant long term trends. The net sediment loss experienced from beaches in the Durban area cannot therefore be attributed directly to wave climate and wind changes since they are too small to be major contributors. Nevertheless should the observed trends continue then they could play a more significant role in the future.

Sea level rise has been shown to be a plausible cause of the current morpho-

logical trends. Furthermore the analysis has shown that the coincidence of large wave events with higher than average tide levels has coincided with extreme beach erosion events. This is a harbinger of the implications of future sea level rise due to global climate change.

We suggest that terrestrial anthropogenic activities such as the construction of dams and the mining of river sand has reduced the sediment supply and is an important factor in the observed erosion trends of the beaches in the case study area.

Trends in natural processes such as beach erosion are often assumed to be associated with global climate change. Although climate change and related factors can cause significant impacts its role should not detract from other local anthropogenic factors that may have more significant impacts before the full effects of climate change are realized.

References

Bruun, P.: Sea Level Rise as a Cause of Shore Erosion, Journal of Waterway, Port, Coastal and Ocean Engineering, American Society of Civil Engineering, 88, 117 – 130, 1962. 31, 114, 133

Callaghan, D. P., Nielsen, P., Short, A., & Ranasinghe, R.: Statistical simulation of wave climate and extreme beach erosion, Coast. Eng., 55, 375 – 390, 2008. 20, 31, 58, 85, 121, 155, 182, 191, 192, 207, 236

Chini, N. Stansby, P. Leake, J. Wolf, J. Roberts-Jones, J. & Lowe, J.: The impact of sea level rise and climate change on inshore wave climate: A case study for East Anglia (UK), Coast. Eng., 57, 973 – 984, 2010. 20, 58, 140, 156, 185, 223

Cooper, J.A.G.: The role of extreme floods in estuary-coastal behaviour: contrasts between river- and tide-dominated microtidal estuaries, Sedimentary Geology, 150, 123 – 137, 2002. 16, 140

Cooper, J.A.G. & Pilkey, O.H.: Sea-level rise and shoreline retreat: time to abandon the Bruun Rule, Global and Planet. Change, 43, 157 – 171, 2004. 133

CSIR: Sand Supply from Rivers within the eThekwini Jurisdiction, implications for coastal sand budgets and resource economics, Report No. CSIR/NRE/ECO/ER/2008/0096/C, Stellenbosch, 2008. 16, 51, 87, 101, 106, 139, 140

Dai, S.B. Yang, S.L. & Cai, A.M.: Impacts of dams on the sediment flux of the Pearl River, southern China, Catena, 76, 36 – 43, 2008. 16, 115

Dang , T. H. Coynel, A. Orange, D. Blanc, G. Etcheber, H. Le, L. A.: Long-term monitoring (19602008) of the river-sediment transport in the Red River

Watershed (Vietnam): Temporal variability and dam-reservoir impact, Sci. Total Environ., 408, 4654 – 4664, 2010. 16, 115

Diedericks, H.: Personal Communication, eThekwini Municipality Coastal and Stormwater Department 166 KE Masinga Road, Durban, RSA, 29 June 2009, 2009. 54, 120

Dodet, G. Bertin, X. Taborda, R.: Wave climate variability in the North-East Atlantic Ocean over the last six decades, Ocean Modelling, 31, 120 – 131, 2010. 138, 139, 196

GESAMP: Anthropogenic Influences on Sediment Discharge to the Coastal Zone and Environmental Consequences, Joint Group of Experts on the Scientific Aspects of Marine Environmental Protection (GESAMP), GESAMP Reports and Studies No 52, UNESCO, 1994. 16, 86, 114

Golyandina, N. Nekrutkin, V. Zhigljavsky, A.: Analysis of Time Series Structure: SSA and related techniques, Chapman and Hall/CRC, London 305 pp., 2001 18, 118

Han, W. Meehl, G. A. Rajagopalan, B. Fasullo, J.T. Hu, A. Lin, J. Large, W.G. Wang, J. Quan, X. Trenary, L. L. Wallcraft, A. Shinoda, T. Yeager, S.: Patterns of Indian Ocean sea-level change in a warming climate, Nat. Sci., 3, 546 – 550, 2010. 11, 114, 139

Hassani, H.: Singular Spectrum Analysis: Methodology and Comparison, Data Sci., 5, 239 – 257, 2007. 18, 118

Hsu, S. Lin, F. Jeng, W. Chung, Y. Shawb, L. Hung, K.: Observed sediment fluxes in the southwesternmost Okinawa Trough enhanced by episodic events: flood runoff from Taiwan rivers and large earthquakes Deep-Sea Res. Pt. I 51, 979 – 997, 2004. 16, 115

Huang, G.: Time lag between reduction of sediment supply and coastal erosion, Int. J. Sediment Res., 26, 27 – 35, 2011. 16, 115

Keim,B.D., Muller, R.A., & Stone, G.W.: Spatial and temporal variability of coastal storms in the North Atlantic Basin, Mar. Geol., 210, 7 – 15, 2004. 12, 115, 140

Kinmont, A.: Beach Erosion and Protection. The Institute of Municipal Engineers, Thirty third annual conference, Durban, 1954. 114, 247, 252, 277

Knutson, T.R. & Tuleya, R.E.: Impact of $C0^2$- Induced warming on simulated hurricane intensity and precipitation: Sensitivity to the choice of climate model and convective parameterization, J. Climate, 17, 3477 – 3495, 2004. 12, 138

Komar, P. D. & Allan, C. J.: Increasing Hurricane-Generated Wave Heights along the U.S. East Coast and Their Climate Controls, J. of Coastal Res., 24, 479 – 488, 2008. 12, 115, 140, 275

Lambert, S.: Changes in winter cyclone frequencies and strengths in transient enhanced greenhouse warming simulations using two coupled climate models, Atmos.-Ocean, 42, 173 – 181, 2004. 12, 138

Liquete, C., Canals, M., Ludwig, W., & Arnau, P.: Sediment discharge of the rivers of Catalonia, NE Spain, and the influence of human impacts, J. of Hydrol., 366, 76 – 88, 2009. 16, 115

Mather, A.A.: Linear and nonlinear sea-level changes at Durban, South Africa, South African J. of Sci., 103, 509 – 512, 2007. 17, 116, 133, 141, 186

Mather, A. A.: Sea Level Rise for the East Coast of Southern Africa, Seventh International Conference of Coastal and Port Engineering in Developing Countries, COPEDEC VII, 2008, 173, 11, Dubai, UAE. 2008. 11, 14, 114, 186, 275

Mavume, A. F., Rydberg, L. Rouault, M. & Lutjeharms, J. R. E.: Climatology and Landfall of Tropical Cyclones in the South-West Indian Ocean, Western Indian Ocean J. Mar. Sci. 8, 1, 15 – 36, 2009. 140

Perrie, W., Jiang, J., Long, Z., Toulany, B., & Zhang, W.: NW Atlantic wave estimates and climate change, Proceedings of the Eighth International Workshop on Wave Hindcasting and Forecasting, Oahu, Hawaii, 2004. 12, 138

Pugh, D.T.: Tides, Surges and Mean Sea Level, John Wiley and Sons, Avon, United Kingdom, 472 pp., 1987. 13, 14, 131, 187

Rouault, M., Penven, P., & Pohl, B.: Warming in the Agulhas Current system since the 1980's, Geophys. Res. Lett., 36, L12602, doi:10.1029/2009GL037987, 2009. 11, 114

Rouault, M., Pohl, B., & Penven, P.: Coastal oceanic climate change and variability from 1982 to 2009 around South Africa, African J. Mar. Sci., 32, 237 – 246, 2010. 11, 114, 138

Rossouw, J.: Review of Existing Wave Data, Wave Climate and Design Waves for South African and South West African (Namibian) Coastal Waters, Coastal Engineering and Hydraulics National Research Institute for Oceanology Council for Scientific and Industrial Research, CSIR report,No. T/SEA 8401, Stellenbosh, 1984. 50, 52, 120

Rovira, A., Batalla, R.J., & Sala, M.: Fluvial sediment budget of a Mediterranean river: the lower Tordera (Catalan Coastal Ranges, NE Spain), Catena, 60, 19 – 42, 2005. 16, 115

Ruggiero, P., Komar, P. D., & Allan, J. C.: Increasing wave heights and extreme value projections: The wave climate of the U.S. Pacific Northwest, Coas. Eng., 57, 539 – 552, 2010. 13, 20, 58, 115, 139, 156, 185, 186, 196, 223

Seymour, R, J.: The Influence of Global Climate Change on Extreme Wave Occurrence on the West Coast of the United States, Proceedings of the 28th International Coastal Engineering Conference, Cardiff, 1, 52 – 60, 2002. 12, 140

Shore protection manual. U.S. Army Engineer Waterways Experiment Station, U.S. Government Printing Office, Washington, DC. 4th Edn., Vol. 2, 1984. 139

Singh, B.: Climate related global changes in the southern Caribbean: Trinidad and Tobago, Global Planet. Chang., 15, 93 – 111, 1997. 114

Theron, A., Rossouw, M., Barwell, L., Maherry, A., Diedericks, G., & de Wet, P.: Quantification of risks to coastal areas and development: wave run-up and erosion, The 3rd biennial CSIR conference, Reference: NE20-PA-F, 2010. 115, 139, 196

Tinmouth, N: Mgeni Estuary, Pre- and Post- Inanda Dam Estuarine Dynamics. Unpublished MSc thesis, University of KwaZulu-Natal, South Africa. 2010. 140

van Gent, M. R. A., van Thiel de Vries, J. S. M., Coeveld, E. M., de Vroeg, J. H., & van de Graaff, J.: Large-scale dune erosion tests to study the influence of wave periods, Coast. Eng., 55, 1041 – 1051, 2008. 21, 54, 138, 151, 219

van Thiel de Vries, J. S. M., van Gent, M. R. A., Walstra, D. J. R., & Reniers, A. J. H. M.: Analysis of dune erosion processes in large-scale flume experiments, Coast. Eng., 55, 1028 – 1040, 2008. 21, 54, 138, 151, 219

Wang, X. L. & Swail, V. R.: Changes of Extreme Wave Heights in Northern Hemisphere Oceans and Related Atmospheric Circulation Regimes, J. Climate, 14, 2204 – 2221, 2001. 12, 115, 138

Wang, X. L. & Swail V. R.: Trends of Atlantic wave extremes as simulated in a 40-year wave hindcast using kinematically reanalyzed wind fields, J. Climate, 15, 1020 – 1035, 2002. 12, 115, 138

Wang, X. L., Zwiers, F. W., & Swail, V. R.: North Atlantic Ocean Wave Climate Change Scenarios for the 21st Century. J. Climate, 17, 2368 – 2383, 2004a. 12, 115, 138

Wang, X. L., Swail, V.R, & Zwiers, F.W.: Changes in extra-tropical storm tracks and cyclone activity as derived from two global reanalyses and the Canadian CGCM2 projections of future, Proceedings of the Eighth International Workshop on Wave Hindcasting and Forecasting, Oahu, Hawaii, 2004b. 12, 115

Weisse, R. & Stawarz, M.: Long-term changes and potential future developments of the North sea wave climate. Proceedings of the Eighth International Workshop on Wave Hindcasting and Forecasting, Oahu, Hawaii. 2004. 12, 115, 138, 140

Woodroffe, C. D.: Coasts: form, process and evolution, Cambridge University Press, Cambridge, United Kingdom, 2003. 14, 15, 114, 131, 150

Zhang, K., Douglas, B. C., & Leatherman, S. P.: Global warming and coastal erosion, Climatic Change, 64, 41 – 58, 2004. 15, 114, 186

Chapter 6

Simulating a multivariate sea storm using Archimedean Copulas

This chapter is based on a paper submitted to Coastal Engineering.

Abstract

Process based numerical models for coastal environments aim to realistically model physical processes. These models may contain forcing errors and/or errors within the model itself. Although the model errors generally outweigh the forcing errors they are an issue and they should be minimised to improve the simulation results. In order to provide realistic storm simulations the dependence between the storm parameters such as wave height, wave period and storm duration need to be considered. Copulas provide a means to satisfy these requirements by enabling the development of a multivariate statistical model of sea storms. The dependencies between wave height, wave period, storm duration, water level and storm inter-arrival time (or calm period) were investigated in a case study on the east coast of South Africa using Kendall's tau correlation coefficient as a depen-

dency metric. Three methods of creating multivariate copulas were applied and the results were compared using (1) Kendall's measure (2) empirical multivariate distributions, and (3) simulation. Only the wave height, wave period and storm duration were found to be significantly associated. Hierarchical copulas provided the best trivariate model for the case study data. The trivariate analysis extends previous bivariate analyses and thereby enables a more detailed description of sea storms to be incorporated in statistical models.

6.1 Introduction

The quantification of coastal storm risk has traditionally been done by considering only the wave height (H) of an event [Isaacson & MacKenzie, 1981]. This practice is flawed since the destruction potential of the wave event is also a function of the storm duration (D), water level (L), inter-arrival time or calm period (I), wave direction (A) and peak period (T). In turn these factors are interdependent and these dependencies have to be considered when modelling the sea state.

It is intuitive that the larger the wave height, the higher the damage potential, and that the longer a storm's duration, the more damage can be inflicted. The effects of the other variables are not as intuitive with regard to risks and require further discussion. A high water level alters the shoaling of waves allowing larger waves to occur closer to shore and consequently act further inland which heightens the risk to the shoreline. Woodroffe [2003] and Sorensen [2006] both state that the significance of storm surge coinciding with high tide or spring tide cannot be over emphasized. The inter-arrival time is of particular importance to coastal erosion. Beaches act as a defense to coastal developments. These beaches are eroded during storm events and will have less dry beach width to defend inland developments while they are recovering from those events. According to equilibrium profile theory a given water level or wave condition will produce a specific equilibrium profile once those conditions have been maintained for a long enough time. Provided the equilibrium profile has not been achieved during the initial storm a subsequent storm, of appropriate magnitude, may be thought of as an extention to the previous storms duration allowing it to reach the equilibrium profile. Erosion aside, if another storm event occurred during

the recovery period the lack of beach buffer may mean the wave-runup reaching coastal developments. Therefore the smaller the inter-arrival time the greater the risk. The wave direction is significant for sediment movement as well as for loadings on structures. For example the closer a wave is to striking a structure at right angles the larger the force it exerts [Goda, 2008]. Wave direction is also important from a sheltering perspective as a beach may have a lower risk to the most probable extreme events. For example a beach sheltered by a headland from south easterly swell may erode less from a 12 m south easterly wave than a 6 m north easterly wave. An increase in wave period has been shown to result in an increase in erosion [van Gent *et al.*, 2008; van Thiel de Vries *et al.*, 2008]. Having said that, in terms of fluid acceleration, all else remaining constant, the shorter the wave period the greater the fluid acceleration and conseqentially the greater the bottom shear stress. Wave periods are also both deterministically and randomly tied to wave height and storm duration. They are deterministic in terms of their physical limitations such as maximum wave steepness but are random as different combinations of wave height and period may be produced from similar meteorlogical forcings depending on the travel distance. Although the relationship between wave period, erosion and meteorlogical forcing is complicated it is not a major concern for a statistical model because the probabalistic relationship between wave height and period will include randomness while the consequential erosion effects will be modelled in a numerical morphological model. The consideration of all these factors allows the true risk of an event to be considered. Copulas provide a tool to model the dependence between all the aforementioned variables that characterize coastal storm events.

Wave climate simulation models and beach morphology models are becoming increasingly popular in coastal, port and marine engineering (e.g. SWAN, Delft3D, Mike3, SBeach, Xbeach, Unibest). The application of these models often requires the simulation of the effects of sea storms. To model a series of sea storms without considering the dependencies between the storm parameters can degrade the realism of these simulations. For example extreme wave height may be unlikely to occur during short duration storms. Similarly the coincidence of extreme wave heights with an extremely long storm duration may also be improbable. Incorporating the statistical dependencies between extreme wave heights

and storm durations should produce a more realistic set of storm events. The proposed multivariate copula model can provide a simulation of a wave climate for a given probability level or be used to conditionally simulate storm events.

The creation of mathematically consistent multivariate copulas is a difficult problem and methods of combining three 2-copulas into a 3-copula are still debated [Salvadori & De Michele, 2006]. An appreciation of the difficulty associated with constructing n-copulas is given by Nelsen [2006]. There have been numerous methods proposed for the construction of multivariate copulas. For Archimedean copulas some examples include: hierarchical [Nelsen, 2006], conditional mixtures [De Michele *et al.*, 2007] and the structure proposed by Chakak & Koehler [1995]. Recently multi-parameter multivariate extreme value (MEV) copulas have been proposed by Salvadori & De Michele [2010]; Salvadori *et al.* [2011]. This paper focuses on multivariate Archimedean copulas and since only the Gumbel copula is both MEV and Archimedean we preclude multi-parameter extreme value copulas.

This paper aims to determine which sea storm parameters are interdependent and tests which multivariate construction technique is appropriate to model and simulate sea storms.

We initially provide an overview of Archimedean copulas and the available multivariate construction techniques. The selection of an appropriate copula is then described followed by the associated dependencies. We then use hierarchical, condition mixtures and the Chakak & Koehler [1995] structure to construct multivariate Archimedean copulas for wave data from a case study on the east coast of South Africa. We identify the best model through a simulation study.

6.2 Theoretical Background & Methods

6.2.1 Archimedean Copulas

Copulas are mathematical functions that join or couple multivariate probability distribution functions $H(x_1, \ldots, x_n)$ to their one-dimensional marginal distribution functions $F_1(x_1), \ldots, F_n(x_n)$. For a detailed introduction to copulas refer De Michele *et al.* [2007]; Joe [1997]; Nelsen [2006]; Salvadori & De Michele [2010].

Archimedean copulas are a special class of copulas. They have been used in a

wide range of applications because of properties that make them easy to construct [Nelsen, 2006]. An Archimedean copula C is a solution to the functional equation

$$\varphi(C(u,v)) = \varphi(u) + \varphi(v) \tag{6.1}$$

where $u = F(x)$ and $v = F(y)$ are marginal distribution functions (u, v) and φ is the generator function. Simply put a copula maps a combination of two or more probabilities to a single joint probability of non-exceedance. An example of an Archimedean copula is the Clayton copula with generator function

$$\varphi(t) = \frac{1}{\theta}(t^{\theta} - 1) \tag{6.2}$$

where θ is the dependence parameter and t is a number from 0 to 1. Nelsen [2006] provides an extensive list of other Archimedean copulas.

Kendall's tau τ_K is the sample version of the measure of association defined in terms of concordance, namely

$$\tau_K = \frac{(c-d)}{(c+d)} \tag{6.3}$$

where c is the number of concordant pairs and d is the number of discordant pairs. A valuable property of Archimedean copulas is that τ_K can be expressed as a function of the generator:

$$\tau_K = 1 + 4\int_0^1 \frac{\varphi(t)}{\varphi'(t)}dt \tag{6.4}$$

The dependence parameter θ can be found from Eqn. 6.4 using Kendall's tau.

6.2.2 Constructing multivariate Archimedean copulas

An n-copula cannot simply be used to "couple" another $(n-1)$-copula with a variate by setting them as its marginal distributions. For example attempting to solve

$$C^n(u_1, u_2, \ldots, u_n) = C(C^{n-1}(u_1, u_2, \ldots, u_{n-1}), u_n) \tag{6.5}$$

often fails and is referred to as the compatibility problem [Nelsen, 2006]. The literature does however offer various techniques to create multivariate distributions from copulas. Some of these techniques are presented below. The first two techniques we describe are based on conditional laws. A conditional distribution describes the probability of observing a variate given that we know the probability of occurrence of an associated variate. In physical terms, we may want to know, given that there will be a wave height of 8.5 m, what storm durations can occur. So $F_{(X|Y)}$ would be the probability of observing X for a known value of Y. Mathematical details of the below methods are provided in the appendix.

Chakak & Koehler [1995] present one of the simplest ways of forming a 3-copula. This method uses bivariate conditional distributions to create a trivariate copula (Eqn. 12.1). The Chakak & Koehler [1995] method is appealing because of its simple form and the fact that all the dependence parameters are available from the corresponding 2-copulas. However the resulting 3-copula is not uniquely determined and is dependent on the order the copulas are combined.

The conditional mixtures approach was used by Salvadori *et al.* [2007], Joe [1997] and De Michele *et al.* [2007] to combine two 2-copulas to form a 3-copula. This method is conceptually similar to that of Chakak & Koehler [1995]. In this case the three dimensional distribution is obtained from the conditional bivariate distributions.

Other methods considered have mainly been used in financial modelling. They are the fully nested and partially nested methods suggested in Joe [1997] and presented by Savu & Trede [2006] as a joint distribution of asset returns. The method was also applied by Grimaldi & Serinaldi [2006], Nelsen [2006], Whelan [2004] and Embrechts *et al.* [2001]. The term used is 'hierarchical Archimedean copulas' which is a copula that joins two or more bivariate or higher order copulas by another Archimedean copula.

Hierarchical Archimedean copulas can either be created by the fully nested method or the partially nested method. The partially nested method is more flexible than the fully nested [Savu & Trede, 2006]. It is however not possible to create a 3-copula as the lowest dimension is $n = 4$.

The major modelling limitation of hierarchical Archimedean copulas is that not all combinations of joint distribution are modelled uniquely. This is not

general enough for modelling a sea state and needs to be considered if the method is used for that application. The fully nested method provides an improved model in this regard.

The partially nested method has the benefit of producing a 4-copula from only two 2-copulas but is unable to produce a 3-copula. Three 2-copulas are required to create a 3-copula via the conditional mixtures approach (Eqn. 12.3) and by the Chakak & Koehler [1995] method (Eqn. 12.1). Equation 12.3 is likely to provide the most complete model as it allows all the dependencies to be modelled by different copulas.

6.3 Case study

The east coast of South Africa has 18 years of reliable wave data from a wave recording buoy near the city of Durban. Corbella & Stretch [2012a] provide details of the data set. The data was aggregated into storm events following the methods of De Michele *et al.* [2007] and the three multivariate copula construction techniques were applied to the wave data to create a storm sea state model.

6.3.1 Univariate analysis

A storm event was defined as a wave event that exceeded a threshold significant wave height H of 3.5 m (Fig. 6.1). Experience has shown that a wave height exceeding 3.5 m is associated with erosion. The storm commenced when the wave height exceeded 3.5 m and ended when the wave height fell below 3.5 m and stayed there for a period of at least two weeks. The two week delay was intended to ensure that consecutive storm events were statistically independent and was selected based on the decay time of the autocorrelation. This two week period is consistent with [Callaghan *et al.*, 2008]. The reduced storm data set was then manually assessed to ensure that each storm event represented one meteorological system. Finally we select the 3 largest storms, on average, per year. This method of selecting independent storms is similar to those of Callaghan *et al.* [2008]; Salvadori *et al.* [2007]; Mendez [2008]; U.S. Army Corps of Engineers [2006]. The storm duration D was the time in hours between the storm start and end times.

The storm inter-arrival time or calm period I was defined as the time in hours between the end of one storm and the start of the next storm. The maximum peak period T that coincided with the storm event was also considered along with simulated water levels L. Wave direction was not considered due to insufficient data.

The relative goodness of fit of various statistical models was assessed using the Akaike information criterion, namely

$$AIC = 2K - 2\ln(\mathcal{L}) \tag{6.6}$$

where K is the number of parameters in the fitted probability distribution and $\mathcal{L}$ is the maximized value of the likelihood function for the estimated parameters. The variates H, D, T and L were best fitted with the generalized extreme value (GEV) distribution. The GEV distribution has been used to model wave heights by Chini *et al.* [2010]; Guedes Soares & Scotto [2004]; Mendez [2008]; Minguez *et al.* [2010] and Ruggiero *et al.* [2010] and is defined as

$$y = \sigma^{-1} e^{-\left(\frac{(x-\mu)}{\sigma}\right)^k} e^{-e\left(\frac{(x-\mu)}{\sigma}\right)} : \quad -\infty < x < \infty \tag{6.7}$$

where μ is a location parameter, σ is a scale parameter, k is a shape parameter.

The storm frequency $1/(I + D)$ was modelled with the Poisson distribution

$$y = \frac{\lambda^x e^{-\lambda}}{x!}, \tag{6.8}$$

where λ is the mean and variance. Seasonality of storm frequency can be included by making λ vary in time. Seasonality has no relevance in this paper and will not be discussed further.

De Michele *et al.* [2007] used a storm magnitude based on an equivalent triangular storm model (see Fig. 6.1), following Boccotti [2000]. Let the storm magnitude be $M = (H - \eta)D/2$, where η is the wave height threshold taken here as 3.5 m. The storm magnitude provides a single quantity to measure the magnitude of a storm produced by the interdependence of H and D. We extend

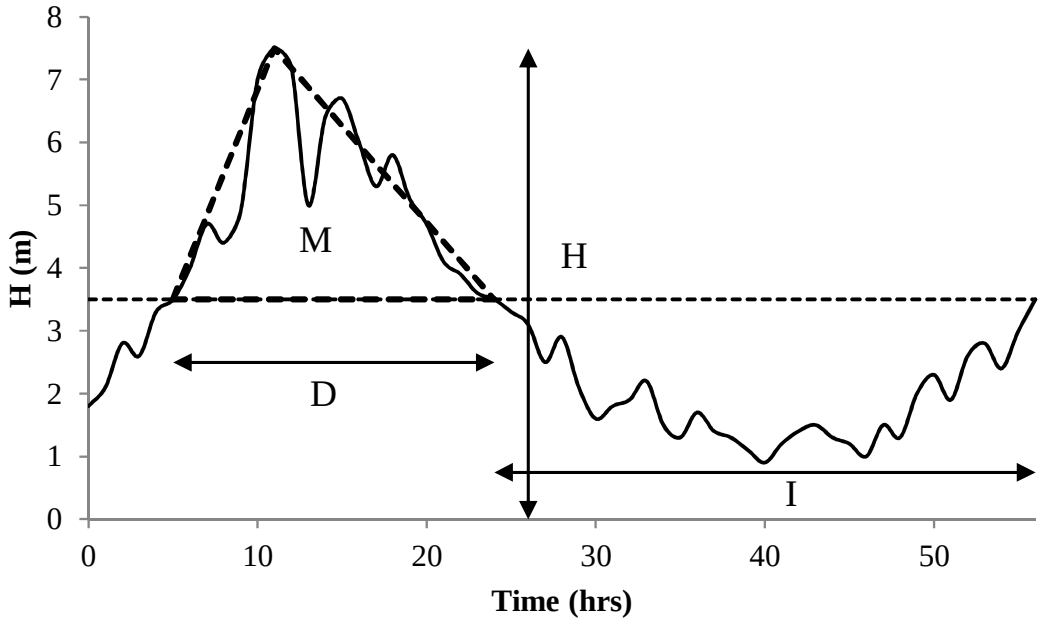

Figure 6.1: Definition of storm magnitude (M), storm duration (D), calm period (I) and wave height (H)

this concept by also considering the wave power

$$P = \left(\frac{gT}{4\pi}\right) E \tag{6.9}$$

where g is gravitational acceleration, ρ is the density of salt water and the average wave energy E is given by

$$E = \frac{1}{8}\,\rho g H^2 \tag{6.10}$$

The wave power is an instantaneous measure of the storm peak and quantifies the interdependence of H and T in a single value. It will be referred to as the peak wave power. The storm magnitude and the peak wave power are examples of how risk may arise from an association between all three variables H, D and T.

6.3.2 Bivariate analysis

The dependence between the variates is required prior to constructing the multivariate copulas. Kendall's tau is a nonparametric measure of correlation and was used, along with the corresponding p value, to determine the degree of dependence between the pairs: HD, HT, HI, HL, DT, DI, DL, TI, TL, IL. Kendall's τ_b considers the number of tied pairs and is given by

$$\tau_b = \frac{(n_c n_d)}{\sqrt{(n_0 n_1)(n_0 n_2)}} \tag{6.11}$$

where $n_0 = n(n-1)/2$, $n_1 = \sum_i t_i(t_i - 1)/2$, $n_2 = \sum_j u_j(u_j - 1)/2$, t_i is the number of tied values in the i^{th} group of ties for the first quantity, u_j is the number of tied values in the j^{th} group of ties for the second quantity, n_c is the number of concordant pairs, n_d is the number of discordant pairs. A p value less than 0.05 was considered acceptable to reject the null hypothesis of $\tau_b = 0$. Kendall's tau was also calculated for the pairs as a function of storm magnitude and peak wave power.

6.3.3 Selecting 2-copulas

The following Archimedean copulas were considered: Clayton, Gumbel, Ali-Mikhail-Haq, Frank and copula 12 in Nelsen [2006] Table 4.1. These copula functions, their generator functions and the relationship between their dependence parameter θ and Kendall's tau are shown in Table 6.1.

We determined the best-fitting Archimedean copula using a nonparametric estimation procedure proposed by Genest *et al.* [1993] which has been successfully applied by numerous authors [Accioly*et al.*, 2004; Dowd, 2008; Zhang & Singh, 2007]. Let $Z = H(X, Y)$ have a distribution function $K(z) = P\{H(X, Y) \leq z\}$ in the interval $(0, 1)$. An empirical distribution of $K(z)$ can be determined as $\hat{K}(z) =$ proportion of $Z_i's \leq z$, where $Z_i =$ number of $(X_j Y_j)$ such that $X_j < X_i$ and $Y_j < Y_i$.

Genest *et al.* [1993] showed that a parametric estimator of K could be found using the generators of the Archimedean copulas. The generator estimate of K,

Table 6.1: The Clayton, Gumbel, Ali-Mikhail-Haq, Frank and copula 12 in Nelsen [2006] with corresponding generator functions and Kendall's tau.

Family	**Function, C(u,v)**	**Generator**	**Kendall's Tau**
Clayton	$\left[max\left(u^{-\theta}+v^{-\theta}-1,0\right)\right]^{-1/\theta}$	$\left(t^{-\theta}-1\right)/\theta$	$\theta/\left(\theta+2\right)$
Gumbel-Hougaard	$\exp\left(-\left[\left(-\ln u\right)^{\theta}+\left(-\ln v\right)^{\theta}\right]^{1/\theta}\right)$	$\left(-\ln t\right)^{\theta}$	$\left(\theta-1\right)/\theta$
Ali-Mikhail-Haq	$uv/\left(1-\theta\left(1-u\right)\left(1-v\right)\right)$	$\ln\frac{1-\theta(1-t)}{t}$	$\frac{3\theta-2}{\theta}-\frac{2}{3}\left(1-\frac{1}{\theta}\right)^{2}\ln\left(1-\theta\right)$
Frank	$-\frac{1}{\theta}\ln\left(1+\frac{(e^{-\theta u}-1)(e^{-\theta v}-1)}{(e^{-\theta}-1)}\right)$	$-\ln\frac{e^{-\theta t}-1}{e^{-\theta}-1}$	$1+\frac{4}{\theta}D_1(\theta)-1$ $\left(D_1(\theta)=\int_0^{\theta}e^{-2t}/(1+t)^{\theta}dt\right)$
Nelsen (2006)	$\left(1+\left[\left(u^{-1}-1\right)^{\theta}+\left(v^{-1}-1\right)^{\theta}\right]^{1/\theta}\right)^{-1}$	$\left(\frac{1}{t}-1\right)^{\theta}$	$1-\frac{2}{3\theta}$

denoted by $\tilde{K}_{\varphi}(z)$, is given by

$$\tilde{K}_{\varphi}(z) = z - \frac{\varphi(z)}{\varphi'(z)} \tag{6.12}$$

The best fitting copula was determined by plotting $\tilde{K}_{\varphi}(z)$ against $\hat{K}(z)$ (known as a $Q-Q$ plot) and performing a Chi-squared and Kolmogorov-Smirnov goodness of fit test. All p-values were calculated for a 95 % level of confidence. The smallest Chi-squared value, calculated from

$$\chi^2 = \sum_{i=1}^{m} \frac{(\hat{K}(z)_i - \tilde{K}_{\varphi}(z)_i)^2}{\tilde{K}_{\varphi}(z)_i}, \tag{6.13}$$

was used to select the best fitting copula.

6.3.4 Empirical non-exceedance probabilities

Various authors have proposed empirical non-exceedance probabilities as plotting position formulae and those appropriate to wave parameters are presented by the U.S. Army Corps of Engineers [2006]. We use the plotting position formula proposed by Gringorten [1963] since Zhang & Singh [2007] successfully applied it to a trivariate probability distribution. The empirical trivariate probability distribution can be expressed as

$$\begin{aligned} F(u,v,w) &= P(U \leq u_i, V \leq v_i, W \leq w_i) \\ &= \frac{\sum_{l=1}^{i}\sum_{m=1}^{i}\sum_{p=1}^{i} n_{lmp} - 0.44}{N + 0.12} \end{aligned} \tag{6.14}$$

where N is the sample size and n_{lmp} is the number of occurrences of the combinations of u_l and v_m and w_p.

Table 6.2: Kendall's tau and p values for the pairs HD, HT and DT

Variables	Kendall's tau	p-value
HD	0.594	1.22×10^{-11}
HT	0.214	0.0159
DT	0.249	0.00492

6.4 Results

6.4.1 Dependence between variables H, D, T, I and L

Kendall's tau and the corresponding p values were calculated for the following pairs: HD, HT, HI, HL, DT, DI, DL, TI, TL, IL. Only HD, HT and DT showed a significant correlation (Table 6.2). This is not unexpected as it shows that the three variates H, D and T are dependent while I and L are likely to be independent. This weakness in association allows us to simplify our model as I and L may be simulated independently from the other variates using only their marginal distributions.

The results in Table 6.2 show the chosen variate pairs to be positively dependent. This implies that the larger the wave heights and periods the longer the storm duration. That is the longer the storm duration the greater the wave power. Similarly the greater the storm magnitude the greater the wave period.

Figure 6.2 shows the correlation between (H, D) pairs for storm magnitudes exceeding specified threshold values. Similarly the correlation between (H, T) pairs with peak wave powers above specified thresholds are also shown in Fig. 6.2. Both (H, D) and (H, T) correlations are positive for low thresholds, but become negative as the thresholds increase. The (H, D) correlation becomes positive again at the high storm magnitudes. The (H, T) correlation behave differently for high peak wave power where after an initial increase it subsequently changes from positive to (perfectly) negatively correlated. This is thought to be attributable to the very few available data pairs in that extreme range. It is expected that with more data pairs the increase to positive correlations would continue into the upper range of peak wave power.

The trend of the storm magnitude can be explained as follows: small mag-

nitudes are associated with positive HD correlations because as relatively small wave events increase so do the event durations. The middle range becomes negative because relatively small waves coincide with long durations or large waves coincide with short durations. The trend becomes positive again because extreme storm magnitudes are formed by large wave events having long durations and the larger the waves the longer the duration. A similar explanation can be applied to the peak wave power. These results can be significantly influenced by the storm event definition and De Michele *et al.* [2007], following Boccotti [2000], concluded that the association should converge towards the limit of -1 as the peak wave power does in Fig. 6.2, when considering increasingly extreme events. We appreciate that the negative correlation may exist as a result of large events being caused by either large wave heights with short durations or small wave heights with long durations. However, we propose that there is an additional higher range that produces more extreme events with large waves coinciding with long periods. Overall both H, D and H, T will be modelled with a positive correlation (Table 6.2) and so our explanation is appropriate and can be well described by copulas. The Clayton copula can model lower tail dependence and becomes less associative in the upper tail. This is an appropriate copula to model the storm proposed by Boccotti [2000]. The model we propose requires a positive dependence to be modelled in the upper and lower tail. Charpentier & Segers [2007, 2009] evaluated tails of Archimedean copulas and showed that Archimedean Copula 12 from Nelsen [2006] can model both upper and lower tail positive dependencies.

6.4.2 Creating a multivariate Archimedean copula

The results of the Chi-squared test between the parametric measure ($\tilde{K}_{\varphi}(z)$) and the empirical estimate ($\hat{K}(z)$) of K is presented in Table 6.3 with the dependence parameters of the various copulas. $Q - Q$ plots of the best fitting copulas are shown in Fig. 6.3. The Clayton copula was the best fit for all the pairs.

The copulas in Table 6.1 were then used to create multivariate copulas based on the three construction methods described in Sect. 6.3.2. The conditional mixtures and the procedure proposed by Chakak & Koehler [1995] do not require

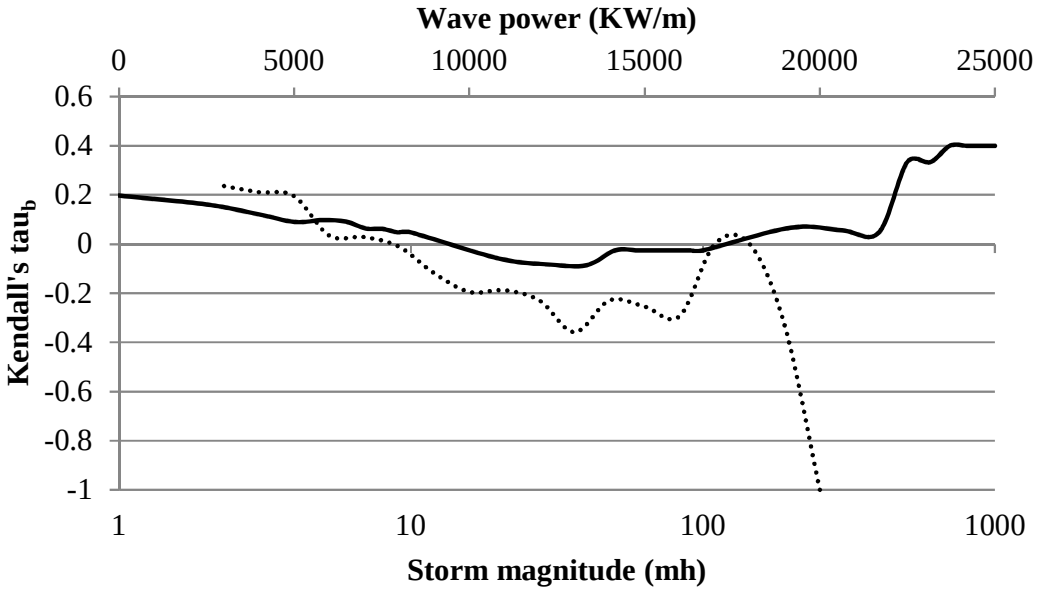

Figure 6.2: Kendall's tau for HD pairs as a function of storm magnitude threshold (solid line) and HT pairs as a function of peak wave power threshold (dotted line).

any further fitting as the trivariate copula can be determined from the 2-copulas. The fully nested method requires an additional copula to fit the 2-copula to the univariate marginal distribution to create a 3-copula. A dependence parameter for this additional copula was calculated and the results are presented in Table 6.4.

6.4.3 Fully nested hierarchical copulas

In an attempt to explore the compatibility problem the trivariate copulas were constructed with different 2-copulas as well as with different copulas that did and did not satisfy the requirement $\theta < \theta_{12}$. Table 6.4 shows the fitting results of the trivariate copulas, Kendall's tau, dependence parameters and goodness of fit between the empirical trivariate distribution and the copula based trivariate distribution. Let the marginal distribution functions of wave height, wave period and storm duration be $F(H) = h$, $F(T) = t$ and $F(D) = d$ respectively. Table 6.4 shows that $C(h, d)$ and t nested with the Clayton copula has the best fit to the empirical distribution. $C(h, t)$ and d does not satisfy the condition $\theta < \theta_{12}$.

Table 6.3: The best fitting copulas, dependence parameters and the Chi-squared (χ^2) and Kolmogorov-Smirnov (ks) statistics for the pairs H, D; H, T and D, T. The p-value at a 95 % level of confidence is also shown

Pairs	**Copula**	**Dependence Parameter (θ)**	**Goodness of fit**		
			χ^2	ks	p-value
H, D	Clayton	2.08	0.219	0.100	0.911
H, T	Clayton	0.543	0.210	0.100	0.911
D, T	Clayton	0.662	0.187	0.067	0.999

Table 6.4: The best fitting hierarchical copulas for the nesting of $C(h, t)$ and d and $C(h, d)$ and t, with the dependence parameters. The goodness of fit is shown as the Chi-squared (χ^2) and Kolmogorov-Smirnov (ks) statistics, with a p-value calculated at a 95 % level of confidence.

Nesting	**Copula**	**Kendall's tau**	**Dependence Parameter (θ)**	**Goodness of fit**		
				χ^2	ks	p-value
$C(h, t)$ & d	Gumbel-Hougaard	0.495	1.90	1.02	0.133	0.629
$C(h, d)$ & t	Clayton	0.244	0.646	0.742	0.117	0.784

Figure 6.4 shows that the empirical cumulative distributions of both trivariate copulas are similar. The nesting should be performed with $C(h, d)$ and t which satisfies the condition $\theta < \theta_{12}$.

6.4.4 Conditional mixtures and the Chakak-Koehler approach

The conditional mixtures and the Chakak & Koehler [1995] approach can be used to construct multivariate copulas from only the 2-copulas. Chakak & Koehler [1995] had the smallest Chi-squared value of 1.04 while the conditional mixtures approach was 4.43.

6.4.5 Simulation comparison

We initially simulate $F(H)$, $F(T)$ and $F(D)$ from the bivariate copulas $C(h, t)$ and $C(h, d)$. The bivariate simulations yields a scatterplot very similar to the measured data (Fig. 6.5).

The bivariate Clayton copulas provide an appropriate model for the association between HD and HT. We now attempt to determine which construction technique yields the best trivariate model.

The construction of the trivariate copula $C(h, d, t)$ following both Chakak & Koehler [1995] and the conditional mixtures approaches are performed by coupling three 2-copulas into a 3-copula conditionally. The similarities in the techniques suggest that the simulations should be similar. The results are shown in Fig. 6.6 where it is evident that both methods do indeed produce similar results.

Figure 6.7 shows that the simulation results of the hierarchical copula $C(C(h, d), t)$ are also similar to those of the Chakak & Koehler [1995] and conditional mixtures methods. A visual comparison with Fig. 6.5 indicates that the hierarchical model has the most similar simulation results to the bivariate copula simulations. The hierarchical copula is expected to produce the best simulation results as it had the best fit to the empirical data.

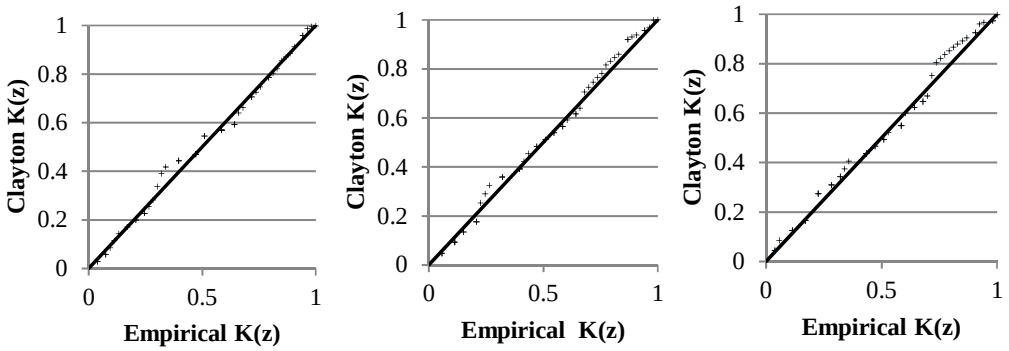

Figure 6.3: $Q-Q$ plots of the best fitting copulas to the pairs (a) H, D; (b) H, T; (c) D, T

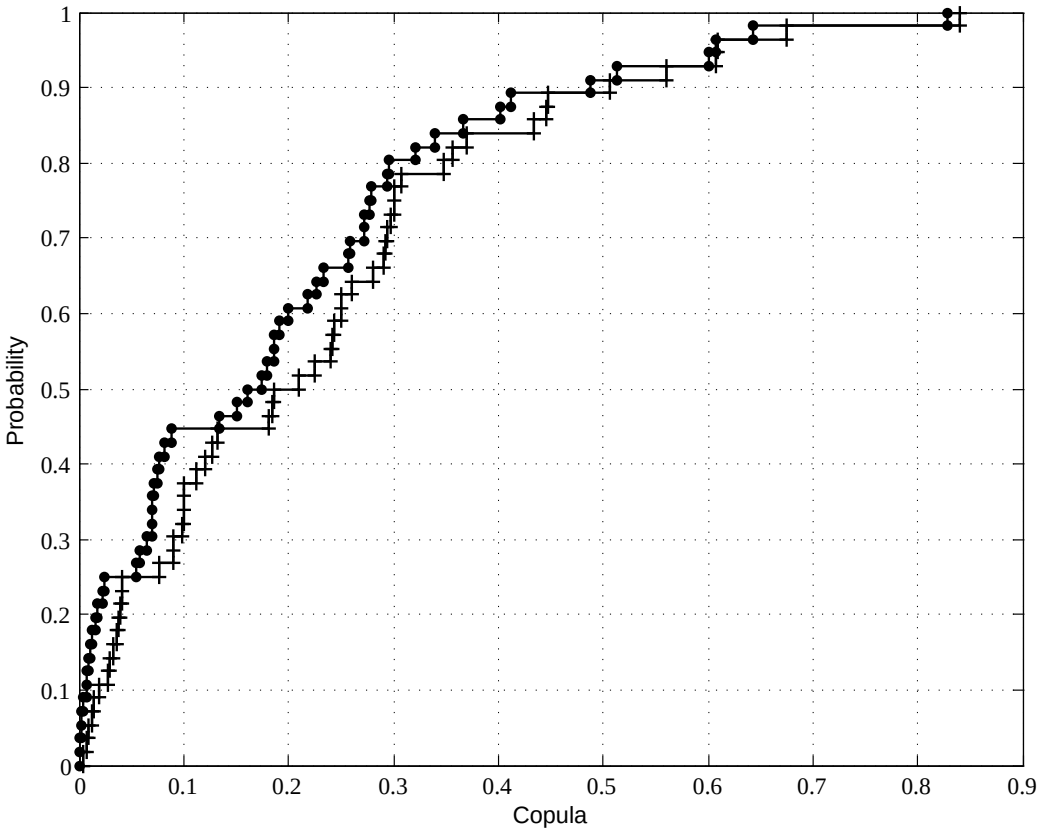

Figure 6.4: The empirical cumulative distribution of $C(h,t)$ and d nested with the Ali-Mikhail-Haq copula (shown by the dots) and $C(h,d)$ and t nested with the Clayton copula (shown by the crosses)

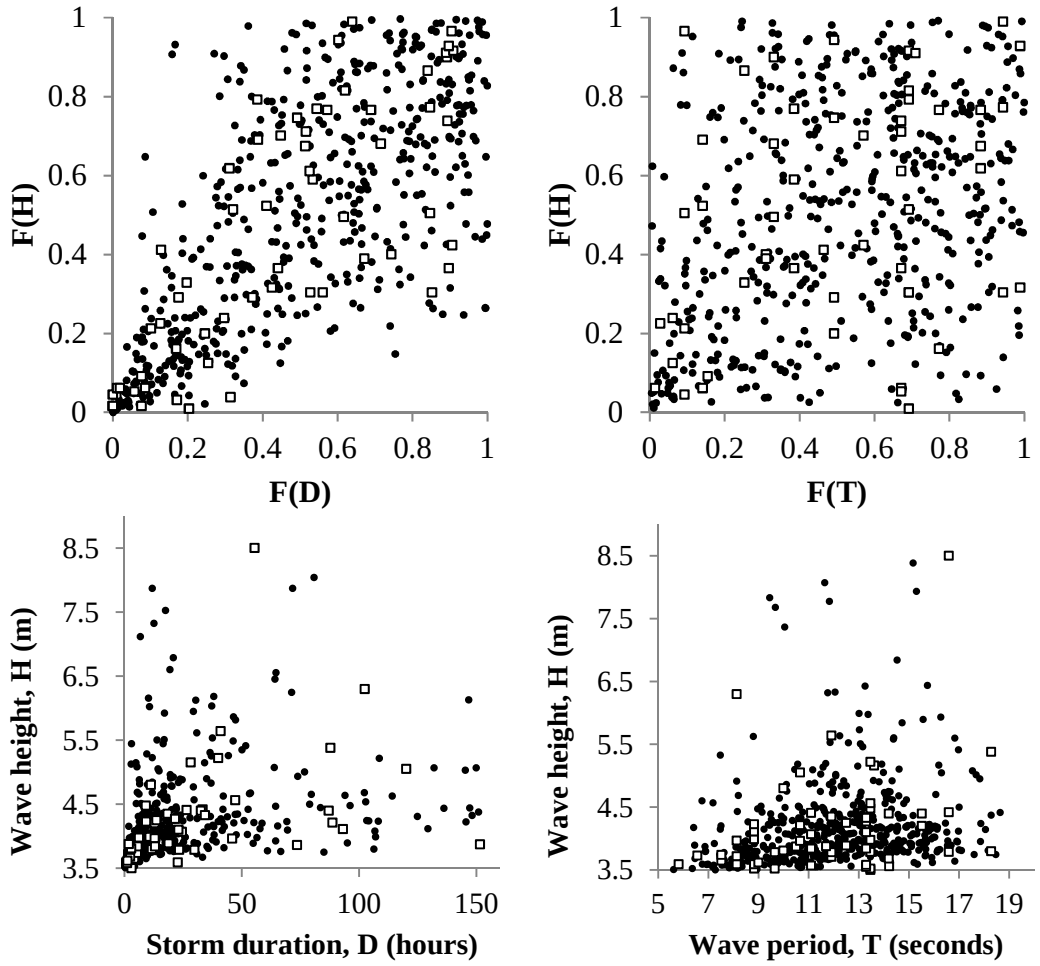

Figure 6.5: Simulations of: (a) wave height and storm duration shown in the top plot as marginals $F(H)$ and $F(D)$ and in the bottom plot as physical parameters H and D; (b) wave height and wave period shown in the top plot as marginals $F(H)$ and $F(T)$ and in the bottom plot as physical parameters H and T from the bivariate Clayton copulas. The simulated data is shown by the dots and the empirical data is shown by the squares.

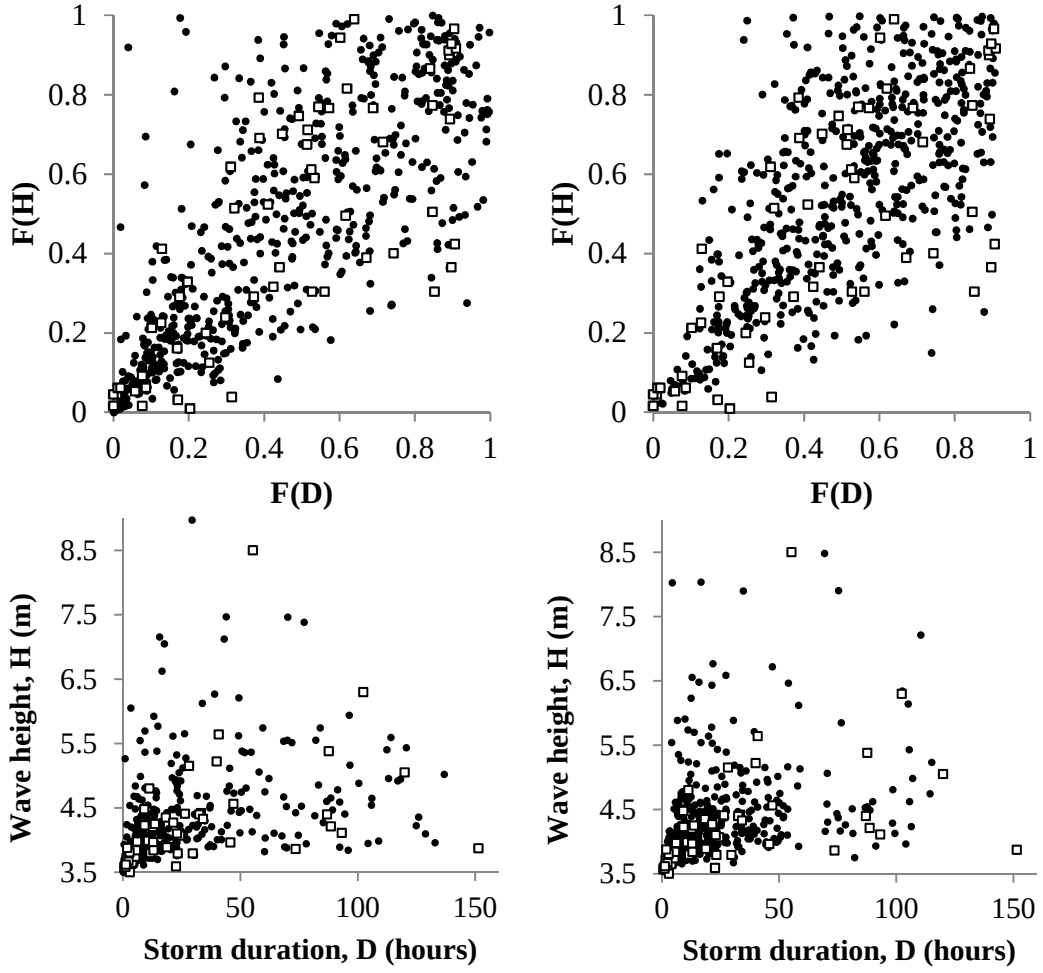

Figure 6.6: Simulations of wave height and storm duration as marginals $F(H)$ and $F(D)$ (top plot) and physical parameters H and D (bottom plot) from a trivariate copula (a) constructed by Chakak and Koehler (1995) and (b) constructed by the conditional mixtures. The simulated data is shown by the dots and the empirical data is shown by the squares.

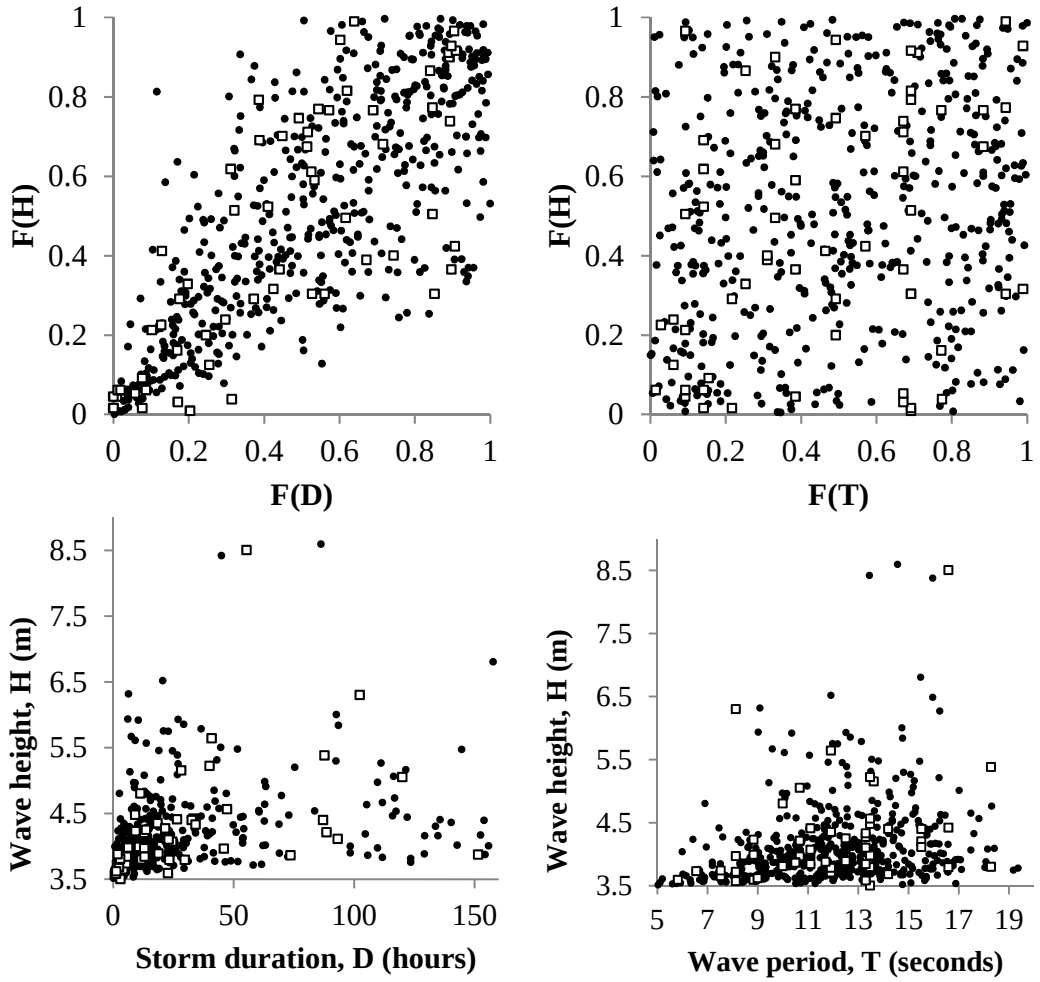

Figure 6.7: Simulations of wave height and storm duration as marginals $F(H)$ and $F(D)$ (top plot) and physical parameters H and D (bottom plot) from a trivariate hierarchical Clayton. The simulated data is shown by the dots and the empirical data is shown by the squares.

Table 6.5: A goodness of fit comparison between the three different trivariate copula $C(h, t, d)$ construction techniques

Construction technique	**Goodness of fit**		
	χ^2	ks	p-value
Hierarchical (Clayton nested in Clayton)	0.742	0.214	0.133
Chakak & Koehler [1995]	1.04	0.196	0.205
Hierarchical (Copula 12 nested in Clayton)	2.43	0.268	0.029
Conditional mixtures	4.43	0.357	0.001

6.5 Discussion

The p-values in Table 6.5 show that the conditional mixtures construction technique did not provide an appropriate fit to the empirical trivariate distribution. The hierarchical trivariate Clayton copula has the best Chi-squared value while the Chakak & Koehler [1995] construction technique had the best Kolmogorov-Smirnov statistic. Ultimately both techniques provide equally acceptable results. The appropriateness of the trivariate Clayton copula is dependent on the bivariate relationships. All our bivariate models are best modelled by the Clayton copula and $C(h, t)$ and $C(d, t)$ have similar dependence parameters (Table 6.3). This means that in our case study the limitations of hierarchical copulas are not realized. It is expected that one of the other two construction techniques would produce a better model if the bivariate distributions were not all described by the Clayton copula. So although the fully nested hierarchical copula provided the best fitting model it is unlikely to do so in all other circumstances as it does not uniquely model all the dependencies between variates.

The Chakak & Koehler [1995] construction technique is the simplest and provided satisfactory model results (see Sect. 6.4.4 and Fig. 6.6). The fully nested hierarchical technique provides the smallest Chi-squared statistic and is relatively simple to apply. The conditional mixtures approach is the most difficult construction technique of the three. The integral cannot be solved explicitly and a numerical solution can be demanding. Chakak & Koehler [1995] is the most appealing model from a practical point of view because it is so easy to apply.

The Clayton copula best represents the Durban data set and satisfies the storm

model described by De Michele *et al.* [2007] [following Boccotti, 2000] where it is assumed that the lower tail has a positive correlation and that the association converges towards the limit of -1 in the upper tail. We however have hypothesized that there exists a return to positive correlations for the most extreme events. As we approach a physical limit to wave height and storm duration the only way the storm magnitude can increase is by extreme waves coinciding with extreme storm durations. This will result in a positive correlation in the upper tail. The Clayton copula is not appropriate for such a model but copula 12 from Nelsen [2006] can model both upper and lower tail dependencies, but has the worst fit to our case study data. However, Fig. 6.8 shows that the simulation results of copula 12 appear to have an appropriate scatter when compared to the empirical data. Figure 6.9 illustrates the changes in the simulations using copula 12 for cases where the dependence parameter increases (i.e. the correlation approaches 1). Figure 6.9b shows that even with a strong correlation copula 12 still models a weaker association about the centre.

It is likely that most data sets will be modelled best by the Clayton copula. This is because most data sets would not have enough upper tail data to describe the positive correlation and so we suggest that the Clayton copula would only be modelling the lower tail and the central bulk of the distribution. We suspect that a more substantial data set including numerous extreme events would be more appropriately modeled by copula 12.

6.5.1 The model limitations

This paper has been intended to identify appropriate techniques for creating multivariate statistical models. In the model's current form it has numerous limitations, some of which can be improved. Firstly the model has no link to cyclonic forcings. On the east coast of South Africa storm waves are generally produced by either tropical cyclones, cut-off lows or cold fronts. Tropical cyclones are most frequent in February and cut-off lows in March. These events behave similarly in terms of wave production with the exception of wave direction. Tropical cyclones generally produce north easterly swell while cut-off lows produce south easterly swell. Although 93 % of all the South African east coasts' offshore wave heights

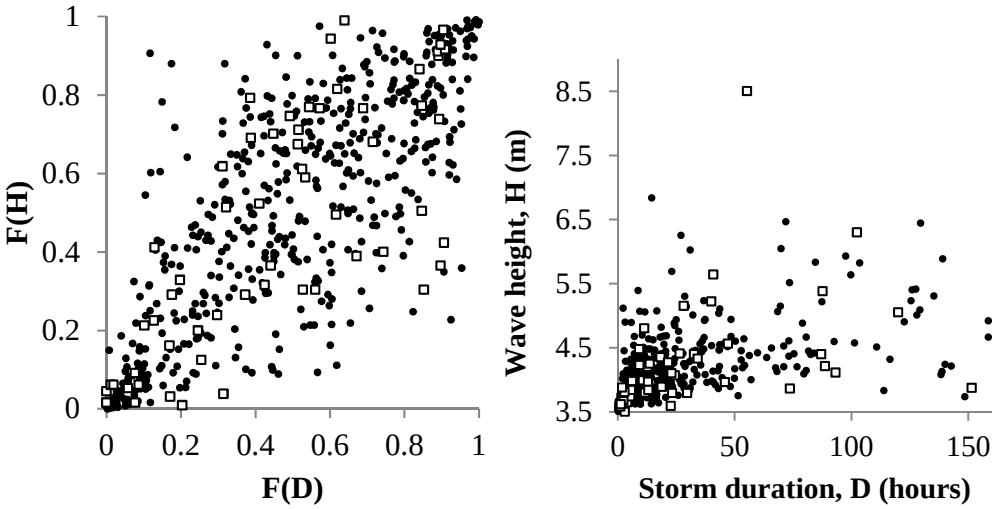

Figure 6.8: Simulations of (a) the wave height marginals $F(H)$ and the storm duration marginal $F(D)$ and (b) the wave height and storm duration from the bivariate copula 12 from Nelsen [2006]. The simulated data is shown by the dots and the empirical data is shown by the squares.

exceeding 3.5 m have directions which fall between south and east, inclusion of the wave direction would improve the model. Between 1962 and 2005 only seven cyclones affected the eastern parts of South Africa [Kruger *et al.*, 2010]. Assuming an average of 3 wave events per year means that cyclones only account for 5 % of the wave events. Similarly only 4 % of the case study's wave data is produced by cyclones of which the wave characterists are very similar to those produced by cut-off lows. The statistical model is therefore modelling a mixture of cold fronts and cut-off lows. The cut-off lows form further out to sea than the cold fronts. The cut-off lows are associated with the large wave heights and wave periods while the cold fronts produce the smaller wave heights and shorter wave periods.

Seasonality effects the frequency and intensity of events and as explained in Sect. 6.3.1 this can be included by using non-stationary probability distributions. This is considered a major limitation in the current model and must be included for realistic simulations.

The copula model also has no physical constraints such as maximum wave

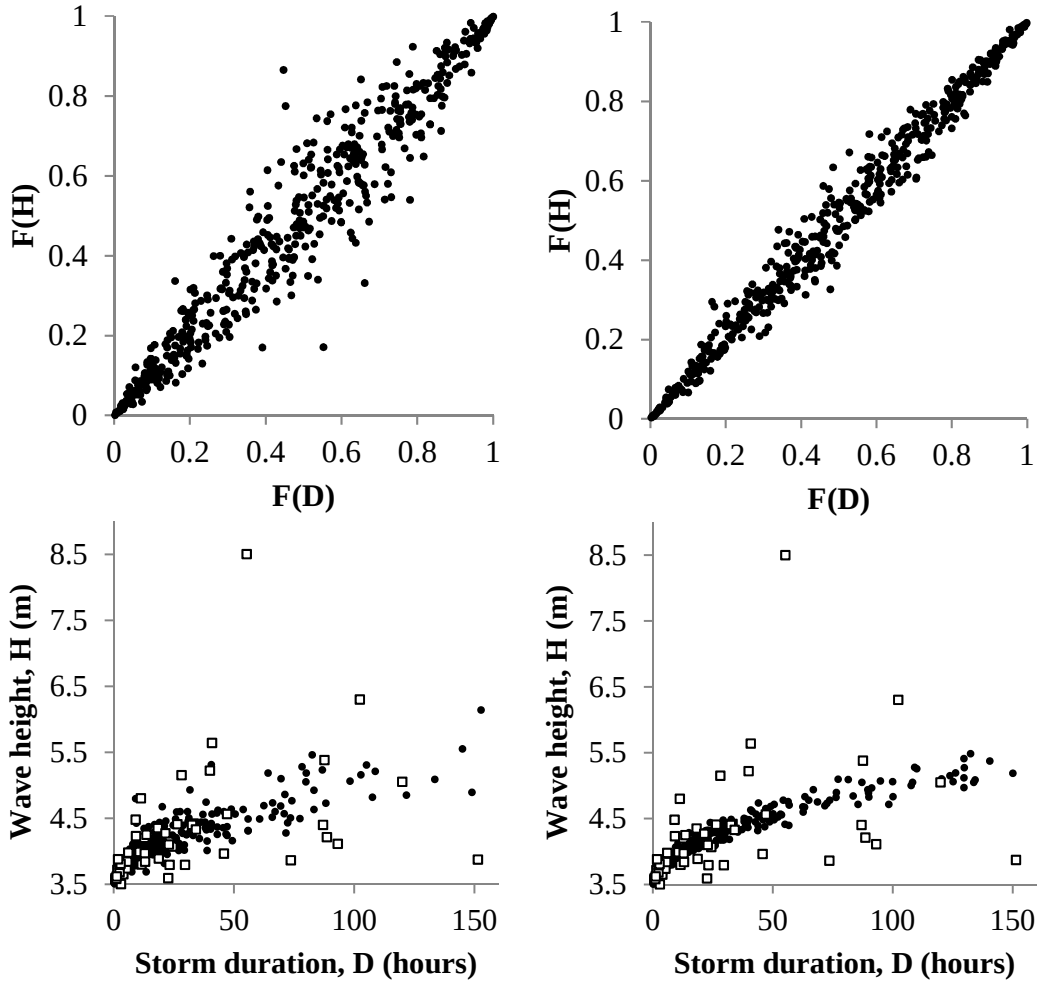

Figure 6.9: Simulations of wave height and storm duration shown in the top plot as marginals $F(H)$ and $F(D)$ and in the bottom plot as physical parameters H and D. Simulated from the bivariate copula 12 from Nelsen [2006] for a dependence parameter of (a) 4 and (b) 8.

steepness or a maximum water depth at wave breaking. The model is purely statistical and could therefore produce a wave height that might not exist at the given water depth. This however is not a major concern as the simulation results may be conditioned to restrict physically impossible events.

6.6 Conclusion

The dependencies of sea storm parameters have been analyzed. Only the parameters H, T and D displayed a significant interdependence all of which were positively correlated. The dependence between H and D was the strongest, followed by H and T. Three construction techniques were investigated for the creation of a trivariate copula. It was found that in general from a theoretical perspective the conditional mixtures approach provides the most complete model with no limitations regarding dependencies. The Chakak & Koehler [1995] method is the most appealing from a practical point of view as it provides similar results to the conditional mixtures, only requires 2-copulas to create a 3-copula and avoids solving the complicated integral produced by the condition mixtures. This simple technique is likely to be very appealing to practitioners. The fully nested method of creating hierarchal copulas provided the best results for our case study. This method does not model all the dependencies uniquely and the reason why it provided the best results is largely a function of the case study data set. The results highlight the importance of doing a thorough analysis of the bivariate data prior to creating a multivariate model because a simple construction technique may be appropriate and allow one to avoid the difficulties associated with the more complete conditional mixtures.

We have extended De Michele *et al.* [2007]'s bivariate analysis of sea storm data. De Michele *et al.* [2007] considered the dependencies of wave height and duration as a function of storm magnitude, while we have included an analysis of wave height and period as a function of peak wave power. From these bivariate analyses we have proposed an extension to the sea storm model suggested by Boccotti [2000]. We propose that there are three levels of storm magnitude and peak wave power: the lowest levels display positive associations, the middle levels negative associations, and as storms approach their physical limits there

is another positive correlation. This concept can be modelled well by copula 12 from Nelsen [2006], which can mimic both the lower and upper tail dependencies. The Boccotti [2000] model is well modelled by the Clayton copula.

In order to fully exploit the realism of numerical models the storm event inputs have to be equally realistic. Statistical models and copula methods provide appropriate tools to simulate realistic events to be used in numerical models of coastal and marine processes.

References

Accioly, R. S. Chiyoshi, F. Y.: Modeling dependence with copulas: a useful tool for field development decision process, Journal of Petroleum Science and Engineering, 44, 83 – 91, 2004. 158

Boccotti, P.: Wave mechanics for ocean engineering, Elsevier Oceanography Series, Elsevier Science, Amsterdam, 2000. 156, 162, 171, 174, 175, 183

Callaghan, D. P., Nielsen, P., Short, A., & Ranasinghe, R.: Statistical simulation of wave climate and extreme beach erosion, Coast. Eng., 55, 375 – 390, 2008. 20, 31, 58, 85, 121, 155, 182, 191, 192, 207, 236

Chakak, A. Koehler, K. J.: A strategy for constructing multivariate distributions, Communications Statistics-Simulation and Computation, 24 537 – 50, 1995. 25, 27, 28, 152, 154, 155, 162, 165, 170, 174, 313, 316

Charpentier, A. Segers, J.: Lower tail dependence for Archimedean copulas: Characterizations and pitfalls, Insurance: Mathematics and Economics, 40, 525 – 532, 2007. 162

Charpentier, A. Segers, J.: Tails of multivariate Archimedean copulas, Journal of Multivariate Analysis, 100, 1521 – 1537, 2009. 162

Chebana F. Ouarda T.B.M.J.: Multivariate quantiles in hydrological frequency analysis, Environmetrics, 22 (1), 63 – 78, 2011. 28, 30, 316

Chini, N. Stansby, P. Leake, J. Wolf, J. Roberts-Jones, J. Lowe, J.: The impact of sea level rise and climate change on inshore wave climate: A case study for East Anglia (UK). Coastal Engineering, 57, 973 – 984, 2010. 20, 58, 140, 156, 185, 223

Corbella, S. & Stretch, D. D.: The wave climate on the KwaZulu-Natal coast, South Africa., J. S. Afr. Inst. Civ. Eng., 54(2), 45 – 54, 2012. 94, 101, 155, 183, 220

De Michele, C. Salvadori, G. Passoni, G. Vezzoli, R.: A multivariate model of sea storms using copulas, Coastal Engineering, 54, 734 – 751, 2007. 22, 25, 27, 78, 152, 154, 155, 156, 162, 171, 174, 189, 190, 223, 224, 313, 315

Dowd, K.: Copulas in Macroeconomics, Journal of International and global Economic Studies, 1(1), 1 – 26, 2008. 158

Embrechts, P. Lindskog, F. McNeil, A.J.: Modelling dependence with copulas and applications to risk management, http://www.risklab.ch/ftp/papers/DependenceWithCopulas.pdf 2001. 26, 28, 154, 316

Genest, C. Rivest, L.: Statistical inference procedures for bivariate Archimedean copulas, Journal of the American Statistical Association, 88, 423, 1034 – 1043, 1993. 158, 226

Goda, Y.: Random Seas and Design of Maritime Structures (2nd Edition), World Scientific Publishing Co. Pte. Ltd, Singapore, 2008. 20, 21, 28, 58, 59, 151, 187, 188, 225, 233

Grimaldi, S. Serinaldi, F.: Asymmetric copula in multivariate flood frequency analysis, Advances in Water Resources, 29, 1155 – 1167, 2006. 26, 27, 154, 315

Gringorten, I. I.: A plotting rule for extreme probability paper, Journal of Geophysical Research, 68(3), 813 – 814, 1963. 160

Guedes Soares, C. Scotto, M. G.: Application of the r largest-order statistics for long-term predictions of significant wave height. Coastal Engineering, 51, 387 – 394, 2004. 20, 21, 58, 156, 185, 223

Hofert, M.: Sampling Archimedean copulas, Computational Statistics and Data Analysis, 52, 5163 – 5174, 2008. 27, 315

Hofert, M.: Efficiently sampling nested Archimedean copulas, Computational Statistics and Data Analysis, 55, 57 – 70, 2011. 27, 315

Isaacson, M. S. MacKenzie, N. G.: Long-term distributions of ocean waves: a review, Journal of Waterway, Port, Coastal and Ocean Division, ASCE, 107, WW2, 1981. 19, 58, 59, 150

Joe, H.: Multivariate Models and Dependence Concepts, Chapman & Hall, London, 1997. 25, 26, 152, 154, 313

Kruger, A. C. Goliger, A. M. Retief, J. V. Sekele, S.: Strong wind climatic zones in South Africa, Wind and Structures, 13, 1, 2010. 52, 172

Mendeza, F. J. Menendez, M. Luceno, A. Medina, R. Graham, N. E.: Seasonality and duration in extreme value distributions of significant wave height. Ocean Engineering, 35, 131 – 138, 2008. 155, 156, 185, 186, 187, 223

Minguez, R. Menndez, M. Mndez, F.J. Losada I.J.: Sensitivity analysis of time-dependent generalized extreme value models for ocean climate variables. Advances in Water Resources, 33, 833 – 845, 2010. 156, 185, 186, 223

Nelsen, R.B.: An introduction to copulas, (second edition), Springer Series in Statistics, Springer, New York, 2006. xxi, xxviii, 22, 24, 25, 26, 27, 29, 152, 153, 154, 158, 159, 162, 171, 172, 173, 175, 189, 190, 223, 224, 315

Ruggiero, P. Komar, P. D. Allan, J. C.: Increasing wave heights and extreme value projections: The wave climate of the U.S. Pacific Northwest. Coastal Engineering, 57, 539 – 552, 2010. 13, 20, 58, 115, 139, 156, 185, 186, 196, 223

Salvadori, G. De Michele, C.: Statistical characterization of temporal structure of storms, Advances in Water Resources, 29, 827 – 842, 2006. 152

Salvadori, G. De Michele, C. Kottegoda, N.T. Rosso, R.: Extremes in Nature. An Approach Using Copulas, Water Science and Technology Library, Springer, 56, 292, 2007. 25, 154, 155, 225, 313

Salvadori, G. De Michele, C.: Multivariate multiparameter extreme value models and return periods: A copula approach, Water Resources Research, 46, W10501, doi:10.1029/2009WR009040 2010. 152, 189, 223, 225

Salvadori, G. De Michele, C. Durante, F.: Multivariate design via Copulas, Hydrol. Earth Syst. Sci. Discuss., 8, 5523 – 5558, 2011. 29, 30, 152, 219, 220, 225, 226, 227, 240

Savu, C. Trede, M.: Hierarchical Archimedean copulas, http://www.uni - konstanz.de/micfinma/conference/Files/papers/Savu_Trede.pdf (2008-11-01), 2006. 26, 27, 154, 190, 224, 314, 315

Savu, C. Trede, M.: Hierarchies of Archimedean copulas, Quantitative Finance, 10 (3), 295 – 304, 2010. 27, 190, 224, 315

Sklar, A. Fonctions de repartition a n dimensions et leurs marges, Publications de l'Institut de Statistique de l'Universit de Paris, 8, 229 – 231. 1959. 23

Sorensen, R. M.: Basic Coastal Engineering, Third Edition, Springer Science and Business Media, Inc. New York, 2006. 13, 14, 150

U.S. Army Corps of Engineers.: Coastal Engineering Manual, EM 1110-2-1100, Part II: (Chapter 8), 9 – 11. 2006. 155, 160

van Gent, M. R. A. van Thiel de Vries, J. S. M. Coeveld, E. M. de Vroeg, J. H. van de Graaff, J.: Large-scale dune erosion tests to study the influence of wave periods, Coastal Engineering, 55, 1041 – 1051, 2008. 21, 54, 138, 151, 219

van Thiel de Vries, J. S. M. van Gent, M. R. A. Walstra, D. J. R. Reniers, A. J. H. M.: Analysis of dune erosion processes in large-scale flume experiments, Coastal Engineering, 55, 1028 – 1040, 2008. 21, 54, 138, 151, 219

Whelan, N.: Sampling from Archimedean copulas Quantitative Finance, 4 (3), 339 – 352, 2004. 26, 28, 154, 316

Woodroffe, C. D.: Coasts: form, process and evolution, Cambridge University Press, Cambridge, United Kingdom, 2003. 14, 15, 114, 131, 150

Zhang, L. Singh, V. P.: Trivariate Frequency Analysis Using the Gumbel-Hougaard Copula, Journal of Hydrologic Engineering, 12(4), 431 – 439, 2007. 158, 160

Chapter 7

Predicting coastal erosion trends using non-stationary statistics and process-based models

This chapter is based on a paper published in Coastal Engineering, 70, 40 – 49, 2012.

Abstract

Storms and water levels are subject to seasonal variations but may also have decadal or longer trends that need to be included when estimating risks in the coastal zone. We propose a non-stationary multivariate generalised extreme value model for wave height, wave period, storm duration and water levels that is constructed using Archimedean copulas. The statistical model was applied to a South African case study to test the impacts of decadal trends on beach erosion. Erosion was estimated using three process-based models – SBEACH, XBEACH, and the Time Convolution model. The XBEACH model provided the best calibration results and was used to simulate potential future long-term trends in beach erosion. Based on the simulated erosion results of 5 beach profiles for storms with 25, 50 and 100 year return periods, it is estimated that the erosion rate could increase

by 0.20 %/year/storm and should therefore be a significant factor in long-term planning.

7.1 Introduction

Increasing awareness of future climate change impacts has added a new dimension to traditional design practice. The predicted and/or the measured increases in storm intensity and frequency should be accounted for in failure risk assessment based on an average recurrence interval. Erosion of coastlines is dominated by three factors: sediment supply; wave forces and sea level rise. This paper attempts to consider all these factors and forecast the erosion potential of future storms using a non-stationary multivariate generalised extreme value statistical model based on Archimedean copulas together with process-based models of the beach response.

Numerous authors have proposed a combination of process-based models and statistical models to estimate the potential impacts of climate trends. Only the most relevant examples are mentioned here. Wang *et al.* [2004] analysed potential changes in significant wave heights using a global climate model and a non-stationary generalised extreme value distribution. They concluded that there was variability of about 20 % between decadal extreme significant wave heights. Coles & Tawn [1994, 1990, 1991] provide methods relating to multivariate statistical modelling in a coastal context while Coles & Tawn [1994] used these methods with an empirical formula for overtopping of a seawall to estimate a probability zone of failure. Wang & Reeve [2010] presented a probabilistic model of long-term beach evolution near detached breakwaters using the numerical model developed by Hanson *et al.* [2006]. Callaghan *et al.* [2008] used a joint distribution of wave parameters to estimate erosion in combination with the time convolution shoreline response model of Kriebel & Dean [1993]. Zacharioudaki & Reeve [2011] performed a statistical analysis of beach response to wave conditions arising from climate change scenarios. Zacharioudaki & Reeve [2011] used a one-line beach response model which is appropriate for beaches dominated by long-shore sediment transport. Our study is concerned with storm waves and so uses cross-shore morphological models. Although much work has combined

statistical models with numerical models this paper presents a unique use of a copula based non-stationary multivariate statistical model in combination with process-based models to quantify potential future storm induced erosion.

We initially provide a brief theoretical background to the statistical and process-based models and outline the methods used. The methodology is tested by applying it to a case study on the east coast of South Africa. The results are then presented and discussed before concluding.

7.2 Theoretical Background and Methods

7.2.1 Case study site

The east coast of South Africa has 18 years of reliable wave data from wave recording buoys near the city of Durban (Fig. 7.1). Corbella & Stretch [2012a] provide details of the data set. A storm event was defined in terms of a significant wave height threshold similar to the triangular storm concept proposed by Boccotti [2000]: a storm event begins when a significant wave height Hs exceeds a threshold of 3.5 m and ends when the significant wave height falls below 3.5 m for a period of at least 2 weeks based on the decay time of the autocorrelation. The reduced storm data set was then manually assessed to ensure that each storm event represented one meteorological event. Finally we select, on average, the 3 largest storms per year. The period between the start and the end time is the storm duration D and the time between the events is the calm period I. The storm definition is illustrated in Fig. 7.2.

Corbella & Stretch [2012b] analysed Durban's wave data and identified increasing trends in significant wave heights exceeding the 3.5 m threshold. They also noted an increase in peak period T and in the frequency of storm events (or similarly a decrease in the average calm period). Only the increase in peak period was found to be statistically significant.

The case study site at Durban also has a 37 year record of beach profiles which exhibit a long term erosion trend [Corbella & Stretch, 2012b]. The records of interest to this study are those that bound storm events. Only the 1998 and 2007 events met these requirements. The analysis is limited to profiles A, C, D,

Figure 7.1: A map of (a) South Africa showing Durban and a map of (b) the Durban Bight showing the locations of profile A, C, D, F and 13 and the Durban harbour

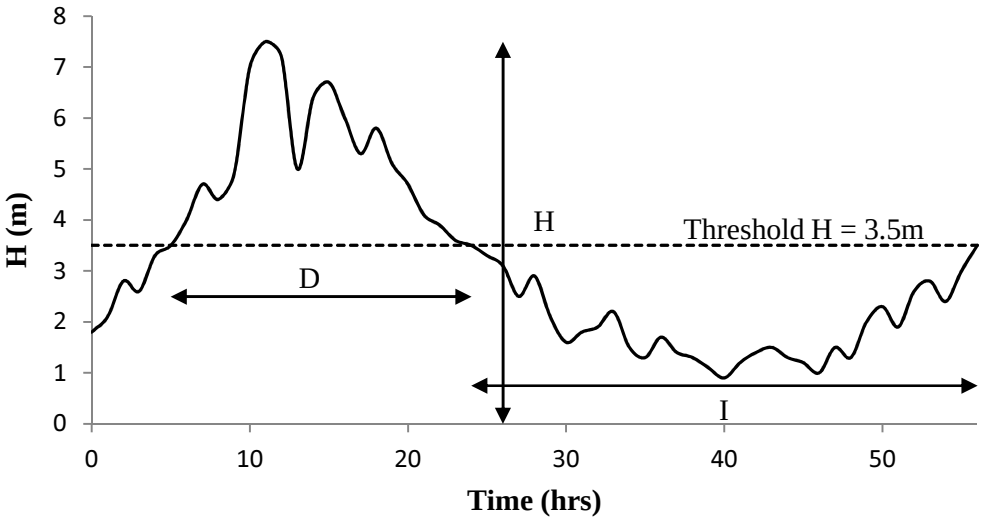

Figure 7.2: Illustration of the storm definition showing the significant wave height Hs, storm duration D and calm period I.

F and 13 (Fig. 7.1) as they have the most frequent bathymetry data and provide a good representation of the Durban Bight while avoiding most of the sheltering near the harbour entrance and the influence of perpendicular beach structures and sand bypass scheme.

In March 2007 Durban experienced its largest wave event on record. The 8.5 m significant wave height and 16.6 second peak period coincided with an extreme high tide of 2.2 m above chart datum (CD) and devastated the coastline. This storm was a realisation that much of the current infrastructure is not capable of withstanding potentially more frequent and intense events in the future. Since the damage of the 2007 event can be easily quantified it will be used as a base line to demonstrate the potential impacts of storm and water level trends.

7.2.2 The Generalised Extreme Value model

The Generalised Extreme Value (GEV) distribution has been used extensively for extreme value analysis of hydrological events and specifically for wave heights by Chini *et al.* [2010]; Guedes Soares & Scotto [2004]; Mendez [2008]; Minguez *et al.* [2010] and Ruggiero *et al.* [2010]. The GEV encompasses three distributions often

referred to as Types I, II and III. The probability density function is given by

$$y = \sigma^{-1} \exp\left(-\left(1 + k\frac{x-\mu}{\sigma}\right)^{-\frac{1}{k}}\right)\left(1 + k\frac{x-\mu}{\sigma}\right)^{-1-\frac{1}{k}} \tag{7.1}$$

for $(1 + k\frac{x-\mu}{\sigma}) < 0$, where μ is the location parameter, σ is the scale parameter and k is the shape parameter. This traditionally stationary model can be adapted to model non-stationary events by making the GEV parameters time dependent [Mendez, 2008; Katz *et al.*, 2002; Minguez *et al.*, 2010]. Non-stationarity is usually limited to time varying location and scale parameters $\mu(t)$ and $\sigma(t)$. For example Ruggiero *et al.* [2010] and Zhang *et al.* [2004] model the location parameter as a linear function of time and the shape parameter as an exponential function of time. Others who have been interested in cyclic behaviour (such as seasonality) have used trigonometric functions to model the location and shape parameters [Mendez, 2008; Katz *et al.*, 2002; Minguez *et al.*, 2010]. For the present study we have assumed that the time dependency can be expressed simply as

$$\mu(t) = \mu_0 + \mu_1 t,\ \sigma(t) = \sigma_0,\ k(t) = k_0, \tag{7.2}$$

where the location parameter is assumed to be linearly dependent on time and the shape and scale parameters are assumed to be constant based on the findings of Wang *et al.* [2004]. Corbella & Stretch [2012b] identified increasing trends in Hs, T and the frequency of storm events. However, only the wave height Hs was modelled with a non-stationary GEV model in the present study, while changes in T and D were included through their dependence on Hs as captured by a multivariate statistical model based on copulas and described in Sect. 7.2.5

7.2.2.1 Sea level estimating with the GEV model

Sea level can be broadly divided into astronomical forcing and sea level rise. Sea level rise is well documented and the trend is usually described linearly (Mather [2008] and references therein). A rate of 2.7 mm/year for sea level rise was assumed for the present study based on the work of Mather [2008, 2007]. The increase in sea level is included in the GEV through the location parameter and

is expressed as

$$\mu_{SLR}(t) = 0.0027t, \tag{7.3}$$

where $\mu_{SLR}(t)$ denotes the sea level rise component of the location parameter.

The sinusoidal nature of astronomical forcing as well as the numerous cycles makes it more complicated to include in the GEV model. Examples of the long-term astronomical forcings include the 18.6 year nodal cycle due to the regression of the lunar nodes and the 4.5 year cycle when the lunar perigee coincides with the equinox [Pugh, 1987]. These two cycles do not have the same phase and the interaction of these two cycles should be included in the model. To reduce the complexity of the model we only consider the 18.6 year nodal cycle in the present study. We include the nodal cycle in the location and scale parameter as described by Mendez [2008], whence

$$\mu_N(t) = \beta_{N_1} \cos(2\pi t/18.6) + \beta_{N_2} \sin(2\pi t/18.6), \tag{7.4}$$

$$\sigma_N(t) = \alpha_{N_1} \cos(2\pi t/18.6) + \alpha_{N_2} \sin(2\pi t/18.6), \tag{7.5}$$

where $\mu_N(t)$ and $\sigma_N(t)$ denote the nodal cycle component of the location and scale parameters respectively, and β and α describe the amplitudes of the nodal cycle. The nodal cycle components were estimated from simulated tidal data between the years 1980 and 2010.

7.2.3 Fitting the Generalised Extreme Value model

The fitting of these distributions requires the sampling of extreme events. The simplest sampling method is the annual maximum method which fits a probability distribution to the annual maxima wave heights. The peak over threshold method samples all events exceeding a specific threshold. Unlike the annual maximum method the peak over threshold method allows more than one event per year to be sampled and is therefore commonly used for analysing short data sets. Generally the GEV is used to model block maxima while the generalised pareto distribution (GP) is used to model data that has a threshold. However, there is no theoretical ground to recommend a specific distribution function for the peak over threshold method [Goda, 2008]. For our data set the GEV and the GP provide similar

results with the GEV having a superior akaike information criteria. We therefore use the GEV to model all the parameters of interest. It should be noted that the marginal distributions do no affect the dependence modeled by the copulas and may be replaced with any preferred distribution.

The maximum likelihood method maximizes the joint probability of observing the data in the sample. This intuitive method has been referred to as the most popular and best technique for deriving estimators [Casella & Berger, 1990; Montgomery & Runger, 2003]. The maximum likelihood method is popular with statisticians because its characteristics are underpinned by a well developed theory [Goda, 2008]. The method was therefore selected for this study.

The significance of non-stationarity in the GEV distributions was evaluated using a log-likelihood ratio test. The test identifies the statistical significance of a trend when compared to a model without a trend. Let M_1 be a model with a trend and M_0 be a model without a trend. If the corresponding log-likelihoods are given by ℓ_{M_0} and ℓ_{M_1} respectively, then the log-likelihood ratio statistic given by

$$LRS = 2(\ell_{M_1} - \ell_{M_0}), \tag{7.6}$$

which is asymptotically chi-squared distributed with degree-of-freedom equal to the difference between the number of free parameters in the two models. We reject the no trend M_0 hypothesis at a significance level of 95 % if LRS exceeds the upper 95^{th} percentile of the chi-squared distribution.

7.2.4 Event frequency

The non-stationary GEV distribution has been used to model the change in wave height. The annual increase in the frequency of these events still has to be included in the model. The definition of an average recurrence interval for a partial duration series is given by [Goda, 2008; Salvadori, 2004]

$$\tau = \frac{\lambda}{1-p}, \tag{7.7}$$

where τ is the average recurrence interval, λ is the average event inter-arrival time $1/(D+I)$ (or inverse of the annual average event frequency f_0) and p is

the non-exceedance probability of an event. A trend in event frequency can be included by making λ time dependent. Assuming a linear trend we represent the trend in $\lambda(t)$ as

$$\lambda(t) = \frac{1}{f_0 + f_1(t)}, \tag{7.8}$$

Equation 7.7 can then be used to express p as a time dependent function of τ, namely

$$p = 1 - \frac{1}{\tau\left(f_0 + f_1(t)\right)}, \tag{7.9}$$

This frequency model can now be used in combination with the non-stationary GEV model to estimate a future wave height for a given recurrence interval based on the trend in frequency and intensity.

7.2.5 Archimedean Copulas

Erosion is not only dependent on wave heights but also on wave period, storm duration, wave angle and sea level. A multivariate statistical model was therefore used to model the dependency between these parameters. Since the physical relationships between the parameters are not expected to change they can be used with both stationary and non-stationary GEV distributions.

The multivariate model was constructed using Archimedean copulas. Copulas are mathematical functions that join or couple multivariate probability distribution functions $F(x_1, \ldots, x_n)$ to their one-dimensional marginal distribution functions $F_1(x_1), \ldots, F_n(x_n)$. For a detailed introduction to copulas refer to De Michele *et al.* [2007]; Nelsen [2006]; Salvadori & De Michele [2010]. Using a 2-dimensional case as an example, an Archimedean copula C is defined as

$$C(u, v) = \varphi^{-1}[\varphi(u) + \varphi(v)], \tag{7.10}$$

where $u = F(x)$ and $v = F(y)$ are marginal distribution functions and φ is the generator function.

Corbella & Stretch [2012c] found that only Hs, T and D of the case study wave data are significantly inter-dependent. Based on this observation they created a fully nested trivariate hierarchical Clayton copula. The same trivariate model

was used for the present study. The Clayton copula generator function is given by

$$\varphi(s) = \frac{1}{\theta}(s^{\theta} - 1) \tag{7.11}$$

where θ is the dependence parameter and $s \in [0, 1]$. The 3-dimensional hierarchical copula has 2 generators, φ_1 and φ_2 and is expressed as

$$C(u_1, u_2, u_3) = \varphi_2^{-1}\left(\varphi_2\left(\varphi_1^{-1}\left[\varphi_1(u_1) + \varphi_1(u_2)\right]\right) + \varphi_2(u_3)\right) \tag{7.12}$$

This model can be used to simulate events conditionally given the expected future wave heights estimated by the non-stationary GEV model. We perform this simulation using the conditional inversion method [De Michele *et al.*, 2007; Nelsen, 2006; Savu & Trede, 2006, 2010]. Given the non-exceedance probability of a wave height h the non-exceedance probability of duration d can be estimated from the conditional law G of the bivariate copula as

$$G_2(d \,|\, h) = \partial_h C(h, d) \tag{7.13}$$

The non-exceedance probability of the wave period t can then be estimated conditionally based on the given values of h and d from the bivariate and trivariate copulas as

$$G_3(t \,|\, h, d) = \frac{\partial_{h,d} C(h, d, t)}{\partial_{h,d} C(h, d)} \tag{7.14}$$

Sampled values for Hs, D and T can then be found by inverting the associated GEV models. It should be noted that Hs, D and T are also dependent on wave direction. Wave direction was not included in the copula model because all the sampled storm events fall between 110° and 180° with an average direction of 147°. There is no significant rank correlation between wave height and wave direction so we assume that all extreme events are equally likely to arrive from any direction between 110° and 180°.

The main advantage of copulas is that they are not limited to dependence described by linear correlation. Dependence measured as a linear correlation is only suitable for a special class of distribution (i.e. elliptical distributions) and its uses outside of these distributions leads to numerous fallacies (see McNeil

et al. [2005]). We therefore use Kendall's tau rank correlation as a measure of dependence. The Clayton copula interpolates between dependency structures. For the limits $\theta \rightarrow 0$ the Clayton copula becomes the independence copula. For $\theta \rightarrow$ inf the comonotonicity copula is produced and for $\theta \rightarrow$ -1 the Frechet-Hoeffding lower bound is obtained. The Clayton copula therefore interpolates between countermonotonicity, independence and comonotonicity.

7.2.6 Erosion estimation by numerical modelling

There are numerous numerical models available for estimating cross-shore erosion [Schoonees & Theron, 1995]. We limit our analysis to SBEACH [Larson *et al.*, 1990], the Time Convolution model [Kriebel & Dean, 1993], and XBEACH [Roelvink *et al.*, 2009]. Although SBEACH has been found to under estimate erosion [Seymour *et al.*, 2005; Zheng & Dean, 1997] it generally provides reasonable predictions [Schoonees & Theron, 1995; Zheng & Dean, 1997]. Kriebel and Dean's model is the simplest of the three models and is based on the theory of idealised equilibrium profiles where the water depth

$$h = \begin{cases} -B & x \leq -\frac{B}{m} \\ mx & -\frac{B}{m} \leq x \leq \frac{4A^3}{9m^3} \\ A\left(x - \frac{4A^3}{27m^3}\right)^{\frac{3}{2}} & x \geq \frac{4A^3}{9m^3}, \end{cases} \tag{7.15}$$

where x is the cross-shore distance offshore, B is the dune height above mean sea level, and A is an empirical coefficient that depends on the sediment settling velocity [Kriebel & Dean, 1993]. Storm surge for the Time Convolution model was limited to the sum of the tidal anomaly and wave setup. Assuming saturated wave conditions and ignoring bed shear stresses the maximum wave setup can be estimated as (Callaghan *et al.* [2008] citing Dean & Dalrymple [1991])

$$\bar{\eta}_{max} = \frac{40 - 3\gamma_b^2}{128}\gamma_b H_b, \tag{7.16}$$

where $\gamma_b = H_b/h_b$ and H_b is the wave height where wave breaking initially occurs and h_b is the depth that wave breaking occurs. The values of H_b and h_b were

estimated for the simulated events in the SWAN model (refer to Sect. 7.2.6.1).

The Time Convolution model has been previously applied to estimating erosion (e.g. Callaghan *et al.* [2008]). However, it is not intended to accurately reproduce erosion processes but rather to provide a fast and easy method to estimate profile retreat.

The XBEACH model is a relatively new public-domain model that is still under development. Although XBEACH has not yet been tested as extensively as the SBEACH model, it has been used for a number of recent studies and has given satisfactory results (e.g. Hartanto *et al.* [2011]; Roelvink *et al.* [2009]).

The three models were calibrated using the 2007 storm event and verified using the 1998 event. The 1998 event had profile measurements one day before the storm peak and two days after the peak. The 2007 event had measured profiles one month before the event and 9 days after the event. These were the only two storm events that had profile data close enough to the event for calibration purposes.

All the models predict erosion of the profile but the sediment remains within the model domain and there is no net loss of sediment. Therefore, only the erosion above mean sea level (MSL) was calculated and compared with the field data.

The wave events simulated by the statistical model are based on recordings from the waverider buoy and so we use the numerical wave model SWAN (Simulating WAves Nearshore) to transform these events to the required locations. The significant wave height and storm duration estimated from the statistical model are used to create an idealised time series of a storm (Fig. 7.8). This time series is transformed to a nearshore time series by the SWAN model and the transformed time series is used in the cross-shore models.

Since the statistical model did not include wave direction we simplify the erosion simulations by setting all the offshore deepwater wave directions equal to 145 ° (south east).

7.2.6.1 The SWAN model

The SWAN model used in this study was set up using three grid resolutions. The largest, offshore rectangular grid had approximately 1000 m × 1000 m grid

Table 7.1: The calibration parameters of the SWAN model

Parameter	**Value**
Water level (Mean Sea Level) (m)	0.0
Directional sector	0 – 360
No. directions in directional space	72
Lowest frequency (Hz)	0.05
Highest frequency (Hz)	1
No. frequency bins	36
Spectrum	JONSWAP
Spectral peak enhancement factor	2.5
Directional energy spreading	15 (Cosine power)
Depth induced breaking	Battjes and Janssen
Alpha - breaking	1
Gamma - breaking	0.73
Bottom friction	Madsen *et al.* [1988]
Friction coefficient	0.01
Non-linear triad interaction	De-activated
Wind growth	De-activated
Whitecapping	Komen *et al.* [1984]
Quadruplets	De-activated
Frequency shift	Activated

cells. A medium grid had 400 m × 400 m cells and the smallest curvilinear grid had approximately 100 m × 50 m cells. The statistically simulated wave conditions were transformed to 20 m water depths in front of each of the selected profile locations. Hind-cast data for the two storms were obtained from the WAVEWATCH-III global wave model [Tolman *et al.*, 2010] and used as offshore boundary conditions to calibrate and verify the SWAN model with the wave recording buoy data. Table 7.1 shows the SWAN model setup and Fig. 7.3 shows time series comparison of the measured and SWAN simulated significant wave heights during the 1998 storm event. The average measured significant wave height over the 1998 storm duration was 3.5 m and the modeled wave height was 3.4 m. The results were similar for the 2007 event.

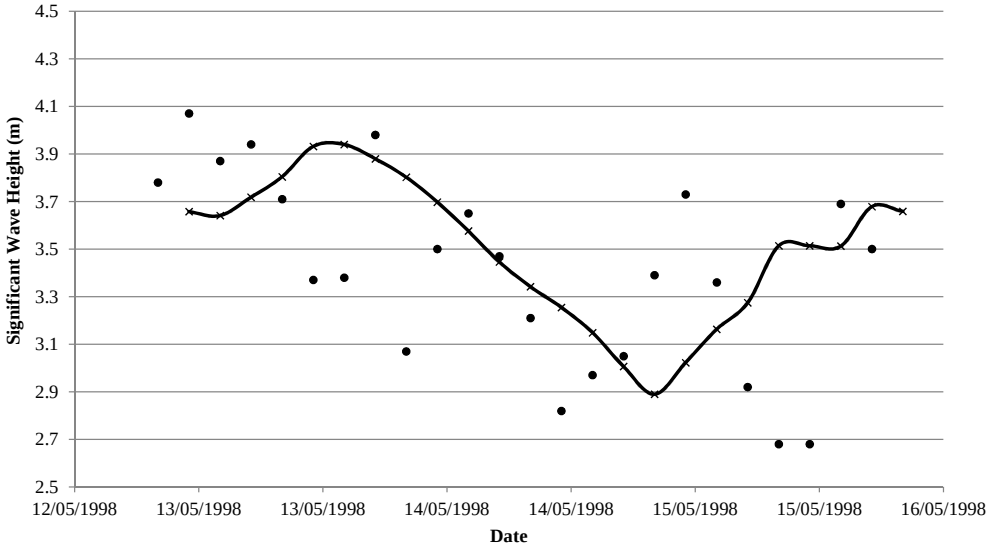

Figure 7.3: A time series comparison of the measured and SWAN simulated significant wave heights during the 1998 storm event. The dots are measured significant wave heights from a Waverider buoy. The line and crosses are SWAN simulated significant wave heights

7.2.7 Summary

We have outlined the creation of a time dependent statistical model and have described four numerical models. We now summarise the section by providing an algorithm for the process used to quantify future erosion.

1. Sample storm parameters Hs, D, T and λ using the POT method and the storm definition given in Sect. 7.2.1.
2. Identify appropriate functions to model any trends in Hs and λ.
3. Fit a non-stationary GEV distribution to Hs.
4. Fit GEV distributions to D and T.
5. Create a copula model of Hs, D and T.
6. Estimate the time dependent non-exceedance probability p (Eqn. 7.9) of Hs corresponding to a 31-year recurrence interval τ (the 2007 event) for a forecast of 10, 25, 50 and 100 years.

7. Simulate 1 000 000 non-exceedance probability samples, at specified non-exceedance probabilities of h, for storm duration d and wave period t from the conditional laws of the bivariate (Eqn. 7.13) and trivariate copulas (Eqn. 7.14).

8. Calculate an event equivalent to the probability levels of the 2007 event from the 1 000 000 samples of d and t.

9. Estimate the value of Hs, D and T from the inverse of the cumulative GEV distribution with the time dependent location parameter (Eqn. **??**).

10. Simulate sea levels for a 10, 25, 50 and 100 year forecast from the inverse of the cumulative GEV distribution using the time dependent parameters (Eqn. 7.3 to 7.5).

11. Use the simulated values of Hs and D to create an idealised storm time series with the maximum significant wave height occurring at half the storm duration (Fig. 7.8).

12. Use the simulated sea level and a sine function to create a time series of the tide. Make the high tide coincide with the maximum wave height.

13. Calibrate the SWAN, SBEACH, XBEACH and Time Convolution model using past storm events.

14. Use the SWAN model to transform the simulated wave events to the required locations and to calculate the wave breaking heights and water depths for the Time Convolution model.

15. Use the SBEACH, XBEACH and Time Convolution model to estimate the erosion corresponding to the simulated wave events.

The shoreline response models require Hs, T, D, wave direction and water level as inputs. Wave direction could not be included in the statistical model because the 7 years of data is too short to establish a trend or dependence between the other parameters. We therefore use the most common wave direction of south east as a constant wave angle in the models.

7.3 Results

7.3.1 Trend analysis

As previously mentioned we limit our analysis of trends to Hs and water levels. We then use the dependency between the storm parameters Hs, D and T to estimate the associated changes of D and T. Water levels were modelled separately because Corbella & Stretch [2012c] found them to be independent of the other storm parameters.

7.3.1.1 Trends in significant wave height

The observed trend in the significant wave height was not found to be statistically significant at a 95 % confidence level [Corbella & Stretch, 2012b]. The difficulty in establishing trends from a relatively short data set is illustrated by the return period estimates using the stationary GEV model in Fig. 7.4. The limited data in the upper tail causes the bootstrapped 95 % confidence interval to become large very quickly. Despite the uncertainty, the observed trend in Hs was modelled and is shown in Fig. 7.5. The rate of increase of significant wave heights exceeding 3.5 m was estimated to be 0.02 m/year. This trend was incorporated into the GEV model using the location parameter as described in Sect. **??**. The negative log-likelihood method estimated the rate of change of the location parameter to be 0.0057 m/year. The log-likelihood ratio test between the stationary and non-stationary models confirmed that the trend in Hs was not statistically significant. The 0.020 m/year trend is similar to the trends identified by Bacon & Carter [1991]; Dodet *et al.* [2010]; Ruggiero *et al.* [2010]; Theron *et al.* [2010], but because there is limited statistical confidence in the data we analyse both the 0.0057 m/year and 0.02 m/year trends.

The significance of an increasing wave height is illustrated in Fig. 7.6. The plot shows how the same recurrence interval corresponds to larger events as time proceeds.

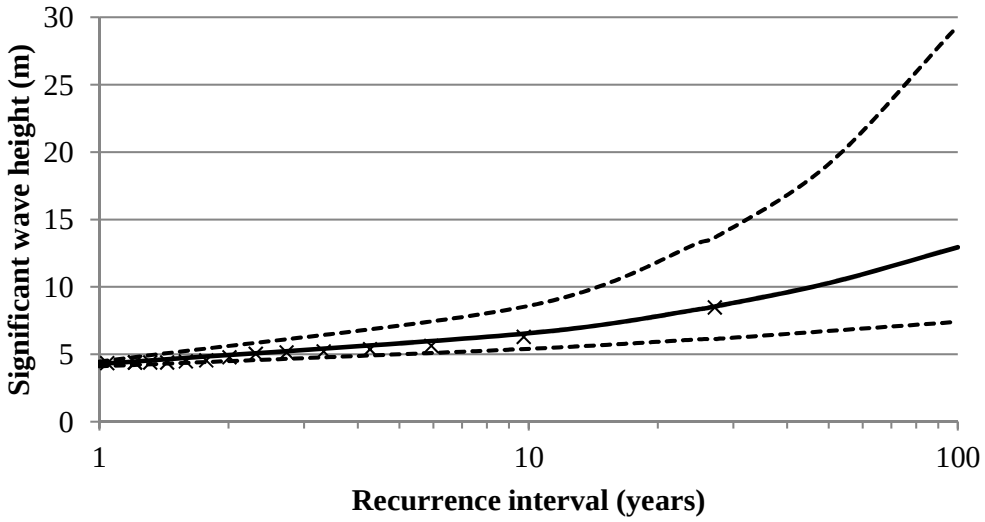

Figure 7.4: The recurrence intervals of significant wave height and the bootstrapped 95 % confidence. The crosses show the empirical recurrence intervals

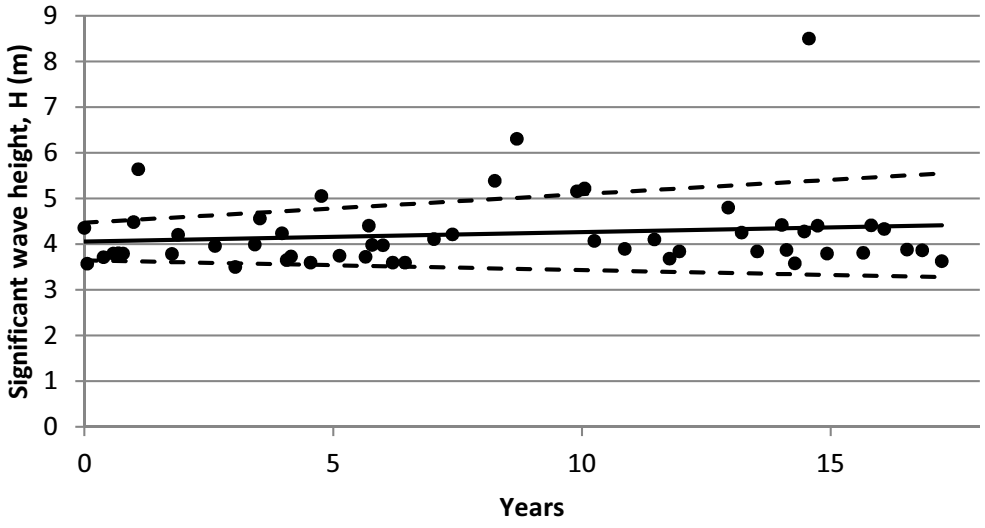

Figure 7.5: The significant wave height events exceeding 3.5 m between 1992 and 2010 and their linear regression shown by the solid line and the 95 % confidence intervals shown by the dashed lines

Figure 7.6: The 100 year forecasted increase in significant wave heights for recurrence intervals between 1 and 100 years for: (a and b) a 0.0057 m/year increase in Hs and (c and d) a 0.02 m/year increase in Hs

7.3.1.2 Trends in storm frequency

The trend in storm frequency was estimated from the occurrence of wave heights exceeding 4 m. It was found that the average of $f_0 = 3$ events/yr was increasing at an average rate of $f_1 = 0.01$ events/yr.

7.3.1.3 Trends in water level

Unlike the GEV model of Hs which used the POT method, the GEV for the water levels was fitted to the annual maxima tide levels. As previously mentioned an estimate of 0.0027 m/year was assumed for sea level rise. Similar to Mendez *et al.* [2007] the contribution of the scale parameter to the nodal cycle was found to be negligible. The amplitude of the nodal cycle $(\beta_{N_1}^2 + \beta_{N_2}^2)^{1/2} = 0.03$ is similar to Mendez *et al.* [2007] and Sobey [2005]. $\beta_{N_1} = 0.004$ and $\beta_{N_2} = 0.03$ while the nodal cycle contribution in the scale parameter $(\alpha N_1, \alpha N_1)$ is not significant. Figure 7.7 shows the linear trend in sea level, the sinusoidal trend in the nodal cycle, and the combination of the two trends in the GEV model.

7.3.2 Simulated events

Table 7.2 shows the simulated events. The copula model incorporates the dependence between the significant wave height, duration and peak period. This dependence allows the trends in duration and peak period to be modelled conditionally on the trend in significant wave height. Table 7.2 shows an increasing trend in duration. The simulated rates of D and T are not consistent with the findings of Corbella & Stretch [2012b]. The reason for this is because the trivariate copula has no upper tail dependence and does not represent the average trend of the data set. If an event in the centre of the distribution, such as a wave height of 5 m was used, then there would be a larger change in D and T. For a detailed explanation of this concept the reader is referred to Corbella & Stretch [2012c]. This concept of tail dependence makes the use of copulas very powerful when forecasting conditionally dependent events.

Figure 7.8 illustrates the evolution of an idealised 2007 storm event over time. If we define the storm magnitude as the area under the plots in Fig. 7.8 it can

Table 7.2: The storm parameters of the 2007 event (significant wave height Hs, duration D, peak period T and water level WL) and the equivalent event storm parameters forecasted 10, 25, 50 and 100 years. The un-parenthesised values are for a 0.0057 m/year increase in significant wave height and the parenthesised values are for a 0.02 m/year increase in significant wave height.

Forecast (years)	**0**	**10**	**25**	**50**	**100**
Hs (m)	8.5	8.64 (8.78)	8.84 (9.20)	9.18 (9.89)	9.82 (11.3)
D (hrs)	55.4	55.5 (55.6)	55.6 (55.9)	55.7 (56.1)	55.9 (56.4)
T (s)	16.6	16.6 (16.6)	16.6 (16.6)	16.6 (16.6)	16.6 (16.6)
WL (m)	1.33	1.36	1.42	1.45	1.62

be seen that the overall storm magnitude increases with time. This increase in combination with the increase in peak period means that the total wave power will increase. Furthermore this increased storm magnitude and wave power are able to act further inland as a result of the increase in water level, which will in turn increase erosion.

7.3.3 Comparison of the numerical erosion models

We do not present the Time Convolution results as a goodness of fit because the method only shifts an equilibrium profile that has been fitted to a historic profile. Instead the results are presented in Table 7.3 as relative percentage errors between the measured and modelled retreat and erosion volumes.

The average error for the two events and for all the profiles is 48 %. This may be an acceptable initial estimate but is not a suitable alternative to a process-based model. The profiles that show the best results are those that have the closest approximation to the equilibrium profile described by Eqn. 7.15. The limitation of assuming a constant wave breaking height is one of the reasons why the erosion of profiles F and 13 is over estimated in Table 7.3.

SBEACH is a more sophisticated model than the Convolution model but because it's calibration parameters are limited it does not have the same flexibility as XBEACH. Figure 7.9 shows the modelled beach response of profile A for both the SBEACH and XBEACH models. XBEACH modelled the response of profile 13 worse than any other profile while it was the best of the SBEACH simulations.

Table 7.3: Relative errors of the Convolution method for profile retreat and volume erosion fro profiles A, C, D, F and 13.

Storm event	Profile	Retreat error (%)	Volume error (%)	Average error (%)
1998	A	-66	-6	36
	C	9	-35	22
	D	-61	24	42
	F	101	-49	75
	13	-58	95	76
2007	A	-67	-38	52
	C	75	-47	61
	D	-57	-44	50
	F	-35	-29	32
	13	-53	-19	36

SBEACH estimates the correct profile shape but shows no net erosion while XBEACH has a similar shape and over estimates the erosion by almost 20 %. The SBEACH results are not tabulated as they mostly show no net erosion above the 0 m MSL contour.

The XBEACH calibration results are shown in Table 7.4. The model was calibrated on the 2007 event and predicts the erosion volumes within 10 % on average. The calibration was verified with the 1998 event and simulated erosion volumes were between 1 % and 57 % of the measurements with an average error of 30 %. XBEACH is the preferred of the three models and will be used to estimate the erosion of the forecasted events. The calibration is acceptable given that it does not include longshore currents and that we are essentially interested in relative erosion volumes.

7.3.4 Predicted erosion

The forecast storm conditions and modelled erosion trends are shown as relative percentage changes in Fig. 7.10. The significant wave height and water levels were modelled with increasing trends with the 18.6 year nodal cycle included in the water level trend. The peak period and duration have a minor increasing trend, neither of which contributes to the estimated increase in erosion. The average

Table 7.4: XBEACH 1D model relative profile erosion volume errors and Chi-squared statistics for profiles A, C, D, F and 13.

Storm event	Profile	Volume error (%)	Chi-squared (χ^2)
1998	A	-31	0.98
	C	36	3.94
	D	57	0.63
	F	-27	4.93
	13	1	0.86
2007	A	-9	2.17
	C	4	1.00
	D	-4	0.64
	F	-7	0.72
	13	19	0.45

annual erosion trend of the profiles was estimated to be 0.14 %/year/storm and 0.20 %/year/storm as a result of the 0.16 % and 0.32 % increase per year in wave height respectively and the 0.21 %/year increase in water level.

7.4 Model limitations

The non-stationary GEV and copula method proposed here for forecasting storm events is more appropriate than simulating events based purely on marginal distributions because it includes the dependence between parameters. The method however assumes that the dependence relationships that exist between storm parameters do not change over time. This may not be correct because there could be changes in the meteorological forcing processes. For example Durban's storm waves are produced by either cut-off lows, cold fronts or tropical cyclones. It is estimated that only 5 % of Durban's storm waves are produced by cyclones and so the current model is mainly representative of a mixture of cold fronts and cut-off lows. Although the relationship between the meteorological forcing and storm durations is still unclear at the case study location, it appears that the larger wave heights and longer period waves are associated with cut-off lows. If there is a trend in only a single forcing process it may eventually affect the relationship modelled by the multivariate copula. If only one of the forcing pro-

cesses is increasing our assumption of a constant dependence relationship will be incorrect.

The proposed method of conditionally simulating peak wave period from a significant wave height should be applied cautiously. In the presented case study the method performs well because of the above described forcing processes. If local storm conditions produce extreme waves the proposed method will overestimate the peak wave period and thus the extreme storm conditions. If there is a possibility of this occurring at the location of interest the copula based simulation of peak wave period may be replaced by a preferred method described by Monbet & Prevosto [2001] or references therein.

Further caution must be observed for the use of Archimedean Copulas. Copulas provide a very general model of dependence and although they have found various successful applications their generality makes it difficult to estimate copulas from data. Copulas that are derived from multivariate distributions (e.g. the Gaussian copula) provide powerful models because the marginal distributions and the dependence structure can be disentangled and handled independently. Archimedean Copulas however do not stem from multivariate distributions and have their structure mainly because of mathematical tractability. Therefore their appropriateness as natural models for dependence should be verified for each application.

The erosion simulations have been performed from a constant average profile. This method does not allow for long term retreat due to sea level rise. The method also neglects any trends in wave direction. The long term erosion effects of changing wave directions are an important factor [Zacharioudaki & Reeve, 2011] and a notable weakness in the current study. Although the method is not realistic but it allows the effects of storms to be quantified separately to that of long term sea level rise and wave direction effects. Since cross-shore erosion processes are dominant during storms the absence of wave direction trends does not significantly affect the quantification of storm erosion trends.

The trends used for the case study are based on analysis of limited data and are not statistically significant. This is expected to be a common problem since most areas in the world have short wave data sets. The absence of statistically significant trends is not a sufficient justification to dismiss the inclusion of such

trends in medium to long term planning. The methods outlined in this paper are intended to allow potential future impacts to be quantified so that they can be assessed as part of a holistic planning and design process.

7.5 Discussion

Three cross-shore erosion models have been evaluated for predicting the impacts of wave and water level trends. The Time Convolution model [Kriebel & Dean, 1993] was the simplest model evaluated and showed an average relative error between the measured and modelled erosion volumes of 48 %. SBEACH is considered a far more sophisticated model than the Time Convolution model. SBEACH modelled the erosion volumes well with regards to shape but the erosion volume was largely balanced by the accretion volume above 0 m MSL and therefore yielded no net erosion. The Time Convolution model provides reasonable initial estimates of profile erosion relative to its simplicity. SBEACH is an appealing model because it has an easy to use graphical user interface and the simulation times are short. The user interface unfortunately removes a degree of flexibility. The calibration parameters are also limited to the Transport Rate Coefficient and the Coefficient for Slope-Dependent term [Sommerfeld *et al.*, 1996]. XBEACH gave the best calibration results and was therefore selected for predicting future trends. A disadvantage of XBEACH is that the simulation times are significantly longer than the other two models. Simulation times can be reduced to some extent by using a morphological time factor. The required length of the XBEACH simulations necessitates the use of a multivariate statistical model. The more pragmatic engineering approach (e.g. Reeve [1998]) would require a lengthy time series as an input into XBEACH. Although the results of the engineering approach can be simply analysed as univariate erosion the extensive XBEACH simulations make the engineering approach impractical.

Average erosion was estimated to increase at a rate of 0.14 %/year/storm and 0.20 %/year/storm for increases in wave height Hs of 0.0057 m/yr and 0.02 m/yr respectively. Corbella & Stretch [2012b] found that most of the Durban beach profiles have a long term erosion trend and they identified numerous reasons for the erosion trends. Although this paper has only analysed the erosion associated

with storm trends at a single probability level, the results provide an indication of general storm erosion trends. We can therefore estimate the proportion of long-term erosion due to either trends in storm characteristics or to sea level rise. Table 7.5 shows the long term erosion trends estimated from historical profile data compared to the erosion estimated due to storm and water level trends. Table 7.5 shows that the storm and water level trends potentially contribute 25 % to 42 % of the overall erosion trend. The remaining 58 % to 75 % of the erosion can be attributed to a decrease in sediment budget and long term sea level rise. Corbella & Stretch [2012b] suggested that the decrease in sediment budget is due to a combination of sediment mining and trapping by dams and the episodic nature of large flood events. These results should be interpreted cautiously. The simulations show that the maximum potential contribution to long term erosion may be the result of storm and sea level trends. However, these trends may not contribute to long term erosion at all if there is sufficient recovery time between the storms for the beaches to recover to their pre-storm volumes. Corbella & Stretch [2012d] found that on average the shoreline recovery takes 2 years, regardless of the storm magnitude. In this regard, based on our current model and estimates, it is not anticipated that storm trends will contribute to long term erosion for the next 100 years. Sea level rise on the other hand will influence long term erosion based on the Bruun rule. Corbella & Stretch [2012b] found that the Bruun Rule attributes 75 % of the current beach erosion to sea level rise. The combination of sea level rise and storm trends is therefore likely to become an issue prior to the year 2100, without storm trends contributing to long term erosion.

Table 7.5: Comparison between long-term profile erosion and erosion estimated from storm and water level trends as percentage relative change. The percentage contribution of the estimated erosion to the long-term erosion is also shown.

Profile	**Long-term annual erosion (%)**	**Storm & water level erosion (%)**		**Contribution of trends to long-term erosion (%)**	
		0.0057 m/year	0.02 m/year	0.0057 m/year	0.02 m/year
A	NA	0.12	0.17	NA	NA
C	0.32	0.10	0.20	31	61
D	-0.21	0.13	0.13	NA	NA
F	1.43	0.19	0.22	14	16
13	0.57	0.18	0.28	32	50
Averages	0.53	0.14	0.20	25	42

7.6 Conclusion

In this paper we have introduced an integrated modelling approach for assessing future coastal erosion trends under changing climatic conditions. The method combines a multivariate, copula based, non-stationary statistical model for storm waves with deterministic shoreline response models.

The non-stationary GEV model is a useful means for forecasting time dependent wave parameters. Coupling non-stationary GEV models via copulas allows the time dependent parameters to be modelled conditionally based on the dependence between parameters. This paper has used both of these methods to create a multivariate statistical model of a time dependent sea state.

The statistical model has been used to estimate future storm erosion trends for a South African case study. The investigation of three morphological models (Time Convolution, SBEACH and XBEACH) showed the XBEACH model to have the best results while the Convolution model provided a simple means to find reasonable erosion estimates. Callaghan *et al.* [2008] concluded that their reliance on the Kriebel & Dean [1993] model was a limitation to their full temporal simulation method. The use of the XBEACH process-based model is an improvement on the Convolution model. We have also improved the statistical description of storm events by including the dependence between wave height, wave period and storm duration using copulas. The predicted future erosion due to storm and sea level trends was estimated to increase at a rate of 0.14 %/year/storm and 0.20 %/year/storm as a result of the 0.0057 m/yr and 0.02 m/yr increase wave height respectively. It has been estimated that storm trends are unlikely to contribute to long term erosion prior to the year 2100 while it is plausible that sea level rise is already contributing to long term erosion.

The methods presented in this paper should be useful for medium to long term planning by coastal managers and decision makers.

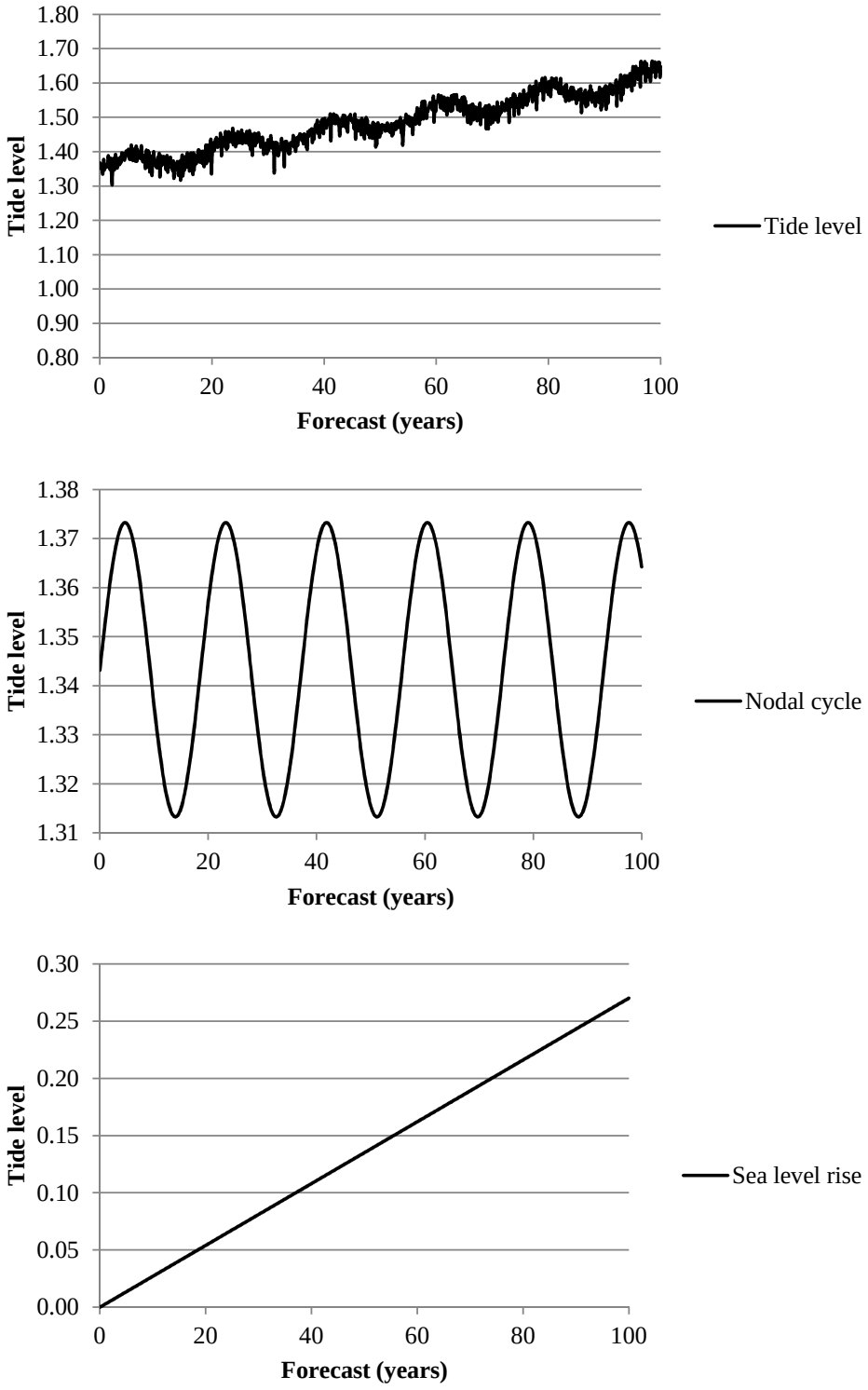

Figure 7.7: A 100-year forecast of sea levels from the non-stationary Generalised Extreme Value model showing the nodal cycle and sea level rise components of the trend

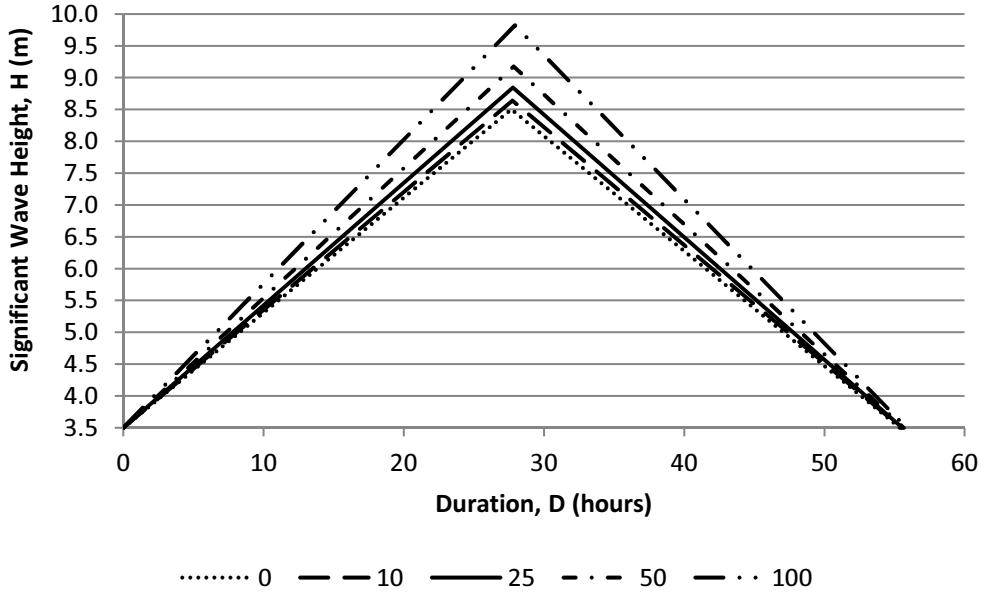

(a)

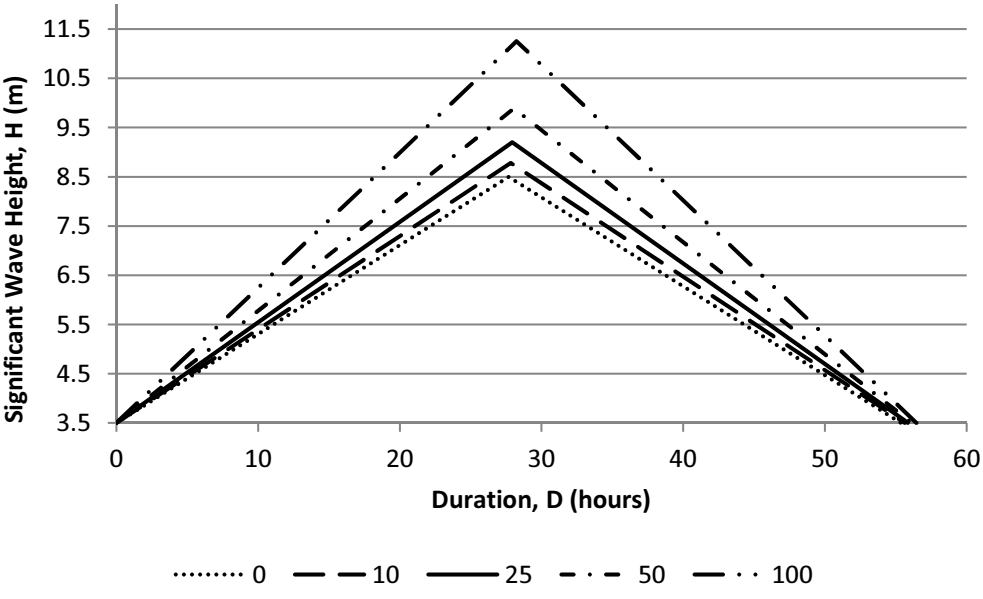

(b)

Figure 7.8: Plots of the idealised 2007 equivalent storm event over 10, 25, 50 and 100 year forecast for (a) a 0.0057 m/year increase in Hs and (b) a 0.02 m/year increase in Hs

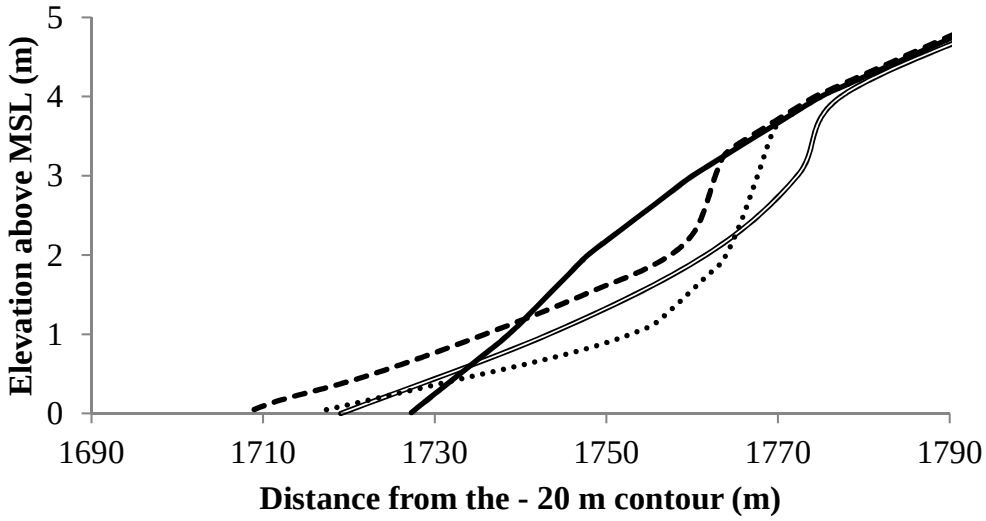

Figure 7.9: A model comparison of the response of profile 13 to the 2007 storm event. The solid line shows the pre-storm profile and the double line shows the post-storm profile. The dashed line is the SBEACH simulated storm response and the dotted line is the XBEACH simulated storm response.

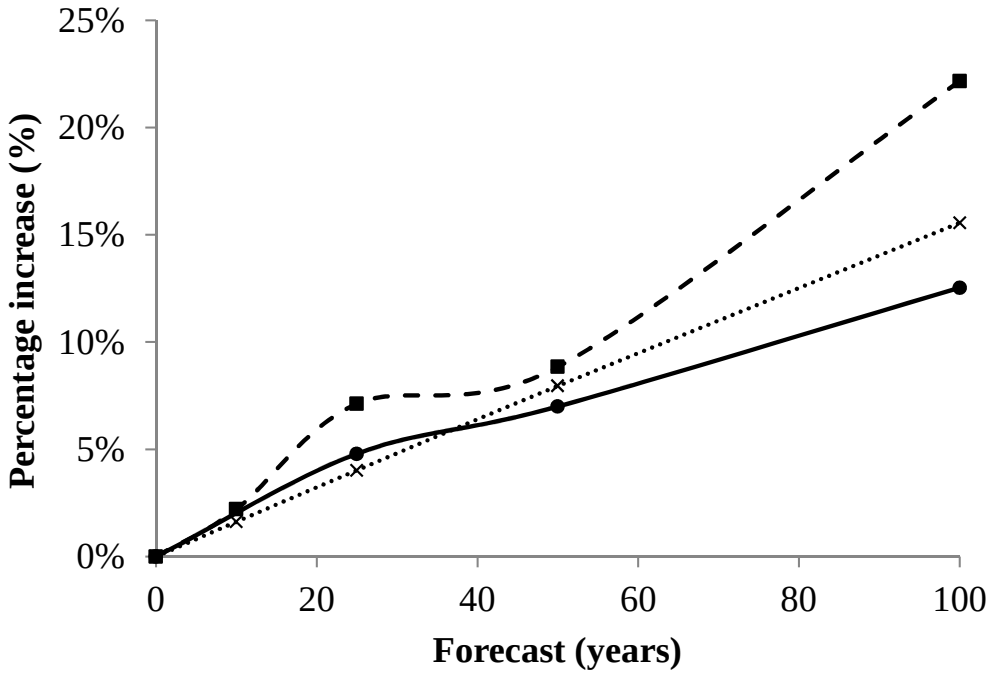

(a)

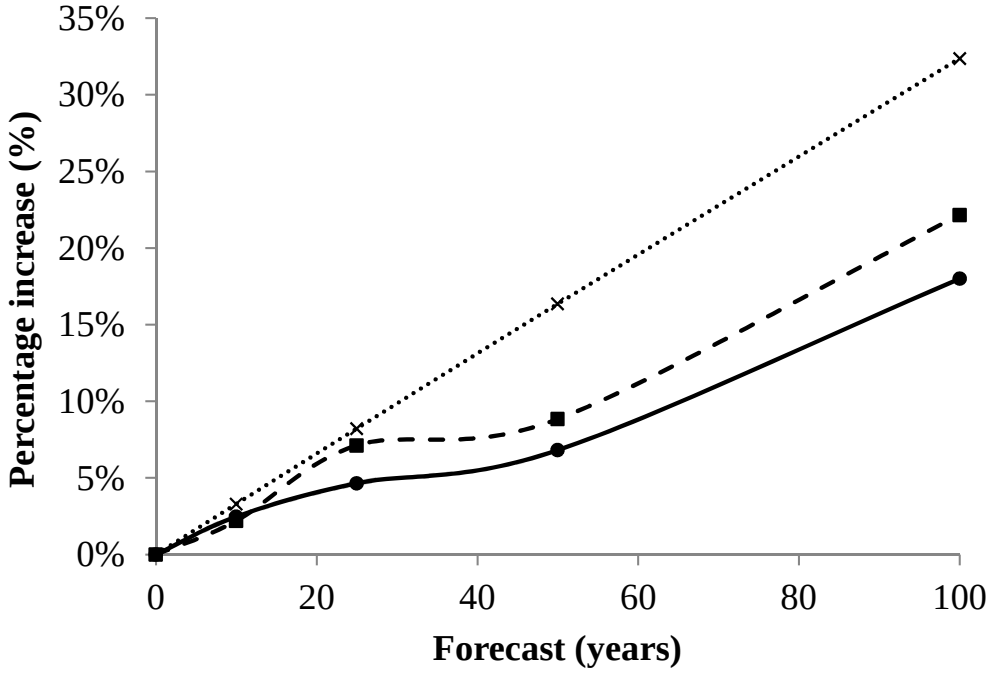

(b)

Figure 7.10: The forecast percentage increase of: significant wave height shown by the dotted line; water level shown by the dashed line and erosion shown by the solid line.

References

Bacon, S. Carter, D.J.T.: Wave climate changes in the north Atlantic and North Sea. International Journal of Climatology, 11, 545 – 558, 1991. 196

Boccotti, P.: Wave mechanics for ocean engineering, Elsevier Oceanography Series, Elsevier Science, Amsterdam, 2000. 156, 162, 171, 174, 175, 183

Casella, G. Berger, R. L.: . Statistical Inference, Wadsworth and Brooks/Cole. Pacific Grove, CA 1990. 21, 59, 188

Callaghan, D. P., Nielsen, P., Short, A., & Ranasinghe, R.: Statistical simulation of wave climate and extreme beach erosion, Coast. Eng., 55, 375 – 390, 2008. 20, 31, 58, 85, 121, 155, 182, 191, 192, 207, 236

Chini, N. Stansby, P. Leake, J. Wolf, J. Roberts-Jones, J. Lowe, J.: The impact of sea level rise and climate change on inshore wave climate: A case study for East Anglia (UK). Coastal Engineering, 57, 973 – 984, 2010. 20, 58, 140, 156, 185, 223

Coles, S. G. Tawn, J.A.: Statistics of coastal flood prevention, Philos. Trans. Roy. Soc. Lond. A, 332, 457 – 476, 1990. 182

Coles, S. G. Tawn, J.A.: Modelling extreme multi variate events, J Roy. Statist. Soc. B, 53, 377 – 392, 1991. 182

Coles, S. G. Tawn, J.A.: Statistical methods for multivariate extremes: an application to structural design, Appl. Statist., 43, 1 – 48, 1994. 182, 239

Corbella, S. Stretch, D. D.: The wave climate on the east coast of South Africa, J. S. Afr. Inst. Civ. Eng., 54 (2), 45 – 54, 2012a. 94, 101, 155, 183, 220

Corbella, S. Stretch, D. D.: Decadal trends in beach morphology on the east coast of southern Africa and likely causative factors. Nat. Haz. Earth Sys. Sci., 2515 – 2527, 2012b. 94, 183, 186, 196, 199, 204, 205

Corbella, S. Stretch, D. D.: Simulating a multivariate sea storm using Archimedean Copulas. Submitted to *Coastal Engineering* 2012c. 189, 196, 199, 223, 224

Corbella, S. Stretch, D. D.: Shoreline recovery from storms on the east coast of Southern Africa. Nat. Hazards Earth Syst. Sci., 12, 11 – 22, 2012d. 205, 220

Dean, R.G. Dalrymple, R.A.: Water Wave Mechanics for Engineers and Scientists. Advanced Series on Ocean Engineering, vol. 2. World Scientific, Singapore. 353, 1991. 191

De Michele, C. Salvadori, G. Passoni, G. Vezzoli, R.: A multivariate model of sea storms using copulas, Coastal Engineering, 54, 734 – 751, 2007. 22, 25, 27, 78, 152, 154, 155, 156, 162, 171, 174, 189, 190, 223, 224, 313, 315

Dodet, G. Bertin, X. Taborda, R.: Wave climate variability in the North-East Atlantic Ocean over the last six decades, Ocean Modelling, 31, 120 – 131, 2010. 138, 139, 196

Goda, Y.: Random Seas and Design of Maritime Structures (2nd Edition). World Scientific Publishing Co. Pte. Ltd. Singapore, 2008. 20, 21, 28, 58, 59, 151, 187, 188, 225, 233

Guedes Soares, C. Scotto, M. G.: Application of the r largest-order statistics for long-term predictions of significant wave height. Coastal Engineering, 51, 387 – 394, 2004. 20, 21, 58, 156, 185, 223

Hanson, H. Larson, M. Kraus, N.C. Gravens, M.B.: Shoreline response to detached breakwaters and tidal current: comparison of numerical and physical models. Proceeding of the 30th International conference of Coastal Engineering, 2006. 182

Hartanto, I.M., Beevers, L., Popescu, I., Wright, N.G.: Application of a coastal modelling code in fluvial environments. Environmental Modelling & Software, 26 (12), 1685 – 1695, 2011. 31, 192, 228

Katz, R. W. Parlange, M. B. Naveau, P.: Statistics of extremes in hydrology. Advances in Water Resources 25, 1287 – 1304, 2002. 186

Komen, G. Hasselmann, S. Hasselmann, K.: On the existence of a fully developed wind-sea spectrum. Journal of Physical Oceanography 14. 1271 – 1285, 139, 1984. 193

Kriebel, D.L., Dean, R.G.: Convolution method for time-dependent beach-profile response. Journal of Waterway, Port, Coastal and Ocean Engineering, 119 (2), 204 – 226, 1993. 31, 85, 182, 191, 204, 207, 228

Larson, M. Kraus, N. C. Byrnes, M. R.: SBEACH: Numerical model for simulating storm-induced beach change, Report 2, Numerical formulation and model tests, Technical report CERC-89-9, US Army Engineer Waterways Experiment Station, Vicksburg, MS. 1990. 31, 191, 228

Madsen, O.S., Poon, Y.K. Graber, H.C.:Spectra wave attenuation by bottom friction: theory. Proceedings of the 21st International Conference on Coastal Engineering, ASCE, New York: 492 – 504, 1988. 193

Mather, A. A.: Linear and nonlinear sea level changes at Durban, South Africa, South African Journal of Science, 509 – 512, 2007. 17, 116, 133, 141, 186

Mather, A. A.: Sea Level Rise for the East Coast of Southern Africa, Seventh International Conference of Coastal and Port Engineering in Developing Countries, COPEDEC VII, 2008, 173, 11, Dubai, UAE. 2008. 11, 14, 114, 186, 275

McNeil, A. Frey, R. Embrechts, P.: Quantitative Risk Management: Concepts, Techniques and Tools. Princeton University Press. 2005. 190

Mendez, F. J. Menendez, M. Luceno, A. Losada, I.J.: Analyzing Monthly Extreme Sea Levels with a Time-Dependent GEV Model. Journal of atmospheric and oceanic technology. 24, 894 – 911, 2007. 199

Mendez, F. J Menendez, M. Luceno, A. Medina, R. Graham, N. E.: Seasonality and duration in extreme value distributions of significant wave height. Ocean Engineering, 35, 131 – 138, 2008. 155, 156, 185, 186, 187, 223

Minguez, R. Menndez, M. Mndez, F.J. Losada, I.J.: Sensitivity analysis of time-dependent generalized extreme value models for ocean climate variables. Advances in Water Resources, 33, 833 – 845, 2010. 156, 185, 186, 223

Monbet, V. Prevosto, M.: Bivariate simulation of non stationary and non Gaussian observed processes application to sea state parameters. Applied Ocean Research, 23, 139 – 145, 2001. 203

Montgomery, D. C. Runger, G. C. Applied Statistics and Probability for Engineers (3rd Edition). John Wiley & Sons, New York, 2003. 21, 59, 188

Nelsen, R.B.: An introduction to copulas, (second edition), Springer Series in Statistics, Springer, New York, 2006. xxi, xxviii, 22, 24, 25, 26, 27, 29, 152, 153, 154, 158, 159, 162, 171, 172, 173, 175, 189, 190, 223, 224, 315

Pugh, D.T.: Tides, Surges and Mean Sea Level, John Wiley and Sons, Avon, United Kingdom, 1987. 13, 14, 131, 187

Reeve, D. E.: On coastal flood risk. ASCE J. Waterway, Port, Coastal & Ocean Engineering, 124 (5), 219 – 228, 1998. 204, 239

Roelvink, D., Reniers, A., van Dongeren, A., van Thiel de Vries, J., McCall, R., Lescinski, J.: Modelling storm impacts on beaches, dunes and barrier islands. Coastal Engineering, 56, 1133 – 1152, 2009. 31, 191, 192, 220, 228

Ruggiero, P. Komar, P. D. Allan, J. C.: Increasing wave heights and extreme value projections: The wave climate of the U.S. Pacific Northwest. Coastal Engineering, 57, 539 – 552, 2010. 13, 20, 58, 115, 139, 156, 185, 186, 196, 223

Salvadori, G.: Bivariate return periods via 2-Copulas, Statistical Methodology, 1, 129 – 144 2004. 28, 29, 188, 225

Salvadori, G. De Michele, C.: Multivariate multiparameter extreme value models and return periods: A copula approach, Water Resources Research, 46, W10501, doi:10.1029/2009WR009040, 2010. 152, 189, 223, 225

Savu, C. Trede, M.: Hierarchical Archimedean copulas, http://www.uni - konstanz.de/micfinma/conference/Files/papers/Savu_Trede.pdf (2008-11-01), 2006. 26, 27, 154, 190, 224, 314, 315

Savu, C. Trede, M.: Hierarchies of Archimedean copulas, Quantitative Finance, 10 (3), 295 – 304, 2010. 27, 190, 224, 315

Schoonees, J.S. Theron, A.K.: Evaluation of 10 cross-shore sediment transport/morphological models, Coastal Engineering, 25, 1 – 41, 1995. 31, 191, 228

Seymour, R. Guza, R.T. OReilly, W. Elgar, S.: Rapid erosion of a small southern California beach fill, Coastal Engineering, 52, 151 – 158, 2005. 31, 191

Sobey, R. J.: Extreme low and high water levels, Coast.Eng., 52, 63 – 77. 2001. 199

Sommerfeld, B.G. Kraus, N.C. Larson, M.: SBEACH-32 INTERFACE USER'S MANUAL, Final report, TAMU-CC-CBI-95-12, U.S. Army Corps of Engineers, 44, 1996. 204

Theron, A. Rossouw, M. Barwell, L. Maherry, A. Diedericks, G. de Wet, P.: Quantification of risks to coastal areas and development: wave run-up and erosion, The 3rd biennial CSIR conference, Reference: NE20-PA-F, 2010. 115, 139, 196

Tolman, H. L.: User manual and system documentation of WAVEWATCH-III version 1.18. NOAA/NWS/NCEP/OMB Technical Note 166, 110, 1999. 193

Wang, B. Reeve, D. E.: Probabilistic Modelling of Long-term Beach Evolution near Segmented Shore-parallel Breakwaters, Coastal Engineering, 57, 732 – 744, 2010. 182

Wang, X. L. Zwiers, F. W. Swail, V. R.: North Atlantic Ocean Wave Climate Change Scenarios for the Twenty-First Century, Journal of Climate, 17, 2368 – 2383, 2004. 182, 186

Zacharioudaki, A. Reeve, D. E.: Shoreline evolution under climate change wave scenarios, Climatic Change, 108(1-2), 73 – 105, 2011. 182, 203

Zhang, X. Zwiers, F. W. Li, G.: Monte Carlo Experiments on the Detection of Trends in Extreme Values, Journal of Climate, 17, 1945 – 1952, 2004. 15, 114, 186

Zheng, J. Dean, R. G.: Numerical models and intercomparisons of beach profile evolution, Coastal Engineering, 30, 169 – 201, 1997. 31, 191

Chapter 8

Multivariate return periods of sea storms for coastal erosion risk assessment

This chapter is based on a paper published in Natural Hazards and Earth System Sciences, 12, 2699 – 2708, 2012.

Abstract

The erosion of a beach depends on various storm characteristics. Ideally, the risk associated with a storm would be described by a single multivariate return period that is also representative of the erosion risk, i.e. a 100 yr multivariate storm return period would cause a 100 yr erosion return period. Unfortunately, a specific probability level may be associated with numerous combinations of storm characteristics. These combinations, despite having the same multivariate probability, may cause very different erosion outcomes. This paper explores this ambiguity problem in the context of copula based multivariate return periods and using a case study at Durban on the east coast of South Africa. Simulations were used to correlate multivariate return periods of historical events to return periods of estimated storm induced erosion volumes. In addition, the relationship of the

most-likely design event [Salvadori *et al.*, 2011] to coastal erosion was investigated. It was found that the multivariate return periods for wave height and duration had the highest correlation to erosion return periods. The most-likely design event was found to be an inadequate design method in its current form. We explore the inclusion of conditions based on the physical realizability of wave events and the use of multivariate linear regression to relate storm parameters to erosion computed from a process based model. Establishing a link between storm statistics and erosion consequences can resolve the ambiguity between multivariate storm return periods and associated erosion return periods.

8.1 Introduction

Return periods based on univariate statistical analysis of independent extreme events are widely used to quantify risk in order to specify design conditions in engineering. Typical examples are the estimation of design flood conditions for dam or stormwater designs. In coastal zone management the characterization of storm events that result in beach erosion is an important issue. Univariate return periods are not sufficient for describing a sea storm as it's rarity and destructiveness are a function of wave height (H), wave period (T), storm duration (D), wave direction (A), water level (W) and storm inter-arrival time (I). With respect to coastal erosion the larger the wave height, storm duration and water level the greater the erosion. The contribution of wave period to erosion is less intuitive. van Gent *et al.* [2008] and van Thiel de Vries *et al.* [2008] found that an increase in wave period leads to an increase in erosion. However, local fluid particle accelerations decrease with increasing T, all else remaining equal, which in turn should provide less erosion potential. The wave direction is not only important from a longshore and cross shore current perspective but also in terms of sheltering. For example, a beach sheltered in a given direction from a 100-yr wave height may experience less erosion than a 50 yr wave height from its exposed direction. The effect of storm inter-arrival time (or it's inverse the storm frequency) is complementary to that of storm duration. If the inter-arrival time between two consecutive storms is short, the beach will not have sufficient time to recover and therefore will be eroding from a lower level. Short inter-arrival

times are therefore in effect similar to an increase in the duration of individual events.

The synthetic design storm [Carley & Cox, 2003] only considers wave height and duration and it assumes that an x-yr storm produces x-yr erosion. Considering the interdependence of H, T, D, A, W and I together with their individual and collective influence on erosion, it is overly simplistic to assume that the return period of H and D corresponds to the return period of the corresponding erosion volume. The return periods of design events should therefore be derived from multivariate statistics. In this paper we estimate these multivariate return periods using the approach of copulas and Kendall's return periods as described by Salvadori *et al.* [2011].

A relationship between sea storm multivariate return periods and erosion return periods could be established from empirical data. However, this is difficult to achieve in practice since beach survey data must be available for both before and after storm events and be close enough to the events that only the effects of the storm are measured. This type of data is often too rare to establish a confident statistical model. In this study we overcome this data shortage by calculating the consequential erosion from historical storm events using the process-based XBEACH model [Roelvink *et al.*, 2009]. We then calculate the average recurrence intervals for the simulated erosion volumes and identify which multivariate return periods correspond to the erosion return periods. In essence we attempt to verify the assumptions of the synthetic design storm. We also investigate the selection of a multivariate design event using the Salvadori *et al.* [2011] most-likely design event method.

8.2 Case study

The east coast of South Africa has 18 yr of reliable wave data from wave recording buoys near the city of Durban (Fig. 8.1a). Corbella & Stretch [2012a] provide details of the data. Corbella & Stretch [2012d] defined a storm event in terms of a significant wave height threshold as follows: a storm event begins when a significant wave height H exceeds a threshold of 3.5 m and ends when the significant wave height falls below 3.5 m for a period of at least 2 weeks. The

Figure 8.1: A map of **(a)** South Africa showing Durban and a map of **(b)** the Durban Bight showing the location of profile C and the Durban harbour.

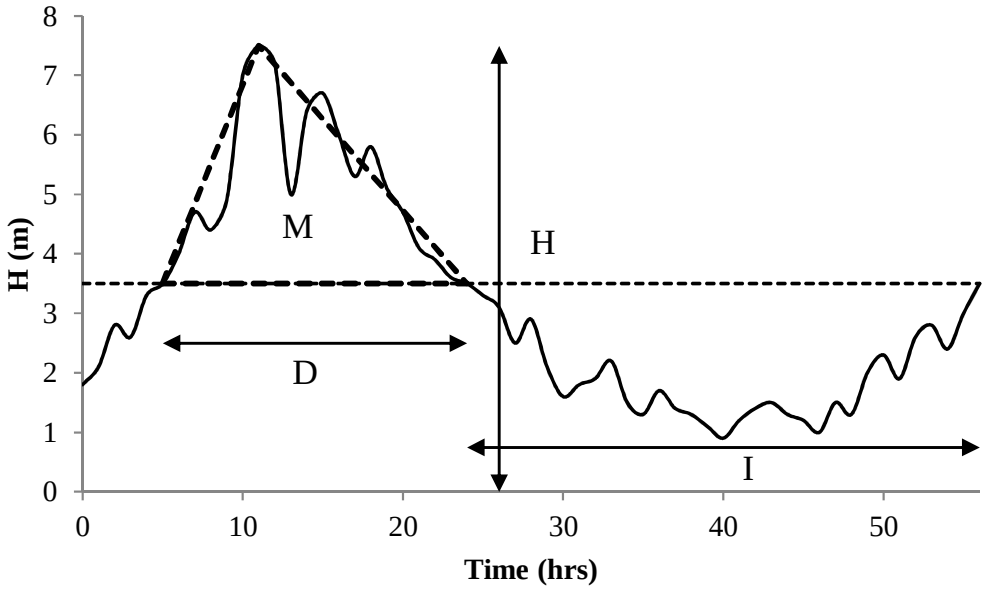

Figure 8.2: Illustration of the storm definition showing the significant wave height H, storm duration D and calm period I.

period between the start and end time, not including the 2 weeks, is the storm duration D and the time between the events is the calm period I. The storm definition is illustrated schematically in Fig. 8.2. The values H, D, T and W are all defined in deep water and experience no sheltering effects.

Durban has an extensive record of beach profiles over 37 yr. Profile C (Fig. 8.1b) was used exclusively for the present study as it is representative of the Durban Bight, while avoiding most of the sheltering influence of the harbour breakwaters and from the perpendicular beach structures. The records of interest in this study are those that bound storm events and only two events from 1998 and 2007 met these requirements.

8.3 Theoretical background and methods

8.3.1 Marginal distributions

The generalized extreme value (GEV) distribution was used as the marginal distributions of H, D, T and W. The GEV has been used extensively for extreme

value analysis of hydrological events and specifically for wave heights by Chini *et al.* [2010]; Guedes Soares & Scotto [2004]; Mendez [2008]; Minguez *et al.* [2010], and Ruggiero *et al.* [2010]. The GEV encompasses three distributions often referred to as Type I, II and III. The probability density function is given by

$$y = \sigma^{-1} \exp\left(-\left(1 + k\frac{x-\mu}{\sigma}\right)^{-\frac{1}{k}}\right)\left(1 + k\frac{x-\mu}{\sigma}\right)^{-1-\frac{1}{k}} \tag{8.1}$$

for $(1+k\frac{x-\mu}{\sigma}) < 0$ and where μ is the location parameter, σ is the scale parameter and k is the shape parameter.

The maximum likelihood method was used to estimate the GEV parameters and the Akaike information criterion (AIC) was used to evaluate the appropriateness of the GEV model. The AIC is given by

$$\mathrm{AIC} = 2n - 2\ln(\mathcal{L}), \tag{8.2}$$

where n is the number of parameters in the probability distribution and $\mathcal{L}$ is the maximized value of the likelihood function for the estimated parameters.

8.3.2 Archimedean copulas

Copulas provide a method of modeling the dependencies between the variables responsible for erosion. They are mathematical functions that join or couple multivariate probability distribution functions to their one-dimensional marginal distribution functions. A detailed introduction to copulas is provided by De Michele *et al.* [2007]; Nelsen [2006]; Salvadori & De Michele [2010].

An Archimedean copula C is a solution to the functional equation

$$\varphi(C(u,v)) = \varphi(u) + \varphi(v) \tag{8.3}$$

where $u = F(x)$ and $v = F(y)$ are marginal distribution functions and φ is the generator function.

Corbella & Stretch [2012c] concluded that only H, T and D of the Durban wave data are inter-dependent and they created a fully nested trivariate hierar-

chical Clayton copula to represent this wave climate. The Corbella & Stretch [2012c] model will be used in this paper. It should be noted that this is typical of a deep ocean coast and shallow seas will have a strong correlation between wave height and water level. The Clayton copula has a generator function expressed as

$$\varphi(q) = \frac{1}{\theta}(q^{\theta} - 1) \tag{8.4}$$

where θ is the dependence parameter and q is a number between 0 and 1. The 3-dimensional hierarchical copula has 2 generators, φ_1 and φ_2 and is expressed as

$$C(u_1, u_2, u_3) = \varphi_2^{-1}\left(\varphi_2\left(\varphi_1^{-1}\left[\varphi_1(u_1) + \varphi_1(u_2)\right]\right) + \varphi_2(u_3)\right) \tag{8.5}$$

The simulations presented in this paper have been performed by the conditional inversion method [De Michele *et al.*, 2007; Nelsen, 2006; Savu & Trede, 2006, 2010]. Given the non-exceedance probability of a wave height h the non-exceedance probability of duration d can be estimated from the conditional law G of the bivariate copula as

$$G_2(d|h) = \partial_h C(h, d). \tag{8.6}$$

The non-exceedance probability of the wave period t can then be estimated conditionally based on the given values of h and d from the bivariate and trivariate copula as

$$G_3(t|h, d) = \frac{\partial_{h,d} C(h, d, t)}{\partial_{h,d} C(h, d)}. \tag{8.7}$$

The non-exceedance probability of water level w is assumed independent of h, d and t and is therefore simulated independently.

It should be noted that H, T and D are also dependent on wave direction. Wave direction was precluded from the copula model as all the sampled storm events fall between 110° and 180° with an average direction of 147°. Since there is no significant rank correlation between H and wave direction, we assume that all storm events are equally likely to arrive from any direction between 110° and 180°.

8.3.3 Return periods

A return period or average recurrence interval τ is the average time (usually expressed in years) between the realizations of two independent successive events. For a given probability level $0 < p < 1$, the return period can be expressed as [Goda, 2008]

$$\tau(p) = \frac{\mu_T}{(1-p)} \tag{8.8}$$

where μ_T is the average inter-arrival time of the storms.

8.3.3.1 Multivariate return periods

An engineer may be concerned with the risks associated with storm events that have various combinations of wave height, storm duration, wave period, etc. With regards to erosion we are interested in the most-likely combination of H, D, T and W for a given probability of exceedance. Unlike dam design where droughts make non-exceedances important, in coastal engineering we are usually only interested in the probability of exceedance. Storm inter-arrival time is an exception, but if parameterized in terms of its inverse, namely as a storm frequency, then the same consideration applies.

The usefulness of multivariate return periods in design work is often debated and the difficulty in their application is associated with linking the statistics to physical consequences. Examples of previous work on multivariate return periods from copulas are Salvadori *et al.* [2007]; Salvadori [2004]; Salvadori & De Michele [2010]; Salvadori *et al.* [2011].

A multivariate return period is inherently ambiguous because different combinations of probabilities may produce the same return period. Events that have an equal probability of exceedance define iso-hyper-surfaces or critical layers L_q^F for a critical level q. We adopt the notation from Salvadori *et al.* [2011] and define a critical layer as

$$L_q^F = \left\{ \vec{x} \in R^d : F(\vec{x}) = q \right\} \tag{8.9}$$

where $\vec{x}$ is a vector, F is a d-dimensional distribution $F = C(F_1, ..., F_d)$ and

$F \in (0, 1)$. This definition provides 3 probability regions:

1. a sub-critical region $R_q^<$ that includes events with $F < q$;
2. a critical, set on L_q^F where all events have a constant $F = q$;
3. a super-critical $R_q^>$ that includes events with $F > q$.

From a coastal engineering perspective we are interested in potentially destructive events, or in other words events in the super-critical region. Salvadori *et al.* [2011] define a super-critical return period τ_x for a multivariate random variable $\vec{X}$ as,

$$\tau_x = \frac{\mu}{P(\vec{X} \in R_q^>)}. \tag{8.10}$$

Alternatively, τ_x can be defined in terms of the sub-critical region $R_q^<$ as

$$\tau_x = \frac{\mu}{1 - K_C(q)} \tag{8.11}$$

where K_C is the Kendall's distribution function [Genest *et al.*, 1993] associated with the d-copula C and is given by

$$K_C(q) = P(C(U_1, ..., U_d) \leq q). \tag{8.12}$$

Kendall's K_C expresses a multivariate quantile relationship [Genest *et al.*, 2001] and measures the probability of events occurring in the region $R_q^<$, i.e. in the sub-critical region delineated by L_q^F. Since a general analytical expression for K_C does not exist for all copula families [Salvadori *et al.*, 2011], we estimate K_C from simulations such that for a simulated sample of m variables $\mathbf{u}_1, \ldots, \mathbf{u}_m$, from a d-copula C, the estimate of the Kendall's distribution function is

$$\hat{K}_C(q) = \frac{1}{m} \sum_{i=1}^{m} 1(C(\mathbf{u}_i) \leq q). \tag{8.13}$$

8.3.4 Kendall's return period

The return period τ_x in Eqn. (8.11) is referred to as the Kendall's return period (KRP). In order to use the KRP in practice, a relationship between the critical

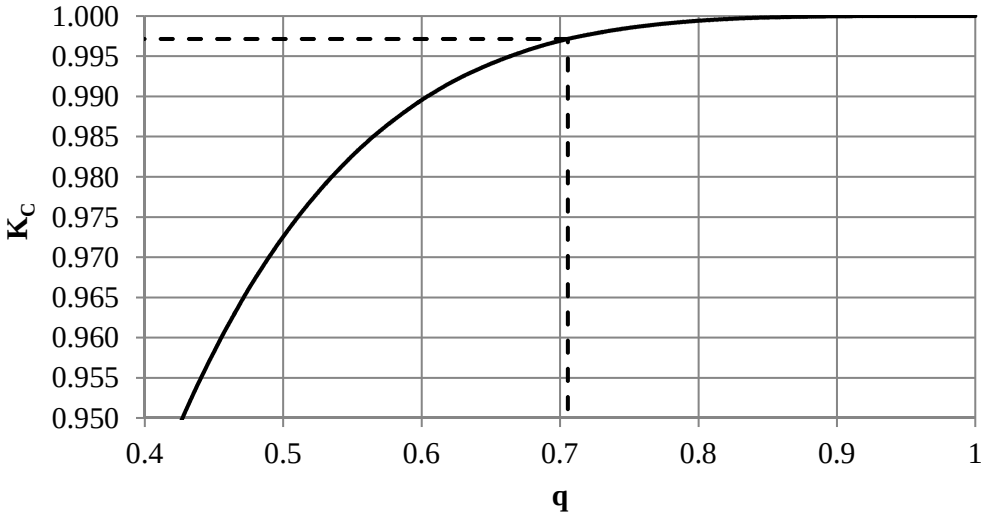

Figure 8.3: Simulated relationship between the Kendall's distribution function K_C and the critical level q (solid line). The dashed line represents a KRP of 100 yr given by $K_C = 0.997142$ for a critical level of q = 0.705626.

level q and K_C is required. Using Eqns. (8.6) and (8.7), we simulate 5 000 000 samples of h, d, t and w in an attempt to produce an almost continuous distribution. The samples were then used to estimate K_C for various critical levels q. The resulting relationship is shown in Fig. 8.3 and the dotted line shows the value of K_C and q corresponding to a KRP of 100 yr. The critical levels corresponding to KRP's of 25, 50 and 100 yr were all calculated and corresponding critical layers inferred for the copula $C(h, d, t, w)$.

8.3.5 The most-likely design realization

Salvadori *et al.* [2011] presented a solution to the ambiguity problem discussed in Sect. 8.3.3.1 by proposing the most-likely design event method. The method essentially uses the density of the multivariate distribution to identify which values lying on L_q^F are relatively more likely to occur than others. The most-likely design realization δ_{ML} for a critical level q was defined as

$$\delta_{\mathrm{ML}} = \arg\max_{\vec{x} \in L_q^F} f(\vec{x}) \tag{8.14}$$

where $f(\vec{x})$ is the multivariate density and for our model is given by

$$f(\vec{x}) = f(H, T, D, W) \tag{8.15}$$

$$= c\Big(F(H), F(T), F(D)\Big)\ f(H).f(T).f(D).f(W) \tag{8.16}$$

and where $c(\cdot)$ is the trivariate copula density given by

$$c(h, d, t) = \frac{\partial^3}{\partial_h \partial_t \partial_d} C(h, t, d). \tag{8.17}$$

The most-likely design realization unfortunately does not have any direct link to physical processes and so cannot in general provide a design storm event that is meaningful in terms of its physical consequences. This can only be achieved by linking storm characteristics to erosion, which is considered in Sect. 8.4.3.

8.3.6 Erosion estimation by process-based models

There are numerous process-based numerical models available for estimating cross-shore erosion [Schoonees & Theron, 1995]. Corbella & Stretch [2012e] compared XBEACH to SBEACH [Larson *et al.*, 1990] and the Time Convolution model [Kriebel & Dean, 1993]. They concluded that XBEACH provided the best results for the Durban beaches and it was therefore adopted for the present study. XBEACH is a public-domain model and although it is not yet fully developed, it has been used in numerous recent studies that have shown it's results to be satisfactory [e.g. Hartanto *et al.*, 2011; Roelvink *et al.*, 2009].

The copula model was constructed from wave data recorded in a water depth of approximately 40 m. Simulated waves therefore need to be transformed into nearshore conditions. The SWAN model was used to transform the wave conditions to a 20 m depth at the seaward boundary of the XBEACH model domain.

8.4 Results

8.4.1 Empirical erosion

The empirical erosion data was limited to storms that occurred in the years 1998 and 2007. The 1998 storm event caused profile C (refer Fig. 8.1) to erode $133\,\mathrm{m^3\,m^{-1}}$ and the 2007 storm event caused the profile to erode $137\,\mathrm{m^3\,m^{-1}}$. Using the relationship developed between KRP and the critical level q in Sect. 8.3.3.1, the return periods for the 2007 and 1998 storms were estimated as 120 yr and 15 yr, respectively.

Although there is a large difference in the storm return periods, the resulting erosion was almost identical. This demonstrates the difficulties associated with multivariate return periods. The relationship between storm return periods and erosion return periods is non-linear and different profiles can behave differently.

8.4.2 Erosion return periods

In order to calculate erosion volumes a beach profile measurement is required before and after a storm. Since such data was only available on two occasions we estimate the erosion of past events using XBEACH. The historical storm events were first idealized using the definition in Fig. 8.2 and then used to quantify the erosion at profile C. The limitations of these simulations are the idealization of the wave height, the constant wave direction of 147° (refer to Sect. 8.3.2) and the identical pre-storm beach profile shape. Figure 8.4 shows the calculated erosion volumes ($\mathrm{m^3\,m^{-1}}$) for recurrence intervals up to 100 yr with a fitted exponential distribution. These erosion return periods represent a volume lost from the average volume of profile C and do not consider storm inter-arrival time[1]. If a designer is concerned with the effects of inter-arrival times we suggest that it can be included by increasing the storm duration or alternatively modeling the calm period using a non-stationary Poisson process.

In an attempt to identify which storm return periods best represent erosion return periods we calculate Kendall's tau rank correlation coefficients between

[1]Note that the volumes are calculated above 1 m Chart Datum while mean sea level is about 1.1 m Chart Datum at this location.

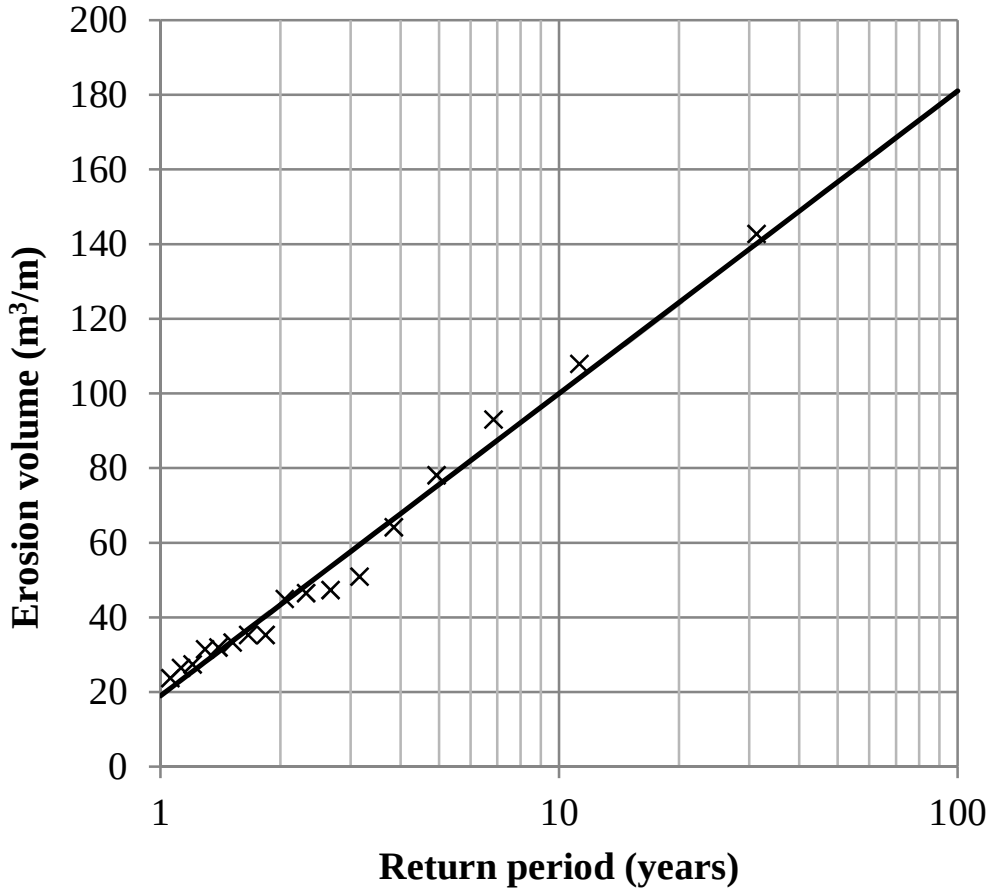

Figure 8.4: The return periods of XBEACH simulated erosion volumes for profile C with the fitted exponential distribution (solid line).

the erosion return periods and univariate storm return periods $\tau(H)$, $\tau(D)$, $\tau(T)$, $\tau(W)$, and multivariate storm return periods, $\tau(HD)$, $\tau(HDT)$ and $\tau(HDTW)$. The results are shown in Table 8.1. Storm duration D had the strongest correlation with erosion, followed by wave height H. Wave period T has a moderate correlation and water level W has no significant correlation. The Kendall's return period $\tau(HDTW)$ has a weaker correlation than $\tau(H)$ mainly because it includes the water level that has no correlation. The multivariate return period correlations improve with fewer variables – the correlation with $\tau(HDT)$ improves on $\tau(HDTW)$, and $\tau(HD)$ gives a further improvement. Note that all these correlation results may be expected to depend on the definition used for the storm events (Fig. 8.2).

Table 8.1: Kendall's tau correlation coefficients between the simulated erosion return periods and the various multivariate storm return periods. The statistical significance of the correlations are indicated by their corresponding p-values.

Erosion vs	**Correlation coefficient**	**p-value**
$\tau\ (D)$	0.78	$6.77\ \times 10^{-17}$
$\tau\ (H)$	0.56	$2.88\ \times 10^{-09}$
$\tau\ (T)$	0.30	$1.49\ \times 10^{-03}$
$\tau\ (W)$	0.03	$7.50\ \times 10^{-01}$
$\tau\ (HD)$	0.76	$4.47\ \times 10^{-16}$
$\tau\ (HDT)$	0.63	$1.94\ \times 10^{-11}$
$\tau\ (HDTW)$	0.50	$9.21\ \times 10^{-08}$

The correlations provide insight into an appropriate multivariate description of an erosion event but do not undisputedly determine the combination of H and D as the best multivariate descriptor. To illustrate this we consider the 2007 event. The 2007 event was the largest event ever recorded in Durban. The Kendall's return periods $\tau(HDTW)$ and $\tau(HD)$ of the 2007 event were 120 yr and 57 yr, respectively. Return periods $\tau(HDT)$ and $\tau(H)$ were 34 yr and 31 yr, respectively. The return period of the erosion predicted by XBEACH for the idealized storm event was 34 yr. This demonstrates that in this case $\tau(HDT)$ or $\tau(H)$ provide the best descriptions of the probability of the erosion event. In fact, considering the 5 largest erosion volumes, the erosion return periods may be described best by any of the return periods $\tau(H)$, $\tau(D)$, $\tau(T)$, $\tau(W)$ or $\tau(HDT)$ depending on which parameter dominates the erosion process. Generally $\tau(HD)$ provides a reasonable estimate of the erosion return period.

Ideally, the erosion return period would be identical to the storm return period. The following section is an attempt to provide a method to estimate events with improved correspondence.

8.4.3 Selecting design storms

The most-likely design realization is a purely statistical definition. It could be a rare event that does not cause significant erosion of the coastline. For example it may select the storm with the smallest significant wave height and water level,

Table 8.2: The most-likely design realizations for multivariate return periods 25, 50 and 100 yr and the associated erosion return periods.

Storm return period (yr)	**25**	**50**	**100**
Storm characteristics:			
H (m)	4.51	4.67	4.87
T (s)	16.0	16.7	16.7
D (h)	29.9	39.9	51.4
W (m)	1.00	1.01	1.03
Erosion volume ($m^3\,m^{-1}$)	50	70	93
Erosion return period (yr)	3	4	8

but with an extremely improbable duration. That combination of parameters may result in a long return period but in reality the duration of such an event may be infinitely long without causing any erosion, i.e. erosion may be insensitive to duration for that parameter range.

Table 8.2 shows the results of the most-likely design estimate. Significant wave heights between 4 m and 5 m were estimated for the return periods of 25, 50 and 100 yr. The actual observed values ranged between 3.5 m and 8.5 m which places the most-likely design events at the lower end of the observed range. The most-likely design method selects events that we can expect to see more often. However there is an immediate problem evident – all the event parameters share an equal weighting statistically but not in terms of their physically influence on erosion. Given that wave height is a principal parameter in erosion it should have greater importance. The result is that the 25, 50 and 100 yr storm return periods correspond to erosion return periods of 3, 4 and 8 yr, respectively (Table 8.2). The risks associated with the recurrence of the storm events are not consistent with those associated with their consequential erosion levels.

The following sections consider ways of constraining or refining the selection of the most-likely design realization by including the physical relationships between H, T, D and W, and the sensitivity of the erosion consequences to each.

8.4.3.1 Constraints due to wave mechanics

The statistical model has no accommodation for the mechanics of water waves, namely the processes in the generation and propagation of ocean waves. Purely statistical models may need to be constrained to avoid unrealistic results. For example there is a physical limitation on wave steepness before they break and dissipate. Wave steepness is defined as the wave height (H) divided by the wave length (L) and for deep water waves is given by [e.g. Goda, 2008]

$$\frac{H}{L} = \frac{2\pi H}{gT^2}. \tag{8.18}$$

The maximum wave steepness is usually assumed to be $\frac{1}{7}$ [Michell, 1893]. It should be noted that the $\frac{1}{7}$-th relationship is for regular waves and has limited value when applied to random wave conditions.

Physical constraints on wave heights and/or periods may also be associated with the wave generation processes and their distance from the area of interest. Storm durations may have realizability constraints related to atmospheric circulation patterns or other factors. All these additional constraints are highly location specific.

Applying the wave steepness constraint alone to the selection of the most probable design event does not change the results shown in Table 8.2 for the case study site.

8.4.3.2 Linking erosion to storm characteristics

The next issue is to link the storm characteristics directly to their erosion consequences. As already noted in Sect. 8.4.1, direct measurements of the erosion due to specific storm events are rare and difficult to obtain. A method of overcoming this limitation is to use a process-based model, such as XBEACH, to quantify the erosion due to each storm event. Since the model attempts to represent the dominant physical processes that drive erosion, this approach should reflect the underlying physics of the problem. However, identical antecedent conditions are assumed for each profile response simulation which does not reflect the actual situation for all events. Furthermore, it is currently not practical to use this

approach to accurately map the erosion caused by a comprehensive range of all possible storm parameters. Instead we use the simulation results previously employed for the analysis of the erosion return periods (Fig. 8.4) and extrapolate from this sample by relating the erosion magnitudes to the storm parameters H, T, D and W using multiple linear regression. The regression equation was chosen to have the form of a truncated Taylor series expansion, namely

$$\begin{aligned} E = E_0 &+ E_H H + E_D D + E_T T + E_W W \\ &+ E_{HH} H^2 + E_{HD} HD + E_{HT} HT + E_{HW} HW \\ &+ E_{DD} D^2 + E_{DT} DT + E_{DW} DW \\ &+ E_{TT} T^2 + E_{TW} TW \\ &+ E_{WW} W^2 \\ &+ \epsilon \end{aligned} \tag{8.19}$$

where the coefficients E_0, E_H, ... are chosen to minimize the sum of the squared errors ϵ. The results are plotted in Fig. 8.5 and indicate that the regression model is adequate in this case. Higher order terms could be included in Eqn. (8.19) to improve the results if necessary. The important outcome of this analysis is that Eqn. (8.19) allows iso-surfaces of erosion (and their associated return periods) to be located in the H, T, D, W parameters space. For example Fig. 8.6 shows a surface plot of erosion, together with iso-erosion contours, for a constant wave period, $T = 16\,\mathrm{s}$, and water level $W = 1.0\,\mathrm{m}$ above mean sea level. In this way individual storms can be related directly to their erosion consequences. For example to estimate a storm event ($HTDW$) representative of a 100 year erosion level ($180\,\mathrm{m^3\,m^{-1}}$) we use the regression model to determine the H, T, D, and W combinations that produce the erosion within a specified tolerance. We then use the most-likely design event to choose the most probable events associated with the desired erosion level. The method is illustrated in Fig. 8.7 that shows level curves for storms (solid lines) and erosion (dashed lines) for return periods of 100, 50 and 25 yr and for constant $T = 15\,\mathrm{s}$ and $W = 1\,\mathrm{m}$ above mean sea level. The intersection of storm lines with the erosion lines represents a point where the erosion return period is equal to the storm return period. In four

Table 8.3: The storm parameters associated with the multivariate return periods 25, 50 and 100 yr and the associated erosion return periods calculated by incorporating a multiple linear regression with the most-likely design event.

Storm return period (yr)	**25**	**50**	**100**
Storm characteristics:			
H (m)	4.63	5.00	10.3
T (s)	16.9	17.5	17.4
D (h)	90.4	95.0	83.9
W (m)	0.85	0.86	0.87
Erosion volumes ($m^3\,m^{-1}$)	132	160	193
Erosion return periods (yr)	25	56	141

dimensions this intersection is not unique and so the most-likely design event is used to select the most probable event. This method was performed for 25, 50 and 100 yr erosion return periods. The resulting storms (combinations of H, T, D, W) were then run through XBEACH to verify the method. Table 8.3 shows that the method produces erosion return periods that are consistent with the storm return periods. The 25 yr return periods correspond exactly and there is only a minor difference between the 50 yr events. The 100 yr storm event translates to an erosion of 141 yr. Although this difference seems significant, when comparing the erosion volumes there is less than 10 % difference between the 100 yr ($180\,m^3$) and 141 yr ($193\,m^3$) erosion event. The difference can be attributed to errors and/or uncertainties in the regression model and the erosion probability distribution for extreme events.

8.5 Discussion

In an ideal situation a multivariate return period of a storm would be equivalent to that of the erosion associated with that storm. This would provide a quantifiable risk to the multivariate return period and make the design process simpler.

The most-likely design event has been suggested as a method for identifying design events, but without a direct link to its physical consequences (in this case erosion) it cannot provide a meaningful measure of the associated risks. A link can be provided by using a "structure function" approach (e.g. Hawkes, 2008 and

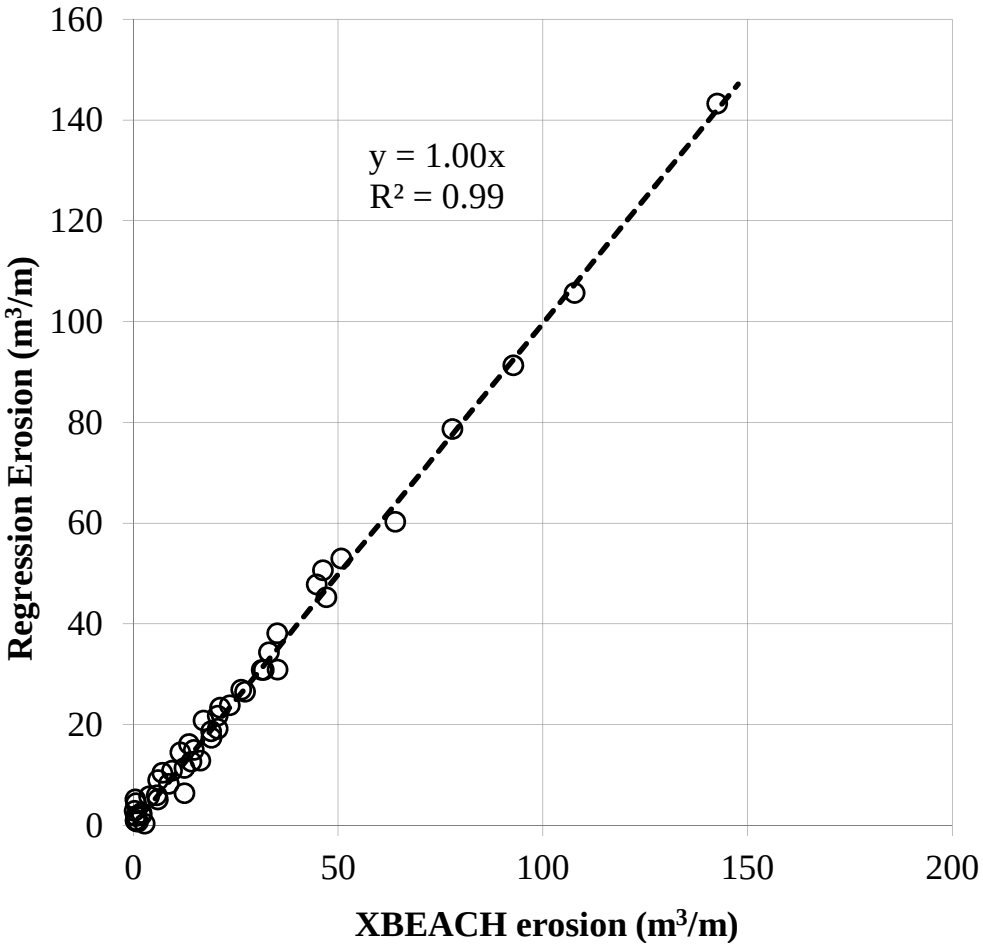

Figure 8.5: A comparison of the erosion estimated from the multiple linear regression and XBEACH.

Callaghan *et al.*, 2008). The complexity in achieving this can be appreciated by considering the effects of storm duration. Equilibrium profile theory suggests that an increased water level and wave height will cause a beach profile to retreat to a new equilibrium level. For this new equilibrium to be established the sea conditions must be sustained for a certain amount of time. Once this threshold of time has been exceeded the profile will cease to change further. This means that a statistical model may predict a rare storm duration of say 300 h but it will not cause any more erosion than a 100-h storm. That is, the sensitivity of erosion to the storm duration may decrease as the duration increases. Therefore, beyond a certain duration threshold it may be more appropriate to consider the

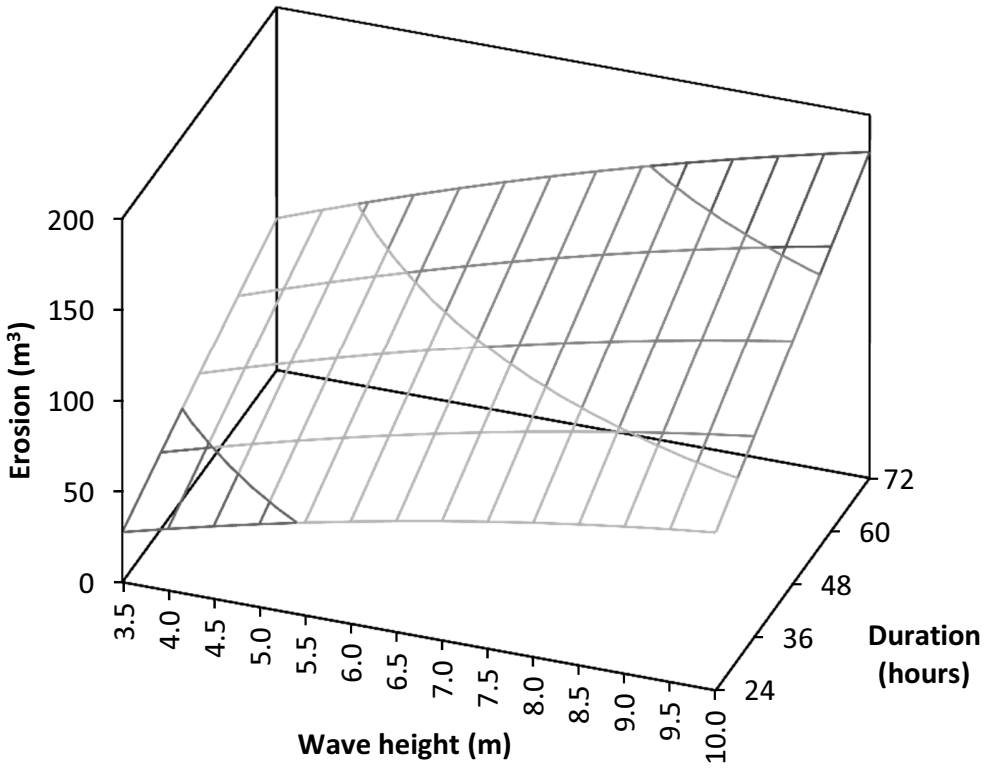

Figure 8.6: Surface plot of erosion as a function of wave height H and storm durations D, for the given wave period $T = 16\,\mathrm{s}$ and water level $W = 1.0\,\mathrm{m}$ above mean sea level. Contours of erosion levels 50, 100, 150, 200, $250\,\mathrm{m^3\,m^{-1}}$ are shown on the surface. Corresponding erosion return periods can be inferred from Fig. 8.4.

occurrence of larger wave heights instead of longer durations.

The ambiguity of multivariate return periods has not been sufficiently developed for practicing designers to employ them in coastal applications. We have proposed a method that can estimate storm events that are analogous to that of associated erosion events. The multivariate analysis is fairly complicated to implement and although it is the correct way to define a storm return period, we suggest a univariate analysis of H and D and a bivariate analysis of HD may provide a reasonable engineering estimate of the associated erosion return period. We suggest that if the wave height return period is significantly larger than that of the duration then the erosion return period will approximate the wave height return period and vice versa. If the wave height and duration return periods are

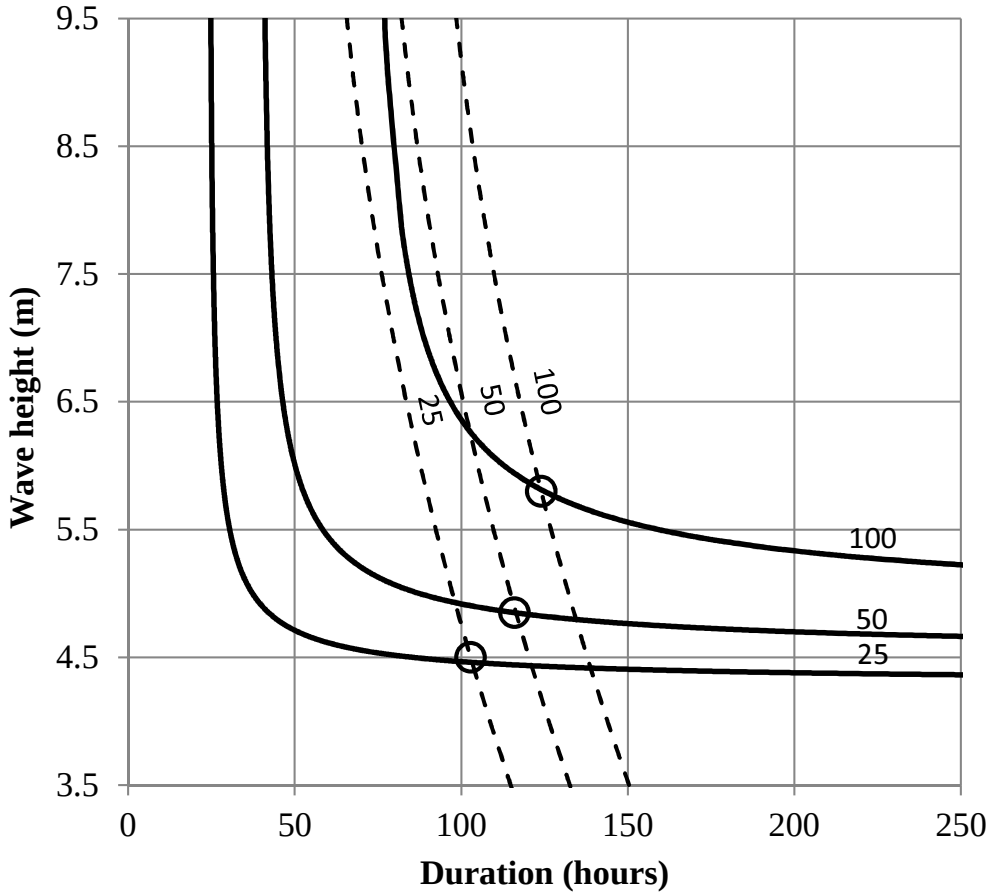

Figure 8.7: Level curves of storm parameters H and D for storm (solid lines) and erosion (dashed lines) return periods of 100, 50 and 25 yr for $T = 15$ s and $W = 1.0$ m above mean sea level

similar then the bivariate return period may be representative of the erosion and thus satisfy the assumptions of the synthetic design storm [Carley & Cox, 2003].

Typically, a univariate analysis of storm parameters inadequately describes the erosion potential of a multivariate storm event. Table 8.4 shows the various return period definitions for the events presented in Table 8.3. None of the return periods except the trivariate $\tau(HDT)$ are close to being consistent with the corresponding erosion return periods. In this case the lower dimensional return periods overestimate the risk (or underestimate the return periods) associated with the storm erosion.

The use of return periods that are directly linked to erosion consequences is

Table 8.4: The magnitude of different return periods (univariate, bivariate, etc.) for the events listed in Table 8.3 which were selected to have multivariate return periods of 25, 50 and 100 yr with matching associated erosion return periods.

Storm return period (yr)	**25**	**50**	**100**
Return period definition (yr):			
$\tau(H)$	2.0	3.1	58
$\tau(T)$	7.3	13	11
$\tau(D)$	3.2	3.3	3.0
$\tau(W)$	1.6	1.7	1.8
$\tau(HD)$	4.0	6.3	14
$\tau(HDT)$	16	37	100

important for well-informed coastal management. Coastal managers often make decisions on wave parameter based return periods without understanding that the associated impact may be significantly different. The method demonstrated in this paper allows the estimation of an unambiguous return period from limited field data by simulating sea storm erosion in XBEACH. Combined with multivariate regression, this essentially yields a structure function in the spirit of those described by Coles & Tawn [1994] and Reeve [1998]. The regression derived structure function is expected to be site and project specific and would have to be re-computed using XBEACH (or from a detailed record of beach surveys) for each application.

8.6 Conclusions

This paper has explored the relationship between multivariate return periods and erosion return periods through a simulation study. Kendall's return period provides a promising description of copula based return periods. Durban's largest storm event on record, the 2007 storm, was estimated to have a 120 yr (multivariate) return period with a 34 yr erosion return period. Based on simulations of idealized historical storms, the multivariate return period with the strongest correlation to erosion return period was a bivariate return period of wave height and duration. We have shown that a univariate analysis of storm parameters cannot adequately describe erosion risks and will lead to overestimation. Cau-

tion is required when attempting to define erosion risks by simple return periods of few dimensions. The most-likely design event proposed by Salvadori *et al.* [2011] provides a means to overcome the ambiguity of multivariate return periods by selecting the most probable events for a specified exceedance probability. However, the method is purely statistical and the lack of any link to the underlying physical consequences limits its usefulness for design applications. We have created a type of erosion structure function using multiple linear regression and based on the XBEACH model. This erosion structure function has been used to improve the appropriateness of the design event estimates. The results suggest that appropriate conditioning can provide a method for estimating multivariate storm return periods that are consistent with the return periods of their consequential erosion events. Further research is required to investigate the generality of this approach and should involve testing at other locations with different wave climates and shoreline characteristics.

References

Callaghan, D. P., Nielsen, P., Short, A., & Ranasinghe, R.: Statistical simulation of wave climate and extreme beach erosion, Coast. Eng., 55, 375 – 390, 2008. 20, 31, 58, 85, 121, 155, 182, 191, 192, 207, 236

Carley, J. T. & Cox, R. J.: A methodology for utilising time-dependent beach erosion models for design events. Proceedings of the 16th Australasian Coastal & Ocean Engineering Conference, Auckland, New Zealand, 2003. 220, 238

Coles, S. G. & Tawn, J. A.: Statistical Methods for Multivariate Extremes: an Application to Structural Design, Appl. Statist., 43, 1 – 48, 1994. 182, 239

Corbella, S. & Stretch, D. D.: The wave climate on the KwaZulu-Natal coast, South Africa., J. S. Afr. Inst. Civ. Eng., 54(2), 2012a. 94, 101, 155, 183, 220

Corbella, S. & Stretch, D. D.: Simulating a multivariate sea storm using Archimedean Copulas, Coast. Eng., submitted, 2012c. 189, 196, 199, 223, 224

Corbella, S. & Stretch, D. D.: Shoreline recovery from storms on the east coast of Southern Africa, Nat. Hazards Earth Syst. Sci., 12, 11 – 22, doi:10.5194/nhess-12-11-2012, 2012d. 205, 220

Corbella, S. & Stretch, D. D.: Predicting coastal erosion trends using non-stationary statistics and process-based models. Coast. Eng., 70, 40 – 49, 2012e. 228

Chini, N., Stansby, P., Leake, J., Wolf, J., Roberts-Jones, J., & Lowe, J.: The impact of sea level rise and climate change on inshore wave climate: A case

study for East Anglia (UK), Coast. Eng., 57, 973 – 984, 2010. 20, 58, 140, 156, 185, 223

De Michele, C., Salvadori, G., Passoni, G., & Vezzoli, R.: A multivariate model of sea storms using copulas, Coast. Eng, 54, 734 – 751, 2007. 22, 25, 27, 78, 152, 154, 155, 156, 162, 171, 174, 189, 190, 223, 224, 313, 315

Genest, C. & Rivest, L.-P.: Statistical inference procedures for bivariate Archimedean copulas, J. Am. Stat. Assoc., 88, 1034 – 1043, 1993. 158, 226

Genest, C. & Rivest, L.-P.: On the multivariate probability integral transformation, Stat. Probab. Lett., 53, 391 – 399, 2001. 29, 226

Goda, Y.: Random Seas and Design of Maritime Structures, 2nd Edn., World Scientific Publishing Co. Pte. Ltd. Singapore, 2008. 20, 21, 28, 58, 59, 151, 187, 188, 225, 233

Guedes Soares, C. & Scotto, M. G.: Application of the r largest-order statistics for long-term predictions of significant wave height, Coast. Eng., 51, 387 – 394, 2004. 20, 21, 58, 156, 185, 223

Hartanto, I. M., Beevers, L., Popescu, I., & Wright, N. G.: Application of a coastal modelling code in fluvial environments. Environ. Model. Softw., 26, 1 – 11, 2011. 31, 192, 228

Hawkes, P. J.: Joint probability analysis for estimation of extremes, J. Hydraul. Res., 46, 246 – 256, 2008. 235

Kriebel, D. L. & Dean, R. G.: Convolution method for time-dependent beach-profile response, J. Waterw. Port C., 119, 204 – 226, 1993. 31, 85, 182, 191, 204, 207, 228

Larson, M., Kraus, N. C., & Byrnes, M. R.: SBEACH: Numerical model for simulating storm-induced beach change, Report 2, Numerical formulation and model tests, Technical report CERC-89-9, US Army Engineer Waterways Experiment Station, Vicksburg, MS, 1990. 31, 191, 228

Mendez, F. J., Menendez, M., Luceno, A., Medina, R., & Graham, N. E.: Seasonality and duration in extreme value distributions of significant wave height, Ocean Eng., 35, 131 – 138, 2008. 155, 156, 185, 186, 187, 223

Michell, J. H.: On the Highest Wave in Water, Phil. Mag., 36, 430–435, 1893. 233

Minguez, R., Menendez, M., Mendez, F. J., & Losada, I. J.: Sensitivity analysis of time-dependent generalized extreme value models for ocean climate variables, Adv. Water Resour., 33, 833 – 845, 2010. 156, 185, 186, 223

Nelsen, R. B.: An introduction to copulas, 2nd Edn., Springer Series in Statistics, Springer, New York, 2006. xxi, xxviii, 22, 24, 25, 26, 27, 29, 152, 153, 154, 158, 159, 162, 171, 172, 173, 175, 189, 190, 223, 224, 315

Reeve, D. E.: Coastal Flood Risk Assessment, J. Waterway Port C., 124, 219 – 228, 1998. 204, 239

Roelvink, D., Reniers, A., van Dongeren, A., van Thiel de Vries, J., McCall, R., & Lescinski, J.: Modelling storm impacts on beaches, dunes and barrier islands, Coast. Eng., 56, 1133 – 1152, 2009. 31, 191, 192, 220, 228

Ruggiero, P., Komar, P. D., & Allan, J. C.: Increasing wave heights and extreme value projections: The wave climate of the US Pacific Northwest, Coast. Eng., 57, 539 – 552, 2010. 13, 20, 58, 115, 139, 156, 185, 186, 196, 223

Salvadori, G.: Bivariate return periods via 2-Copulas, Stat. Methodol., 1, 129 – 144, 2004. 28, 29, 188, 225

Salvadori, G. & De Michele, C.: Multivariate multiparameter extreme value models and return periods: A copula approach, Water Resour. Res., 46, W10501, doi:10.1029/2009WR009040, 2010. 152, 189, 223, 225

Salvadori, G., De Michele, C., Kottegoda, N. T., & Rosso, R.: Extremes in Nature, An Approach Using Copulas, Water Science and Technology Library, Springer, 56, 292pp, 2007. 25, 154, 155, 225, 313

Salvadori, G., De Michele, C., & Durante, F.: On the return period and design in a multivariate framework, Hydrol. Earth Syst. Sci., 15, 3293 – 3305, doi:10.5194/hess-15-3293-2011, 2011. 29, 30, 152, 219, 220, 225, 226, 227, 240

Savu, C. & Trede, M.: Hierarchical Archimedean copulas, available at: `http://www.uni-konstanz.de/micfinma/conference/Files/~papers/` (last access: 1 November 2011), 2006. 26, 27, 154, 190, 224, 314, 315

Savu, C. & Trede, M.: Hierarchies of Archimedean copulas, Quant. Financ., 10, 295 – 304, 2010. 27, 190, 224, 315

Schoonees, J. S. & Theron, A. K.: Evaluation of 10 cross-shore sediment transport/morphological models, Coast. Eng., 25, 1 – 41, 1995. 31, 191, 228

Sklar, A.: Fonctions de repartition a n dimensions et leurs marges, Publications de l'Institut de Statistique de l'Université de Paris, 8, 229 – 231, 1959. 23

van Gent, M. R. A., van Thiel de Vries, J. S. M., Coeveld, E. M., de Vroeg, J. H., & van de Graaff, J.: Large-scale dune erosion tests to study the influence of wave periods, Coast. Eng., 55, 1041 – 1051, 2008. 21, 54, 138, 151, 219

van Thiel de Vries, J. S. M., van Gent, M. R. A., Walstra, D. J. R., andReniers, A. J. H. M.: Analysis of dune erosion processes in large-scale flume experiments, Coast. Eng., 55, 1028 – 1040, 2008. 21, 54, 138, 151, 219

Chapter 9

Coastal Defences on the KwaZulu-Natal coast: a review with particular reference to geotextiles

This chapter is based on a paper published in the Journal of the South African Institution of Civil Engineering, 54 (2), 55 – 64, 2012.

Abstract

Modern coastal defences have to satisfy economic, environmental and sustainability criteria. The balancing of these criteria can make the implementation of coastal defences socially, environmentally and politically complicated. Durban's local authority, the eThekwini Municipality, has had experience with numerous forms of coastal defences in its attempts to balance the operations of a port and associated beach erosion problems. Recently, in March 2007, the KwaZulu-Natal coastline suffered severe damage from an extreme storm event which necessitated the installation of additional coastal defences. This paper evaluates Durban's experiences of coastal defences and details the successes and failures in order to

provide practical insight to those faced with similar circumstances or considering the implementation of coastal defence.

9.1 Introduction

The implementation of coastal defences has historically been dependent on the value of the hinterland and the nature of the coastline. Environmental and sustainability considerations have become more prevalent in the implementation of coastal defences and are often the governing factors when determining an appropriate defence [Airoldi *et al.*, 2005; Moschella *et al.*, 2005; Zanuttigh *et al.*, 2005]. Consideration of these three factors often leaves municipalities and coastal engineers struggling to find a solution that optimally satisfies all the considerations.

Durban is an important port city located on the east coast of South Africa (Fig. 9.1). The local government was faced with a challenge concerning coastal defences when an extreme event in March 2007 devastated the KwaZulu-Natal coastline. This paper reviews the defences implemented before, during and after the event and identifies their successes and failures. The description of these successes and failures is intended to aid authorities and interested and affected parties to make insightful decisions when undertaking a coastal defence. The review also identifies the importance of monitoring with respect to coastal management. Durban's beach profiles have been recorded since 1973 and have played an integral part in the Municipality's coastal management.

Gilbert & Vellinga [1990] identified five alternative ways to mitigate the damage of coastal storms, namely accommodation; protection; beach nourishment; retreat and the do-nothing alternative. These solutions can be further divided into two major categories of "hard" and "soft" engineering solutions. Hard solutions typically result in permanent structures that have continual effects on the environment. Soft solutions are the environmentally preferred options and do not involve permanent structures. Durgappa [2008] defined groynes, breakwaters, seawalls, revetment etc. as hard solutions and only beach nourishment as a soft solution. We suggest that the soft category should include accommodation, retreat and the use of geotextile sand filled containers (GSC). Although soft solutions are always a priority they are often difficult to implement effectively.

Accommodation is essentially part of a management or planning programme to reduce risk, an example is the establishment of setback lines or designing structures to accommodate occasional flooding. Retreat is the relocation of existing structures to a less vulnerable area and is often seen as a last resort because of its socio-economic complications [French *et al.*, 2001].

While the eThekwini Municipality (Durban's local government authority) did implement retreat and the do-nothing approach in the aftermath of the March 2007 event, the experiences from these solutions were trivial and did not warrant inclusion in this review. Minor public owned structures were relocated outside of vulnerable zones following their failure without any public objections. Private properties were not protected with public funds and many of them recovered naturally. Setback lines were successful in mitigating damage during the March 2007 event and are consider an essential part of coastal planning. This review is limited to physical defences and precludes setback lines.

The review aims to compare Durban's coastal defence experiences with international experiences in an attempt to highlight and recommend successful practices. The review commences with a brief history of Durban's beach protection and then describes Durban's coastal defence experiences with respect to: groynes; beach nourishment; loffelstein walls; geotextile sand filled containers; geotextile tubes and geotextile wraps. The conclusion recommends coastal defences based on the Durban experience.

9.2 A brief history of Durban's beach protection

Durban's history of beach protection has largely revolved around efforts to effectively operate a port. There is evidence of the beaches being stable for a period of almost 100 years prior to the commencement of harbour works [CSIR, 1976; Kinmont *et al.*, 1954].

In 1857 construction began on the North and South breakwaters of the harbour. It soon became necessary to deepen the channel to cater for vessels with larger drafts, and dredging operations commenced in 1895. Dredging operations intensified from 1897 onwards and this marked the onset of erosion [Kinmont *et al.*, 1954]. The channel dredging remained approximately 650 000 $m^3/year$

Figure 9.1: A map of South Africa showing KwaZulu-Natal and Durban and a map showing the Durban harbour and the relevant local areas

which was approximately equal to the longshore drift estimated at that time meaning no sand was reaching the beaches north of the harbour.

In response to the beach erosion the eThekwini Municipality started pumping sediment as beach nourishment to the South and Central beaches in 1935 [Barnett *et al.*, 1999]. What followed were a series of different schemes implemented to discharge dredged material to the beaches. These schemes included a failed fixed bypass scheme attempted between 1950 and 1953.

The so called Paterson Groynes were built between 1954 and 1956. These two groynes were constructed to stabilise the central beaches in light of the fact that maintenance dredging was not providing the required quantities. The groynes did little to alleviate the problem.

Further effort was made to mitigate beach erosion in 1966 when construction of the underwater mound commenced. The mound was a large underwater sand bank constructed from dredged sediment and was aimed at protecting the Central and Northern beaches against storm waves. The mound was never completed to its design height [Barnett *et al.*, 1999] and in 1977 the CSIR had found it more beneficial to pump the sand available for the mound directly to the beaches.

The long standing sediment supply problem was eventually solved by the sand bypass scheme, completed in 1982 and the new groynes completed in 1985. These groynes called the Bay of Plenty and North Beach Piers (Fig. 9.2) replaced the Paterson Groynes. In 1989 a third groyne, the Dairy Beach Pier (Fig. 9.2), was constructed [Mather *et al.*, 2003]. The sand bypass scheme consisted of a concrete hopper and a series of four booster stations, each approximately 700 m apart and connected with a 400 mm diameter high density polyethylene pipe. The hoppers could receive 5000 m^3 of fluidised sand. This sand would then be re-dredged by a fluidising and pumping mechanism at the hopper station and could then be pumped to various outlets between Vetch's (Fig. 9.1) and Bay of Plenty beach, totalling approximately 3.5 km.

The widening of the Durban harbour in 2007 necessitated the demolition of the hopper station. A new design has been completed and the scheme is due to be operational by 2013. Until such time there is a temporary scheme, consisting of a bund in the northern breakwater and operating similarly to the original scheme.

Table 9.1 provides an inventory of all the physical defences that have been

installed in the eThekwini Municipality. Table 9.1 shows the date of installation, the length of coast defended and comments on the defences' performance. The length of the defence is only an estimation and does not include ad hoc defences that have been installed by private home owners. The eThekwini coastline is approximately 100 km and it is estimated that 11 % of it is defended. Almost 90 % of these defences are made up of rock revetments, loffelstein walls and geotextile sand bags. The bulk of the defences are loffelstein walls which were installed in the Bluff, Umdloti and Umhlanga Rocks in the 1980s. These retaining walls make up 34 % of all eThekwini's coastal defences. The oldest form of coastal defence is rock revetments. Almost the entire stretch of Durban's central beaches is protected by rock revetments. The rock that was installed in the 1900s is now permanently covered by sand but makes up 29 % of eThekwini's coastal defences. The first geotextile sand bags were installed in 2007 but already make up 24 % of the eThekwini coastal defences.

9.3 The March 2007 event

The March 2007 storm event refers to the storm's climax on the 19th and 20th of March 2007. Approximately 350 km of the KwaZulu-Natal (KZN) coastline was subject to severe erosion [Breetze *et al.*, 2008].

An extreme high tide cycle of 18.6 years and an offshore storm coincided to produce wave heights of up to 8.5 m. The combination of equinox tide level and peak storm wave setup resulted in a water level of almost 2.7 m above chart datum [Phelp *et al.*, 2009].

What followed were a multitude of coastal defences, many implemented under emergency conditions. The remainder of this paper reviews the successes and failures of defences pre and post the 2007 event.

9.4 Groynes

Groynes are shoreline stabilisation structures that retard the natural flow of sediment causing accretion. They are constructed perpendicular to the shoreline and are designed to provide a minimum beach width.

Table 9.1: Coastal defences along the eThekwini Coastline, their installation dates, physical characteristics and encountered issues

Defence	Locations	Installation Date	Physical characteristics	Encountered issues
Groynes	Bay of Plenty North Beach Dairy Beach	1985 1985 1989	214 m long 214 m long 214 m long Affects 1000 m	In 1998, following a large storm event, the seaward southern piles of Bay of Plenty Groyne kicked from excessive scour. The structure required repair.
Beach nourishment	Vetch's to South Beach	1982 2009 2010	650 000 m^3 250 000 m^3 250 000 m^3 Affects 2000 m	High beach scarp
Gabion baskets	South Beach	1982	100 m	No known issues
Gabion baskets filled with 20 kg sand bags	Ansteys Beach	2007/2008	20 m	The gabion baskets deformed from the sand bag movement. They look untidy but have performed well.
Loffelstein walls	Brighton Beach Umhlanga Rocks Umdloti	1980s	1000 m 2000 m 850 m	Numerous walls failed in 2007. A section failed in 2011 at Brighton Beach and Umhlanga Rocks.
Fibreglass sheet piles	Ansteys Beach	2008	70 m	No issues to date
Geotextile sand bags	Vetch's Beach Ushaka Beach Addington Beach Battery Beach Thekwini Beach Country Club Beach Blue Lagoon Ansteys Beach Umdloti Umhlanga Rocks Total	2007 2007 2009 2010 2010 2012 2012 2012 2008 2007/2008 2011 2008	120 m 300 m 200 m 200 m 250 m 110 m 100 m 300 m 100 m 300 m 300 m 300 m 2660 m	See GSC section
Geotextile tubes	Amanzimtoti	2008	50 m	No issues to date
Geotextile wrap	Numerous private homes	2008	500 m	Inappropriate materials (such as non-woven polyester/bidim) suffer from severe abrasion and pull apart. The wrap was also used as a secondary defence behind the bags at Umdloti and Addington.
Rock revetments	Umdloti sewer pump station Amanzimtoti The Bluff Central beaches (South Beach to Bay of Plenty Beach)	2007 2007 1900s 1900s	30 m 30 m 1200 m 2000 m	Social issues but are very effective.
The mound	Bay of Plenty Beach	1966	1000 m	Never completed. Waves of sufficient height break on the mound.

Durban's groyne field was constructed between 1985 and 1989 (Fig. 9.2). This groyne field, in conjunction with the sand bypass scheme has been successfully maintaining a stable beach over their existence. The groynes are semipermeable rock groynes, making the beach width dependent on the rock elevation. The rock levels are monitored annual by the eThekwini Municipality and were adjusted to their design levels in 2009 with a combination of rock and geotextile sand bags.

The piers are constructed on precast friction piles and so the elevation of the sand determines the stability of the structure. The dynamic environment necessitates monitoring and scour levels around the piles are determined every 6 months.

Corrosion of reinforcing steel is a major concern for all coastal structures. Although the groynes are still in good condition it is worth noting corrosion observations. When the Bay of Plenty and North Beach Groynes were constructed in 1985 the handrail posts were reinforced with ordinary high tensile steel bars with a concrete cover of 50 mm (a minimum cover of 25 mm was specified). The Dairy Beach Groyne was constructed four years later in 1989 with handrail posts consisting of hot-dipped galvanised high tensile steel reinforcing bars but with only 25 mm concrete cover. By 2010 all of the Dairy Beach handrail posts had to be replaced with polymer concrete posts as a result of server concrete spalling. The superstructures and piles of all three piers were constructed similarly but the galvanised Dairy Beach Pier was in a far superior condition than the two older groynes. The fact that the steel in the handrail posts was galvanised, had less concrete cover and was installed more recently implies that concrete cover cannot be neglected because the reinforcing is galvanised. A 20 mm concrete cover is inadequate to protect a galvanised bar under highly corrosive conditions [Yeomans, 2004] and SANS 10100-2:1992 specifies 60 mm concrete cover in extreme environments for normal density concrete. The eThekwini Municipality Coastal Department use galvanised steel in all their coastal structures with a minimum cover of 60 mm.

Groynes are an expensive investment and are often difficult to construct. They also have the potential to intensify erosion if not designed correctly. This was the case in 1936 when a loose stone groyne was constructed. It accentuated erosion on either side of the groyne and so it had to be removed [Kinmont *et al.*, 1954]. A

strong rip current is often induced by a groyne and although a pleasure for surfers they can be precarious to an uninformed bather and consequentially require the presence of life guards. Their effective and safe functionality necessitates a fair amount of monitoring and consequentially requires a good management structure.

The groyne field did not prevent the 2007 event from overtopping the promenade and damaging the adjacent commercial node. The wave heights also exceeded the soffit of the deck and broke numerous precast concrete slabs. With such an extreme event it is not expected that the groynes will completely prevent damage but they did minimise the impacts by providing a beach buffer between the promenade and ocean.

In Durban's case the groynes have been worth the expense and effort, providing not only stable beaches but a recreational attraction to the public. The groynes are currently exceeding their 20 year design life and, other than some minor concrete spalling, are still in a safe operating condition.

9.5 Beach Nourishment

Beach nourishment is the supply of sand to beaches usually from offshore dredging and is an environmentally preferred method of shore protection [Belkessa *et al.*, 2008]. This technique is used worldwide usually in combination with a shoreline stabilisation technique. Europe has adopted beach nourishment as central to its soft engineering strategy [Hamm *et al.*, 2002; Hanson *et al.*, 2002]. The additional sediment on the beach essentially shifts the wave run-up further away from inland infrastructure creating a buffer.

To protect dunes from erosion the dry beach has to be flat and wide enough to approximate to the Bruun-type equilibrium profile at the raised water level [Dette & Raudkivi, 2002]. This profile shape and thus a nourishment volume are difficult to estimate. The so called equilibrium profile develops from predominant wave action and so a storm profile will be different from a calm weather profile. This is also true when widening a beach as the wave conditions may change seaward. A way of avoiding this is to base the nourished profile on a desired historic profile. This in itself is erroneous since a beach that is being nourished is typically eroding and so is not at an equilibrium profile. A numerical beach

Figure 9.2: Photograph looking south-west across the main Durban beachfront showing the Bay of Plenty, North Beach and Dairy Beach Piers, from closest to furthest, 3 June 2010.

response model is usually used to predict changes in the nourished profile. When attempting to reclaim beach for recreational purposes the inability to predict a fill volume can result in a failed project. The recently acquired dry beach can adjust under wave action and return the dry beach width to the pre-nourishment dry width. Although the sand is not lost but simply moved to an unstable portion in the lower profile the nourishment in terms of reclaiming recreational beach would have failed. The existence of a good and substantial beach profile record is needed to perform a suitable nourishment design.

Failure of nourishment projects that are generally government funded are criticised by the public who may not support a future beach nourishment scheme. In relation to other coastal protection nourishment is cheaper but it is still very expensive to not see a visible result. Tax payers are often happier knowing that their contribution is in a visible seawall as opposed to thousands of cubic meters

of sand sitting just offshore. It is therefore extremely important to not under nourish a beach.

The 2007 storm event had left the beaches in a similar state to 1982 and the hopper was no longer available to replenish the starved beaches. The issue was intensified by the looming 2010 World Cup and prompted the city engineers to initiate a beach nourishment project where offshore sediment would be dredged and pumped ashore.

A 900 mm diameter pipe was laid 1,4 km from the Harbour's North Breakwater to Addington beach (Fig. 9.3). An offshore borrow site that had previously been used to reclaim Berth's D to G within the harbour was used. The site was surveyed and sediments sampled to ensure that the grading was suitable. Sediment grading is important as fines produce plumes and increase the sediments erosion susceptibility. At the same time the sediment cannot be too coarse as traversing the beach can become an uncomfortable barefoot experience. A good way of determining a suitable grading is to compare the grading of a popular and stable recreation beach with the borrow site. It was found that the borrow site was slightly coarser (a mean of 304 μm) than the destinations, Vetch's and Addington Beach (Fig. 9.1). The project was undertaken in two phases the first in 2009 and the second in 2010, each phase contributing approximately 250 000 m^3 of sediment to the beaches.

A project of such a nature is technically trivial but management intensive. The dredger is chartered on an hourly rate and so the more sand that is pumped the smaller the cubic meter cost. At the time the dredgers stand by rate was R 36 000.00 an hour necessitating that no delays were incurred at the discharge pipe. The success of the project was largely indicative of good project management.

The project was successful as it introduced new high quality coarse sediment (about 500 000 m^3) into the system, aiding a correction in the sediment budget. The project was unfortunately not a complete success. The importance of creating a suitable beach profile was neglected in the first phase of pumping, largely due to time constraints. The resulting profile was quickly corrected to an equilibrium profile which produced unexpected earthworks costs to counteract the 3 m scarp that formed. The borrow site was originally surveyed with a single scan sonar as

Figure 9.3: Beach nourishment at Addington Beach (Dredging International, June 2009)

a higher resolution multibeam was considered an unnecessary expense since the site had been dredged extensively in the past. The initial dredging phase was without incident except dredging of small ammunitions. The second dredging phase saw the dredging of steel elements (Fig. 9.4) resulting in the cracking of the dredger impeller.

The cracking of the impeller was a major setback in the project and resulted in a large insurance claim. In hindsight an expensive multibeam survey may have been more economical should the insurance not cover the delays.

9.6 Retaining walls

Retaining walls in the coastal context are different from seawalls. In Durban a large number of dry stacking, interlocking retaining walls have been used inappropriately or have developed into an inappropriate situation as a result of chronic erosion. Although there are various types of dry stacking, interlocking walls Durban's coastal retention structures are loffelstein walls. Water loffel is a variation of loffelstein having interlocking wings. They are commonly used for hydraulic applications and had been extensively used as seawalls at Brighton Beach, Umh-

Figure 9.4: Dredged steel elements and cracked dredger impeller (Dredging International, April 2010)

langa and Umdloti. Seawalls are the most common form of coastal defence and the physical barrier between the land and sea is often considered most desirable by residents [French *et al.*, 2001]. Unfortunately they can create a static coast and are one of the least environmentally acceptable solutions. Loffelstein walls are essentially coastal retention structures that are constructed at the backshore and are not intended to withstand direct wave action. Unfortunately due to chronic erosion the walls at Umhlanga and Umdloti are exposed to wave attack fairly regularly. Although in these situations a more substantial defence, such as the fibreglass sheet piles at Ansteys Beach, is preferable the loffelstein walls have performed relatively well.

A large amount of these walls failed during the 2007 event. The failures were a result of water down rush and overtopping washing sediment out from behind the walls. This combination of sediment loss caused the walls to collapse on themselves (Fig. 9.5). This failure mechanism highlights the need to have substantial drainage and filtration behind the walls. A geotextile filter layer ensures that water can drain from behind the wall while the filter retains the

Figure 9.5: Failure of loffelstein seawall at Umhlanga main beach (eThekwini Municipality data base, 20 March 2007)

sediment. Some of the walls that had a geotextile filter parallel to the wall still failed, while none of the walls that had a filter parallel and perpendicular to the wall failed. It is felt that having these perpendicular geotextile tiebacks (Fig. 9.6) limits the likelihood of sediment escaping through gaps in the parallel filter. This was the only failure mechanism experienced during the event as none of the walls were undermined. This was a consequence of the walls being either founded on rock or on a bed of gabion mattresses below the lowest scour profile.

Although Loffelstein walls are not a favourable solution, the majority of the loffels that failed during the event were reinstated. Only certain sections of the walls had failed and it was more aesthetically pleasing and economical to retain a continuous loffel wall. Where walls were severely damaged they were replaced with geotextile sand bags.

9.7 Geotextile sand filled containers (GSC)

The use of GSCs was initiated in the USA, the Netherlands and in Germany more than 50 years ago [Saathoff *et al.*, 2007]. GSCs have become increasingly popular because of their multitude of applications as well as their environmental benefits. GSCs are often spoken of as a soft engineering solution. This is not entirely correct because a soft solution is one that does not impede the natural morphology of the

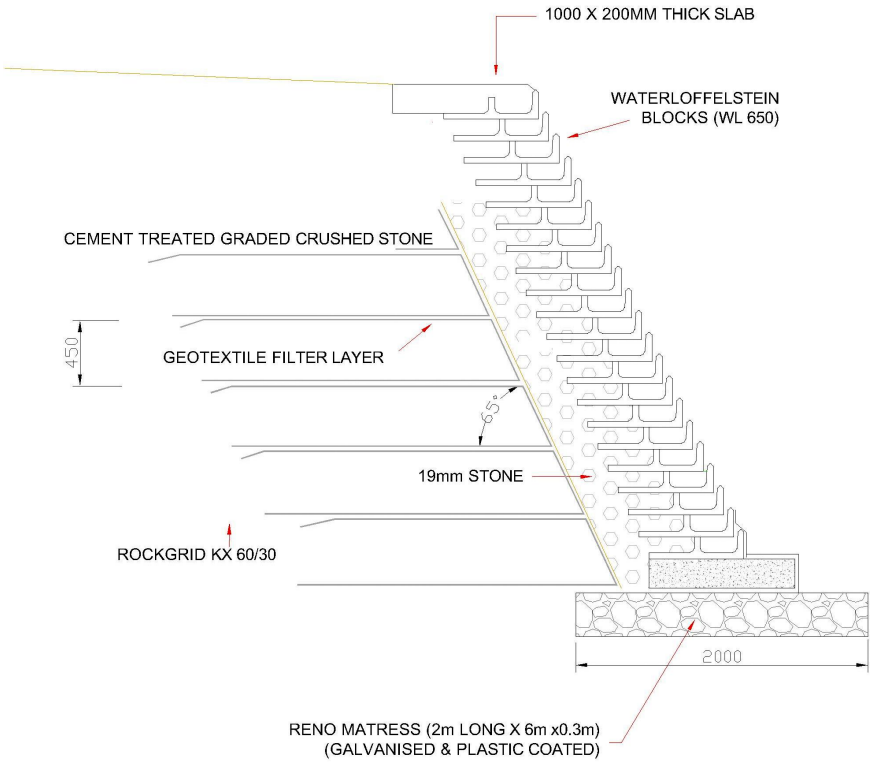

Figure 9.6: Typical section through loffelstein wall

coast. The GSCs prevent erosion and so can develop a static shoreline. They are considered a soft solution because if an unforeseen environmental impact ensues they can easily be sliced open and removed spilling sand back onto the beach.

Allan & Komar [2002] observed the effectiveness of an artificial dune for shore protection by surveying a dune constructed with sand-filled geotextile bags covered by loose sand and dune vegetation from 1999 to 2002. They reported that the dune survived fairly extreme conditions which included overtopping, but noted that it was still to be seen if it would cope with the more severe storms.

Heerten *et al.* [2008] did extensive research into the effectiveness of GSCs to mitigate coastal erosion. They described the successful use of GSCs on the island Sylt in Germany where geotextile cushions were covered with sand and sand trap fences. The geotextile was exposed after the second largest storm surge yet it had prevented a 2.5 m above normal water level and waves exceeding 5 m from eroding the dune.

Recio & Oumeraci [2008] also did extensive research on geotextile bags. Through rigorous model testing they were able to consider all the forces acting on the containers as well as the effects of container deformation. The impact of wave action and submergence causes sand to be moved inside the bag from the back to the exposed face. This movement has two negative effects. It decreases the contact area between bags thus reducing the friction forces and it increase the surface area in the front of the bag making it more susceptible to drag forces.

GSCs are a relatively new technology and have only recently found application in South Africa. Their advantages include being cost effective and easily transported which makes them ideal for emergency work. The geotextile can be easily cut and removed if required but at the same time permanent containers are susceptible to vandalism. This issue has been combatted by a composite vandal-deterrent geotextile which traps 3 kg of sand per square meter within the geotextile. Although this significantly increases the resilience and durability of the container [Saathoff *et al.*, 2007] it has little effect on the penetration of a knife. GSCs used to protect dunes should always be covered with sand and vegetated to protect them from vandals and to restore a natural appearance to the coastline. Vegetation has the advantage of mitigating blown sediment and stabilising backshore morphology [Udo *et al.*, 2002].

Based on the documented success of GSCs in Australia [Restall *et al.*, 2002; Saathoff *et al.*, 2007], the Municipality decided to pursue their installation as an emergency and permanent measure. The use of GSCs or geotextile sand bags became the eThekwini Municipality's favoured form of sea defence after the 2007 event. Their extensive use warrants an extended section dedicated to their application.

9.7.1 Manufacture

Kaytech Engineered Fabrics was approached to manufacture and supply the GSCs. The bag dimensions were initially 2 x 2.5 x 0.5 m which resulted in a fill weight of approximately 4 tons. These dimensions were based on a geotextile container of 2.6 x 1.9 x 0.58 m used in Australia [Hornsey *et al.*, 2011]. After the emergency production of bags had subsided Kaytech refined their manufac-

Figure 9.7: Filling of Geotextile Sand Bags with frame (April 2007)

ture and optimised the bag size to 2.1 x 1.8 x 0.55 m. The bags consist of a double layer, an inner geotextile and an outer UV stabilised staple filament polypropylene. The two fabrics are bonded together and stitched into a bag. The bag contains two chutes that can be extended from the bag creating a conduit to convey sand into the bag. Since the pioneering of the first bags numerous manufactures have entered the market.

The filling of the bags required a steel frame (Fig. 9.7). The manufacture of this frame should be governed by the geometry and layout of the bag. This proved to be an issue as new bag manufacturers entered the market and the manufacture of the bag evolved. When the bag's chute diameter varied the frame's funnel diameter remained constant, this necessitated the removal of some stitching to allow installation of the bag into the frame. This is problematic as the stitching has a tendency to run, potentially causing the bag to pull open.

The stitching of the bags is done in the factory by sewing machines and the seam has 80 % of the bag material strength. The chutes however have to be sealed onsite and this is done by hand stitching with nylon string. This stitch is therefore the weakest part of the bag and has been mitigated by placing the bags with the hand stitched portion facing landwards. Supervision and quality control of the hand stitching is essential as labour have a tendency to fluctuate quality which may lead to the leaking of sand. A manufacturing technique which has proved to successfully increase quality is the pre punching of holes. This means the spacing of hand stitches is predefined and so ensures more consistency with regards to the quality of stitch. All that still has to be ensured is that the nylon is knotted correctly. A handheld sewing machine was initially used to stitch the bags but was abandoned during the emergency work following associated installation delays. The reintroduction of the sewing machine has not been supported due to cost implications as well as there being no present evidence of the adverse effects of hand stitching. It is the authors' opinion that the bags should be sewed similarly to the factory stitching.

9.7.2 Installation

The bags are filled to 80 % of their capacity (based on the German construction technique [Oumeraci *et al.*, 2003] ensuring that the sand is sufficiently compacted by flooding with water. If the bags are filled any more it becomes difficult to stitch them closed, jeopardising the quality of the stitch. Overfilling the bags also causes rounding. Since some of the bag's stability is determined by its mass and friction, it was hypothesised that the more rounded it is the less contact each bag will have with the surrounding bags, lowering the stability. Not filling the bags to capacity allows them to be levelled for the next bag layer as well as providing a large contact area. It must be noted that Hornsey *et al.* [2011] findings contradict this theory showing that the Australian practice of filling bags to capacity is more stable.

In certain circumstances there may be uncertainty as to where the lowest scour level is or additional confidence is required in minimising the undermining risk. This was accommodated by providing a Dutch toe (self-healing toe). A Dutch

toe is a row of bags in front of the wall's toe and tied back into the bottom bags. The theory is that as the beach profile approaches the founding level of the bag wall the Dutch toe will settle giving the structure an additional 2 m (length of one bag) scour resistance.

9.7.3 Slope

The slope of the bag protected dune is still debated, with engineers designing slopes from 30 to 45 degrees. The stability of the bag wall is dependent on the friction forces developed between the bags which is a function of their roughness, the net normal force (weight above the contact area) and the contact area. Recio & Oumeraci [2008] identified, from flume tests, that the friction between containers affects the hydraulic stability much more than assumed in past and present literature. In order for the bags to be stable this frictional force must be equal to or greater than the active soil force behind the bags Fig. 9.8. So although the friction increases as the bag wall approaches the vertical so does the active soil pressure. A balance of these two forces was used to calculate an optimum bag slope. Figure 9.9 shows a plot of how many bags will be stable out of the 20 bags retaining 10 m of soil, through a range of slopes. The calculation includes a safety factor used on the soil properties as advised by Henkel [1981]. For comparativeness, results shown ignore cohesion, place the water table below the bag wall, and use a constant soil weight of 18 kN/m^3 and a friction angle of 30 degrees. Active pressures were calculated using Coulomb's active earth pressure coefficient. The bag dimensions and weight are as previously stated.

Figure 9.9 illustrates that the angle range of 18 – 26 degrees can retain the most soil. The flatter the slope of the wall the less the wave loading but the greater the wave run-up. This simply calculation does not consider the hydraulic stability of the bags and because the sand is displaced to the bags front face by the lifting and dropping of the exposed portion it is thought that the less bag length that can be lifted the more stable the bags. It is felt that the increased restriction of this movement is what makes the bags more stable at steeper slopes [Hornsey *et al.*, 2011] and not the increased friction.

The bags are prone to vandalism and degradation by ultraviolet radiation.

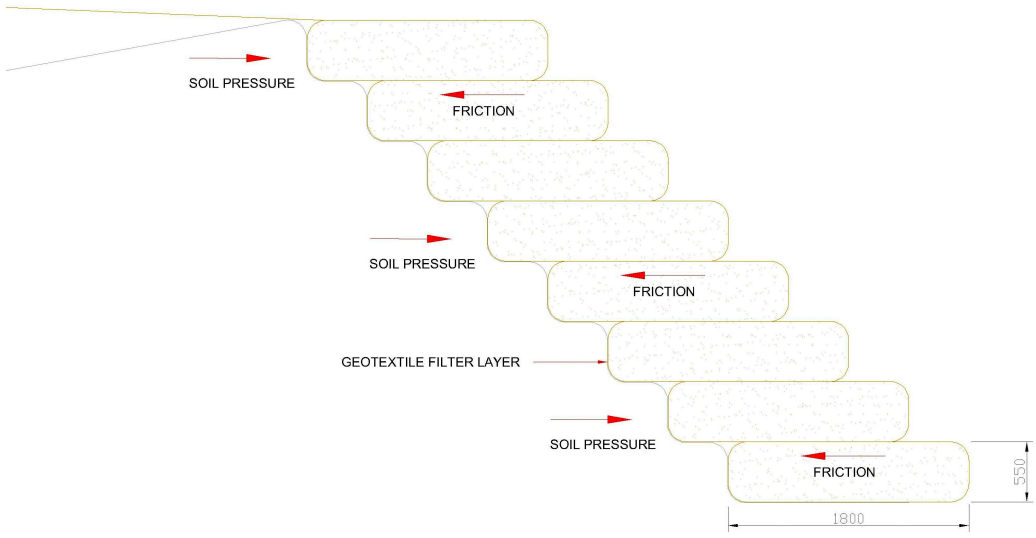

Figure 9.8: A typical section through a geotextile sand bag wall illustrating the soil pressure and bag friction

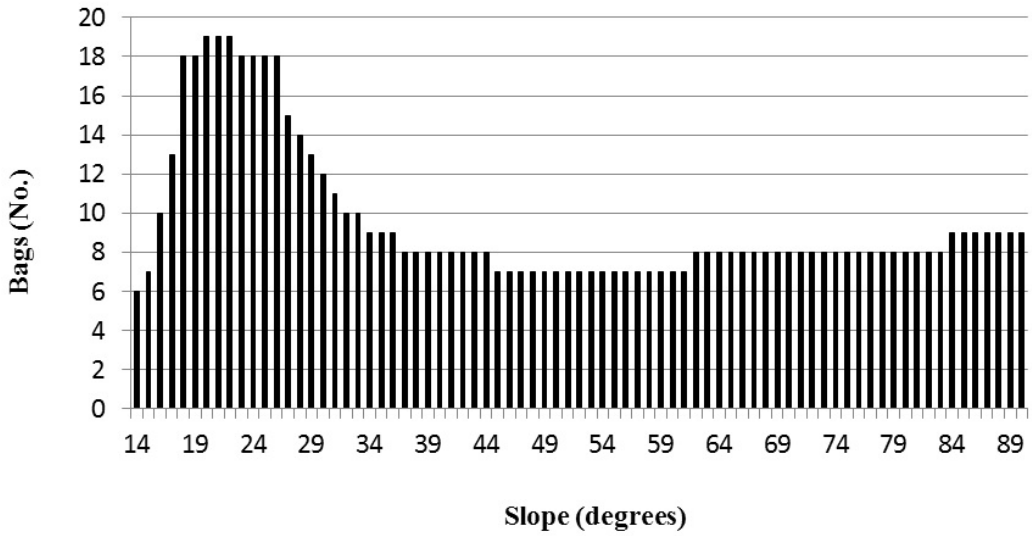

Figure 9.9: The number of stable retaining bags per wall inclination

They also look untidy once people have traversed them and have been subject to wave action. The bags should therefore be covered with sand and vegetated. Since beach sand generally cannot maintain a slope greater than 30 degrees it also dictates that the bags should follow a similar slope. The ground conditions, space restrictions and retained height all influence the bag wall slope and thus a standard orientation cannot be specified and each situation should be considered independently.

9.7.4 Geotextile sand bag performance

The bags endured their first substantial test on the 26 July 2011 from a significant wave height of 5 m and all the issues identified in the literature were realised. Vandalised bags leaked sand and created weak spots in the walls. The lower layers of bags shifted forward making the lower wall face steeper. This appears to be the combination of three factors: the bags not being filled sufficiently, the bags leaking sand and the bags' geotextile elongating. All these factors enable the sand to move to the bag's exposed face lowering the friction forces and increasing the drag forces. In an extreme case a bag was completely removed from the lower portion of a wall (Fig. 9.10). We propose that our local bags need some refinement in terms of elongation and that stringent quality controls are required during installation. The significance of bag deformation is perhaps more evidence that the Australian method of filling the bags to capacity and using a 45° slope is more appropriate.

9.8 Geotextile tube

Geotextile tubes have been used all over the world and have been particularly successful in the construction of artificial reefs. The geotextile tube was experimented with as it was potentially faster, cheaper and more structurally sound than using geotextile sand bags. The theory was that the 1.4 m diameter by 25 m tube could be laid in position and then pumped full of sand (Fig. 9.11). This however was not as simple in practice.

Pumping slurry into the tube caused air to be trapped in the tube which had

Figure 9.10: A geotextile bag wall failure at Isipingo (July 2011). The red rectangle highlights where a bag was removed from the wall and the red circle identifies the removed bag.

limited venting points. The slurry was also pumped at a ratio of about 30 % sand to 70 % water. The geotextile drained slowly causing the tube to fill with water and air faster than it could expel them, resulting in the slurry discharge pipe being forced out the tube inlet. This issue was overcome by having scuba divers inside the tube directing the pump discharge. The tube also had to be braced every 5 m.

The tube was successfully installed and has been in place for almost 4 years without any issues. Structurally the tube is more stable than individual bags as it is continuous, weighs more and only has one piece of hand stitching. The tube has the added advantage of being able to be placed and filled in the water. With all the tube's complication's it ended up costing twice as much as installing the geotextile sand bags. Although it was discontinued due to its difficult installation and associated costs their use has been successful in other applications [Alvarez *et al.*, 2007; Cantr *et al.*, 2002; Shin & Oh, 2007]. We propose that similar success is possible if more appropriate equipment is used.

Figure 9.11: Geotextile tube installation at Amanzimtoti (April 2008)

9.9 Geotextile wrap

The geotextile wrap was used as an alternative to the geotextile sand bags where access was limited and have proved to be a reliable alternative [Yasuhara & Recio-Molina , 2007]. A 5.3 m by 25 m geotextile fabric was used to create an insitu sand bag or tube. The geotextile is laid flat, half is topped with sand and the other half is then folded over and stitched on the landward side. This method allows all the work to be done by hand. If the wrap will not be exposed (always be covered by sand or by geotextile bags) bidim may be used. If the bidim will be exposed to sunlight and wave action it should be replaced with 1200 g/m^2 ultraviolet (UV) treated geocontainer fabric as the bidim is not UV protected and pulls apart under wave attack. The long continuous hand stitching is the wrap's main weakness but also makes the installation cost effective and has become increasingly popular

amongst private home owners along the KwaZulu-Natal coast.

9.10 Conclusion

Durban has had a long history of beach protection and some of its recent experiences have been shared in this review. From these experiences it is recommended that soft solutions, primarily as a combination of coastal setback lines, beach nourishment and GSCs be prioritised. Admittedly soft solutions are not always practical or appropriate.

Durban's groyne field has been a valuable investment aiding in successfully stabilising the central beaches since their construction. Experience has shown that concrete cover should be seriously considered as corrosion mitigation even when providing galvanised reinforcing. It is recommended that all structures, including seawalls and GSCs, are founded on rock or at a depth that ensures structural stability when the lowest historical scour level is exceeded.

Beach nourishment and geotextile sand bag seawalls are the eThekwini Municipality's preferred soft protection to be implemented in conjunction with coastal setback lines. A successful beach nourishment project can be executed by substantial preliminary research of the borrow site as well as good project management. For a geotextile sand bag defence it is recommended that the bags are filled to capacity and installed at a slope of 45 degrees, covered in sand and vegetated. Although geotextile wraps have proven their reliability as coastal protection [Yasuhara & Recio-Molina , 2007] the Municipality's experiences have only found them to be an appropriate substitute for the bags in severely restricted areas. In areas of high vulnerability it is recommended that a bidim wrap be installed and draped with bidim prior to overlaying it with one or two layers of geotextile sand bags. The bidim wrap acts as a second defence against extreme events as well as a substantial filter layer, which has proven to be significant. A Dutch toe should also be installed as additional risk mitigation of undermining. The bags elongation at breaking point still needs to be refined and parity has to be achieved on the filling percentage of the bags' capacity.

Many situations require more robust solutions than geotextile sand bags or beach nourishment. Such situations need to be individually accessed but rock

revetments and sheet piled seawalls have been successfully installed in Durban.

A good monitoring system is essential for successful coastal management. The beach profiles recorded in Durban since 1973 have been instrumental in the design of all its coastal defences from seawalls to beach nourishment. To the authors' best knowledge the record is the most extensive in South Africa and is the core of the eThekwini Municipality's coastal management and defences.

The March 2007 event gave the eThekwini Municipality the opportunity to be innovative. It is hoped that other organisations will be able to convert the failures into successes and use the stories of success to improve the sustainability of defending our coast.

References

Allan, J. C., Komar, P. D., 2002. "A dynamic revetment and artificial dune for shore protection". In: Proceedings, The 28th International Coastal Engineering Conference, Cardiff, Vol. 2, 2044 – 2056. 33, 259, 276

Alvarez, I. E., Rubio, R., Ricalde, H., 2007. "Beach restoration with geotextile tubes as submerged breakwaters in Yucatan, Mexico". Geotextiles and Geomembranes Vol. 25, 233 – 241. 34, 266, 296

Airoldi, L., Abbiati, M., Beck, M. W., Hawkins, S. J., Jonsson, P. R., Martin, D., Moschella, P. S., Sundelf, A., Thompson, R. C., & berg, P., 2005. "An ecological perspective on the deployment and design of low-crested and other hard coastal defence structures". Coastal Engineering Vol. 52, 1073 – 1087. 246, 275

Belkessa, R., Houma, F., Ciortan, R., Mezouar K.: "Protection works of the sea coast in Algeria". Seventh International Conference of Coastal and Port Engineering in Developing Countries, COPEDEC VII, 196, 11. Dubai 2008. 32, 253

Breetze, T., Parak, O., Celliers, L., Mather, A., & Colenbrander, D. R. (eds.), 2008. "Living with coastal erosion in KwaZulu-Natal: a short-term, best practice guide". KwaZulu-Natal Department of Agriculture and Environmental Affairs, Cedara, Pietermaritzburg. 250

Barnett, K. A., 1999. "The Management of Durban's Beaches: An Historical Perspective". In: Proceedings, Fifth International Conference of Coastal and

Port Engineering in Developing Countries, COPEDEC V, 1999, Cape Town. 87, 249, 277

Cantr, S., 2002. "Geotextile tubes - analytical design aspects". Geotextiles and Geomembranes Vol. 20, 305 – 319. 34, 266

CSIR, 1976. "Status quo of the Durban Beach protection investigation". Report No. C/SEA 7607, Stellenbosch. 247, 277

Dette, H. H., Raudkivi, A. J., 2002. "Beach and storm-tide protection on the coast of the Baltic Sea". In: Proceedings, 28th International Coastal Engineering Conference, Cardiff, Vol. 3, 3298 – 3307. 16, 32, 253

Durgappa, R., 2008. "Coastal protection works". In: Proceedings, Seventh International Conference of Coastal and Port Engineering in Developing Countries, COPEDEC VII, 2008, Dubai. 85, 246, 275

French, P. W., 2001. "Coastal Defences: processes, problems and solutions". Routledge, New York. 247, 257, 275

Gilbert, J., Vellinga, P., 1990. "Strategies for Adaption to Sea Level Rise", Report of the Coastal Zone Management Subgroup, Intergovernmental Panel on Climate Change, World Meteorological Organization and U.N. Environmental Programme. The Netherlands. 246

Hamm, L., Capobianco, M., Dette, H. H., Lechuga, A., Spanhoff, R., Stive, M. J. F., 2002. "A summary of European experience with shore nourishment". Coastal Engineering Vol. 47, 237 – 264. 32, 253

Hanson, H., Brampton, A., Capobianco, M., Dette, H. H., Hamm, L., Laustrup, C., Lechuga, A., Spanhoff, R., 2002. "Beach nourishment projects, practices, and objectives - a European overview. Coastal Engineering". Vol. 47: 81 – 111. 32, 253

Heerten, G., Klompmaker, J., Partridge, A., 2008. "Design and construction of waterfront structures with special designed non-woven geotextiles". In: Proceedings, Seventh International Conference of Coastal and Port Engineering in Developing Countries, COPEDEC VII, Dubai. 33, 259, 276

Henkel, D. J., 1981. "The design of sheet pile walls". Geotechnics Seminar, session No.7, Sheet pile walls. 263, 294

Hornsey, W. P., Carley, J. T., Coghlan, I.R., Cox, R. J., 2011. "Geotextile sand container shoreline protection systems: Design and application". Geotextiles and Geomembranes, Vol. 29(4), 425 – 439. 33, 260, 262, 263, 274, 276, 282, 283, 286, 287, 290, 291, 292, 294, 296, 299, 300

Kinmont, A., 1954. "Beach Erosion and Protection". In: Proceedings, The Institute of Municipal Engineers, Thirty third annual conference, Durban. 114, 247, 252, 277

Mather, A. A., Kasserchun, R., Wenlock, H., 2003. "City of Durban Sand Bypass Scheme: 20 year performance evaluation". In: Proceedings, Sixth International Conference of Coastal and Port Engineering in Developing Countries, COPEDEC VI, Colombo, Sri Lanka. 249, 277

Mather, A. A., 2008. "Sea Level Rise for the East Coast of Southern Africa". In: Proceedings, Seventh International Conference of Coastal and Port Engineering in Developing Countries, COPEDEC VII, Dubai, UAE. 11, 14, 114, 186, 275

Moschella , P. S., Abbiati, M., berg, P., Airoldi, L., Anderson, J. M., Bacchiocchi, F., Bulleri, F., Dinesen, G. E., Frost , M., Gacia, E., Granhag, L., Jonsson, P. R., Satta, M. P., Sundelf, A., Thompson, R. C., Hawkins, S. J., 2005. "Low-crested coastal defence structures as artificial habitats for marine life: Using ecological criteria in design". Coastal Engineering, Vol. 52, 1053 – 1071. 246, 275

Oumeraci, H., Hinze, M., Bleck, M., dan Kortenhaus, A., 2003. "Sand-Filled geotextile containers for Shore protection". In: Proceedings, COPEDEC VI, Colombo, Sri Lanka. 33, 262, 291

Phelps, D., Rossouw, M., Mather, A. A., & Vella, G. F., 2009. "Storm damage and rehabilitation of coastal structures on the East coast of South Africa". In: Proceedings, Institute of Civil Engineers Conference, Edinburgh, Scotland. 51, 250, 277

Recio, J., Oumeraci, H. 2008. “Hydraulic Stability of Geotextile Sand Containers for Coastal Structures: Process Oriented Studies Towards New Stability Formulae”. In: Proceedings, Seventh International Conference of Coastal and Port Engineering in Developing Countries, COPEDEC VII, Dubai. 33, 259, 263, 279, 294, 297

Restall, S. J., Jackson, L. A., Heerten, G., Hornsey, W. P., 2002. “Case studies showing the growth and development of geotextile sand containers: an Australian perspective”. Geotextiles and Geomembranes. Vol. 20(5), 321 – 342. 33, 260, 276, 277, 296

Saathoff, F., Oumeraci, H., Restall, S., 2007. “Australian and German experiences on the use of geotextile containers”. Geotextiles and Geomembranes, Vol. 25 (4-5), 251 – 263. 32, 33, 34, 258, 260, 275, 277, 285, 286, 287, 288, 289

SANS 10100-2:1992. 1992. Code of practice for the structural use of concrete. Part 2: Materials and execution of work, Pretoria: South African Bureau of Standards.

Shin, E. C., Oh, Y. I., 2007. “Coastal erosion prevention by geotextile tube technology”. Geotextiles and Geomembranes, Vol. 25, 264 – 277. 34, 266, 296

Udo, K., Takewaka, S. & Nishimura, H., 2002. “Long-term morphological change of backshore dunes”. In: Proceedings, The 28th International Coastal Engineering Conference, Cardiff. 260, 285

Yasuhara, K., Recio-Molina, J., 2007. “Geosynthetic-wrap around revetments for shore protection”. Geotextiles and Geomembranes, Vol. 25, 221 – 232. 34, 267, 268

Yeomans, S. R., 2004. “Galvanized steel reinforcement in concrete”. Elsevier, Oxford. 252

Zanuttigh, B., Martinelli, L., Lamberti, A., Moschella, P., Hawkins, S., Marzetti, S., Ceccherelli, V. U., 2005. “Environmental design of coastal defence in Lido di Dante, Italy”. Coastal Engineering, Vol. 52 1089 – 1125. 246, 275

Chapter 10

Geotextile sand filled containers as coastal defence: South African experience

This chapter is based on a paper published in Geotextiles and Geomembranes, 35, 120 – 130, 2012.

Abstract

Geotextile sand filled containers (GSC) have rapidly become the preferred coastal defence on the east coast of South Africa. Their growth can be attributed to political, social and environmental factors. This paper details South African experiences and the observed performance of GSCs. The main failure mechanism of geotextile sand bag seawalls is identified to be the movement of sand within the bags. This movement is observed to be a result of insufficient filling, bag elongation and sand leaking. Through a review of local and international manufacturing and construction techniques we identify methods of reducing the internal movements of sediment. The observed performance of local bags provide a practical full scale validation of the physical model findings of Hornsey *et al.* [2011]; Recio

& Oumeraci [2007].

10.1 Introduction

Sandy beaches make up approximately 20 % of the world's coastline and Durgappa [2008] claimed that of these more than 60 % have been eroding in recent decades. Erosion is likely to intensify with predicted trends in sea level rise, storm frequency and storm intensity [Komar & Allan, 2008; Mather, 2008]. The erosion trends, combined with the estimate that over 60 % of the global population lives within the coastal zone [EEA, 1999], will necessitate more widespread use of coastal defence systems. An increasing awareness of anthropogenic impacts on the environment has driven demands for "soft" defences to replace "hard" defences such as groynes and seawalls. The development of geotextile sand-filled containers (GSCs) has been pursued as such a replacement.

The use of GSCs was initiated in the USA, Netherlands and Germany more than 50 years ago [Saathoff *et al.*, 2007]. Durgappa [2008] did not include GSCs as a soft solution, although they are often placed into this category. Defining GSCs as a soft solution is not strictly correct because a soft solution is one that does not impede the natural morpho-dynamics of the shoreline. The GSCs prevent erosion and so can develop a static shoreline. However they can be considered to be a "pseudo-soft" solution since, in certain applications, they can be removed relatively easily if an unforeseen environmental impact ensues, and do not require the mining of rock.

The authors believe the increasing popularity of GSCs in South Africa has been driven by (1) social, (2) political and (3) environmental factors. Coastal residents often perceive a physical barrier between the land and the sea as a more desirable defence [French *et al.*, 2001] than soft mitigations such as beach nourishment. A seawall is also preferred from a political perspective as it serves as a reminder and measure of a political contribution. The potential for seawalls to develop static shorelines and accentuate erosion makes them environmentally unacceptable. Environmental and sustainability considerations are becoming the governing factors when implementing coastal defence (e.g. Airoldi *et al.* [2005]; Moschella *et al.* [2005]; Zanuttigh *et al.* [2005]). The GSCs provide a middle

ground that is appealing to both politicians and residents while being environmentally acceptable.

Allan & Komar [2002] discussed the effectiveness of an artificial dune for shore protection. They monitored a dune constructed with sand-filled geotextile bags and covered by vegetated loose sand. The dune was reported to have survived fairly extreme conditions which included overtopping. The 3-year monitoring period was too short to confirm the dune's survival under extreme conditions.

Heerten *et al.* [2008] reported extensive research into the effectiveness of GSCs for mitigating coastal erosion. They described the successful use of GSCs on the island Sylt in Germany where geotextile cushions were covered with sand and sand trap fences. Although the GSCs were exposed after a large storm they prevented the high tide levels (2.5 m above normal) and large waves (exceeding 5 m) from eroding the dune.

Hornsey *et al.* [2011] and Restall *et al.* [2002] described the successes of GSC revetments at Stockton and Maroochydore beaches in Australia where they have been in place since 1996 and 2001 respectively.

The implementation, successes, and failures of GSCs are well documented in Europe and Australasia but this relatively new technology has only recently found application in South Africa. This paper aims to contribute to this body of knowledge by describing the use of GSCs from a South African perspective. To the authors' best knowledge this paper is the first to document the successes and failures of GSCs in South Africa. We start by describing the case study area and it's local wave conditions. The observed performance of local non-woven GSCs are reported and attempts made to link the observations to local manufacturing and construction methods. South African practice is then compared to international practice, followed by conclusions and recommendations for future research and development.

10.2 Case Study: Durban, South Africa

Large GSCs as coastal defences were first installed in South Africa in 2003. The geotextile bags were used to construct two groynes at Langebaan [McClarty *et al.*, 2006]. Since then the use of large GSCs for coastal defence in South Africa has

been dominated by Durban. Durban is an important port city located on the east coast of South Africa (Fig. 10.1). Durban's history of beach protection is linked to the development of the port since the beaches were stable for a period of almost 100 years prior to the commencement of harbour works [CSIR, 1976; Kinmont *et al.*, 1954]. The city implemented beach nourishment, constructed an underwater mound and a unsuccessful groyne field [Barnett *et al.*, 1999] before successfully stabilising the beaches with a new groyne field and a permanent sand bypass scheme [Mather *et al.*, 2003]. Durban has also implemented various seawalls and therefore has a range of experience in coastal defence systems.

Durban's coastal defence issues received renewed attention after an extreme storm event devastated the KwaZulu-Natal coastline in March 2007. A wave recording buoy, in 22 m of water, measured a significant wave height of 8.5 m and a peak wave period of 16.6 seconds. The wave height was the largest ever recorded and the combination of an equinox tide level and peak storm wave setup resulted in a water level almost 2.7 m above chart datum or about 1.7 m above mean sea level [Phelp *et al.*, 2009]. The long-term average significant wave height along the east coast of South Africa is 1.65 m with a peak period of 10 seconds and an average wave direction from the south east. Based on the documented success of GSCs in Australia [Restall *et al.*, 2002; Saathoff *et al.*, 2007] and the successful installation at Langebaan [McClarty *et al.*, 2006], the local government authority (eThekwini Municipality) decided to pursue GSC installations as an emergency and permanent measure. The use of GSCs became the eThekwini Municipality's favoured form of sea defence after the 2007 event and over 20 000 units have been installed in seawalls along a 100 km long section of coastline.

10.2.1 Performance of geotextile sand bag seawalls

The bags endured their first substantial test on the 26 July 2011 from a significant wave height of 5 m (measured by a wave recording buoy in a water depth of 18 m). The event highlighted numerous short comings in the bag manufacture and installation. Although there was damage to some seawalls none of them failed and considering the total failure of certain loffelstein seawalls (Fig. 10.2 and 10.3) the bags performed relatively well. A bag seawall near the failed loffelstein seawall

Figure 10.1: A map of South Africa showing KwaZulu-Natal and Durban and a map of the eThekwini Municipality showing the relevant locations

is shown in Fig. 10.4. During the event the slope of the bag seawalls steepened near the toe and flattened near the crest and in an extreme case a bag was completely removed from the lower portion of a seawall (Fig. 10.5). It appears that the lower bags were being pulled out of the seawall in a similar manner to that described by Recio & Oumeraci [2007, 2008]. Basically the sand within the bags is moved to the exposed face under wave action. This movement decreases the contact area between bags thus reducing the friction forces and increasing the surface area in the front of the bag making it more susceptible to drag forces. The sand movement also means that the bags above no longer have sufficient support underneath them and so the bag seawall settles and moves forward. The bag seawall in Umhlanga Rocks (Fig. 10.1) settled about 0.5 m and moved forward about 0.3 m. The vertical settlement of the wall was almost 10 % of the wall height. This movement is shown in Fig. 10.4 and illustrated in Fig. 10.6. The bags were never intended to take full wave loading but rather wave run-up. As indicated in Fig. 10.6 the bags did not experience direct wave impacts but run-up of approximately 4 m MSL. The up-rush and down-rush of the water moved the bag's internal sediment and displaced the bags seawards. These observations have essentially provided a full scale validation of the deformation effects analysed by Recio & Oumeraci [2007]. The movement of sand within the bags has been identified to be the main cause of failure and is attributed to the bags not being filled sufficiently, the geotextile elongating, and the leaking of sand.

The remainder of this paper identifies why this failure mechanism occurs and proposes ways of avoiding it. The specification of the GSCs as a sea defence has recently been revised for the Durban Central Beachfront Upgrade. The new specification (Table 10.2) is in part intended to minimize the failures described here.

10.3 Manufacture

GSC's are unlike the usual applications of geotextiles as they are required to function for a considerably longer design life under exposure to the elements. This significant difference has to be accounted for in their manufacture.

Kaytech Engineered Fabrics were initially contracted to be a specialist con-

(a) (b)

Figure 10.2: (a) Waves breaking on a loffelstein seawall in Umhlanga (03/07/2011) and (b) the subsequent failure of the loffelstein seawall (02/08/2011)

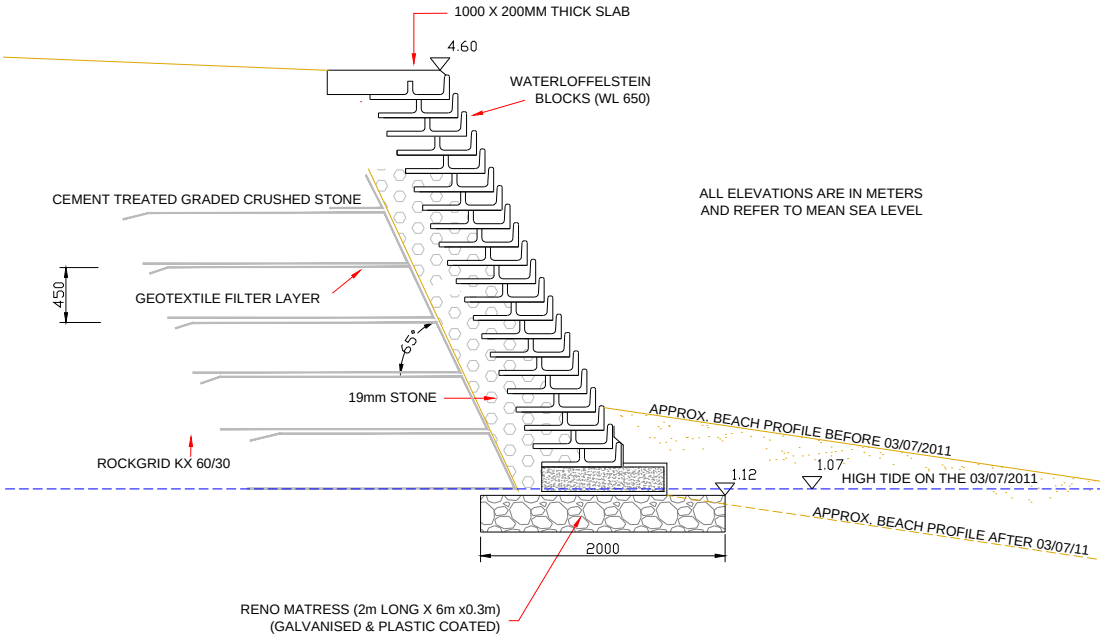

Figure 10.3: A cross-section of the loffelstein wall that failed at Umhlanga Rocks.

(a) (b)

Figure 10.4: A bag seawall in Umhlanga Rocks (29/08/2011) showing (a) the movement of the seawall relative to its original position and (b) the steepening of the seawall toe and the flattening of the seawall crest

Figure 10.5: A geotextile bag seawall failure at Isipingo (July 2011). The red rectangle highlights where a bag was removed from the seawall and the red circle identifies the removed bag

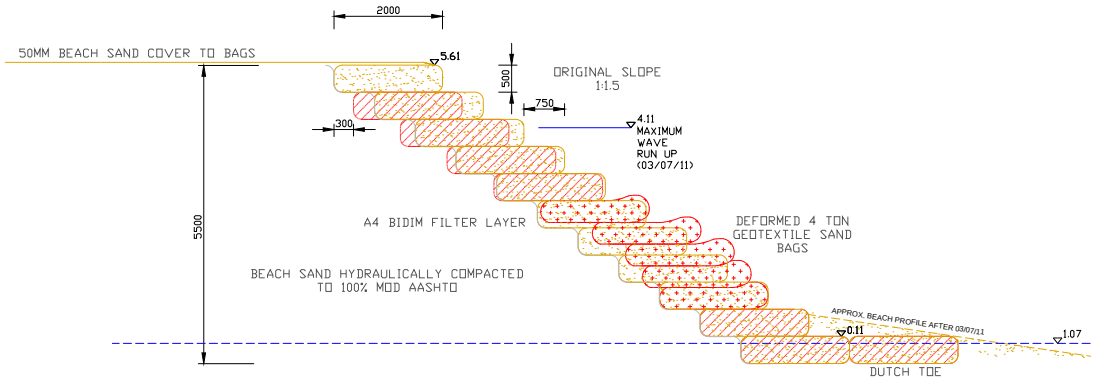

Figure 10.6: A cross-section of the geotextile bag seawall at Umhlanga Rocks. The red bags show the location of the bags after the 26/07/2011.

sultant and manufacturer of the GSCs. The filled bag dimensions were initially $2.5 \times 2 \times 0.5$ m which resulted in a fill weight of approximately 4 tons. These dimensions were based on a filled geotextile container of $2.6 \times 1.9 \times 0.58$ m used in Australia [Hornsey *et al.*, 2011]. After the emergency production of bags had subsided Kaytech refined their manufacture and optimised the bag size to $2.1 \times 1.8 \times 0.55$ m. The slight change in dimensions was to optimise the component geotextiles as they come off the production line. The optimisation was essentially to mobilise the stronger cross direction strength of the bag's outer staple fibre component. The bags consist of a double layer - an inner polyester and an outer ultraviolet (UV) stabilised staple filament polypropylene. The two fabrics are bonded together and stitched into a bag. The bag contains two chutes that can be extended to create a conduit for conveying sand into the bag.

The lifetime of a geotextile is difficult to determine and estimates are based on limited case studies. In an attempt to estimate their lifetime, three of the bags were tested, each from a different location. Table 10.1 shows the exhumed bag locations, approximate installation date and the corresponding test results. All the bags came from seawalls with 30 – 35 degree slopes. The bag wall at Vetch's Beach was approximately 3 m high, the Umdloti seawall was approximately 4 m high and the Umhlanga seawall was only 1.5 m high. The oldest bag was 4 years old and was exhumed from Vetch's Beach. This bag had periodic UV exposure and was estimated to be overtopped by the sea on at least three

occasions. The Vetch's bag lost the most tensile strength of the three exhumed bags – approximately 10 % of its strength in the cross direction and none in the machine direction. It also lost 5 % of its seam strength. The newest bag was from Umhlanga Rocks and was installed for approximately 2.5 years. These bags were used as a cofferdam during the reconstruction of a loffelstein seawall and so sustained wave impacts and UV exposure for approximately 2 months. Since then these bags have been completely covered with sand. The bag only lost 4 % of its tensile strength in the machine direction. All the bags exceeded the specified elongation of 50 % (Table 10.1). The fact that many of the bag properties exceeded the original specification (Table 10.1 & 10.2) may be evidence of the variability in the manufacturing process although it has been proposed that the ingress of sand into the fabric may affect the geotextile properties. Oberhagemann & Hossain [2011] reviewed existing literature of geotextiles used in hydraulic, coastal and landfill applications and noted that their life expectancies ranged from 35 to 110 years, although some geotextiles protected from weather and sunlight have reportedly survived for several centuries. Based on local observations of geotextile sand bags the authors agree with Oberhagemann & Hossain [2011] that an appropriate lifetime estimate of a geotextile bag is 30 years, provided that UV exposure is seasonal and/or the wall consists of multiple geotextile bag layers to limit the weather exposure.

The new bags comprise multi-component geotextiles as apposed to the preceding bi-component geotextiles.

10.3.1 Durability

A bag is only contributing to the stability of a seawall if it is full of sand. The leaking of sand is therefore a risk to the structural and hydraulic stability of the seawall. Although minor loss of sediment may occur through the geotextile [Muthukumaran & Ilamparuthi, 2006] the major losses occur from damaged geotextiles. Hornsey *et al.* [2011] categorized potential damage to the GSC as either incidental or due to vandalism. Applications in South Africa have been restricted to situations that minimize or eliminate incidental damage such as that from from boats or vehicles. The main concern regarding GSC damage is that

Table 10.1: The test results of three exhumed bags from Vetch's Beach, Umdloti and Umhlanga (refer Fig. 10.1).

Properties	**Original specs**	**Vetch's Beach** (2008 – 2011)	**Umdloti** (2009 – 2011)	**Umhlanga Rocks** (mid 2009 – 2011)	**Test method**
Mass (g/m^2)	2100	2429	2534	4542	AS 3706.1
Thickness (mm)	12	12.6	12.1	13.7	AS 3706.1
MD Tensile strength (KN/m)	50	55.5	51.0	47.6	AS 3706.2
XD Tensile strength (KN/m)	95	85.3	105.6	105.7	AS 3706.2
Penetration CBR (N)	12000	13878	12780	12885	AS 3706.4
Elongation (%)	50	67.5	69	55.6	AS 3706.4
Seam strength (KN/m)	40	38.1	49.0	65.8	ASTM D4884.09

NOTES: MD = machine direction; XD = cross direction

(a) (b)

Figure 10.7: Geotextile sand bags that have been (a) cut and (b) burnt

due to vandalism and is well documented. An observation that has not been well documented is biological damage to GSCs. For an extended discussion regarding the durability of GSCs as coastal protection the reader is referred to Oumeraci & Recio [2010].

10.3.1.1 Vandalism

Geotextiles can be cut with a knife. This issue has been combatted by a composite vandal-deterrent geotextile which traps 3 kg of sand per square meter within the geotextile. Although this significantly increases the resilience and durability of the container [Saathoff *et al.*, 2007] it has little effect on the penetration of a knife (Fig. 10.7a). GSCs have also been burnt by vandals (Fig. 10.7b). GSCs used to protect dunes should always be covered with sand and vegetated to protect them from vandals and to restore a natural appearance to the coastline. Vegetation also has the advantage of mitigating blown sediment and stabilising backshore morphology [Udo *et al.*, 2002].

10.3.1.2 Biological damage

Encouraging vegetation cover in order to mitigate vandalism is important but sufficient depth of growing medium must be provided as dune vegetation can otherwise root into the GSC (Fig. 10.4). This is an issue if the GSCs are intended as a sleeping defence because storm surges may cause the vegetation to be stripped

from the GSCs thus creating sand leaks.

Rats have also been observed nesting between installed bags. There is no visible evidence that the rats have gnawed into the containers but it is plausible. The existence of rats is thought to be a result of adjacent restaurants and vagrants that often take shelter in coastal structures such as piers. The risk of encountering both rodents and vandals in such locations should be carefully considered when installing GSCs.

10.3.2 UV Resistance

South African UV radiation is of order 180 kilo-Langleys making UV degradation of GSCs a major concern. South African bags have been subjected to the Australian UV resistance testing standard, AS 3706.11, which is based on the American standard, ASTM D4355. The UV stabilised geotextile experiences less than 20 % change in ultimate tensile strength after being exposed to a Xenon arc-type apparatus for 672 hours. Saathoff *et al.* [2007] claimed that this is equivalent to a minimum design life of 10 years, while TenCate [2010] found that 500 hours of Xenon arc testing equates to roughly 0.5 to 2 years of field exposure. The correlation between UV laboratory testing and field exposure is unclear and design life estimates are still restricted to limited case studies. In this regard Hornsey *et al.* [2011] found that the GSCs in the Maroochydore beach groynes had lost less than 15 % of their tensile strength after 6 – 8 years. Although long-term testing is defined as exposure greater than 500 hours Hornsey *et al.* [2011] recommends testing to a minimum of 2000 hours. This uncertainty in UV resistance has been combatted by covering the bags in sand while all new bags will be required to retain a minimum of 90 % of their geo-composite tensile strength after 2000 hours as per ASTM D4355. In 2008 Kaytech commissioned Roediger Agencies, an analytical laboratory at the University of Stellenbosch, to analyse a recovered sample from Langebaan. The sample at the time was over four years old and its degradation was assumed to be from UV radiation. From the analysis it was concluded that the degradation was mechanical de-lamination of the outer fibre rather than UV light degradation. While the analysis provided some confidence in the bags' UV resistance it ultimately highlighted a manufacturing

Figure 10.8: Delamination of a sample geotextile composite

weakness. This motivated the thermal fusing of the outer fibres to the inside of the inner layer in the new multi-component bags (Sect. 10.6).

10.3.3 Abrasion and delamination resistance

The German rotating drum test method [BAW, 1994] is often considered the best representation of the near-shore surf abrasion environment [Hornsey *et al.*, 2011; Saathoff *et al.*, 2007]. The test uses 10 mm and 4 mm gravel with water to form an abrasive slurry which is used to abrade the fabric. A minimum of 75 % tensile strength retention is recommended [Saathoff *et al.*, 2007]. The rotating drum test has only recently been adopted locally while the American ASTM D4886 abrasion test has been used in the past. The latter uses 300 grit sandpaper as an abrading medium and is well suited for thin fabrics. The local bags have a 95 % tensile strength retention following this test. Since the relationship between the two test methods is unknown all new bags are required to retain 85 % of their tensile strength after 80 000 drum revolutions as described by the German rotating drum test.

The tensile strength of the composite geotextile is determined by the inner polyester. The performance of the material is therefore determined by the extent that the two materials act as one. De-lamination is a concern since if the outer layer is not correctly fused to the inner it can be easily removed exposing the unprotected inner fabric to UV attack. The peel resistance is tested in accordance with ASTM 6496-04a and is not less than 1.9 kN. Figure 10.8 shows the de-lamination of a composite geotextile sample.

10.3.4 Elongation

A high ultimate elongation of the bag geotextile is thought to reduce installation damage and allow flexibility in the structure [Saathoff *et al.*, 1994]. This high elongation allows the bags to mould themselves and to be self-healing during settlements or when bags are removed from a seawall (Fig. 10.4 and Fig. 10.5). Saathoff *et al.* [2007] recommend an ultimate elongation of greater than 50 %. Recent observations have shown the advantages of high elongation but have also highlighted potential disadvantages. As previously noted the only observed failure mechanism was produced by internal sand movement (Sect. 10.2.1). It is believed that the handling of the bags during installation and, to a lesser extent, their service lives, cause them to undergo plastic elongation. This permanent elongation means that the sand-filled volume of the bag decreases relative to the bag dimensions. This volume change allows more sand to move freely within the bag which then becomes more susceptible to the failure mechanism described in Sect. 10.2.1. A solution to the elongation issues is still under debate and the new specification requires that the tensile strength, when measured in both the cross and machine direction, be at least 75 kN/m at an elongation of 10 % when tested to SANS 10221 - 2007. Past bags exceeded elongations of 50 % at these loads and more testing is required to investigate the advantages and disadvantages of reducing the elongation.

10.4 Construction techniques

The effects of different construction techniques on the long term performance of GSCs is not well documented and it is believed that it has a more important role than the literature suggests. The filling of the bags required a steel frame (Fig. 10.9). The manufacture of this frame is governed by the geometry and layout of the bag. This proved to be an issue as new bag manufacturers entered the market and the manufacture of the bag evolved. When the bag's chute diameter varied the frame's funnel diameter remained constant, this necessitated the removal of some stitching to allow installation of the bag into the frame. This is problematic as the stitching has a tendency to run, potentially causing the bag

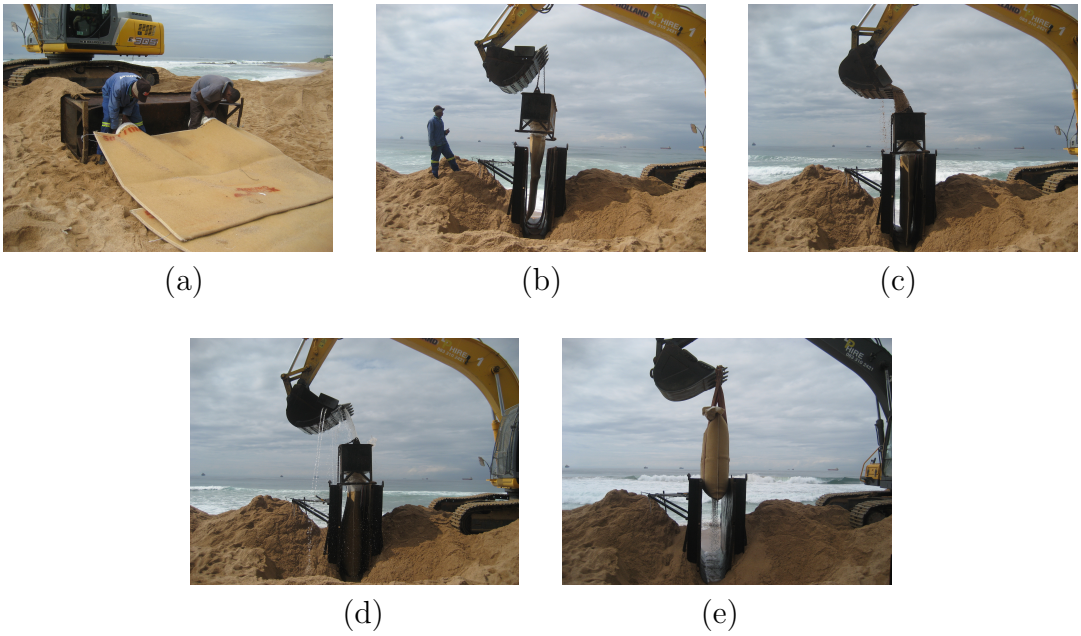

(a) (b) (c)

(d) (e)

Figure 10.9: Sequence of filling a bag using an excavator and a steel frame. (a) The bag's chutes are placed over the frames dual funnels. (b) The bag is loaded into the frame. (c)/(d) The bag is filled alternating between buckets of sand and water. (e) The filled bag is removed from the frame in order to be stitched.

to pull open (Fig. 10.10).

10.4.1 Filling the bags

The filling of the GSCs has become a contentious issue in South Africa. The origin of the issue stems from the difficulty in defining a fill ratio, the construction technique and the uncertainty of an optimal fill ratio with respect to hydraulic stability. The filling of GSCs has been performed in various ways in different countries. They have been commonly filled by dredge pump in underwater applications [Lee & Douglas, 2011; Oh & Shin, 2006] but modified machinery [Martinelli *et al.*, 2011], hand filling [Oberhagemann & Hossain, 2011] and conveyor belt with frame [Heibaum, 1999; Saathoff *et al.*, 2007] have all been used. Locally the bags have been filled either by pumping a sand and water slurry into the bags or by filling with an excavator. Pumping is theoretically superior to that of the excavator but unfortunately it is not more practical. The bags are almost always

Figure 10.10: Running of bag stitching following the widening of the chutes

installed after an erosion event when the beach volume is at a minimum. This means that the bags can be installed at the lowest historic profile level with little or no excavation. The low beach level also means that there is no buffer from wave runup. The slurry pump is therefore under constant attack and a tracked machine is required to periodically re-position it. It was found that the time lost from the pump being disturbed by the waves and tides as well as requiring an excavator available to continuously move the pump, made the operation less efficient and almost more expensive than having two excavators on site filling bags.

The current preferred method is filling the bags by excavator as shown in Fig. 10.9 (this practice is common in Australia [Hornsey *et al.*, 2011]) with one bucket of sand followed by one bucket of water. A second excavator relocates the bag to a safe position where it can be stitched prior to placement.

The bags were originally filled between 80 % and 90 % of their capacity (based

on the German construction technique [Oumeraci *et al.*, 2003] ensuring that the sand is sufficiently compacted by flooding with water. If the bags are filled any more it becomes difficult to stitch them closed, jeopardising the quality of the stitch. Overfilling the bags also causes rounding. Since some of the bag's stability is determined by its mass and friction, it was hypothesised that the more rounded it is the less contact each bag will have with the surrounding bags, lowering the stability. Not filling the bags to capacity allows them to be leveled for the next bag layer as well as providing a large contact area. However, the findings of Hornsey *et al.* [2011] contradict this theory showing that the Australian practice of filling bags to capacity is more stable. The fill ratio was defined as the height of sand within the bag against the height of the bag when suspended in the filling frame. This definition is accurate but impractical to measure within the frame. The fill height can be measured when the bag has been placed for stitching but this is prone to errors because the bags deform substantially. Quality control can be compromised with numerous bags being insufficiently filled. Filling the bags to their physical limit is appealing as it makes the problem of defining a fill ratio less problematic.

Not filling the bags to capacity and insufficient compaction of the sand has been highlighted as a reason why the sediment is able to move within the bags. The geotextile composite has a hydraulic conductivity of 0.03 m/s (the new specification will be 0.05 m/s) while sand is approximately 0.01 m/s [Das, 2002]. This means that the current method of placing an excavator bucket full of sand followed by a bucket full of water is not compacting the sand sufficiently as the water escapes through the geotextile before it can flood the sand and compact it. So if the bags were to be filled to capacity the current method may result in the bags only being about 90 % full. It is not expected that the 10 % of sand movement within the bag will significantly affect the stability but when the target is 80 % of the full capacity the resulting 20 % deficit probably will. There has been an attempt to mitigate this issue by specifying a constant flow of water into the bag. This method has not yet been applied and it is expected that the same issues experienced with the slurry pumping will be encountered. There is now general consensus in KwaZulu-Natal that the bags should be filled to capacity. All bag installations from 2012 have been done at fill capacity. The fill ratio is strongly

Figure 10.11: Hand stitched nylon rope to seal the landward end of the bags

dependent on the filling technique and the excavator filling technique (Fig. 10.9) is unable to consistently achieve a 100 % fill ratio. Although the excavator filling technique has been retained additional hand filling by shovel has been required to ensure capacity filling.

10.4.2 Installation

In South Africa the bags have been orientated with their longitudinal axis perpendicular to the wave attack in a stretcher bond arrangement. This arrangement has undergone physical model tests by Hornsey *et al.* [2011] and Coghlan *et al.* [2009]. While Recio & Oumeraci [2007] conducted physical model tests with the longitudinal axis parallel to the wave attack. Although Recio & Oumeraci [2007] arrangement may improve the hydraulic stability it requires a significantly larger amount of bags and so has a serious cost implication.

Figure 10.12: Cable tied bags as an alternative to nylon stitching

The stitching of the bags is done in the factory by sewing machines and the resulting seam has 90 % of the bag material tensile strength in the machine direction. To minimize the risk of the stitch unravelling there is a Lock stitch over the full depth of the continuous seam which is also covered with an Overlock stitch. The chutes however have to be sealed onsite and this is done by hand stitching with 5 mm diameter nylon rope (Fig. 10.11). This stitch is therefore the weakest part of the bag and has been mitigated by placing the bags with the hand stitched portion facing landwards. Careful supervision and quality control of the hand stitching is essential as labour-based methods can fluctuate in quality which may lead to leaking of sand. A manufacturing technique which has proved to successfully increase quality is the pre-punching of holes (Fig. 10.11 and Fig. 10.12). This means the spacing of hand stitches is predefined and so ensures more consistency with regards to the quality of stitch. All that still has to be ensured is that the nylon is knotted correctly. Nylon cable ties (Fig. 10.12) have

comparative properties to nylon rope and were used as an alternative. The cable ties have not proven to be superior but remain a viable alternative. A handheld sewing machine was initially used to stitch the bags but was abandoned during the emergency work following associated installation delays. The re-introduction of the sewing machine has not been supported due to cost implications as well as there being no evidence at present for the adverse effects of hand stitching. The system of chutes into the bag become sand tight after they have been rolled up and sealed within the bag.

There may be uncertainty as to where the lowest scour level is or additional confidence may be required in minimizing the undermining risk. This has been accommodated by providing a Dutch toe (self-healing toe). A Dutch toe is a row of bags in front of the seawall's toe and tied back into the bottom bags. (refer Fig 10.6). In theory as the beach profile approaches the founding level of the bag seawall the Dutch toe will settle giving the structure an additional 2 m scour resistance (i.e. the length of one bag) .

10.5 Slope

The slope of bag protected dunes is still debated, with engineers designing slopes from 30 to 45°. Flume tests have shown that 45° is the most stable [Hornsey *et al.*, 2011]. The stability of the bag seawall is dependent on the friction forces developed between the bags which is a function of their roughness, the net normal force (weight above the contact area) and the contact area. Recio & Oumeraci [2008] identified, from flume tests, that the friction between containers affects the hydraulic stability much more than assumed in past and present literature. In order for the bags to be stable this frictional force must be equal to or greater than the active soil force behind the bags (Fig. 10.13). So although the friction increases as the bag seawall approaches the vertical so does the active soil pressure. A balance of these two forces was used to calculate an optimum bag slope. Figure 10.14 shows a plot of how many bags will be stable at a specific slope. The calculation includes a safety factor used on the soil properties as advised by Henkel [1981]. For comparison purposes the results shown ignore cohesion, place the water table below the bag seawall, and use a constant soil weight of

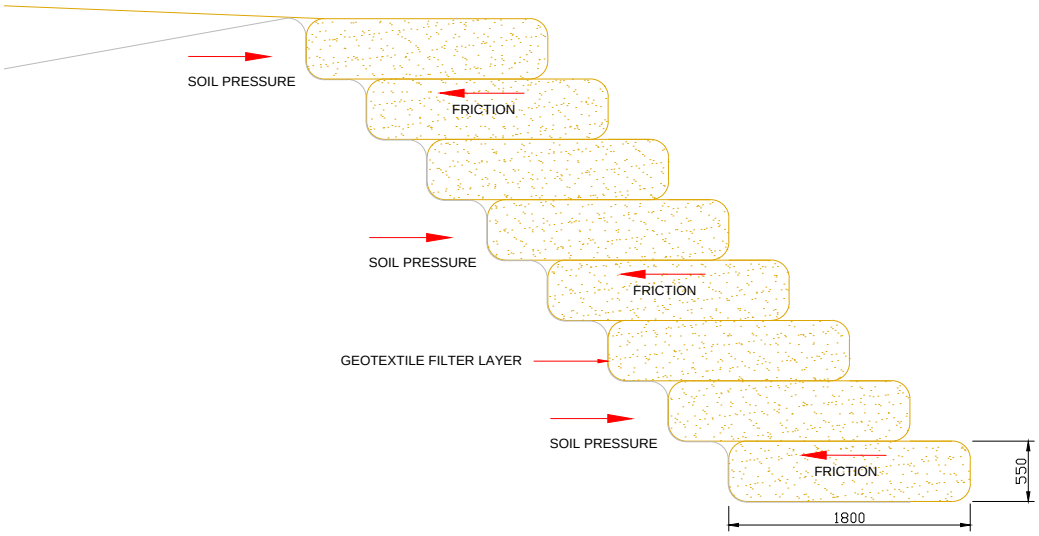

Figure 10.13: Cross-section of a geotextile sand bag seawall showing the bag friction and the lateral earth pressure

18 kN/m^3 and a soil friction angle of 30°. Active soil pressures were calculated using Coulomb's active earth pressure coefficient K_a as given by Lambe & Whitman [1969], namely

$$K_a = \left(\frac{\csc(\beta)\sin(\beta - \phi)}{\sqrt{\sin(\beta + \phi_w)} + \sqrt{\frac{\sin(\phi+\phi_w)\sin(\phi-i)}{\sin(\beta-i)}}} \right)^2 \tag{10.1}$$

where β is the angle of the bag slope measured from the horizontal, i is the surface slope of the retained soil, ϕ is the soil friction angle and ϕ_w is the friction angle of the wall. The bag dimensions are 2.5 x 2 x 0.5 m and have a fill weight of 4.5 tons based on the assumed soil weight of 18 kN/m^3.

Figure 10.14 illustrates that the angle range of 18 – 26° can retain the most soil. For the assumptions used, a 45° bag slope will be unable to retain 5 m of soil while a 30° slope will. This simple calculation does not consider the hydraulic stability of the bags and because the sand is displaced to the front face of the bags by the lifting and dropping of the exposed portion, it is thought that the less bag length that can be lifted the more stable the bags are. Given this apparent

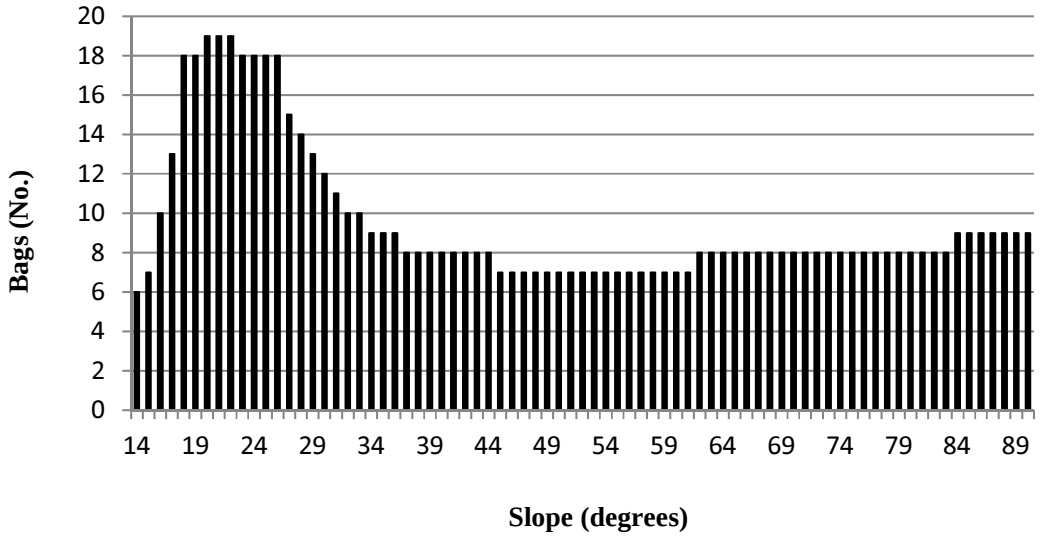

Figure 10.14: The number of stable retaining bags per seawall inclination

contradiction we speculate that the increased restriction of this movement is what makes the bags more stable at steeper slopes (45°) and not the increased friction [Hornsey *et al.*, 2011].

10.6 Bi-component and multi-component bags

Throughout this paper we have identified shortfalls in the geotextile bag design and have described ways to mitigate them either through construction techniques or bag design. Table 10.2 summarises the main improvements to the new bags and Fig. 10.15 provides a visual comparison. The tensile strength has been increased by 154 % in the machine direction and 20 % in the cross direction. Restall *et al.* [2002] discussed the ultimate strengths of GSCs used in 7 projects on the Australian coast of which the maximum GSC tensile strength was 75 kN/m. Alvarez *et al.* [2007] reported an ultimate tensile strength of 90 kN/m for geotextile tubes used as submerged breakwaters, while Shin & Oh [2007] reported geotextile tube tensile strengths of 175 kN/m. The South African bags are in the upper range of tensile strengths with regards to marine and coastal geotextiles. To the authors' best knowledge the bags represent the highest tensile strength of any geotextile

Table 10.2: Comparison of the bi-component (original specification) and multi-component bag specifications

Properties	Bi-component bags	Multi-component bags
Mass (g/m^2)	2100	1566
Thickness (mm)	12	8.8
MD Tensile strength (kN/m)	50	127
XD Tensile strength (kN/m)	95	114
Ultimate elongation (%)	50	17

NOTES: MD = machine direction; XD = across direction

sand bag on record. The higher tensile strengths have been driven by the desire to achieve a lower ultimate elongation. The percentage elongation has been more than halved in the new bags making the bags vulnerable to damage during installation and thus requiring greater tensile strengths. Kaytech were able to achieve these requirements with almost 30 % reduction in geotextile thickness and weight. This was possibly due to the fusion technique that joins the inner polyester to the outer polypropylene resulting in a superior product that is less expensive than its predecessor. The first multi-component bags were installed in 2012 and it remains to be seen if they have the same robustness as the bi-component bags and whether the advantages from the additional stiffness outweigh the disadvantages.

10.7 Conclusion

Coastal defences are necessary in the presence of increasing coastal population densities, sea level rise, and occurrence of extreme events. GSCs have become the preferred defence along the east coast of South Africa as they have political, social and environmental appeal. KwaZulu-Natal installed over 20 000 sand bags between the year 2007 and 2011. The experience of these bags in seawalls has shown that the failure mechanism of the bags is associated with movement of sand within the bags, as described by Recio & Oumeraci [2007, 2008]. Observations of installed bags have shown that this movement is intensified by under filling of the bags, bag elongation, and the leaking of sand. The leaking of sand is mainly caused by vandalism which can only really be minimised by covering the bags in

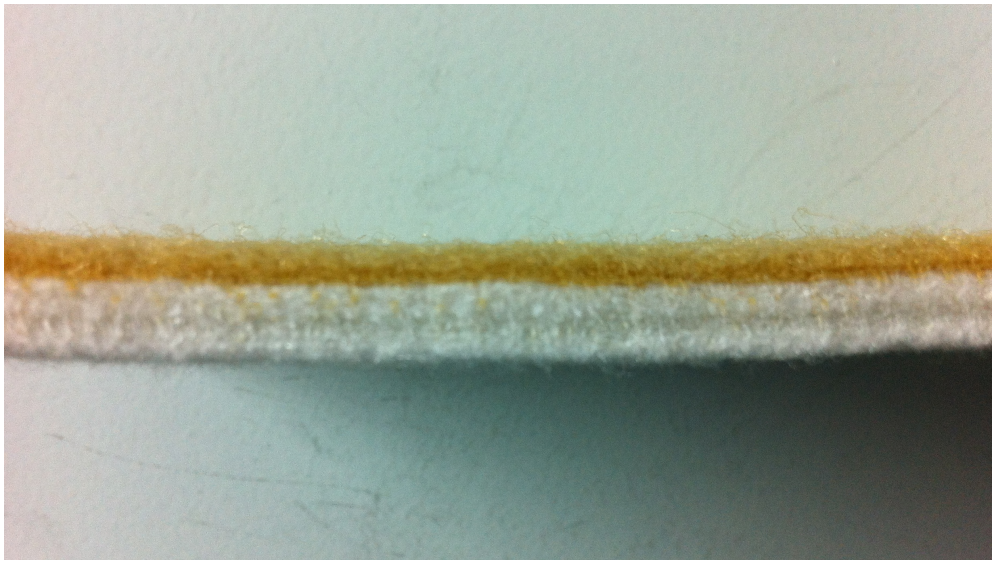

(a)

(b)

Figure 10.15: Geotextile sand bag (a) bi-component and (b) multi-component

sand or by limiting their installation in high risk areas.

Experience has shown that the Australian practice of filling the bags to capacity may make the bags more hydraulically stable as suggested by Hornsey *et al.* [2011]. The fill ratio has significant effects on the long term performance of geotextile sand bags. Under filling of bags increases the potential sand movement within the bags and the related failures. The authors' propose that defining an optimum fill ratio is essential for the long term performance of GSCs and should be a priority candidate for future research and development.

From observations of installed bags the authors' can confidently say that a 45° slope is more stable than 30°. This appears to be the result of more of the bag being confined for the 45° slope rather than the increase in friction which is offset by the forces of the retained dune sand. Since physical model tests have been limited to stabilised retained slopes the authors' suggest that retained sand slopes be modelled to verify these observations.

The use of GSCs for shoreline protection requires UV and abrasion resistance. Although specifications and testing standards are available there is no clear indication how those specifications relate to life expectancy. Such an indication would add considerable value to the cost and risk analysis in using GSCs for shoreline defences and should be considered in future research.

The high elongation of a bag allows it to stretch and thus increases the potential sand movement within the bag. This effect may not warrant limiting the elongation percentage of the geotextile given the benefits of flexibility (Fig. 10.4 and 10.5). Experience has shown that the majority of the bag elongation occurs during installation and construction methods should be revised to limit this initial deformation prior to altering the geotextile characteristics. We propose that the effects of construction techniques on the long term performance of GSCs is an aspect that is poorly understood and should be included in future research and development.

The testing of exhumed bags showed that many of the properties exceeded the specified properties. This may be because of variability in the manufacturing process but it has been suggested that the ingress of sand into the geotextile may alter its properties and this hypothesis should be tested in future studies.

Based on the South African experience it is recommended that the bags be

filled to capacity and where possible be placed at a slope of 45°. Elongation during construction may have significant effects on the long term service life of the bags and it is recommended that a construction method that minimises bag elongation be adopted. The bags are sensitive to abrasion, UV degradation and vandalism. It is therefore recommended that the bags be covered with sand and vegetated wherever possible.

This paper has added the South African experience of GSCs in coastal defences to the well documented experiences of Europe and Australia. We have also provided practical full scale validation of the physical model results of Hornsey *et al.* [2011]; Recio & Oumeraci [2007].

References

Allan, J. C., Komar, P. D., 2002. "A dynamic revetment and artificial dune for shore protection". In: Proceedings, The 28th International Coastal Engineering Conference, Cardiff, Vol. 2, 2044 – 2056, 2002. 33, 259, 276

Alvarez, I. E., Rubio, R., Ricalde, H., 2007. "Beach restoration with geotextile tubes as submerged breakwaters in Yucatan, Mexico". Geotextiles and Geomembranes Vol. 25, 233 – 241. 34, 266, 296

Airoldi, L., Abbiati, M., Beck, M. W., Hawkins, S. J., Jonsson, P. R., Martin, D., Moschella, P. S., Sundelf, A., Thompson, R. C., & berg, P., 2005. "An ecological perspective on the deployment and design of low-crested and other hard coastal defence structures". Coastal Engineering Vol. 52, 1073 – 1087. 246, 275

BAW Federal Waterways Engineering & Research Institute., 1994. "Guidelines for Testing Geotextiles for Navigable Waterways (Germany)". 287

Barnett, K. A., 1999. "The Management of Durban's Beaches: An Historical Perspective". In: Proceedings, Fifth International Conference of Coastal and Port Engineering in Developing Countries, COPEDEC V, 1999, Cape Town. 87, 249, 277

Coghlan, I.R., Carley, J.T., Cox, R.J., Blacka, M.J., Mariani, A., Restall, S.J., Hornsey,W.P., Sheldrick, S.M., 2009."Two-Dimensional Physical modelling of sand filled Geocontainers for coastal protection". In: Proceedings of Australasian Coasts and Ports Conference 2009. The Institution of Engineers Australia, Wellington NZ. 292

CSIR, 1976. “Status quo of the Durban Beach protection investigation”. Report No. C/SEA 7607, Stellenbosch. 247, 277

Das, B. M., 2002. ”Principals of Geotechnical Engineering”. Brooks/Coles, Pacific Grove. 291

Dette, H. H., Raudkivi, A. J., 2002. “Beach and storm-tide protection on the coast of the Baltic Sea”. In: Proceedings, 28th International Coastal Engineering Conference, Cardiff, Vol. 3, 3298 – 3307. 16, 32, 253

Durgappa, R., 2008. ”Coastal protection works”. In: Proceedings, Seventh International Conference of Coastal and Port Engineering in Developing Countries, COPEDEC VII, 2008, Dubai. 85, 246, 275

EEA, 1999. “Coastal and marine zones. Environment in the European Union at the Turn of the Century”. State of Environment Report No. 1/1999. Copenahagen: EEA (Chapter 3.14). Available from: http://reports.eea.eu.int/92-9157-202-0/en. 275

French, P. W., 2001. “Coastal Defences: processes, problems and solutions”. Routledge, New York. 247, 257, 275

Heibaum, M.H., 1999. “Coastal scour stabilisation using granular filter in geosynthetic nonwoven containers”. Geotextiles and Geomembranes, Vol. 17, 341 – 352. 289

Heerten, G., Klompmaker, J., Partridge, A., 2008. “Design and construction of waterfront structures with special designed non-woven geotextiles”. In: Proceedings, Seventh International Conference of Coastal and Port Engineering in Developing Countries, COPEDEC VII, Dubai. 33, 259, 276

Henkel, D. J., 1981. “The design of sheet pile walls”. Geotechnics Seminar, session No.7, Sheet pile walls. 263, 294

Hornsey, W. P., Carley, J. T., Coghlan, I.R., Cox, R. J., 2011. “Geotextile sand container shoreline protection systems: Design and application”. Geotextiles and Geomembranes, Vol. 29(4), 425 – 439. 33, 260, 262, 263, 274, 276, 282, 283, 286, 287, 290, 291, 292, 294, 296, 299, 300

Kinmont, A., 1954. "Beach Erosion and Protection". In: Proceedings, The Institute of Municipal Engineers, Thirty third annual conference, Durban. 114, 247, 252, 277

Komar, P.D., Allan, C. J., 2008. "Increasing Hurricane-Generated Wave Heights along the U.S. East Coast and Their Climate Controls". Journal of Coastal Research, Vol. 24 (2), 479 – 488. 12, 115, 140, 275

Lambe, T. W., Whitman, R. V., 1969. "Soil Mechanics". John Wiley and Sons, New York. 295

Lee, E.C. Douglas, R.S., 2011. "Geotextile tubes as submerged dykes for shoreline management in Malaysia". Geotextiles and Geomembranes, in press, 1 – 8. 289

Martinelli, L. Zanuttigh, B. De Nigris, N. Preti, M., 2011. "Sand bag barriers for coastal protection along the Emilia Romagna littoral, Northern Adriatic Sea, Italy". Geotextiles and Geomembranes, Vol. 29, 370 – 380. 289

Mather, A. A., Kasserchun, R., Wenlock, H., 2003. "City of Durban Sand Bypass Scheme: 20 year performance evaluation". In: Proceedings, Sixth International Conference of Coastal and Port Engineering in Developing Countries, COPEDEC VI, Colombo, Sri Lanka. 249, 277

Mather, A. A., 2008. "Sea Level Rise for the East Coast of Southern Africa". In: Proceedings, Seventh International Conference of Coastal and Port Engineering in Developing Countries, COPEDEC VII, Dubai, UAE. 11, 14, 114, 186, 275

McClarty, A., Cross, J., James, G.M., Gilbert, L, 2006. "Design and construction of coastal erosion protection groynes using geocontainers, Langebaan, South Africa". Geosynthetics, In: Proceedings, 8th International Conference on Geosynthetics, Yokohama, Japan, Vol. 2, 765 – 768. 276, 277

Moschella , P. S., Abbiati, M., berg, P., Airoldi, L., Anderson, J. M., Bacchiocchi, F., Bulleri, F., Dinesen, G. E., Frost , M., Gacia, E., Granhag, L., Jonsson, P. R., Satta, M. P., Sundelf, A., Thompson, R. C., Hawkins, S. J., 2005. "Low-crested coastal defence structures as artificial habitats for marine life: Using

ecological criteria in design". Coastal Engineering, Vol. 52, 1053 – 1071. 246, 275

Muthukumaran, A.E. Ilamparuthi, K., 2006. "Laboratory studies on geotextile filters as used in geotextile tube dewatering". Geotextiles and Geomembranes, Vol. 24, 210 – 219. 283

Oh, Y. I. Shin, E. C., 2006. "Using submerged geotextile tubes in the protection of the E. Korean shore". Coastal Engineering, Vol. 53, 879 – 895. 289

Oberhagemann, K. Hossain, Md. M., 2011. "Geotextile bag revetments for large rivers in Bangladesh". Geotextiles and Geomembranes, Vol. 29 402 – 414. 283, 289

Oumeraci, H., Hinze, M., Bleck, M., dan Kortenhaus, A., 2003. "Sand-Filled geotextile containers for Shore protection". In: Proceedings, Sixth International Conference of Coastal and Port Engineering in Developing Countries, COPEDEC VI, Colombo, Sri Lanka. 33, 262, 291

Oumeraci, H. & Recio, J. 2010. "Geotextile sand containers for shore protection". In: Kim, Y. C. Handbook for Coastal and Ocean Engineering. World Scientific Publishing, Singapore. 285

Phelps, D., Rossouw, M., Mather, A. A., & Vella, G. F., 2009. "Storm damage and rehabilitation of coastal structures on the East coast of South Africa". In: Proceedings, Institute of Civil Engineers Conference, Edinburgh, Scotland. 51, 250, 277

Recio, J., Oumeraci, H. 2007. "Effect of deformations on the hydraulic stability of coastal structures made of geotextile sand containers". Geotextiles and Geomembranes. Vol. 25, 278 – 292. 274, 279, 292, 297, 300

Recio, J., Oumeraci, H. 2008. "Hydraulic Stability of Geotextile Sand Containers for Coastal Structures: Process Oriented Studies Towards New Stability Formulae". In: Proceedings, Seventh International Conference of Coastal and Port Engineering in Developing Countries, COPEDEC VII, Dubai. 33, 259, 263, 279, 294, 297

Restall, S. J., Jackson, L. A., Heerten, G., Hornsey, W. P., 2002. "Case studies showing the growth and development of geotextile sand containers: an Australian perspective". Geotextiles and Geomembranes. Vol. 20(5), 321 – 342. 33, 260, 276, 277, 296

Saathoff, F., Witte, J., 1994. "Use of geotextile containers for stabilizing the scour embankments at the Eidersperrwerk", Geosynthetics World, Part 1 in vol. 5(1), 1994, Vol. 5(2), 1995. 288

Saathoff, F., Oumeraci, H., Restall, S., 2007. "Australian and German experiences on the use of geotextile containers". Geotextiles and Geomembranes, Vol. 25 (4-5), 251 – 263. 32, 33, 34, 258, 260, 275, 277, 285, 286, 287, 288, 289

Shin, E. C., Oh, Y. I., 2007. "Coastal erosion prevention by geotextile tube technology". Geotextiles and Geomembranes, Vol. 25, 264 – 277. 34, 266, 296

TenCate Geosynthetics North America, 2010. "UV durability of TenCate geosynthetics". Technical Note, Pendergrass. 286

Udo, K., Takewaka, S. & Nishimura, H., 2002. "Long-term morphological change of backshore dunes". In: Proceedings, The 28th International Coastal Engineering Conference, Cardiff. 260, 285

Zanuttigh, B., Martinelli, L., Lamberti, A., Moschella, P., Hawkins, S., Marzetti, S., Ceccherelli, V. U., 2005. "Environmental design of coastal defence in Lido di Dante, Italy". Coastal Engineering, Vol. 52 1089 – 1125. 246, 275

Chapter 11

Synthesis and conclusion

11.1 Introduction

This chapter provides a synthesis of the eight papers (Chapters 3 to 10) with regards to coastal risk. The conclusions are then presented in terms of the research questions and recommendations are made for future research.

11.2 Coastal risk

This thesis has identified and analysed trends in waves, water levels and beach profiles. These three trends describe the risk of a beach in terms of increasing wave parameters, water levels, chronic erosion of beaches and the recovery time of beaches.

The most urgent concern is chronic erosion as it is likely to exist in the absence of wave and water level trends. Chronic erosion may be the result of a reduction in sediment supply, an increase in storm trends and sea level rise. It was found that on average storm damaged beaches recovery to their pre-storm profile within 2 years (Chapter 4). This implies that storm trends are not currently contributing to chronic erosion and that the erosion may be attributed to a decrease in sediment budget and sea level rise. The Bruun rule attributes 75 % (Chapter 5) of the total current erosion to sea level rise and we suggest that the remaining 25 % is accounted for by sediment mining and damming of rivers as well as the absence

of large episodic flood events (Chapter 4).

We can put these trends into a time perspective by considering the March 2007 storm event. The narrow beaches did not provide a sufficient buffer to protect coastal developments as well as there not being sufficient recreational beach area. On average more than 20 % of the beach volume was lost from the 2007 event. Therefore a loss of 20 % beach volume from the current level represents a critical level. The current average chronic erosion for all the beach profiles is approximately 0.8 % per annnum (Chapter 5). At this current rate the beaches will be at a critical level by the year 2040. This makes it imperative that the sediment supply deficit is corrected through the restricting of mining permits and the use of beach nourishment (Chapter 9). It is possible that a large flood event will provide the sediment correction (Chapter 4). If the supply is addressed only sea level rise will be contributing to the erosion and consequently will bring the beaches to a critical level by 2060.

Chronic erosion has the potential to be amplified by increasing storm parameters. It was estimated that current storm trends could potentially increase erosion by 0.14 % to 0.20 % per annum (Chapter 7). However, in Chapter 4 it was concluded that beaches make volumetric recoveries within an average of 2 years regardless of the magnitude of the event. There is a threshold of storm frequency and intensity above which beaches will be unable to recover prior to a consecutive storm event and chronic erosion will set in. It is unclear what this theshold is so to be conservative let us assume that the threshold has already been exceeded and beaches are eroding an additional 0.14 %/annum. Once again we define an unacceptable beach volume as 20 % less than the current volumes. The erosion associated with trends in wave parameters and water levels will then be at a critical level before the year 2030. We do not believe this to be the case because the estimated current increase in storm frequency of 1 event in 100 years (Chapter 5) is not expected to contribute to long term erosion prior to the year 2100.

In summary:

1. A combination of all the measured trends will produce a critical beach volume by 2030.

2. A combination of sea level rise and sediment supply reduction will produce a critical beach volume by 2040.

3. An increase in sea level will produce a critical beach volume by 2060.

These results may have great value in coastal management but must still be considered cautiously. As highlighted in Sect. 2.2 over 50 years of data is required to define a coastal climate. This thesis has only analysed 37 years of beach profile data and 18 years of wave data. These limited data sets may describe a period of climate variability as opposed to climate change but are currently the only available estimates.

Although sediment budgets may be corrected via beach nourishment or controlled by legislation, natural climate cycles producing sea level rise will require interim solutions. The author believes that geotextile sand bags will provide a politically, socially and environmentally acceptable sea defence (Chapter 10).

11.3 Research answers

The research questions were presented in Chapter 1 and are repeated below with their answers.

The main research question was:

Can the risks from extreme waves be characterised by simple measures such as a recurrence interval that accurately reflects the associated hazards to developed coastal zones?

This research question was investigated in the context of a case study in the Durban area where it can be posed specifically as:

What is the return period of the waves experienced during the March 2007 storm event, and what are the lasting effects of these storms on the coastline?

This question can be divided into the following questions:

Is there evidence of trends in Durban's wave climate and sediment movement?

This question is answered in Chapter 5. Increasing trends were found in wave height, wave period, storm frequency and a trend towards a more southerly wave direction. Decreasing trends were found in duration and calm period. Of these identified trends only the trends in peak period and mean wave direction were found to be statistically significant at a 95 % confidence level.

There is evidence of chronic erosion along the eThekwini coastline. Approximately 70 % of the measured beach profiles have been eroding from 1973/1988 of which almost 80 % were estimated to be statistically significant at a 95 % confidence level (Sect. 5.3.2)

What are the current and potential future impacts of these trends?

This question is addressed in Chapter 4, 5 and 7. Currently chronic erosion is a major concern and on average, beaches are loosing approximately 0.8 % of their volume per annum. Sandy beaches are a major tourist attraction and the decrease of recreational sandy beach width may have an immediated impact on tourism. It has been estimated that the chronic erosion will become critical before the year 2040.

It is unlikely that the trends in storm parameters are currently affecting erosion. These trends were estimated to increase erosion by 0.14 %/annum to 0.20 %/annum and should become critical, in terms of beach volume, by the year 2200. The trends in sea level, as per the Bruun rule, describe a 40 % loss in beach volume by the year 2100 for a 0.3 m rise. The profile retreat in this case is

critical and relates to 25 m. If any confidence can be put in the Bruun rule we are likely to experience increased coastal flooding by the year 2060.

If all 3 of these trends were contributing to erosion the beaches would be at a critical level by 2030 (Sect. 11.2).

What is the global recovery time of storm damaged beaches?

This question was answered in Chapter 4. It was found that on average, beach profiles take 2 years to make a volumetric recovery to their pre-storm status, regardless of the event magnitude.

Can a sea storm be described as a non-ambiguous multivariate return period, representative of its erosion potential?

This question was explored in Chapters 6 and 8. The author has provided a method of creating non-ambiguous multivariate return periods that are representative of erosion volumes. Although the generality of the method still has to be determined the author is confident that the method will provide a sound foundation for development.

The March 2007 storm event was estimated to have a wave height univariate return period of approximately 30 years (Chapter 3). However, although it's multivariate return period $\tau(H, T, D, L)$ was estimated to be a 120 year return period it resulted in an erosion return period of 34 years. (Chapter 8).

What are the most sustainable coastal defences?

Chapters 9 and 10 address this question. Beach nourishment and geotextile sand bags were found to be the most sustainable forms of coastal defence. These defences will be necessary in short and medium term planning but will eventually become insufficient in the long term.

11.4 Conclusion

This thesis has provided an updated review and analysis of Durban's wave data. Such a review has not been formally presented since 1984.

The global recovery times of storm damaged beaches was estimated to be approximately 2 years.

Trend analysis was performed on wave heights, water levels and beach volumes using the novel approach of singular spectrum analysis. Increasing trends were found in wave height, peak period and wave direction. Only peak wave period and wave direction were found to be statistically significant. Sediment mining, damming of rivers as well as the absence of episodic extreme flood events and sea level rise were estimated to be the principal causes of chronic erosion.

The relationship between storm parameters and wave heights was modelled statistically using the novel method of copulas. A trivariate Clayton copula has been created for the Durban wave climate. The copula model was used, in conjunction with non-stationary probability distributions, to forecast future events with a probability equivalent to that of the 2007 event. From the forecasts it was estimated that future events would contribute an additional 0.14 % erosion volume per year.

This thesis has provided a method of consistently representing multivariate return periods in a non-ambiguous way. Physical constraints have been proposed along with a multivariate linear regression iso-erosion surface to improve the estimates of the most-likely design event method. The 2007 storm event was found to have a multivariate return period (the occurence of wave height, peak period, storm duration and water level) of 120 years and an erosion return period of 34 years.

This thesis provides a review and critical comparison of all Durban's coastal defences to international practices. It suggests that the use of geotextile sand bags and beach nourishment are the most appropriate coastal defences. The South African experience and development of geotextiles for coastal defence has also been added to international knowledge.

This thesis has quantified risks for coastal managers. In order of priority the risks are: a decrease in sand supply; an increase in sea level; an increase in storm

parameters and an increase in storm frequency. Without mitigation these trends will have significant impacts by the year 2030.

11.5 Future research

Multivariate statistical modelling is a difficult subject and one that still needs considerable development. In this thesis independent storm events have been identified by applying a commonly used and well accepted theshold sampling method. Although the author is confident that the method provides suitable sampling of independent events the correct approach would be via climatic forcing. Meteorological events should be identified and associated to wave direction. This would immediately solve the problem of wave period being both deterministic and random (Chapter 6).

Similarly, meteorological trends should be identified (Chapter 7). For example in Durban the three major meteorological forcings are tropical cyclones, cold fronts and cut-off lows but only one of these forcings may have a trend. This would then allow extensive modelling of seasonal cycles and long term trends. The author believes that the inclusion of direction into the statistical model will solve a significant portion of the limitations as sheltering plays a major role in erosion. This study has been unable to include wave direction because of limited data and many years of data collection may still be required before the recommended reseach can be undertaken.

Multivariate return periods should ideally be described in a way that is related or analogous to erosion. This thesis has proposed a method of estimating analogous events. Further research is required to investigate the generality of this approach and should involve testing at other locations with different wave climates and shoreline characteristics.

Chapter 12

Appendix

This appendix provides the mathematical expressions for the three construction techniques described in Sect. 6.2.2 and the simulation algorithm used in this study.

Multivariate copula construction techniques

The Chakak & Koehler [1995] method uses the bivariate conditional distribution of (X, Y), given that $Z = w$, to create a trivariate copula

$$C_{XYZ}(u, v, w) = wC_{XY}\left(\frac{C_{XZ}(u, w)}{w}, \frac{C_{YZ}(v, w)}{w}\right), \tag{12.1}$$

where $u, v, w \in [0, 1]$. The method has the compatibility problem and there is no guarantee that

$$wC_{XY}\left(\frac{C_{XZ}(u, w)}{w}, \frac{C_{YZ}(v, w)}{w}\right) = vC_{XZ}\left(\frac{C_{XY}(u, v)}{v}, \frac{C_{YZ}(v, w)}{v}\right) \tag{12.2}$$

The conditional mixtures approach is conceptually similar to that of Chakak & Koehler [1995] and was used by Salvadori *et al.* [2007], Joe [1997] and De Michele *et al.* [2007] to combine two 2-copulas to form a 3-copula. The three dimensional distribution can be obtained from the conditional distributions by

$$F_{XYZ}(x, y, z) = \int_{-\infty}^{y} C_{XZ}\left(F_{(X|Y)}(x|t), F_{(Z|Y)}(z|t)\right) F_Y(dt) \tag{12.3}$$

where $F_{(X|Y)}$, $F_{(Z|Y)}$ are the conditional distributions and can be found from the fitted two copulas

$$F_{(X|Y)}(x|y) = P(X \leq x|Y = y) = \partial C_{XY}(u, v)/\partial u \tag{12.4}$$

A similar expression exists for $F_{(Z|Y)}$. The notation can be rather confusing but the conditional distributions are simply the partial derivatives of the relevant 2-copulas. Note that C_{XZ} is basically a measure of conditional dependence between X and Z, given the behaviour of Y. Generally an analytic solution of the integrals cannot be found and a numerical method has to be employed.

The construction of a multi-level hierarchical Archimedean copula is conceptually simple but computationally and notationally challenging [Savu & Trede, 2006]. To make the notation slightly less confusing the operation " $\circ$ " is used to indicate the composition of functions such that $\varphi_{n-1} \circ \varphi_{n-2}^{-1}(y) = \varphi_{n-1}(\varphi_{n-2}^{-1}(y))$. The n-dimensional copula for the fully nested case requires $(n-1)$ generators, $\varphi_1, \ldots, \varphi_{1-n}$,

$$\begin{aligned} C(u_1, \ldots, u_n) = \varphi_{n-1}^{-1} \big(\varphi_{n-1} \circ \varphi_{n-2}^{-1} \big[\ldots (\varphi_2 \circ \varphi_1^{-1} [\varphi_1(u_1) + \varphi_1(u_2)] \\ + \varphi_2(u_3)) + \ldots + \varphi_{n-1}(u_{n-1})] + \varphi_{n-1}(u_n)) \end{aligned} \tag{12.5}$$

To make the method clearer consider the 3-dimensional copula $C(u, v, w)$. It can be written as a fully nested hierarchical copula $C(C(u, v), w)$, assuming the same dependence parameter. Writing the copulas in terms of their generating functions φ (Eqn. 6.1) would produce an equation similar to Eqn. 12.5.

Although the partially nested method is more flexible than the fully nested method it is not possible to create a 3-copula as the lowest dimension is $n = 4$, whence

$$\begin{aligned} C(u_1, \ldots, u_4) = \varphi^{-1} \big(\varphi \circ \varphi_{12}^{-1} [\varphi_{12}(u_1) + \varphi_{12}(u_2)] + \\ \varphi \circ \varphi_{34}^{-1} [\varphi_{34}(u_3) + \varphi_{34}(u_4)]\big) \end{aligned} \tag{12.6}$$

with three generators φ, φ_{12} and φ_{34}. The conditions required for nesting are

satisfied if $\theta < \theta_{12}$ and $\theta < \theta_{34}$ [Grimaldi & Serinaldi, 2006; Hofert, 2008, 2011; Savu & Trede, 2006]. Only the random variates U_1 and U_2 along with U_3 and U_4 are interchangeable. The major modelling limitation is that the joint distribution of (U_1, U_3) is equal to the joint distributions of (U_2, U_3), (U_1, U_4) and (U_2, U_4). The fully nested method provides a better model in this regard since for $n = 4$ dimensions, only (U_4, U_1), (U_4, U_2) and (U_4, U_3) will have the same joint distribution. Generally there are $n(n-1)/2$ (the number of bivariate marginals) ways to couple n variables and since there are only $n - 1$ generators only part of all possible mutual dependences will be uniquely modeled.

Simulation

The aim of a simulation is to generate a vector $(U_1, \ldots, U_n)$ whose variables are interdependent and lie in the interval $[0, 1]$. Let their joint distribution be a copula $C = C(u_1, \ldots, u_n)$. A sample from C can be simulated by the conditional inversion method [De Michele *et al.*, 2007; Nelsen, 2006; Savu & Trede, 2006, 2010]. In general a sample u_n can be simulated from U_n based on the conditional law of U_n given the values $U_1, \ldots, U_{n-1}$.

$$\begin{aligned} C_n(u_n|u_1, \ldots, u_{n-1}) &= P(U_n \leq u_n | U_1 = u_1 \ldots, U_{n-1} = u_{n-1}) \\ &= \frac{\partial_{u_1,\ldots,u_{n-1}} C(u_1, \ldots, u_n, 1, \ldots, 1)}{\partial_{u_1,\ldots,u_{n-1}} C(u_1, \ldots, u_{n-1}, 1, \ldots, 1)} \end{aligned} \tag{12.7}$$

for $n = 2, \ldots, d$. The conditional law C_n can then be used in the following algorithm to generate u_n:

1. Simulate d independent random variables $t_1, \ldots, t_d$ on I.
2. Set $t_1 = u_1$
3. For $n = 2, \ldots, d$, evaluate the inverse of the conditional distribution function to generate $u_n = C_n^{-1}(t_n|u_1, \ldots, u_{n-1})$

Evaluation of the inverse conditional distribution becomes increasingly complicated as more variates are included in the model and can usually only be solved

numerically. Other simulation algorithms have been proposed and examples of these can be found in Chebana & Ouarda [2011], Chakak & Koehler [1995], Whelan [2004] and Embrechts *et al.* [2001].

References

Chakak, A. Koehler, K. J.: A strategy for constructing multivariate distributions, Communications Statistics-Simulation and Computation, 24 537 – 50, 1995. 25, 27, 28, 152, 154, 155, 162, 165, 170, 174, 313, 316

Chebana F. Ouarda T.B.M.J.: Multivariate quantiles in hydrological frequency analysis, Environmetrics, 22 (1), 63 – 78, 2011. 28, 30, 316

De Michele, C. Salvadori, G. Passoni, G. Vezzoli, R.: A multivariate model of sea storms using copulas, Coastal Engineering, 54, 734 – 751, 2007. 22, 25, 27, 78, 152, 154, 155, 156, 162, 171, 174, 189, 190, 223, 224, 313, 315

Grimaldi, S. Serinaldi, F.: Asymmetric copula in multivariate flood frequency analysis, Advances in Water Resources, 29, 1155 – 1167, 2006. 26, 27, 154, 315

Hofert, M.: Sampling Archimedean copulas, Computational Statistics and Data Analysis, 52, 5163 – 5174, 2008. 27, 315

Hofert, M.: Efficiently sampling nested Archimedean copulas, Computational Statistics and Data Analysis, 55, 57 – 70, 2011. 27, 315

Joe, H.: Multivariate Models and Dependence Concepts, Chapman & Hall, London, 1997. 25, 26, 152, 154, 313

Nelsen, R.B.: An introduction to copulas, (second edition), Springer Series in Statistics, Springer, New York, 2006. xxi, xxviii, 22, 24, 25, 26, 27, 29, 152, 153, 154, 158, 159, 162, 171, 172, 173, 175, 189, 190, 223, 224, 315

Salvadori, G. De Michele, C. Kottegoda, N.T. Rosso, R.: Extremes in Nature. An Approach Using Copulas, Water Science and Technology Library, Springer, 56, 292, 2007. 25, 154, 155, 225, 313

Savu, C. Trede, M.: Hierarchical Archimedean copulas, http://www.uni - konstanz.de/micfinma/conference/Files/papers/Savu_Trede.pdf (2008-11-01), 2006. 26, 27, 154, 190, 224, 314, 315

Savu, C. Trede, M.: Hierarchies of Archimedean copulas, Quantitative Finance, 10 (3), 295 – 304, 2010. 27, 190, 224, 315

Whelan, N.: Sampling from Archimedean copulas Quantitative Finance, 4 (3), 339 – 352, 2004. 26, 28, 154, 316